UiT The Arctic University of Norway

Faculty of Biosciences, Fisheries and Economics

Rheostasis and timing: A tanycyte-mediated process

Vebjørn Jacobsen Melum

A dissertation for the degree of Philosophiae Doctor

February 2025

Université de Strasbourg

UNIVERSITÉ DE STRASBOURG

École doctorale Sciences de la vie et de la santé | ED 414 Université de Strasbourg

ÉCOLE DOCTORALE Sciences de la vie et de la santé

Institut des Neurosciences Cellulaires et Intégratives (INCI), UP3212
Régulation et Perturbation des Rythmes Neuroendocriniens

THÈSE **présentée par / DISSERTATION presented by :**

Vebjoern Jacobsen Melum

soutenue le /defended on : **20 Mai 2025**

pour obtenir le grade de **/** to obtain the grade of **:**
Docteur de l'Université de Strasbourg / Strasbourg University Doctor

Discipline/Spécialité **/** Discipline/Specialty : Biologie/Neurosciences

Rhéostasie et temporalité : un processus médié par les tanycytes

THÈSE dirigée par / DISSERTATION supervisor :

Shona Wood	Dr., Université de Tromsoe – L´université arctique Norvége
Valerié Simonneaux	Dr., Université de Strasbourg

RAPPORTEURS :

Sylvain Giroud	Dr., Université du nord du Michigan
Fanny Langlet	Prof., Université de Lausanne

AUTRES MEMBRES DU JURY / OTHER MEMBERS OF THE JURY :

Lars Folkow	Prof., Université de Tromsoe – L´université arctique Norvége
James McCutcheon	Prof., Université de Tromsoe – L´université arctique Norvége

Cover photo: Fredrik Markussen

Rheostasis and timing: A tanycyte-mediated process

Vebjørn Jacobsen Melum

A dissertation for the degree of Philosophiae Doctor, February 2025

UiT – The Arctic University of Norway

Faculty of Biosciences, Fisheries and Economics

Department of Arctic and Marine Biology

Arctic Chronobiology and Physiology research group

University of Strasbourg

École doctorale de Sciences de la Vie et la Santé

L'Institut des Neurosciences Cellulaires et Intégratives

Equipe Rythmes neuroendocriniens de la reproduction

Supervisors:

Shona H. Wood, UiT

David G. Hazlerigg, UiT

Valérie Simonneaux, UNISTRA

Résumé détaillé des résultats de la thèse en français

Introduction

Les propriétés géophysiques de la Terre entraînent des changements annuels dans l'irradiation solaire, entraînant des fluctuations saisonnières de la température et de la disponibilité alimentaire. Cela nécessite que les espèces non équatoriales répartissent les processus exigeants en énergie vers des périodes favorables de l'année. La régulation temporelle des fonctions physiologiques nécessite à la fois un réajustement des processus homéostatiques (rhéostasie) et la capacité de suivre les saisons. Les espèces de mammifères utilisent principalement les changements de photopériode (durée du jour) pour permettre d'anticiper les opportunités et demandes saisonnières à venir. La photopériode est représentée en interne par la sécrétion nocturne de mélatonine qui, via la pars tuberalis et les tanycytes du 3ème ventricule de l'hypothalamus, contrôle les adaptations métaboliques saisonnières. Dans ce contexte, l'objectif principal de cette thèse était d'élucider la signature moléculaire des tanycytes dans deux paradigmes saisonniers qui modifient le métabolisme ; la programmation photopériodique maternelle (chez le hamster sibérien, *Phodopus sungorus*) et l'hibernation (chez le hamster doré, *Mesocricetus auratus*).

Objectifs de recherche

Pour comprendre le rôle fonctionnel des tanycytes en tant que médiateurs des changements d'état métabolique, il est d'abord nécessaire de caractériser les modifications de leur biologie chez des animaux traversant de tels changements. Au cours de mon doctorat, j'ai abordé cette question en recourant à deux paradigmes saisonniers modifiant le métabolisme énergétique : la programmation photopériodique maternelle (hamster de Sibérie) et l'hibernation (hamster doré). J'ai combiné ces modèles avec la microdissection par capture laser (LCMD), le RNAseq et des mesures physiologiques à différents temps du cycle saisonnier. Dans cette thèse, j'ai visé à:

1. Synthétiser l'état des connaissances sur la programmation photopériodique maternelle, en particulier le rôle des tanycytes dans ce phénomène;

2. Caractériser la signature moléculaire des tanycytes dans un paradigme de programmation photopériodique maternelle;
3. Mettre en place un paradigme d'hibernation et des outils de suivi physiologique;
4. Caractériser le transcriptome tanycytaire dans un paradigme d'hibernation.

Le premier objectif est atteint dans l'Article I, où j'ai rassemblé la littérature pertinente dans une mini-revue consacrée à la programmation photopériodique maternelle. Le deuxième objectif est traité dans l'Article II : j'y ai appliqué un protocole de programmation photopériodique maternelle pour montrer comment la programmation in utero des petits conduit, une fois ces derniers engagés dans des stratégies métaboliques distinctes, à des caractéristiques sensorielles différentielles des tanycytes. Le troisième objectif est rempli dans l'Article III, via un protocole de manipulation de la photopériode et de la température pour induire l'hibernation, assorti d'un suivi télémétrique affiné de l'état physiologique. Enfin, le quatrième objectif est abordé dans l'Article IV, où le profil transcriptionnel des tanycytes a été étudié à différents états métaboliques avant, pendant et après la saison d'hibernation chez le hamster doré.

Résultats

Article I : Programmation photopériodique maternelle : mélatonine et synchronisation saisonnière avant la naissance

L'Article I est une revue publiée dans « Frontiers in Endocrinology » (doi : 10.3389/fendo.2019.00901). Son objectif était de synthétiser les connaissances actuelles sur le rôle des tanycytes dans le phénomène de programmation photopériodique maternelle (PPM).

En bref, la PPM est un phénomène par lequel, durant la gestation, la descendance est programmée sur le plan métabolique afin d'ajuster son développement postnatal aux conditions environnementales anticipées. Les petits sont programmés pour suivre soit une trajectoire de développement accélérée, soit une trajectoire ralentie, avec un moment de la puberté distinct. Ce phénomène, observé chez certaines espèces de rongeurs vivant dans des habitats où la disponibilité alimentaire et les contraintes thermiques fluctuent saisonnièrement, est supposé favoriser la survie des jeunes et accroître leurs chances de succès reproducteur (Negus, Berger and Forslund, 1977; Negus, Berger and Pinter, 1992; Lee, 1993; Gower, Nagy and Stetson, 1994). Pour que la programmation soit adaptée, l'une des trajectoires doit être initiée au

printemps et en été, périodes favorables où la croissance et la maturation sexuelle s'accélèrent, tandis que l'autre doit être initiée en automne et en hiver, lorsque le coût de la vie est élevé, induisant un ralentissement de la croissance et un report de la maturation sexuelle jusqu'au printemps suivant. L'alignement de ces deux trajectoires sur la saison appropriée requiert une information précise sur la période à venir. Des travaux antérieurs ont montré que l'exposition maternelle aux changements de photopériode se reflète dans le profil de mélatonine. La mélatonine traverse la barrière placentaire et agit sur le cerveau fœtal en développement (voir : (Horton and Stetson, 1992; Horton, 2005)). Comme le fœtus ne synthétise pas sa propre mélatonine mais possède des récepteurs fonctionnels à la mélatonine, la mélatonine maternelle lui sert de fenêtre sur le monde extérieur, indiquant la direction du changement saisonnier. Une étude récente a montré que cette variation de la durée du signal mélatoninergique, via la sécrétion de TSH, programme in utero la couche tanycytaire à engager une trajectoire de développement rapide ou lente (Sáenz de Miera et al., 2017). La programmation qui survient durant la gestation détermine la manière dont les tanycytes, et la descendance, répondront aux changements de photopériode après le sevrage, en modifiant leur sensibilité au signal TSH. La revue résume les éléments indiquant que cette modulation de la sensibilité des tanycytes à la TSH confère une dépendance à l'histoire photopériodique dans le phénomène de PPM.

Article II : Les tanycytes hypothalamiques comme médiateurs de la plasticité saisonnière programmée maternellement

L'Article II est publié dans « Current Biology » (doi : 10.1016/j.cub.2023.12.042) et vise à mieux comprendre comment la PPM des tanycytes modifie leur signature moléculaire après la naissance.

Nous avons cherché à caractériser la signature moléculaire des tanycytes dans un paradigme de PPM. Nous avons utilisé le modèle bien établi du hamster de Sibérie (Phodopus sungorus) et manipulé expérimentalement la photopériode à laquelle les mères étaient exposées durant la gestation : soit une longue photopériode (LP : 16 h de lumière/24 h), soit une courte photopériode (SP : 8 h de lumière/24 h). Les petits sont restés sur la photopériode gestationnelle jusqu'au sevrage (jour postnatal 21). Au sevrage, un sous-groupe de chaque lot a été transféré vers une photopériode intermédiaire (IP : 14 h de lumière/24 h). Ainsi, quatre groupes ont été échantillonnés au jour postnatal 50 : LP, maintenu en LP tout au long de l'expérience ; LPIP,

gesté en LP puis transféré en IP au sevrage ; SPIP, gesté en SP puis transféré en IP au sevrage ; SP, maintenu en SP durant toute l'expérience. Conformément aux travaux antérieurs, nous avons observé que les groupes LP et SPIP suivaient une trajectoire développementale accélérée avec un statut reproducteur actif (augmentation des poids testiculaires), tandis que les groupes SP et LPIP présentaient une trajectoire ralentie avec une activité reproductive interrompue. Chez chaque individu, des cryocoupes hypothalamiques ont servi à réaliser une LCMD de la région tanycytaire vimentine-positive autour du 3V. La spécificité tanycytaire de l'approche LCMD a été confirmée en rapprochant le transcriptome d'un jeu de données de RNAseq unicellulaire avec marqueurs cellulaires connus (Campbell et al., 2017).

Nous avons identifié 6 053 gènes modulés dans les tanycytes en fonction de la photopériode. Plus précisément, les tanycytes d'animaux LP présentaient un enrichissement en gènes liés aux cils par rapport aux animaux SP. Pour tester la traduction au niveau protéique, nous avons recouru à l'immunohistochimie (IHC) ciblant la structure d'ancrage du cil, les corps basaux (γ-tubuline), et leurs projections ciliaires (α-tubuline). Cela a révélé une augmentation des corps basaux et des projections ciliaires chez les animaux LP comparés aux SP. En outre, une augmentation de la photopériode après le sevrage (SPIP) accroissait l'expression de marqueurs de ciliogenèse.

Le cil est une structure cytologique qui sert de plate-forme d'amarrage à de multiples récepteurs, notamment des GPCR et d'autres récepteurs de signalisation, dont le TSH-R (Gerdes, Davis and Katsanis, 2009; Yang, Hong and Kim, 2021). La régulation photopériodique de la ciliation pourrait donc modifier la capacité sensorielle des tanycytes aux signaux de rétrocontrôle métabolique, tels que la TSH. Par ailleurs, des dysfonctionnements ciliaires chez l'humain et la souris entraînent divers phénotypes métaboliques délétères (Badano et al., 2006; Loktev et al., 2013; Lee et al., 2020).

Dans l'ensemble, nos résultats nous ont conduits à proposer un modèle reliant la photopériode in utero et en début de vie à des modifications de la fonction sensorielle des tanycytes, se manifestant par le nombre de cils sensoriels. Ces variations de ciliation pourraient influencer le drive excitateur exercé par les tanycytes sur les régions hypothalamiques régissant la croissance et le développement, conduisant à des phénotypes appropriés à la saison.

Article III : Une méthode affinée pour surveiller le réveil d'hibernation chez le hamster européen
L'Article III est publié dans « BMC Veterinary Research » (doi : 10.1186/s12917-020-02723-7). L'objectif était de mettre en place un paradigme d'hibernation et de développer des outils de suivi.

Étudier l'hibernation requiert de la patience, des vêtements chauds et de bons collègues. L'Article III visait à acquérir l'expérience nécessaire à l'établissement d'un paradigme d'hibernation et des outils de suivi physiologique. Nous avons utilisé le hamster européen (Cricetus cricetus) comme modèle d'hibernation. Pour initier le programme préparatoire à l'hibernation, les hamsters ont été transférés d'une longue photopériode (LP : 14 h de lumière/24 h) à 22 °C vers une courte photopériode (SP : 10 h de lumière/24 h) à 22 °C. Après 8 semaines, la température a été abaissée à 10 °C. Nous avons équipé les animaux pour enregistrer la température corporelle (Tb) avec un enregistreur de température iButton dans la cavité abdominale et une étiquette IPTT (BMDS IPTT-300®) sur le tissu adipeux brun (TBAT) dans la région interscapulaire. Ces deux sites ont été choisis pour augmenter la précision du suivi et détecter les événements précoces d'un réveil naturel lorsque la TBAT commence à s'élever.

Dans les 4 semaines suivant le passage à 10 °C, tous les animaux ont initié un phénotype d'hibernation avec un schéma cyclique : chute de la température centrale à proximité de la température ambiante pendant plusieurs jours (torpeur), puis réchauffement spontané vers l'euthérmie (réveil), un phénomène appelé T-A cycling. Nous avons observé une diminution clé de la Tb avant l'initiation de l'hibernation, qui a servi d'indicateur important utilisé dans l'Article IV.

Après 2 semaines de T-A cycling, nous avons commencé à suivre de près le TBAT lors des réveils de torpeur. Nous montrons que le réchauffement du BAT précède le réchauffement du corps entier de 48,6 minutes (CI : 45,4–51,7 min), tandis que les courbes de température aux deux sites suivent des trajectoires sigmoïdes similaires jusqu'à l'euthérmie. Le début du frisson des muscles de la région du BAT a été noté autour de 15 °C (14,2–16,8 °C). Durant le réveil, la fréquence ventilatoire augmentait et atteignait un pic juste avant le retour à l'euthérmie. En somme, nous montrons comment un enregistrement de température supplémentaire en continu au niveau du BAT classique renseigne sur l'initiation la plus précoce du réveil chez un hibernant.

Une version affinée de cette technique a été appliquée dans une étude distincte non incluse dans cette thèse (Markussen et al., 2024).

Dans le cadre de cette thèse, l'Article III a permis d'acquérir les compétences et outils nécessaires pour étudier les tanycytes pendant l'hibernation.

Article IV : Modification de l'utilisation des substrats énergétiques et de la capacité sensorielle des tanycytes au cours de la saison d'hibernation chez le hamster doré
L'Article IV est un manuscrit accepté dans le « Canadian Journal of Zoology », consacré à la description des changements transcriptionnels des tanycytes au fil de la saison d'hibernation chez le hamster doré.

Nous avons cherché à caractériser les tanycytes par LCMD RNAseq dans un modèle d'hibernation saisonnière chez l'adulte. Bien que l'Article III ait mobilisé le hamster européen, nous avons choisi le hamster doré (Mesocricetus auratus) pour cette expérience, car il est aisément disponible auprès d'un fournisseur agréé, hautement photopériodique et présente un phénotype d'hibernation robuste, avec une progression clairement définie : préparation à l'hibernation régulée photopériodiquement puis fin spontanée de l'hibernation (réfractaire).

Pour initier l'hibernation, les hamsters dorés ont été transférés d'une longue photopériode (LP : 14 h de lumière/24 h) à 22 °C vers une courte photopériode (SP : 10 h de lumière/24 h) à 8 °C. Cela déclenche l'arrêt de l'axe reproducteur, l'abaissement du point de consigne de Tb et l'augmentation du BAT, autant d'événements préparatoires clés avant l'initiation de l'hibernation (Lyman et al., 1982; Markussen et al., 2024), réponse photopériodique dans laquelle les tanycytes sont impliqués (Milesi, Simonneaux and Klosen, 2017). Après 8–12 semaines en SP à 8 °C, les hamsters initient le T-A cycling, caractérisé par des épisodes de torpeur de plusieurs jours avec une Tb s'approchant de la Ta, interrompus par un rapide retour spontané à des températures euthermiques (IBE). Les tanycytes ont été proposés comme jouant un rôle encore non élucidé dans la régulation du TA-cycle (Bratincsák et al., 2007; Markussen et al., 2024). Ce schéma cyclique se poursuit jusqu'à environ 20 semaines en SP, moment où, sans changement de facteurs externes, les hamsters cessent brusquement le T-A cycling, demeurent euthermiques et recommencent à accroître la taille de leurs testicules (réfractaire). Comme dans l'Article II, nous avons prélevé des cerveaux pour LCMD et réalisé un RNAseq, mais en

définissant cette fois nos points de temps à l'aide d'enregistrements télémétriques de Tb afin de capter la phase pré-hibernation, l'IBE, la torpeur et l'installation de l'état réfractaire.

Nos résultats montrent qu'avant l'hibernation et pendant celle-ci, la signature d'expression génique évoque un état catabolique avec dégradation du glycogène et augmentation de la glycolyse. Durant la torpeur, nous avons observé un enrichissement des voies liées à l'hypoxie et à l'épissage de l'ARN, tandis que les tanycytes en IBE présentaient une augmentation de gènes impliqués dans la répression génique et la dégradation protéique. Les tanycytes des groupes réfractaire et LP, tous deux reproductivement actifs (poids testiculaires augmentés), montraient une augmentation de gènes liés à la liaison des ligands des GPCR et à la ciliation. Collectivement, nos résultats suggèrent une modification de l'utilisation des substrats énergétiques et de la capacité sensorielle des tanycytes en réponse à la manipulation photopériodique.

Ces résultats font écho à ceux de l'Article II, où l'exposition gestationnelle et précoce à la LP chez des hamsters de Sibérie juvéniles augmentait l'expression des gènes ciliaires et le nombre de cils présents sur les tanycytes (Melum et al., 2024). Pris ensemble, l'Article IV et l'Article II suggèrent que l'augmentation de l'expression des gènes ciliaires dans la couche tanycytaire pourrait constituer une adaptation saisonnière générale visant à accroître la sensibilité aux signaux de rétrocontrôle métabolique, tels que la TSH, et à amorcer un programme de printemps/été.

Conclusion

En mobilisant deux espèces de rongeurs saisonniers, le hamster de Sibérie et le hamster doré, cette thèse suggère que l'état hivernal des deux espèces se caractérise par une diminution de l'expression des gènes ciliaires et, partant, une sensibilité réduite des tanycytes aux signaux présents dans le CSF, immergeant leur surface apicale. La thèse n'apporte pas de preuve définitive quant aux signaux en cause, mais il est probable qu'une sensibilité modifiée à la TSH joue un rôle clé. Un modèle des diverses réponses cellulaires sous-tendant cette réduction de la capacité sensorielle est proposé. Un tel modèle place les tanycytes — et le remodelage de leur sensibilité aux signaux de rétrocontrôle métabolique — au cœur du point de consigne rhéostatique du métabolisme énergétique chez les espèces de rongeurs saisonniers.

“It`s called precision of thought and economy of expression. Know what your message is, know your audience, and say it in as few words as possible.”

Anthony Fauci, in interview with Jon Cohen (Cohen, 2022)

Table of Contents

List of tables

List of Figures

Acknowledgements

Winter solstice, the shortest day of the year. As the sun dims to its minimum in the southern horizon, these words are typed, their meaning frozen in time.

First and foremost, I would like to thank my supervisors, who have provided me with support and guidance beyond what I could have hoped for. I have enjoyed our stimulating scientific discussions, which have deepened my understanding for the scientific process, and enhanced the development of this final product. Specifically, I would like to thank my main supervisor Shona H. Wood for the trust and the many opportunities granted during this PhD. I am grateful for your tremendous support, guidance and patience. Most importantly your genuinely curiosity and dedication to science are truly inspiring. I would thank my co-supervisor David G. Hazlerigg for eye-opening questions and your insistence of understanding all aspects of our work. I would thank my co-supervisor Valérie Simonneaux for the opportunity to get a French perspective on neuroendocrinology, and for sharing your expertise with me. The welcome and inclusion I received in Strasbourg was unparalleled.

Further, I would like to thank all the members of Team Simonneaux for inspiring discussions, help navigating the labs and society in general and the good lunches. Especially thanks to Béatrice and Marie-Azélie for our collaboration, and Clarisse for invaluable assistance with the hamsters.

Further, I would like to thank all the members of Arctic Chronobiology and Physiology, past and present, for enabling to work in such a unique location, and for the comparative nature of our research group. I am grateful to work alongside so many brilliant scientists that willingly share and contribute their knowledge and skills. Special thanks to Blix for insightful talks and perspectives. I am especially grateful to Team hamster: Sandra, Fernando and Fredrik, for our collaboration and your continuation of the fascinating work on hibernation.

Fredrik, I am eternally grateful for our friendship, from long hours in the cold monitoring hibernating hamsters to tanycyte discussions over coffee, to our days in the mountains. I hope the future has more in store.

To the friends and family who have been there when it mattered most, thank you.

Sanne og Vilja, tusen takk for de dere er og det vi har sammen. Vilja, hverdag minner du meg på å være tilstede i øyeblikket, og jeg setter umåtelig stor pris på vår felles undring og nysgjerrighet for de minste ting. Sanne, takk for alt du gjør for oss, nå går det mot lysere tider.

Thesis abstract

The geophysical properties of the earth result in yearly changes in solar irradiance driving seasonal fluctuations in temperature and food availability. This necessitates non-equatorial species to partition energy demanding processes to favourable times of the year. Temporal gating of physiology requires both a readjustment of homeostatic processes (rheostasis), and the ability to keep track of seasonal time. Mammalian species primarily use changes in photoperiod (day length) to allow anticipation of forthcoming seasonal opportunities and demands. Photoperiod is internally represented by nocturnal melatonin secretion, and via the pars tuberalis and the tanycytes of the 3rd ventricle of the hypothalamus, this results in seasonal metabolic adaptations. Hence, the overarching objective of this thesis was to elucidate the molecular signature of tanycytes in two seasonal paradigms that shift metabolism; maternal photoperiodic programming (Siberian hamster, *Phodopus Sungorus*) and hibernation (golden hamster, *Mesocricetus auratus*).

In **Paper I,** we review the neuroendocrine processes involved in maternal photoperiodic programming (MPP). Here, photoperiod is relayed to small rodents during gestation, via the maternal melatonin signal, programming the tanycytes of the hypothalamus, resulting in distinct after-birth metabolic trajectories, matching the pup to the seasonal environment. In **Paper II**, a MPP experiment using Siberian hamsters characterized the molecular signature of the tanycyte layer. Revealing differences in the expression of cilia-related genes and numbers of cilia present in the tanycyte layer related to the photoperiodic history and subsequent metabolic trajectory. In **Paper III**, we developed and refined methods to study hibernation. Finally, in **Paper IV**, we characterized the tanycyte layer of adult golden hamsters in response to changes in photoperiod, during hibernation and in the spontaneous emergence from hibernation (refractory state). Here, we also observed a change in cilia-related genes in response to photoperiod and the refractory state.

Collectively, the findings presented in this thesis suggest that changes in cilia-related genes and numbers of cilia on tanycytes and, therefore presumably alterations in metabolite signalling via tanycytes, may be a rheostatic mechanism altering metabolic feedback to the hypothalamus allowing an animal to match their metabolic physiology to the environment.

Résumé de these

Les propriétés géophysiques de la Terre entraînent des changements annuels dans l'irradiation solaire, entraînant des fluctuations saisonnières de la température et de la disponibilité alimentaire. Cela nécessite que les espèces non équatoriales répartissent les processus exigeants en énergie vers des périodes favorables de l'année. La régulation temporelle des fonctions physiologiques nécessite à la fois un réajustement des processus homéostatiques (rhéostasie) et la capacité de suivre les saisons. Les espèces de mammifères utilisent principalement les changements de photopériode (durée du jour) pour permettre d'anticiper les opportunités et demandes saisonnières à venir. La photopériode est représentée en interne par la sécrétion nocturne de mélatonine qui, via la pars tuberalis et les tanycytes du 3ème ventricule de l'hypothalamus, contrôle les adaptations métaboliques saisonnières. Dans ce contexte, l'objectif principal de cette thèse était d'élucider la signature moléculaire des tanycytes dans deux paradigmes saisonniers qui modifient le métabolisme ; la programmation photopériodique maternelle (chez le hamster sibérien, *Phodopus sungorus*) et l'hibernation (chez le hamster doré, *Mesocricetus auratus*).

Dans **l'article I,** nous passons en revue les processus neuroendocriniens impliqués dans la programmation photopériodique maternelle (PPM). Ici, la photopériode est transmise aux petits rongeurs pendant la gestation, via le signal maternel de mélatonine qui programme les tanycytes de l'hypothalamus. Ceci entraîne des trajectoires métaboliques de la descendance adaptées à l'environnement saisonnier. Dans **l'article II**, une expérience PPM réalisée chez des hamsters de Sibérie a caractérisé la signature moléculaire de la couche de tanycytes, révélant des différences dans l'expression de gènes liés aux cils et dans le nombre de cils présents dans les tanycytes en fonction de l'histoire photopériodique durant la gestation et de la trajectoire métabolique ultérieure. Dans **l'article III**, nous avons développé et affiné des méthodes pour étudier l'hibernation. Enfin, dans **l'article IV**, nous avons caractérisé la couche tanycytaire de hamsters dorés adultes en réponse aux changements de photopériode, pendant l'hibernation et lors de la sortie spontanée de l'hibernation (état réfractaire). Ici, nous avons également observé une modification des gènes liés aux cils en réponse à la photopériode et à l'état réfractaire.

Collectivement, les résultats présentés dans cette thèse suggèrent que les changements dans l'expression des gènes liés aux cils et dans le nombre de cils sur les tanycytes pourraient, via des altérations dans la signalisation des métabolites, être un mécanisme rhéostatique altérant la régulation métabolique vers l'hypothalamus, permettant à un animal d'adapter sa physiologie métabolique à l'environnement.

Avhandlingens sammendrag

I tempererte og polare områder er det store årlige variasjoner i temperatur og mattilgang, som medfører at arter må gjennomføre energikrevende prosesser på fordelaktige tider av året. Sesongmessig tilpasning av fysiologi krever både homeostatisk rejustering (reostase), og en indre kalender. Pattedyr bruker primært endringer i daglengde for å forutse og forberede seg på den kommende årstiden. Daglengden gjenspeiles i kroppen av nattlig utskillelse av melatonin, som via pars tuberalis og tanycytter i hypothalamus, resulterer i sesongmessige metabolske tilpasninger. Derfor er denne avhandlingens overordnede mål å beskrive den molekylære signaturen til tanycyttene gjennom to sesongmessige paradigmer som drastisk endrer metabolisme: daglengdeprogrammert vekst og utvikling (Sibirsk dverghamster, *Phodopus Sungorus*) og dvale (gullhamster, *Mesocricetus auratus*).

Først oppsummerte vi hva som allerede var kjent om hvordan Sibirsk dverghamster under svangerskapet bruker melatonin til å programmere fosteret sin vekst og utvikling etter fødselen, noe som resulterer i unger med en hurtig utvikling på sommeren og en sakte utvikling på vinteren. Det ble tydelig at tanycyttene er helt sentrale i å sikre et samsvar mellom utviklingsstrategi og årstid (**Artikkel I)**. Derfor gen-sekvenserte vi tanycyttene hos Sibirske dverghamstere som både under svangerskapet og tidlig i livet var utsatt for ulike daglengder. Vi avdekket endringer i både gener relatert til cellehårenes funksjon og antall cellehår, som sammenfalt med de to ulike utviklingsstrategiene (**Artikkel II**). **Artikkel III** videreutviklet metodikk for dvaleforskning ved å studere Europeisk hamster (*Cricetus cricetus*). Til slutt, i **Artikkel IV** beskrev vi hvordan tanycytter hos voksne gullhamstere endrer seg med daglengde, dvaleperioden og når de forlater hiet for å reprodusere. Også her ser vi endringer i gener som styrer cellehårenes funksjon og oppbygning.

Sett under ett, kan funnene i denne avhandlingen tyde på at en reduksjon i antall cellehår og deres funksjon hos tanycytter er en generell tilpasning hos hamstere for å sette kroppen på sparebluss om vinteren, og dermed sikre et samsvar mellom energiforbruk og energitilgang.

Lay person summary of the thesis

As an inhabitant of the sub-arctic, the seasonal changes in daylight and temperature are particularly evident to me. The yearly celebration of the first arriving oystercatcher, the greening of the landscape within a matter of days and the magnificent thrills of the bluethroat are all events marking progression of the seasons. Therefore, perhaps it is not surprising that I wanted to better understand the cellular timing mechanism underpinning these seasonal wonders. Because in Nature, timing is everything. The more extreme environment an animal inhabits, the less margin for error. Throughout this thesis I examine how changes in the function of a specialised brain cell known as the tanycyte, controls the timing of seasonal changes in reproduction, body temperature and feeding. To achieve this, I have used two species of hamsters, that both utilize a metabolic depression strategy to survive the winter.

As a preliminary step, we compiled the existing literature on tanycytes involvement in maternal photoperiod programming. This is a phenomenon where Siberian hamster (*Phodopus sungorus*) dams relay the daylength, via melatonin, to their pups during gestation. The melatonin duration the pups receives programs their development to match the thermal demands and nutrient availability of the environment. Manifested as a fast growth rate and early pubertal onset in pups born under long summer days, and a slow growth rate and delayed pubertal onset until next spring in winter born pups. The summary of the current knowledge resulted in a mini-review putting tanycytes and their altered sensitivity to metabolic feedback signals at the forefront of the phenomenon (**Paper I**). Therefore, in **Paper II** we RNA profiled the tanycyte-layer of Siberian hamsters being exposed to various daylengths during gestation and development, revealing differences in the expression of cilia-related genes and numbers in relation to metabolic trajectory. The second metabolic depression strategy we studied was hibernation, a seasonally prepared state allowing the expression of torpor and a reduction of energy usage up to 88 %. **Paper III** laid the ground work and tools to study the physiology of hibernation and **Paper IV** profiled the tanycytes throughout this seasonal phenomenon. In contrast to **Paper II**, **Paper IV** used adult golden hamsters (*Mesocricetus auratus*) but also showed a decrease in the expression of cilia-related genes in winter adapted hamsters.

Cilia are a sensory “antenna” of the cell, therefore changes in cilia may change how winter-adapted animals sense the energy status of their bodies. Further work is required to test this hypothesis, but this thesis has highlighted that these two seasonally regulated paradigms show similar changes in tanycyte cilia-related gene expression and that this may be a general adaptation contributing to winter survival.

Populærvitenskapelig sammendrag

Naturens vinterstillhet forvandler seg på få uker til et yrende liv med intense lyder og lukter. Før skogen stilner av igjen, når kurtise skifter til yngelpleie. Sommeren går, de små blir store og plutselig blir det mørkt på kvelden. En dag ligger det en hinne av tynn is på vannet og bladene begynner å skifte farge. Bare de mest hardføre velger å bli, de andre setter kursen sørover, eller går i hi under bakken. I naturen er rett handling til rett tid helt avgjørende. For dyr som lever på livets yttergrense, er det lite rom for feil. Derfor har dyr og fugler over tid utviklet både en indre klokke og en indre kalender for å sikre rett handling til rett tid av døgnet og året. I denne doktorgraden ser jeg nærmere på hvordan sensorceller i hjernen kalt tanycytter, bidrar til sesongmessige endringer i kroppstemperatur, reproduksjon og matinntak. Nærmere bestemt har jeg brukt to hamsterarter som begge er avhengig av å sette kroppen på sparebluss for å overleve vinteren.

I naturen ser man hos visse smågnagere at unger født på våren vokser fort og kommer tidlig i puberteten, mens unger født på høsten vokser sakte og utsetter puberteten til neste vår. Hos Sibirsk dverghamster (*Phodopus sungorus*) er det vist at endringer i morens nattlige utskillelse av melatonin forteller fosteret om det går mot sommer eller vinter. Avkommet blir altså født med en funksjonell kalender, og en programmert utviklingsstrategi som samsvarer med mattilgang og temperaturen i miljøet. I **Artikkel I** oppsummerte vi tanycyttenes rolle i en slik kalenderstyrt utvikling, og det ble tydelig at disse sensorcellene, og deres endrede evne til å motta metabolske signaler, står helt sentralt i dette fenomenet. Derfor ville vi forstå hvordan tanycyttene bidrar til en slik kalenderstyrt utvikling (**Artikkel II**). Vi avdekket endringer i gener relatert til cellehår og antall cellehår hos tanycyttene, som sammenfalt med de to ulike utviklingsstrategiene. Dvale er en annen måte hamstere setter kroppen på sparebluss. Denne vinteroverlevelsesstrategien innebærer perioder med en drastisk reduksjon i metabolsk aktivitet og en kroppstemperatur helt ned til 0 °C, noe som kan redusere energibehovet med så mye som 88 %. **Artikkel III** la grunnlaget for å studere dvalefysiologi, og i **Artikkel IV** gen-sekvenserte vi tanycyttene på ulike tidspunkter av dvaleperioden. I motsetning til **Artikkel II** brukte vi i **Artikkel IV** voksne gullhamstere (*Mesocricetus auratus*), men også her er det en reduksjon i gener relatert til cellehårets oppbygning og funksjon hos hamstere som har tilpasset seg vinteren.

Cellehår, også kjent som cilier, fungerer altså som en antenne for metabolske signaler, som for eksempel sukker. Derfor kan en reduksjon i antall cellehår hos sensorceller i hjernen være med å endre hvordan hamstere oppfatter sin egen energistatus. En slik hypotese må testes grundigere, men denne avhandlingen viser at hos to ulike hamsterarter med kroppen på sparebluss finner vi en reduksjon i gener relatert til cellehårets oppbygning og funksjon, noe som kan tyde på en generell tilpasning for å overleve vinteren.

List of papers

Paper I

Maternal Photoperiodic Programming: Melatonin and Seasonal Synchronization Before Birth

Jayme van Dalum[+], Vebjørn J. Melum[+], Shona H. Wood, David G. Hazlerigg

Department of Arctic and Marine Biology, UiT – The Arctic University of Norway, Tromsø, Norway

[+] Joint first authors listed alphabetically

Frontiers in Endocrinology 2020: 10:901: doi: 10.3389/fendo.2019.00901

Published 10. January 2020

Paper II

Hypothalamic tanycytes as mediators of maternally programmed seasonal plasticity

Vebjørn. J. Melum[1], Cristina Sáenz de Miera[2], Fredrik A.F. Markussen[1], Fernando Cázarez-Márquez[1], Catherine Jaeger[4], Simen R. Sandve[3], Valérie Simonneaux[4], David G. Hazlerigg[1], Shona H. Wood[1]

1 UiT — The Arctic University of Norway, Department of Arctic and Marine Biology, Arctic Chronobiology and Physiology research group, Tromsø, Norway

2 University of Michigan Medical School, Department of Molecular and Integrative Physiology, Ann Arbor, Michigan, United States of America

3 Section of Biology, Department of Animal and Aquacultural Sciences (IHA), Faculty of Life Sciences (BIOVIT), Norwegian University of Life Sciences (NMBU), Ås, Norway

4 University of Strasbourg, Institute of Cellular and Integrative Neurosciences, Strasbourg, France

Current Biology 2024: Feb 5;34(3):632-640.e6: doi: 10.1016/j.cub.2023.12.042

Published 04 February 2024

Paper III

A refined method to monitor arousal from hibernation in the European hamster

Fredrik A.F. Markussen[1†], Vebjørn. J. Melum[1†], Béatrice Bothorel[2], David G. Hazlerigg[1], Valérie Simonneaux[2] and Shona H. Wood[1]

1 UiT — The Arctic University of Norway, Department of Arctic and Marine Biology, Arctic Chronobiology and Physiology research group, Tromsø, Norway

2 University of Strasbourg, Institute of Cellular and Integrative Neurosciences, Strasbourg, France

† Joint first authors listed alphabetically.

BMC Veterinary Research: **17**, 14 (2021): doi: 10.1186/s12917-020-02723-7

Published 7th of January 2021

Paper IV

Altered fuel utilisation and sensory capacity in tanycytes throughout the hibernation season in the golden hamster

Vebjørn. J. Melum[1,2], Béatrice Bothorel[2], Marie-Azélie Moralia[2], Valérie Simonneaux[2], David G. Hazlerigg[1], Shona H. Wood[1]

1 UiT — The Arctic University of Norway, Department of Arctic and Marine Biology, Arctic Chronobiology and Physiology research group, Tromsø, Norway

2 University of Strasbourg, Institute of Cellular and Integrative Neurosciences, Strasbourg, France

Accepted manuscript in the Canadian Journal of Zoology

Author contributions

	Paper I	**Paper II**	**Paper III**	**Paper IV**
Concept and idea	VJM, JvD, SHW, DGH	SHW, DGH, VS, CSdM	SHW, DGH, VS	VJM, SHW, DGH, VS
Study design and methods	n/a	SHW, DGH, VS, CSdM, VJM	VJM, FM, SHW, BB, DGH, VS	VJM, SHW, DGH, VS, BB
Data gathering	n/a	VJM, CSdM, CJ, SHW, FM, FC	VJM, FM, BB	VJM, VS, BB, MAM
Data analysis	n/a	VJM, SHW, FM, FC, SRS	VJM, FM	VJM, SHW
Manuscript preparation	VJM, JvD	SHW, DGH, VJM	SHW, VJM, FM	VJM, SHW
Manuscript revision	VJM, JvD, SHW, DGH	SHW, DGH, VS, CSdM, VJM, FM, FC, SRS, CJ	VJM, FM, SHW, DGH, VS, BB	VJM, MAM, BB, SHW, DGH, VS

BB = Béatrice Bothorel

CJ = Catherine Jaeger

CSdM = Cristina Sáenz de Miera

DGH = David G. Hazlerigg

JvD = Jayme Van Dalum

FM = Fredrik Markussen

FC = Fernando Cázarez-Márquez

MAM = Marie-Azélie Moralia

SRS = Simen R. Sandve

SHW = Shona H. Wood

VJM = Vebjørn J. Melum

VS = Valérie Simonneaux

Abbreviations

3V – 3rd ventricle
α – Alpha
AgRP - Agouti-related peptide
Aldh1a1 – Gene, aldehyde dehydrogenase 1 family member A1
ALDH1A1 – Protein, aldehyde dehydrogenase 1 family member A1
ATP – Adenosine Triphosphate
ARC – Arcuate nucleus
β - Beta
BAT – Brown adipose tissue
BBB - blood-brain barrier
BrdU - bromodeoxyuridine
Ca^{2+} - Calcium
CALHM1 – Protein, calcium homeostasis modulator 1
CART - Cocaine- and amphetamine-regulated transcript
Ccrl2 – Gene, C-C motif chemokine receptor-like 2
CSF – Cerebrospinal fluid
CSF-BB - Cerebrospinal fluid - blood-barrier
CX43/GJA1 – Protein, connexin-43/ Gap junction protein alpha 1
Cyp26a1 – Gene, cytochrome P450 family 26 subfamily A member 1
CYP26A1 – Protein, cytochrome P450 family 26 subfamily A member 1
CVO - Circumventricular organ
Dio2 – Gene, type II iodothyronine deiodinase
DIO2 – Protein, type II iodothyronine deiodinase
Dio3 – Gene, type III iodothyronine deiodinase
DIO3 – Protein, type III iodothyronine deiodinase
DMH – Dorso-medial hypothalamus
ERα – Protein, oestrogen receptor 1 alpha
FGF - Fibroblast growth factor
G6P - Protein, glucose-6-phosphate
G6PT – Protein, glucose-6-phosphate transporter
G6PT3 – Protein, glucose-6-phosphate complex 3
GABA - Gamma-aminobutyric acid
Gabbr1 – Gene, gamma-aminobutyric acid type B receptor subunit 1
GnRH - gonadotropin-releasing hormone
GRM4 / MGLUR4 – Protein, Glutamate Metabotropic Receptor 4 / Metabotropic glutamate receptor 4
GPCR - G-protein coupled receptor
Gpr50 – Gene, G-protein coupled receptor 50
GPR50 – Protein, G-protein coupled receptor 50
IBE – Inter-bout euthermic
ICV – Intracerebroventricular
IHC – Immune-histochemistry
IP – Intermediate photoperiod
IP3 - Inositol trisphosphate
Ki67 – Protein, antigen identified by monoclonal antibody Ki 67
LCMD – LASER capture microdissection
Ldha – Gene, lactate dehydrogenase A
LDHA – Protein, lactate dehydrogenase A
LP – Long photoperiod
Lepr – Gene, leptin receptor
LEP-R / Ob-R – Protein, leptin receptor

LH - Luteinizing hormone
MBH – Medio-basal hypothalamus
ME – Median eminence
MPP – Maternal Photoperiodic Programming
MT1 – Protein, melatonin receptor 1
Nfia/b/x – Gene, nuclear factor one family transcription factors
NPY – Neuropeptide Y
POMC - Pro-opiomelanocortin
P2RY1 – Protein, P2Y purinoceptor 1
PANX1 – Protein, pannexin 1
PCNA – Protein, proliferating cell nuclear antigen
Pdk2 – Gene, pyruvate dehydrogenase kinase 2
Pre-hib – Pre-hibernation
STAT3 – Protein, signal transducer and activator of transcription 3
PT – Pars tuberalis
PVN - Paraventricular nucleus
RA – Retinoic acid
RAR – Protein, retinoic acid receptor
Rarres2 – Gene, retinoic acid receptor responder 2
RAX – Protein, retina and anterior neural fold homeobox
RBP2 / CRABP2 – Protein, cellular retinoic acid-binding protein 2 / retinol binding protein 2
RBP4 / CRBP4 – Protein, retinol binding protein 4 /cellular retinol binding protein 4
RDH – Proteins, retinol dehydrogenases
REH – Protein, Retinol ester hydrolyse
RFamide - Arginine-phenylalanine-amide
RFRP – Protein, RFamide-related peptide
RNA - Ribonucleic acid
RXR – Protein, retionid X receptor
SCN - Supra chiasmatic nucleus
SLCO1C1 / OATP1C1 – Protein, solute carrier organic anion transporter family member 1C1 / Organic anion-transporting polypeptide 1c1
Slc2a1 / *Glut1* – Gene, solute carrier family 2 member 1 / Glucose transporter 1
SLC2A1 / GLUT1 – Protein, solute carrier family 2 member 1 / Glucose transporter 1
Slc2a2 / *Glut2* – Gene, solute carrier family 2 member 2 / Glucose transporter 2
SLC2A2 / GLUT2 – Protein, solute carrier family 2 member 2 / Glucose transporter 2
Slc2a3 / *Glut3* – Gene, solute carrier family 2 member 3 / Glucose transporter 3
SLC2A3 / GLUT3 – Protein, solute carrier family 2 member 3 / Glucose transporter 3
Slc2a4/*Glut4* – Gene, solute carrier family 2 member 4 / Glucose transporter 4
SLC2A4 / GLUT4 – Protein, solute carrier family 2 member 4 / Glucose transporter 4
SLC16A1 / MCT1 – Protein, solute carrier family 16 member 1 / Monocarboxylate transporter 1
SLC16A2 / MCT8 – Protein, solute carrier family 16 member 2/ Monocarboxylate transporter 8
SLC16A3 / MCT4 – Protein, solute carrier family 16 member 3 / Monocarboxylate transporter 4
Slc16a10 / Mct10 – Gene, solute carrier family 16 member 10 / Monocarboxylate transporter 10
SLC16A10 / MCT10 – Protein, solute carrier family 16 member 10 / Monocarboxylate transporter 10
SP – Short photoperiod
T3 - Triiodothyronine
T4 – Thyroxine
T-A – Torpor-arousal
TAS1R2 – Protein, taste receptor type 1 member 2
TAS1R3 – Protein, taste receptor type 1 member 3
T_a- Ambient temperature
T_b – Core body temperature
TCA - Tricarboxylic acid

TDN – Tanycyte derived neuron
TH – Thyroid hormone
TRE - Thyroid hormone response elements
TSH – Thyroid stimulating hormone
Tshr – Gene, thyroid stimulating hormone receptor
TSH-R – Protein, thyroid stimulating hormone receptor
VEGF-A – Protein, vascular endothelial growth factor A
VMH – Ventro-medial hypothalamus
YFP - Yellow fluorescent protein

1 Introduction

1.1 Managing the seasonal energy budget

The geophysical properties of the Earth give rise to daily and seasonal cycles in solar irradiance and temperature (Figure 1). The Earth use 24 hours to complete one rotation around its own axis, creating daily changes in solar irradiance and temperature, experienced as day and night. The axis of the Earth has a tilt of 23°, to the orbital plane, resulting in a predictable alteration in day length (photoperiod) across the year at a specific latitude as the Earth orbits the Sun (Figure 1). These yearly changes in solar energy influx create profound seasonal changes in food availability and ambient temperature (T_a) at temperate and polar regions. If one reduces the interaction between an animal and the environment to flux of energy, it is evident how altered T_a and photoperiod, influence two key aspects of animal physiology, namely the cost of thermoregulation, important for mammals, and food availability, which again dictates food intake and the cost of locomotion to search for food (Bronson, 1988). This energetic view provides an eco-evolutionary framework for why animals organize their life-history to fit with the energy availability in their environment (Bronson, 1989).

We can use this framework to consider small rodents living in the tropics, a region with minimal changes in photoperiod throughout the year and with a stable T_a, therefore with minimal predictable changes in food availability (Figure 1). Such an environment would favour mammals that are able to reproduce year-round once an energy threshold is reached. This strategy is termed “opportunism” and would be beneficial in an unpredictable environment with a low thermal constraint (Figure 2) (Bronson, 1988). However, as we move away from the tropics and latitude increases, seasonal changes in photoperiod and T_a are more extreme (Figure 1), and the need for accurately timed physiological adaptions to conserve energy are more obvious (Bronson, 1989). Living in a strongly seasonal environment would mean an evolutionary advantage may be gained if the animal could predict the future energy availability and align their energetic needs/physiology to match the energy availability. Bronson called this the “predictor option”, which enables an animals life-history to be accurately timed to match the forthcoming environmental conditions, for example only breeding at certain favourable parts of the year (Bronson, 1988).

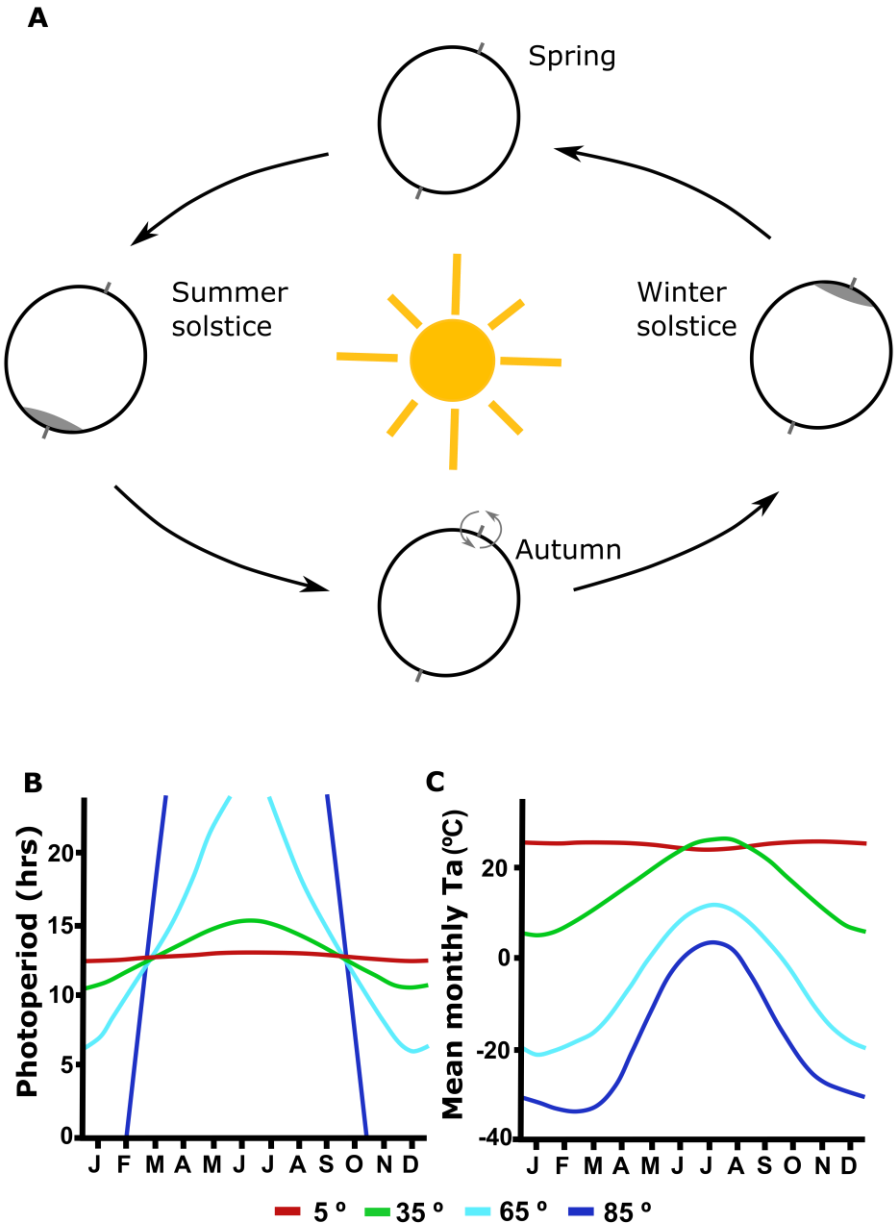

Figure 1 Earth, with its tilt and orbit around the Sun creates daily and seasonal fluctuations in solar irradiance and temperature presenting challenges for species inhabiting non-equatorial regions. The Earth spins around its own axis with one rotation lasting 24 hours, creating changes in solar irradiance (light) on a given spatial point. These 24-hour changes in light are for most of the Earth creating a daily variation between sunlight (day) and the absence of light (night). A) However, due to the elliptical orbit of Earth around the Sun with a passage time of one year, and the axial tilt of 23º, these 24-hour changes in solar irradiance are for non-equatorial regions depending on the orbital phase of the Earth. B) In regions around equator the length of the day and night remains the same throughout the year, while as latitude increase a drastic yearly change in photoperiod is observed. C) Latitudinal mean monthly ambient temperature (T_a) shows the profound relationship between time of year, photoperiod and T_a. Data presented in B and C are for the northern hemisphere. The southern hemisphere would show an opposite time of year for maxima and minima photoperiod and T_a. These geophysical properties of the Earth make predictable yearly changes in solar irradiance, and gives rise to the seasons in non-equatorial regions. Illustration by V.J. Melum. Based on (Hut *et al.*, 2013).

The seasonal regression/activation of the reproductive system is one adaptation to budget energy appropriately across the year, enabling survival. The seasonal regression/activation of reproduction is more plastic at lower latitudes, and becomes increasingly constrained at higher latitudes (Figure 2) (Bronson, 1989; Hazlerigg *et al.*, 2023) . Therefore, temperate species show an increase in the plasticity of the reproductive season compared to polar species.

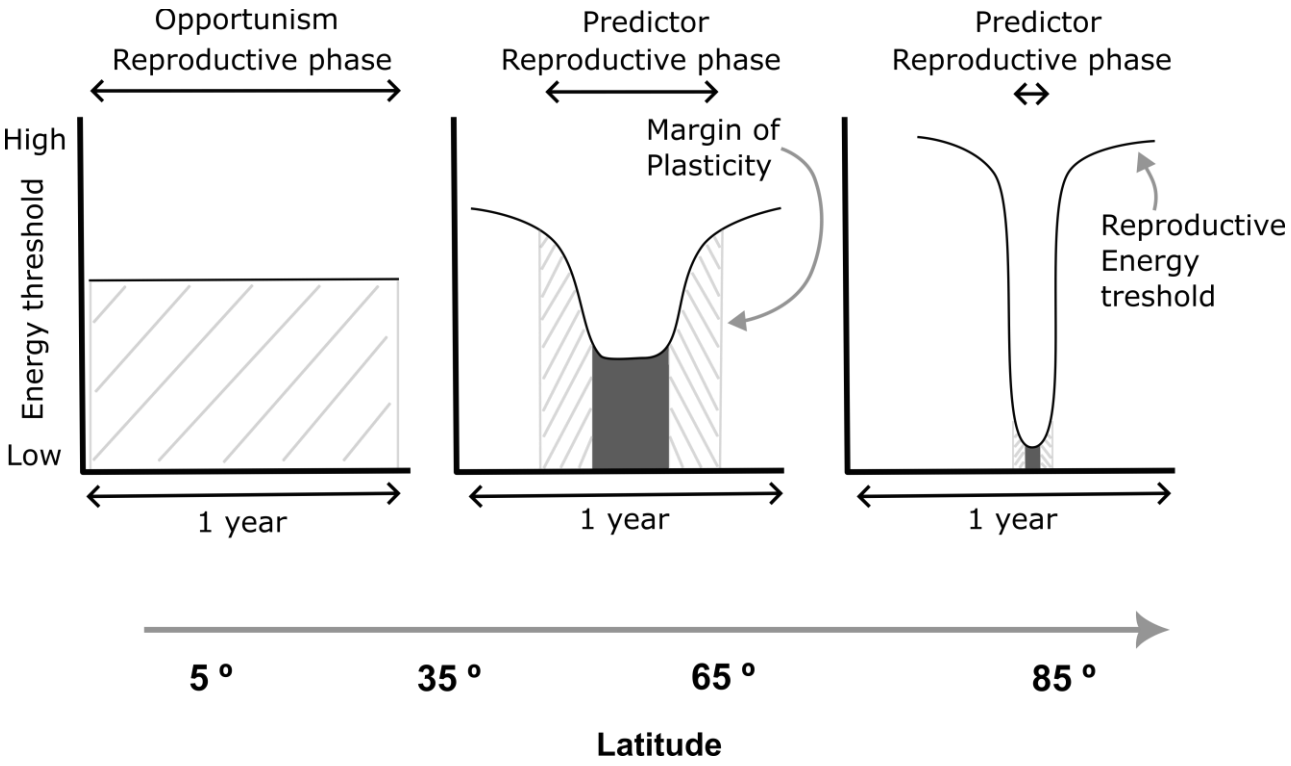

Figure 2 Schematic illustrating opportunism and the predictor option. In mammalian species inhabiting equatorial regions with minimal fluctuations in temperature, their reproductive phase spans the entire year, and only energy availability dictates the reproductive on-set (left). Hence the energy threshold for reproduction is static throughout the year, making these species able to breed whenever the energy supply passes this threshold. Such a reproductive strategy is termed "opportunism", since these species are able to use sudden increases in food availability as an opportunity to breed. In species inhabiting temperate zones, there is a shift from being purely opportunistic, to being relying more on a predictor option. Meaning they confine their reproductive phase to certain parts of the year, when the energy availability and costs are compatible with reproduction (middle). These species show substantial plasticity in their on- and off-set of the reproductive phase depending on environmental conditions. Such a seasonal gating of the reproductive phase requires an environmental cue to aid the animal to predict/anticipate forthcoming seasons. In species inhabiting polar regions, the temporal organization of reproduction is confined to a narrow part of the year, with limited possibilities for utilizing spontaneous available energy opportunities for reproductive purposes (right). Together, these three models for regulation of the reproductive phase illustrate that mammalian species inhabiting regions with seasonal changes in food and temperature display an increased prevalence of a predictor rather than opportunistic breeding strategy. Hatched area indicates the temporal plasticity of reproduction. Illustration by V.J. Melum. Based on (Hazlerigg *et al.*, 2023).

While Bronson primarily focused on the reproductive system there are a range of seasonal physiological adaptations small rodents can use to conserve energy and avoid predation in winter; these include thicker and sometimes different colour pelage, increased fat stores, increased food stores, changes in growth, and metabolic depression strategies (discussed in **1.3** overwintering strategies of small rodents). These physiological and behavioural adaptations are all processes that take time to achieve, and if they were initiated as a passive reactive response to immediate environmental cues, it would be both too risky and too late. Therefore, animals have evolved a "predictor" in the form of an innate biological clock, which can use photoperiod as the primary timekeeping cue and allow the animal to anticipate the forthcoming seasonal energetic constraints. In the next section I will discuss the formal properties of seasonal timekeeping (**1.2**) and then discuss the energetic challenges faced by small rodents in seasonal environments and specifically two overwintering strategies; maternal photoperiodic programming and metabolic depression (**1.3.1** & **1.3.2**).

1.2 Timing of seasonal life histories: photoperiodism & circannual programs

The field of chronobiology focuses on the nature of innate biological clocks and how these synchronise physiological adaptations to the daily and seasonal environment. Daily rhythms of behaviour or physiology can be termed diel (meaning day), if these rhythms also persist under constant conditions and maintain an approximate 24-hour period, they are termed circadian (meaning approximately a day). This persistence in constant conditions is indicative of an innate biological clock. There are also physiological processes occurring on a yearly time scale (seasonal rhythms), if these rhythms persist in constant conditions and maintain an approximate period of 10-12 months, they are termed circannual (meaning approximately a year). One remarkable example of circannual timekeeping is the African Stonechat which maintained cycles of moulting, reproduction and migratory restlessness for 12 years when kept in constant conditions, clearly demonstrating the involvement of an innate biological clock (Gwinner, 1986).

However, there are differences in the level of persistence of circannual rhythms and there are disagreements in the field on the usage of this term. In this thesis I will use the definition of type I and type II circannual rhythms for ease (Dunlap, Loros and DeCoursey, 2004). The example of the African stonechat is a type II circannual rhythm because it persists for multiple years without a changing photoperiodic input. Shorter-lived species, such as small rodents, tend to have type I circannual rhythms which is characterised by the need for a change in photoperiodic signal to complete the seasonal program. Importantly, in type I rhythms there is an innately timed part of the cycle, namely the animal becomes refractory, no longer responding to the prevailing photoperiod and initiating the next part of

its seasonal program. For most small rodents the refractory state is characterized of a re-activation of the gonads and summer physiology. They will remain in a reproductively active state unless reset by a change to a short photoperiod (SP), which will lead to the regression of the gonads and initiation of winter physiology. Whether an animal has a type I or II rhythm is dependent upon their longevity, availability of photoperiodic cues in their environment and the strength of the seasonality in their environment (Hazlerigg *et al.*, 2023). Both type I and II rhythms are entrained/synchronised by changing photoperiod, which is essential to match responses to the 12-month year. This process of synchronising the circannual clock to the solar year using photoperiod is called photoperiodism (Goldman, 2001). Therefore, there must be a mechanism to assess the length of the photoperiod and stimulate physiological responses (photoperiodic time measurement).

The ability of animals to respond to photoperiodic change has been useful in a laboratory setting, allowing the mechanisms behind photoperiodic time measurement to be revealed. In 1960 Bünning proposed that photoperiodic time measurement was based on a circadian oscillator (Bünning, 1960). In this framework, often called the Bünning-hypothesis, light has two roles. First, to keep the circadian system is phase. Second, if light is exposed during a certain part of the circadian phase, it elicits a response. This indicates that long day responses are not necessarily dependent on absolute durations of light exposure, but on the relation between the timing of light exposure and circadian phase. The circadian phase at which light exposure can induce a physiological response is called the photoinducible phase. Since the prediction of the physiological response within this framework depends on external light to coincide with a specific internal phase, it is often called a coincidence timer model (for review see: (Goldman, 2001)). Substantial evidence in temperate animal species supports the involvement of a circadian-based coincidence model underlying photoperiodism (Elliott, Stetson and Menaker, 1972; Ravault and Ortavant, 1977). Laboratory experiments using simplified lighting environments allowed the specific photoperiod required to elicit a physiological response to be defined (the so-called “critical photoperiod”) allowing further probing of photoperiodic response mechanisms, and I will discuss these further in section **1.4**. First, I will return to two specific overwintering strategies of small rodents; maternal photoperiodic programming and metabolic depression (**1.3**) describing the physiological phenomenon and placing them in a timing context.

1.3 Overwintering strategies of small rodents

Small (body mass ≈ 100g) rodents have a large surface to volume ratio which makes them particularly challenged by low ambient temperature (Scholander *et al.*, 1950). As a result, small rodents often live in burrows shielded from environmental temperature fluctuations. This enables them to reduce the thermoregulatory cost at rest. However, at 10 °C a mammal of 25g is only able to store enough fat to meet their energy requirements for a few hours (Perrigo and Bronson, 1983), therefore they must forage, leaving their insulated burrow, and be exposed to the ambient temperature. The longer an animal forages in temperatures below its thermoneutral zone (i.e. the T_a range whereas an animal can keep a stable core body temperature (T_b) without increasing metabolic activity), increase the cost of both locomotion and thermoregulation. This can drive some small rodents to switch from being nocturnal (night active) to being diurnal (day active) (Hut *et al.*, 2012; Van Der Vinne *et al.*, 2014), however this increases predation risk (van der Vinne *et al.*, 2019). Therefore, small rodents living at higher latitudes or living in regions of extreme changes in seasonal T_a (i.e. mountain regions in temperate zones) have overwintering strategies to reduce their energy requirements. As already covered in section **1.1** reproductive regression is a common strategy but despite this gating of breeding, offspring of small rodents can be born in Autumn which requires that they alter their developmental trajectory to limit growth to prepare for winter (discussed in **1.3.1** Maternal photoperiodic programming). Also, in preparation for winter many small rodents use metabolic depression strategies to conserve energy (discussed in section **1.3.2** Metabolic depression: Daily torpor and hibernation).

1.3.1 Maternal photoperiodic programming

One-way small rodents can conserve energy to meet the high energy demands of winter is to have a time of year dependent life-history strategy. Since pups of small rodents have the potential to become reproductively active within two months after birth, they can give rise to multiple generations in one breeding season. This results in pups born early in the breeding season (spring) facing different environmental prospects compared to pups born late in the season (autumn). These discrepancies in future energetics dictate two distinct optimal life-histories of the pup. With early born individuals that face a future environment providing enough energy for the animal to surpass the reproductive energy threshold, favouring a rapid development and early pubertal onset to maximise number of offspring within the same breeding season. Conversely, late born individuals face forthcoming environmental conditions incompatible with surplus energy invested in reproduction, hence favouring a life-history strategy enabling conservation of energy by a slow development and a delayed pubertal onset until the following spring, shifting the energy allocation towards survival rather than reproduction. Hence pups born early in the breeding season commit to a “live fast, die young" strategy, whereas late-born pups commit to a "live slow, die old" strategy. The utilization of these two time of year dependant life-history

strategies is evident in voles and hamsters (Negus, Berger and Forslund, 1977; Hoffmann, 1978; Negus, Berger and Brown, 1986; Negus, Berger and Pinter, 1992).

For such a time of year dependant developmental program to be optimal it needs to be matched to the environment, and laboratory studies in voles spp. and Siberian hamsters (*Phodopus sungorus*), have shown that this is achieved through the combined effects of photoperiod exposure during gestation and during juvenile development, giving a history dependent interpretation of early life photoperiod (Figure 3). As an example, exposure of Montane vole (*Microtus montanus*) pups 14-h of light from birth, delays reproductive development in pups whose mother were exposed to long photoperiod (LP) (16hr of light/24 hrs) during gestation, but stimulates it in pups whose mothers were exposed to SP (8 hrs of light/24 hrs) during gestation (Horton, 1984a, 1984b). This photoperiodic history dependence of developmental program demonstrated the importance of not mere photoperiod in early life, but the direction of change of photoperiod in relation to a previous "recording". Suggesting an ability of the pup to keep track of changes in photoperiod to initiate an appropriate life-history. To resolve if the origin of such a photoperiodic "recording" was achieved *in utero* or neonatally, Milton Stetson, Theresa Horton and colleagues benefitted from the controlled laboratory setting and utilized cross fostering experiments and carefully separated photoperiodic treatment into gestational, neonatal and post-weaning phases ((Horton, 1984b, 1985; Stetson, Elliott and Goldman, 1986) (for review see: (Horton and Stetson, 1992; Horton, 2005)). Collectively these studies demonstrate that the history-dependent response derives from an interaction between gestational- and post-weaning photoperiodic experience, while the neonatal phase represents a photoperiodic "dead zone".

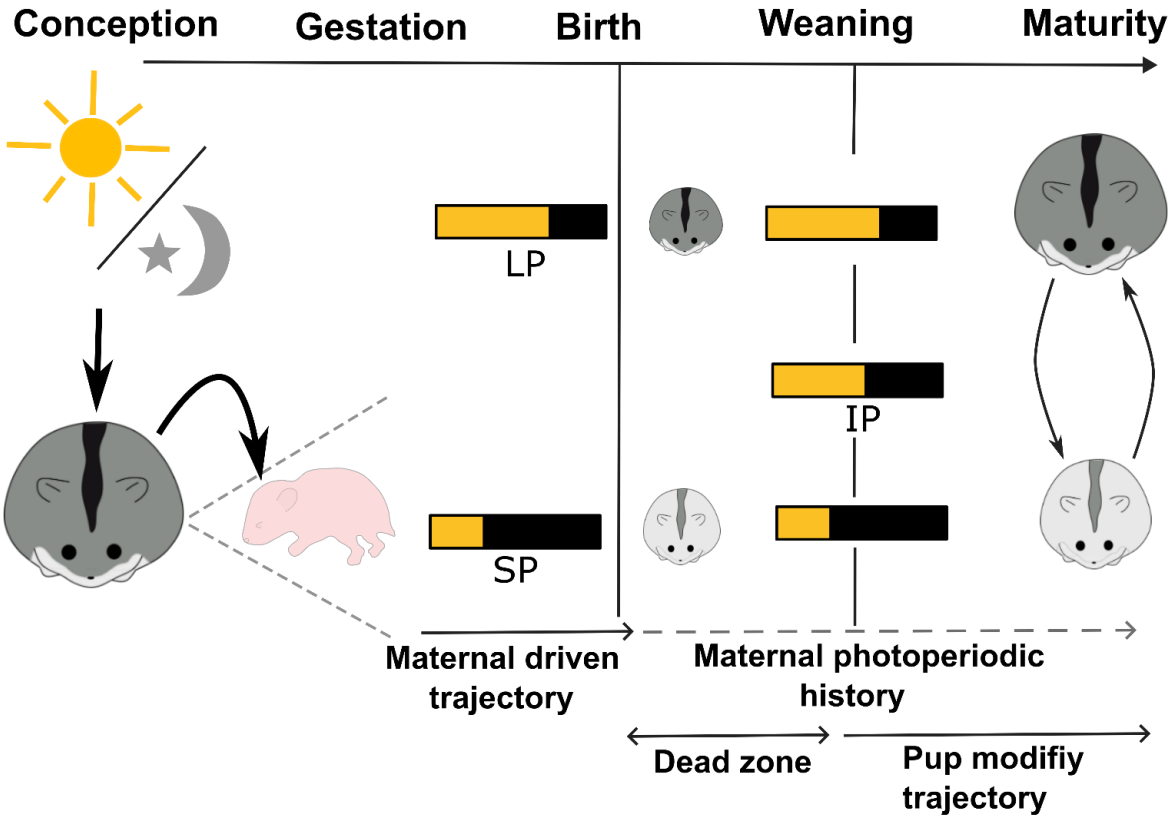

Figure 3 Maternal transfer of the photoperiodic signal during gestation dictates the photoperiodic response of the pup after birth, governing growth and time of sexual maturation. During gestation, maternal relay of the photic environment programs the metabolic trajectory of the pup after birth. If the offspring remains on the same photoperiod as during gestation, this maternally driven trajectory will pervade into two distinct life-histories. Siberian hamster offspring gestated and exposed in early-life to a long photoperiod (LP) constitute a dark pelage, high growth rate and early sexual maturation, a metabolic program beneficial to maximise the reproductive opportunity during summer-like conditions. Conversely, offspring gestated and exposed in early-life to a short photoperiod (SP) show a white pelage, decreased growth rate, and a delay of sexual maturation, a metabolic program enhancing energy conservation and physiological adaptations to winter survival. Once the pup is able to receive and respond to photoperiod (around weaning), it is able to compare the actual photoperiod, with the previous photoperiod experienced by the mother during gestation. This maternal photoperiodic history dictates the response of the pup to an intermediate (IP) photoperiod. If gestated under LP, an intermediate photoperiod (IP) is perceived as an autumnal signal with a decline in photoperiod, and the pup modify its metabolic trajectory to prepare for winter survival. Conversely, if the pup is gestated under SP, an exposure to IP is perceived as a spring signal, with an increase in photoperiod, and the pup switch from a winter survival phenotype to a reproductively active phenotype. Illustration by V.J. Melum.

Cross-fostering experiments in Montane voles demonstrate gestational photoperiod of the mother, *in utero*, to determine the interpretation of the photoperiodic signal by the pup after birth (Horton, 1985). During pregnancy, females were kept under LP (16hr of light/24 hrs) or SP (8 hrs of light/24 hrs). At birth half of the young were moved to a foster mother that had received LP during pregnancy and the other half moved to a foster mother that had received SP during pregnancy (Figure 3). All pups were raised under IP (14 hrs of light/24 hrs) after birth. SP gestated pups accelerated their development and

growth, compared to LP gestated pups, demonstrating *in utero* transfer of the photoperiodic signal from the actual birth mother to be the origin of the photoperiodic "recording" that govern the developmental program. Such an *in-utero* programming of the pups growth and development is termed maternal photoperiodic programming (MPP). A phenomenon also observed in Siberian hamsters (*Phodopus sungorus*) (Stetson, Elliott and Goldman, 1986; Stetson *et al.*, 1989), collared lemmings (*Dicrostonyx groenlandicus*) (Gower, Nagy and Stetson, 1994) and meadow voles (*Microtus pennsylvanicus*) (Lee *et al.*, 1989; Lee, 1993), which all are species that inhabit environments with large annual variations in photoperiod, temperature and food availability. MPP seem to have developed as a strategy to enhance survival and fitness in small rodent species, with timing being paramount in this phenomenon to ensure an optimal fit between the metabolic program of the animal and the available environmental resources and thermal constraints.

In section **1.4**: The photoneuroendocrine system, I will discuss mechanisms through which maternal - fetal communication of photoperiod via maternal melatonin can occur through the pups seasonal timekeeping circuits setting their developmental trajectory.

1.3.2 Metabolic depression: Daily torpor and hibernation

Another winter survival strategy utilized by small rodent species is to reduce the metabolic rate, and hence the cost of living. The period of time when animals show a metabolic depression causing a more than 5 °C decrease in T_b compared to the normothermic resting T_b is termed "torpor" (Ruf and Geiser, 2015). In the smallest mammalian species (<50 grams) torpor follows a daily pattern, forming part of the rest phase, and hence is called daily torpor (Figure 4A&B). In laboratory mice, food-restriction rapidly induces daily torpor, evident as a reduction in metabolic rate and a subsequent drop in T_b to around ~22°C, depending on T_a (Hudson and Scott, 1979). This response to an acute energetic challenge contributes to the energetic savings during the rest phase. However, the animal will still remain active and search for food, and abolish the expression of daily torpor if enough food is present (Hudson and Scott, 1979). Hence this form of daily metabolic suppression is often referred to as induced- or food-restricted daily torpor (Geiser, 2021).

Such a response to caloric restriction is also evident in photoperiodic species such as the Siberian hamster. During LP conditions Siberian hamsters keep a stable T_b, but upon food restriction they start to express daily torpor (Figure 4A). However, under SP conditions, Siberian hamsters display spontaneous daily torpor expression as part of their winter survival strategy (Figure 4B) (Figala, Hoffmann and Goldau, 1973). There is a clear distinction in depth, duration and energy substrate usage between food-restricted daily torpor in a LP adapted Siberian hamster, and daily torpor occurring in a SP adapted Siberian hamster ((Diedrich, Kumstel and Steinlechner, 2015) for review see: (Cubuk, Bank and Herwig, 2016)). Whereas during the whole 24-h period the food-restricted daily torpor utilizes lipids

as an energy substrate, the SP adapted Siberian hamster metabolizes carbohydrates in the active phase and lipids only during daily torpor (Diedrich, Kumstel and Steinlechner, 2015). Highlighting the food-restricted daily torpor as an emergency solution to energy deficits, while daily torpor being part of a photoperiodically driven metabolic program. However, also in SP adapted Siberian hamsters the occurrence of torpor episodes can be increased by food-restriction, while keeping torpor characteristics intact, demonstrating a flexibility to compensate for imposed energy deficits within the controlled program (Ruf *et al.*, 1993; Diedrich, Kumstel and Steinlechner, 2015).

In seasonal species the required homeostatic energy set-point varies throughout the year. This is particularly evident in body weight regulation, where a specific time of year relate to specific body weight set-points, such a dynamic central regulation of body weight is explained with a sliding set-point theory (Mrosovsky and Fisher, 1970). After 8-12 weeks in SP, the body weight of Siberian hamsters drop by about 3-40 %, from ≈42 grams in summer to ≈25 grams in winter (Heldmaier and Steinlechner, 1981a), and fasting and re-feeding experiments reveal that animals, despite continuous access to food follow their seasonal program of body weight regulation (Steinlechner, Heldmaier and Becker, 1983). Collectively, these examples of seasonal adjustments to homeostatic energy set-points have been described as “rheostasis” (Mrosovsky, 1990). Such an expansion to the term homeostasis increases our appreciation of the fundamentally opposing challenges animals face in cyclical environments, and hence the requirement of temporally distinct physiological adaptations.

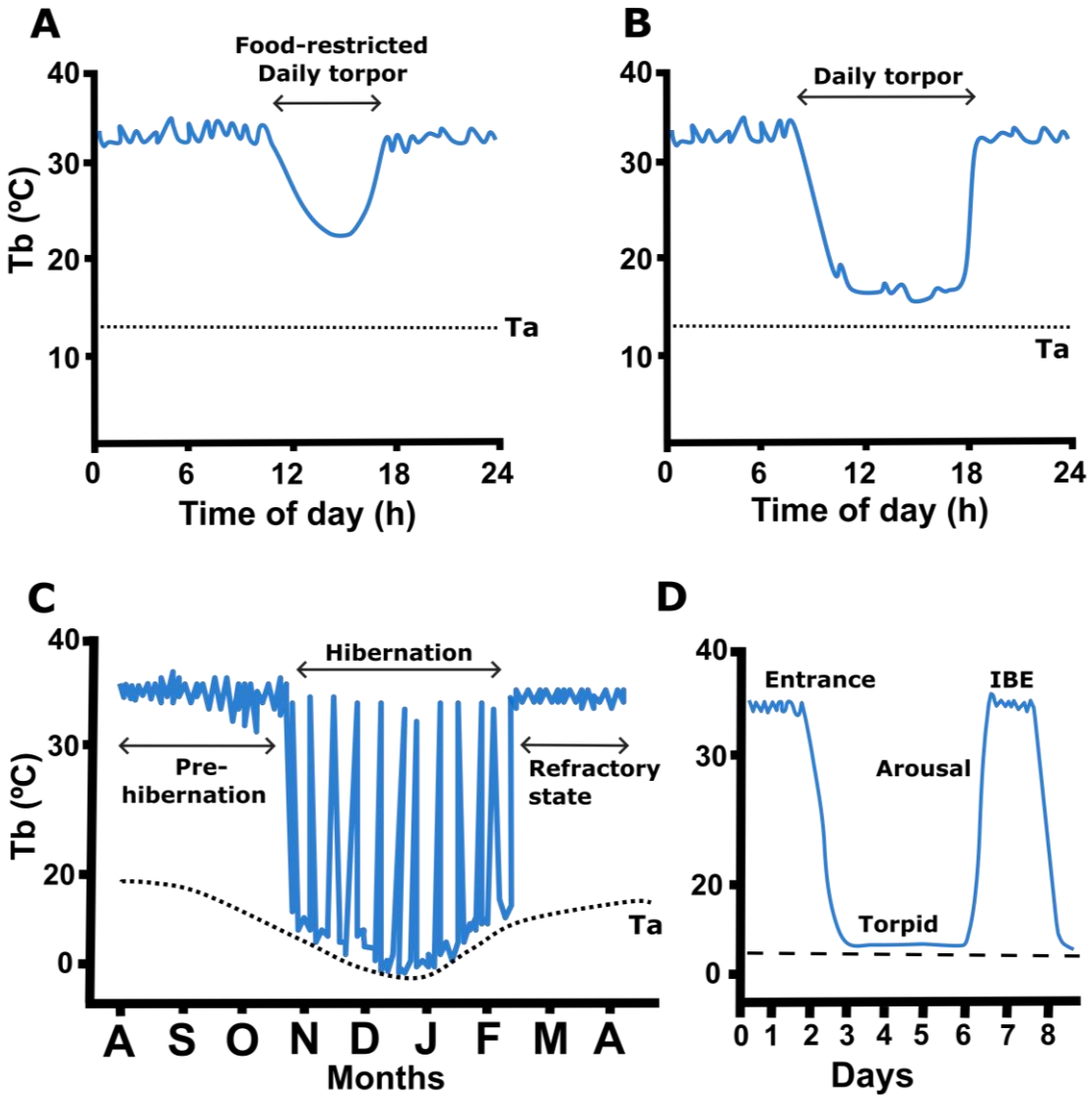

Figure 4 Small rodent species utilize metabolic depression to conserve energy. Two distinct forms of metabolic depression exist, daily torpor (A and B) and hibernation (C and D). Daily torpor, a daily gated decrease in metabolic rate (illustrated by core body temperature - T_b) reduces the energy requirement of the animal, A) either as an acute response to decreased food availability or B) as part of a seasonal program. Food-restricted daily torpor is distinctive from spontaneous daily torpor in the characteristics of the depth and duration of the torpor bout. C) Hibernation is a photoperiodically driven program to reduce the cost of living to a minimum, requiring a preparatory phase (pre-hibernation) to enable physiological adaptations to occur. When ready, the hibernation period starts when an initiation of metabolic depression, leads to a substantial decrease in T_b approaching ambient temperature (T_a), where it remains for multiple days (torpor), before spontaneously rewarming back to a euthermic T_b (arousal). The hibernation period is characterised by this repetitive torpor-arousal (T-A) cycling. By an endogenously driven process, the animal becomes photorefractory to the short photoperiodic signal, stop T-A cycling and initiate reproductive preparatory processes (refractory state). D) A zoomed part of the hibernation period shows how the animal gradually lowers metabolic activity and T_b prior to enter the torpid state (entrance). The torpid state, with an extreme suppression of metabolic activity and low T_b spans over multiple days, which profoundly decreases the energy consumption of the animal, while still able to thermoregulate. The arousal back to an euthermic T_b is achieved within hours, and the brief period with an euthermic T_b is termed inter-bout euthermic (IBE). Illustration by V.J. Melum

The photoperiodically driven reduction in body weight of Siberian hamsters is primarily achieved by a reduction in fat content, which could compromise insulation of the animal ((Heldmaier and Steinlechner, 1981a) reviewed in: (Bartness and Wade, 1985)). An increase in the surface to volume ratio, which promotes heat loss, and a reduction in energy reserves seems like a counterintuitive adaption to tackle the harsh winter. However, in the wild, Siberian hamsters are known to hoard large stashes of seeds, providing an external energy reserve (Bartness and Wade, 1985). Further, a reduced fat mass, if not compromising insulation may decrease the energetic requirements in winter. Indeed, the thermal conductance of Siberian hamsters remain constant throughout the year (Heldmaier and Steinlechner, 1981a), indicative of other adaptations, such as increased fur length, density and coverage compensate for the increased surface to volume ratio in winter. Further, a decreased body weight enables an increased basal metabolic rate (BMR) while still spending less energy in total. Such an increased BMR at rest decrease the lower critical temperature (i.e. the minimum T_a an animal can be exposed to while keeping a stable T_b without an increase in metabolic activity) of the Siberian hamster in winter, contributing to further energy savings (Heldmaier and Steinlechner, 1981a). With these adaptations in place, the large body weight reduction in winter acclimatized Siberian hamsters show around a 35 % reduction in energy requirements at rest with euthermic T_b. If adding the energetic savings of daily torpor, the daily energy requirement of Siberian hamsters during winter is reduced by approximately 40 % (Heldmaier and Steinlechner, 1981a, 1981b). The Siberian hamster represents a strong example of how photoperiodically driven physiological adaptations ensure a fit between the energetic needs of the animal and the environmental conditions, supporting winter survival. In autumn born pups, through MPP (Section **1.3.1**) the physiological adaptations for winter are initiated from birth.

Another similar, but distinct, metabolic depression strategy used by small mammalian rodents to survive the winter is hibernation (Figure 4C) (reviewed in: (Heldmaier, Ortmann and Elvert, 2004)). Hibernation can be an ambiguous term, and will here be defined as "a physiological and behavioural adaptation that permits survival during seasonal periods of energy shortage via a combination of pre-hibernal energy storage and hibernal metabolic depression (torpor)" (Pers. comms. S. Wood). In many hibernators, exposure to shortening photoperiod initiates the pre-hibernation period, a mandatory preparatory phase in which both behavioural and physiological adaptations occur. A key part of this preparation is to ensure enough energy reserves, either through externally stored food, or internally stored fat. The size of the animal influences the capacity to store fat (Ruf and Geiser, 2015); larger hibernators (e.g. arctic ground squirrels, *Urocitellus parryii*, *>500g*) tend to be fat-storing, likely as a result of a large body size being able to carry the required fat reserves to meet the energy demand during the whole hibernation period. Contrastingly, smaller hibernators (e.g. golden hamsters, <150g) lack this capacity and tend to be food-storing. Regardless of strategy, the animal depends on the stored energy during the hibernation season.

During the pre-hibernation period, changes in territorial and social behaviour occur, whilst searching for a place to hibernate. As a key preparation the hibernator builds a nest in an insulated place, often below ground, with insulative materials where the hibernation will occur, therefore called a "hibernaculum". Both the below ground location and insulative properties of the nest materials increase the minimum T_a and buffer thermal fluctuations, reducing thermoregulatory costs. Within the hibernaculum food-storing hibernators pile up hoarded food, as an external energy reserve to rely on during the winter, reducing both predation risk and the cost of thermoregulation during foraging at low T_a. The food cache enables the hibernator to be confined within the hibernaculum during the whole hibernation period. Interestingly, in golden hamsters, removal of the hoarded food, delays hibernation onset, indicating a capability of the hibernator to assess the energy requirement to survive the winter (Lyman, 1954).

During the pre-hibernation period several endocrine organs reduce their secretory activity (Lyman *et al.*, 1982). Most notably, the reproductive system is inactivated, with gonadal regression and a drop in circulating sex steroids (Hoffman, Hester and Towns, 1965; Darrow, Yogev and Goldman, 1987; Darrow *et al.*, 1988). Further, the increase in both amounts and thermogenic properties of brown adipose tissue (BAT) increase the thermogenic capacity of the animal, a prerequisite for a successful hibernation (for review see: (Cannon and Nedergaard, 2004). Concomitantly, in some species a gradual decrease in T_b is observed prior to hibernation on-set (Sheriff *et al.*, 2012; Chayama *et al.*, 2016). At the cellular level multiple molecular adaptations takes place to enhance cellular function at low temperature and during periods without food or water (for review see:(Carey, Andrews and Martin, 2003; Giroud *et al.*, 2021)).

After the preparative period, with considerable between and within species variation, the hibernation period is initiated by metabolic depression followed by a substantial drop in T_b (Figure 4C). This controlled lowering of T_b (Entrance) continues until T_b is a few °C above T_a, where it stabilizes and remains for multiple days (Torpor). During torpor, the hibernator challenges our perception of life, and in a state of suspended animation, the metabolic rate drops to as low as 1 % of euthermic levels, with corresponding reductions in heart rate and breathing frequency (Lyman *et al.*, 1982; Ruf and Geiser, 2015). In the torpid state, as a result of the low T_b, the cellular activity of all processes are slowed. Even in the torpid state, the hibernator is able to thermoregulate and defend a new stable T_b during torpor (Lyman, 1948). The observed minimal T_b show large species variability, but can be as low as 0°C in some species (Barnes, 1989). By defending a lower T_b, hibernators achieve a dramatic reduction in the lower critical T_a below which increased energy expenditure is needed to maintain T_b. The resultant metabolic rate reduction is a clear adaptive benefit of rheostatic adjustment of a hypothalamic set-point (Mrosovsky, 1971, 1990). How this is achieved is not known, but it probably involves a modulation of

the normothermoregulatory circuits in the hypothalamus ((Heller and Hammel, 1972) reviewed in: (Heller *et al.*, 1978)).

During the hibernation season, many hibernators, including the golden hamster, undergo cyclical episodes of torpor and spontaneous rewarming to an euthermic T_b (Arousal), an energy costly process known as torpor-arousal (T-A) cycling (Lyman, 1948; Yousef, Robertson and Johnson, 1967). This is achieved by non-shivering BAT thermogenesis and muscle shivering ((Smith and Hock, 1963), for review see: (Nedergaard and Cannon, 1990)). The arousal poses a particular physiological challenge to the animal, with tissues having to withstand a rapid 30 °C increase in T_b within about 3 hours (Lyman, 1948). This short, but intense arousal phase comprises a large proportion of the total energy budget (up to 86 %) in the hibernation period, and is a paradoxically expensive component of an energy conserving process (Karpovich *et al.*, 2009). Why it occurs have spurred multiple hypothesis without any firm answers (for review see:(van Breukelen and Martin, 2015)). The necessity to arouse to restore a cellular balance of substances that have either accumulated or depleted during torpor seems the most likely general explanation.

During the euthermic phase of the T-A cycle, the animal resumes normal cellular functions and rapidly clears out accumulated waste products. This makes the adaptations to hibernation unique, since the tissues have to be operational at both low and high T_b. In food-storing hibernators, feeding, drinking and sleep makes up the inter-bout euthermic (IBE) period, contrary in fat-storing hibernators no feeding or drinking occur (reviewed in: (Giroud *et al.*, 2021)). Rapidly, often within 24 hours the hibernator enters a new torpor bout (Figure 4D). This repetitive pattern of T-A cycling defines the hibernation period (Figure 4C), and in the Richardson`s ground squirrel (*Urocitellus richardsonii*), the estimated reduced energy requirement is as much as 88 % (Wang, 1979). A saving worth the risks associated with low T_b.

After a certain amount of time, while still remaining in the hibernacula hidden from photoperiodic changes, the hibernator ceases T-A cycling (Lyman *et al.*, 1982). Concomitantly, an increase in gonadal activity, measured as an increase in circulating sex steroids, is seen in relation to the end of the hibernation period (Barnes, 1986; Darrow, Yogev and Goldman, 1987; Barnes *et al.*, 1988; Darrow *et al.*, 1988). Within the laboratory this spontaneous change in metabolic program is evident even if pinealectomised and kept under LP and at a stable T_a, clearly showing T-A cycling and gonadal activity to be driven by an endogenous timing mechanism (Sáenz De Miera *et al.*, 2014). Early observations in field caught thirteen-lined ground squirrel (*Ictidomys tridecemlineatus*), showed a gradual increase in testicular weights during the hibernation period (Wells, 1935). Given that in the laboratory, peripheral injection of gonadal hormones have been shown to block T-A cycling, the temporal dynamics and species-specifics of this observation needs to be further substantiated (Hall and Goldman, 1980; Lee *et al.*, 1990). Regardless, the reversion of physiology while still under SP means the hibernators become refractory to the photoperiodic signal (section **1.2**). In summary, hibernation is a timed metabolic

depression strategy relying on an innate timing mechanism that ensures winter survival, and enable the hamster to participate in the next reproductive event in spring.

To elucidate the neuroendocrine basis for the timing and regulation of metabolic control during hibernation, the golden hamster is an exemplar model species with a robust photoperiodic initiation of the hibernation phenotype (Lyman and Chatfield, 1955). The pre-hibernation period of golden hamsters can be shortened by low T_a, but even T_a of 22 °C will in the laboratory induce hibernation under SP conditions (Malan *et al.*, 2018). Further, the golden hamster is a food-storing hibernator, with a body weight between 90-120 grams and is easily handled in the laboratory. Given the readily induction of hibernation under SP conditions in a controlled laboratory setting, the golden hamster is a good model organism for further work to decipher the still poorly understood mechanisms underlying the extreme metabolic depression seen in hibernators.

1.4 The photoneuroendocrine system

For animals to be photoperiodic (i.e. to schedule seasonal changes in physiology or behaviour based on changes in photoperiod), there must be a decoding of the photic signal to translate it to a physiological response. In mammals, light perceived by the retina depolarizes non-visual photoreceptors which relay the light signal via the retino-hypothalamic tract to the supra chiasmatic nucleus (SCN), the master circadian pacemaker in the body (for review see: (Hastings, Maywood and Brancaccio, 2018) (Figure 5). Further, SCN neurons project to the paraventricular nucleus (PVN) of the hypothalamus, whose neurons further project to the intermediolateral cells of the spinal cord. Here the neuronal signal goes to the superior cervical ganglia neurons which innervate the pineal gland, the site of melatonin synthesis. Under the indirect SCN control, melatonin is synthetized during the night (dark phase), and have a minimal secretion during the day (light phase). Melatonin is not stored in the pineal cells but immediately released in the blood stream, so that there is an inverse relationship between circulating melatonin levels and daylength. The demonstration that pinealectomy of male golden hamsters inhibits testicular regression when exposed to SP, showed the importance of melatonin in driving the photoperiodic response in seasonal animals (Hoffman and Reiter, 1965). Further support for duration of melatonin to be at the core of photoperiodism was evident in a series of elegant studies utilizing the melatonin and the timed infusion paradigm (for review see: (Bartness *et al.*, 1993)). With a specific time between melatonin infusions in pinealectomised animals, these studies demonstrated that the total duration of the melatonin signal during a 24-hour period was essential in eliciting a photoperiodic response. The importance of melatonin in synchronising the circannual rhythm was also demonstrated in pinealectomised sheep which completely lost reproductive synchrony to the annual photoperiod which could be rescued with only a 90-day melatonin infusion (Woodfill *et al.*, 1991, 1994). The fact that only 90 days of a melatonin signal are required to synchronise to the entire 365-day year demonstrates the importance of photoperiodic (or melatonin) history in seasonal timing.

As stated earlier one of the clearest examples of photoperiodic history dependence is the phenomenon of MPP. Here it is also clear that melatonin is the key signal. During gestation, the mother relays changes in daylength via transplacental melatonin to the developing fetus, which are shielded from the photoperiod in the womb, and lack the independent capacity for rhythmic melatonin synthesis. This was demonstrated in detailed studies in Siberian hamsters (*Phodopus sungorus*) which started to elucidate the mechanism behind MPP (Horton, Ray and Stetson, 1989; Stetson *et al.*, 1989; Horton, Stachecki and Stetson, 1990; Horton *et al.*, 1992). With the use of melatonin injection to LP-adapted pregnant pineal-intact females, a time-of-day dependent effect in pup development was revealed (Horton, Ray and Stetson, 1989). Specifically, melatonin injections given prior to the dark-phase, and therefore extending the natural short melatonin profile of the female, resulted in the most pronounced decrease in pup testicular growth (Horton, Ray and Stetson, 1989). In pinealectomised mothers, the *in utero* effect of maternal photoperiod on pup development was abolished (Horton, Stachecki and Stetson, 1990), similarly to pineal-intact mothers with continuous release melatonin implants (Horton *et al.*, 1992). Collectively, these studies resolved that the photoperiodic history of the pups was achieved *in utero*, and that this *in utero* programming was melatonin dependent (for review see:(Horton and Stetson, 1992)).

The sites through which photoperiodic change in melatonin secretion is coupled to seasonal photoperiodic responses have been a topic of major interest in the last 50 years (reviewed in: (Hazlerigg and Simonneaux, 2015)). In mammals, the melatonin signal can be received by cells expressing melatonin receptor 1 (MT1) or melatonin receptor 2 (MT2) (for review see: (Vanecek, 1998)). Within the brain MT1 receptors are the principal receptor type and are found in the medio-basal hypothalamus (MBH), SCN and in the pars tuberalis (PT), a region surrounding the pituitary stalk (Klosen *et al.*, 2002; Dardente *et al.*, 2003; Johnston *et al.*, 2003). Within the PT, the melatonin signal duration regulates transcription translation feedback mechanisms key in seasonal timekeeping (Figure 5). In essence, melatonin exerts a suppressive action on Eya3 expression, which in turn repress Tsh-β transcription. Decreased levels of TSH-β leads to reduced synthesis of thyrotropin/thyroid stimulating hormone (TSH), since it consists of TSH-β and α-GSU (Dardente *et al.*, 2010; Masumoto *et al.*, 2010; Wood *et al.*, 2015, 2020). PT thyrotrophs secrete TSH in a melatonin-dependent manner (Hanon *et al.*, 2008; Nakao *et al.*, 2008; Ono *et al.*, 2008). The TSH is transported in a retrograde manner to the 3rd ventricle (3V) of the hypothalamus where it binds to TSH-receptors (TSH-R) on specialised radial glial cells, tanycytes.

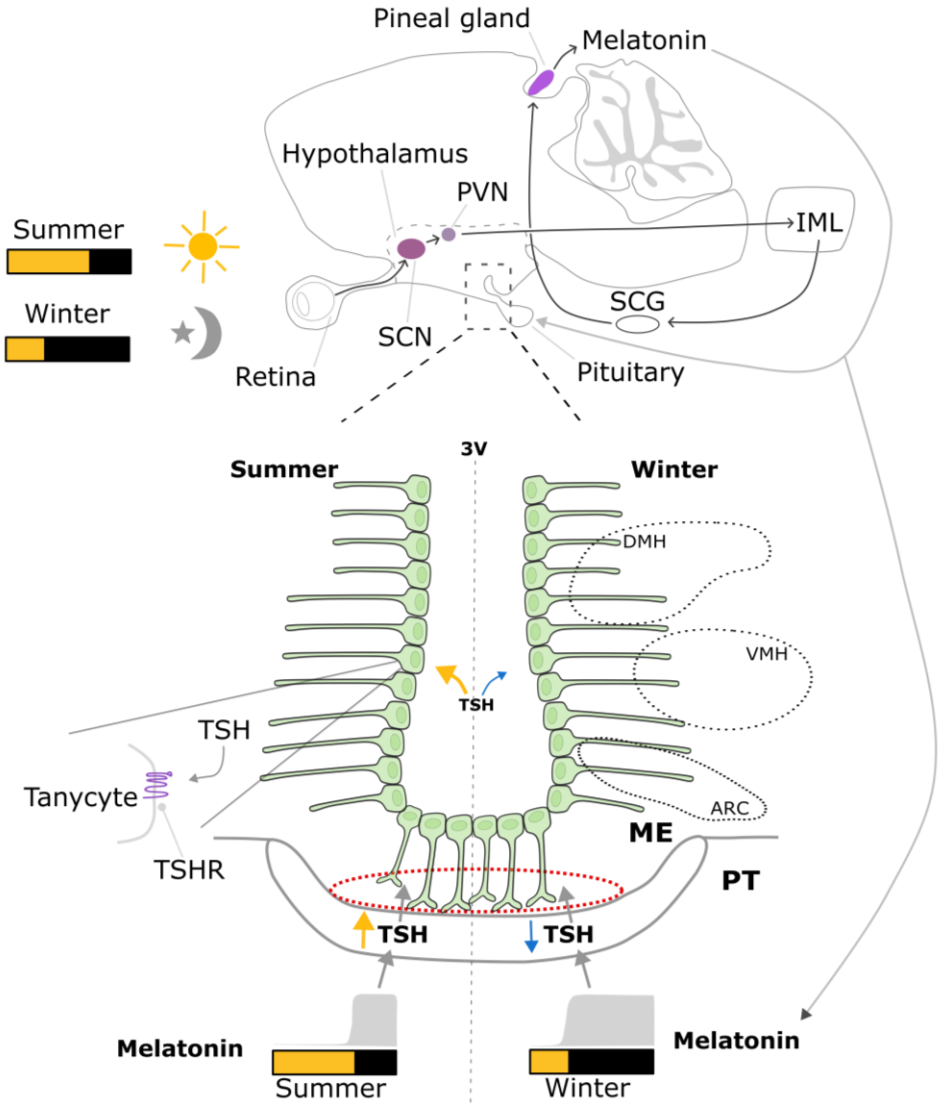

Figure 5 Neuroendocrine mechanisms of photoperiodic time measurements. The photoneuroendocrine system relays photic input from the eyes via the retinohypothalamic tract to the supra chiasmatic nucleus (SCN) which serves as the prime site of circadian rhythm generation in mammals. The SCN further innervate the paraventricular nucleus (PVN) which in turn transmits the photic signal to the intermediolateral nucleus (IML) residing in the spinal cord. From here the signal is relayed to the superior cervical ganglia (SCG) which innervate the pineal gland. Through this multi-synaptic pathway, SCN activity controls the production and secretion of melatonin from the pineal gland in a time-of-day dependent manner. Upon darkness SCN release its inhibition on the melatonin synthesizing cells in the pineal gland, causing a secretion of melatonin confined to the dark phase (night) of the 24-hour day. This results in a short melatonin profile in summer, when the dark part (night) of the 24-hours day is short. Conversely, during winter, when the dark part (night) of the 24-hours day is long, there is a long melatonin profile. These seasonal changes in melatonin signal duration are essential because they are detected and responded to by cells in the pars tuberalis (PT), surrounding the pituitary stalk, which express melatonin receptor 1. These thyroptroph-like cells secrete thyrotropin/thyroid stimulating hormone (TSH) into the fenestrated median eminence (ME) in a melatonin dependent manner, with high levels in summer and low levels in winter. This PT derived TSH binds to TSH-R on the tanycytes, lining the tuberal part of the 3rd ventricle (3V), driving reciprocal changes in enzymatic and transporter activity. Arcuate nucleus (ARC), ventromedial hypothalamus (VMH) and dorso-medial hypothalamus (DMH). Illustration by V.J. Melum. Based on (Hazlerigg and Simonneaux, 2015)

The change of the melatonin signal duration that is conveyed from the PT to the tanycytes via TSH not only regulates the downstream seasonal physiology of adults but also engages with the fetal PT and hypothalamus to programme the metabolic trajectory of the pup, after-birth (MPP) (Sáenz de Miera *et al.*, 2017; Sáenz de Miera, 2019). This places the action of TSH on tanycytes and the function of tanycytes as a pivotal component of the timing of seasonal life histories in mammalian species and the regulation of metabolic physiology.

In the next section I will review the characteristics of tanycytes and their role in energy homeostasis in non-seasonal species (**1.5**); I will return to the actions of TSH on the tanycyte and how this links to the downstream seasonal physiology (**1.6**).

1.5 Tanycyte function in energy homeostasis

Tanycytes are specialised ependymal glial cells, related to radial glia, which are coming to be recognised as important modulators of hypothalamic function. Tanycytes are found along the ventricles in the circumventricular organs (CVO) of the brain, regions that permit exchange of larger peptides between brain and blood (Langlet, Mullier *et al.*, 2013). The previous literature on tanycytes has been focused on the cells lining the tuberal floor of the 3V, in close proximity to the median eminence (ME), one of the seven CVOs in the brain (For review see: Rodríguez *et al.*, 2005; Rodríguez, Blázquez and Guerra, 2010; Prevot *et al.*, 2018; Rodríguez *et al.*, 2019). I will also focus on this population of 3V tanycytes, which extend dorsally overlapping with cuboidal ependymal cells. However, unlike these cuboidal cells, tanycytes are vimentin-positive, have long projections into the brain parenchyma and only possess either a primary cilium (uniciliated) or two cilia (biciliated) (Mirzadeh *et al.*, 2017). The privileged anatomical position of tanycytes in the basal 3V allows them to access and transport signalling molecules both in the blood and cerebrospinal fluid (CSF), enabling them to be the nexus point between the brain and body. Four subtypes, alpha 1 (α1), alpha 2 (α2), beta 1 (β1) and beta 2 (β2), have been categorised using their position in the ventricle and specific protein markers (Figure 6). However, it is evident that the functionality and markers of tanycyte subtypes depend on metabolic state, indicating a more dynamic gradient between tanycyte subtypes than previously appreciated (Sullivan, Potthoff and Flippo, 2022; Brunner *et al.*, 2024).

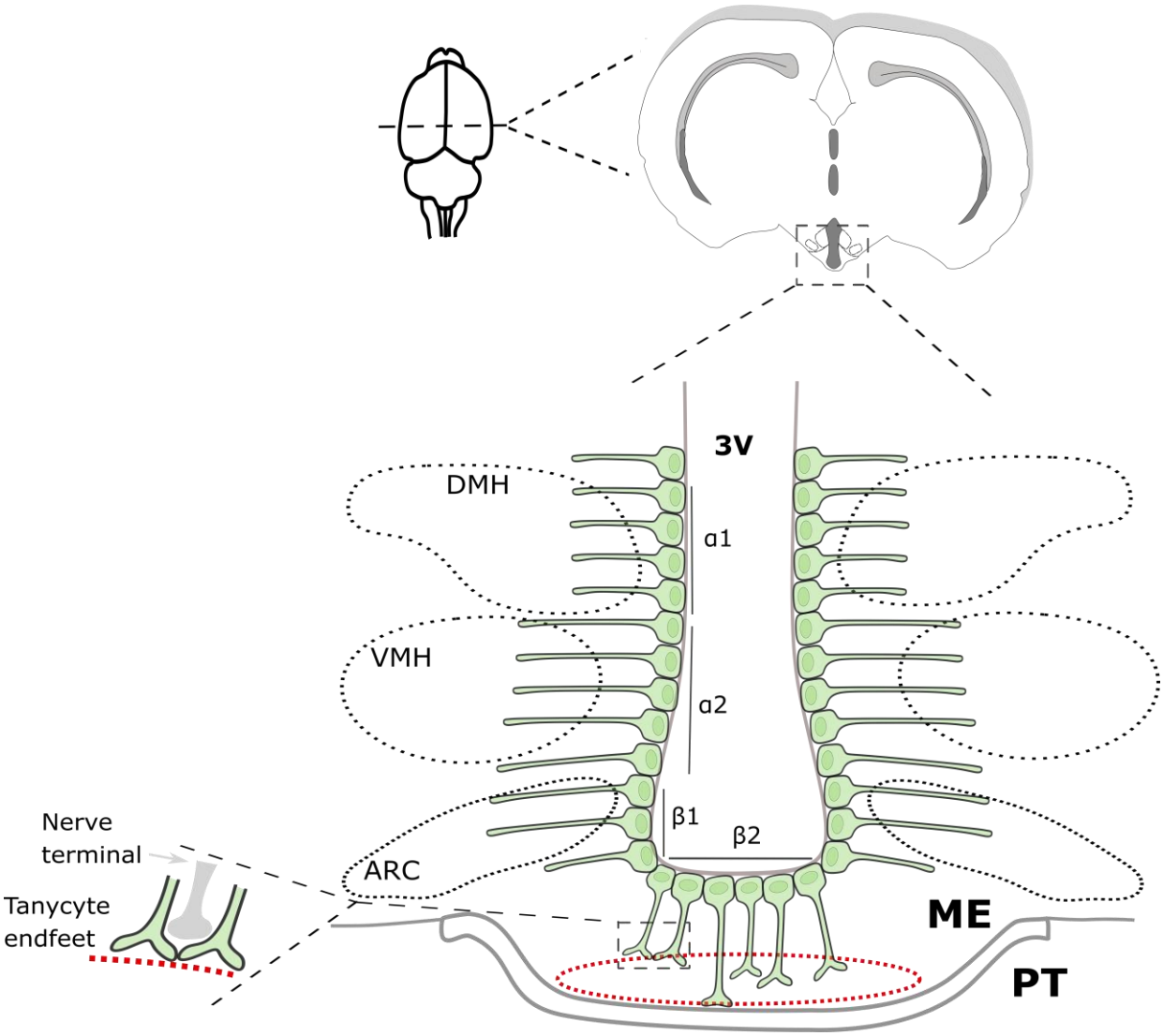

Figure 6 Tanycytes lining the tubular part of the 3rd ventricle constitute an important integrator of peripheral metabolic status to the medio-basal hypothalamus. This tanycyte population, characterised by vimentin-positive long processes, makes close contact to neuronal populations located in different areas of the medio-basal hypothalamus (arcuate nucleus, (ARC), ventro-medial hypothalamus, (VMH and dorso-medial hypothalamus, (DMH)), involved in the regulation of food intake, reproduction and thermoregulation. Classically these tanycytes have been divided into four subtypes, with the most dorsal being alpha 1 (α1), and ventrally transitioning into alpha 2 (α2), beta 1 (β1) and beta 2 (β2), although recent studies report these subtypes to display a plasticity that favours a more gradient view. β2-tanycytes lining the tuberal floor of the 3rd ventricle (3V) constitute a cerebrospinal fluid (CSF)-blood barrier (BB), (CSF-BB) gating the peripheral signal molecules that freely enters the fenestrated median eminence (ME). One of seven circumventricular organs (CVO) in the brain where the protective blood-brain barrier that limit diffusion of larger substances from blood to brain, is shifted from endothelial cells to tanycytes. A shift that enables neuronal secretion of larger peptides into the ME vasculature, for their pituitary target site. Within this hypothalamic-pituitary axis, β2-tanycytes can act as physical barriers with their endfeet ensheathing the secretory nerve terminals, limiting neuropeptide hormone release into the ME. Finally, β2-tanycytes are also in contact with thyrotroph-like cells of the pars tuberalis (PT), a key secretory cell in the relay of seasonal changes in the photoperiodic signal. Illustration by V.J. Melum.

Since the first discovery of tanycytes in 1909 by Ramón y Cajal (Ramón y Cajal, 1909), they have been speculated to exert an array of functions influencing the homeostatic control centre for physiological

functions. In recent decades, this peculiar cell type has had a revival of interest, and technological advances start to equip researchers to reveal their mechanistic function. To date, the key areas tanycytes have been implicated in are their ability to 1) control the secretion of neuropeptides by hypothalamic neurons into the portal vasculature (Prevot *et al.*, 1999; Parkash *et al.*, 2015; Müller-Fielitz *et al.*, 2017), 2) regulate blood-hypothalamus and cerebrospinal fluid-hypothalamus exchange of metabolites both through active transport and barrier properties (Langlet *et al.*, 2013; Lhomme *et al.*, 2021; Rodríguez-Cortés *et al.*, 2022; Barahona *et al.*, 2024), 3) sense and respond to metabolites in blood and CSF (Frayling, Britton and Dale, 2011; Recabal *et al.*, 2018; Bolborea *et al.*, 2020) and 4) respond to environmental cues by modulating hypothalamic neurogenesis, an ability termed neural stem cell properties (Lee *et al.*, 2012; Yoo *et al.*, 2021). Through these diverse actions, tanycytes constitute a pivotal part in the hypothalamic response to peripheral metabolic signals and have been shown to possess the capacity to be modulators of homeostatic hypothalamic circuits (For review see: (Bolborea and Langlet, 2021; Dali, Estrada-Meza and Langlet, 2023)). These insights come from beyond the field of seasonal biology, and often utilize standard laboratory rodent models, such as mice and rats, with the cutting-edge technology that follows. In the following sections I will summarise the evidence for tanycytes as sensors and relays of energy status to the hypothalamic neurons and the contribution of the tanycyte stem cell niche to the hypothalamic neuronal populations both during development and in the adult in response to changing energy status.

1.5.1 Evidence for tanycytes of the 3rd ventricle as relays of energy status to the hypothalamic circuits

The MBH is considered to be the key brain region for peripheral integration of metabolic signals and subsequent regulation of food intake (reviewed in: (Schwartz *et al.*, 2000)). Here, within the arcuate nucleus (ARC) both orexigenic (appetite inducing) Agouti-related peptide (AgRP)/neuropeptide Y (NPY)- and anorexigenic (appetite suppressing) Pro-opiomelanocortin (POMC)/cocaine- and amphetamine-regulated transcript (CART)- neurons reside (reviewed in: (Dietrich and Horvath, 2013)). These neurons are considered principal regulators of food intake through down-stream actions within, among others, PVN of the hypothalamus and brainstem (Cowley *et al.*, 1999). Also, neurons in the ventro-medial hypothalamus (VMH) and dorso-medial hypothalamus (DMH) contribute to the regulation of food intake. The activity of these appetite modifying neurons in the MBH is most importantly regulated by reproductive status (sex steroids), glucose, leptin, ghrelin and lactate (Jansen *et al.*, 1993; Cowley *et al.*, 2001, 2003; Elmquist *et al.*, 2005). Tanycytes modulate these neuronal populations access to metabolic signalling molecules (reviewed in: (García-Cáceres *et al.*, 2019)).

Given the anatomical position of 3V tanycytes, they constitute a physical barrier for peripheral metabolic signals to reach the CSF. Within the brain, blood vessels are ensheathed with endothelial cells, that through tight junction proteins limit larger molecules to passively diffuse from the blood into the brain parenchyma, forming the blood-brain barrier (BBB) (for review see: (Saunders *et al.*, 2018)). However,

in the CVO, the blood vessels are fenestrated, meaning they have an increased permeability due to a lack of tight junction proteins in the endothelial cells surrounding them. This increase in permeability enables larger peptides to enter the CVO. Tanycytes line the ventricular wall of the CVO, and through tight junction proteins, they limit the passage of larger peptides into the CSF (Mullier *et al.*, 2010; Langlet, Mullier *et al.*, 2013). In this way, tanycytes of the ME, and other CVOs, form a physical barrier called CSF-blood-barrier (CSF-BB) in which function is to gate peripheral signalling molecules from the ME into the CSF, and thereby control the accessibility of these signals to neuronal populations.

In addition, tanycytes are able to modulate the dorsal extent of both the CSF-BB and fenestrated blood vessels in the ME influencing hypothalamic access to peripheral metabolic signals. In fasting mice, tanycytes, through the release of vascular endothelial growth factor A (VEGF-A), induce a reorganization of the tight junction proteins between the endothelial cells that ensheathe the blood-vessels, which leads to altered permeability of metabolic signals into the ARC (Langlet, Levin *et al.*, 2013). Such a reorganization of the BBB influence AgRP/NPY neuronal activity, which in turn modulate food intake during refeeding after fasting (Langlet, Levin *et al.*, 2013). Along with the dorsal increase of fenestrated blood vessels, the tanycytic expression of tight junction proteins shifts dorsally to keep an intact CSF-BB (Langlet, Levin *et al.*, 2013). This demonstrates tanycytes to be an active part of a plastic response to energetic status. Since tanycytes contact both the BBB and CSF, they are able to sense a range of metabolites. Given their extension to, and signalling with, neurons makes changes in tanycyte morphology and barrier function influence hypothalamic sensing and signalling to these peripheral metabolic signals (Pasquettaz *et al.*, 2020). In some tanycytes, their processes have boutons, synapse-like structures, which contact both appetite-modifying neurons (NPY and POMC) in the ARC and reproductive neurons in the VMH, suggesting a role for tanycytes in tanycyte-neuronal communication through secretory activity and synaptic plasticity (Figure 7) (Pasquettaz *et al.*, 2020). Collectively, the unique anatomical location and properties of tanycytes suggest them to be important in the relay of metabolic signals in the CSF and blood to hypothalamic circuits involved in energy balance and reproduction. In the next sections I will summarise the information relating to tanycytic sensing of leptin (**1.5.1.1**), ghrelin (**1.5.1.2**), glucose (**1.5.1.3**), lactate (**1.5.1.4**), fatty acids (**1.5.1.5**) and sex steroid hormones (**1.5.1.6**) because of their particular importance in signalling energy status and requirements.

1.5.1.1 Leptin

Leptin is a peptide hormone secreted from adipocytes. It has long been regarded as the hormonal mediator of an organism's fat status, since its plasma levels is proportional to amount of adipose tissue. The implication of leptin in feeding have hence been extensively studied. The brain responds to leptin when it binds to neurons expressing leptin receptor (LEP-R/Ob-R). If leptin is peripherally administered, the response is acutely observed in a small subset of the ARC neurons. The response in all the remaining

leptin-responsive neurons is delayed until 1-2 hours after the injection. However, if given intracerebroventricularly (ICV) leptin responsive neurons in the more dorsal part of ARC, DMH and VMH respond within minutes (Faouzi *et al.*, 2007). This indicates that leptin requires active transport from the ME to the hypothalamic regions, a process proposed to be mediated by tanycytes (Balland *et al.*, 2014). Even though initial replication of the study failed (Yoo *et al.*, 2019), a recent study proposes a LEP-R-EGF-R shuttle in tanycytes to be the main route of leptin entry into the brain (Figure 7) (Duquenne *et al.*, 2021). Selective deletion of LEP-R in tanycytes limits leptin entry to the brain, and results in increased food intake, lipogenesis, and glucose intolerance (Duquenne *et al.*, 2021). This highlights the capacity of tanycytes to regulate energy homeostasis by conveying peripheral metabolic signals to the hypothalamus.

1.5.1.2 Ghrelin

Ghrelin is a metabolic hormone secreted from the stomach. It exerts an orexigenic drive on AgRP/NPY neurons that promote feeding behaviour. How ghrelin accesses the brain is not clear. However, *in vitro* and *in vivo* observations propose a similar mechanism for ghrelin as demonstrated for leptin (Collden *et al.*, 2015; Uriarte *et al.*, 2019). Further, selective deletion of tanycytes insulin receptors influence the AgRP-neuronal response to peripheral ghrelin injections (Porniece Kumar *et al.*, 2021). This indicates a pivotal role for tanycytes in relaying the peripheral hunger signal ghrelin to reach the hypothalamic regions controlling energy homeostasis, albeit the precise mechanism remains elusive.

1.5.1.3 Glucose

The brain assesses peripheral glucose status to modulate components of the glucose homeostatic axis to ensure blood glucose levels are confined within narrow levels. Since there is a correlation between blood and CSF glucose levels, tanycytes relay peripheral glucose status when they respond to CSF glucose in an Adenosine Triphosphate (ATP)-dependent way (Figure 7). This is achieved through uptake of glucose from the CSF by various glucose transporters (GLUTs), within the tanycytes the glucose enters the glycolytic pathway and increase internal levels of ATP which is secreted out of the cell through the hemi-channel connexin-43 (CX43). An increase in external ATP levels increase the cellular activity of P2Y purinoceptor 1 (P2RY1) leading to formation of cytosolic inositol trisphosphate (IP_3). Increased cellular levels of IP_3 cause the endoplasmic reticulum to release its calcium (Ca^{2+}) stores, which forms a calcium-wave that propagate along the tanycytic process and stimulate neuronal activity in the MBH (James and Butt, 2002; Frayling, Britton and Dale, 2011; Orellana *et al.*, 2012). A similar response is demonstrated for certain amino acids as well (Frayling, Britton and Dale, 2011; Lazutkaite *et al.*, 2017) (Figure 7). Recently, optogenetic stimulation of individual tanycytes was shown to trigger calcium wave propagation and activation of neurons in the ARC (Bolborea *et al.*, 2020). This long-lasting effect is achieved through the gap-junctions created by CX43, increasing the connectivity and responsiveness to nutritional signals such as glucose (Recabal *et al.*, 2018). Moreover, the daily variation of peripheral glucose levels was attributed to a SCN-driven circadian reorganization of both tanycytic tight junction

proteins and GLUT1 expression levels influencing ARC glucose responsive neurons (Rodríguez-Cortés *et al.*, 2022). In this way, tanycytes act as a glucose sensor that monitors and relays concentration differences between glucose levels in CSF and the hypothalamic parenchyma, modulating the hypothalamic response to ensure glucose homeostasis.

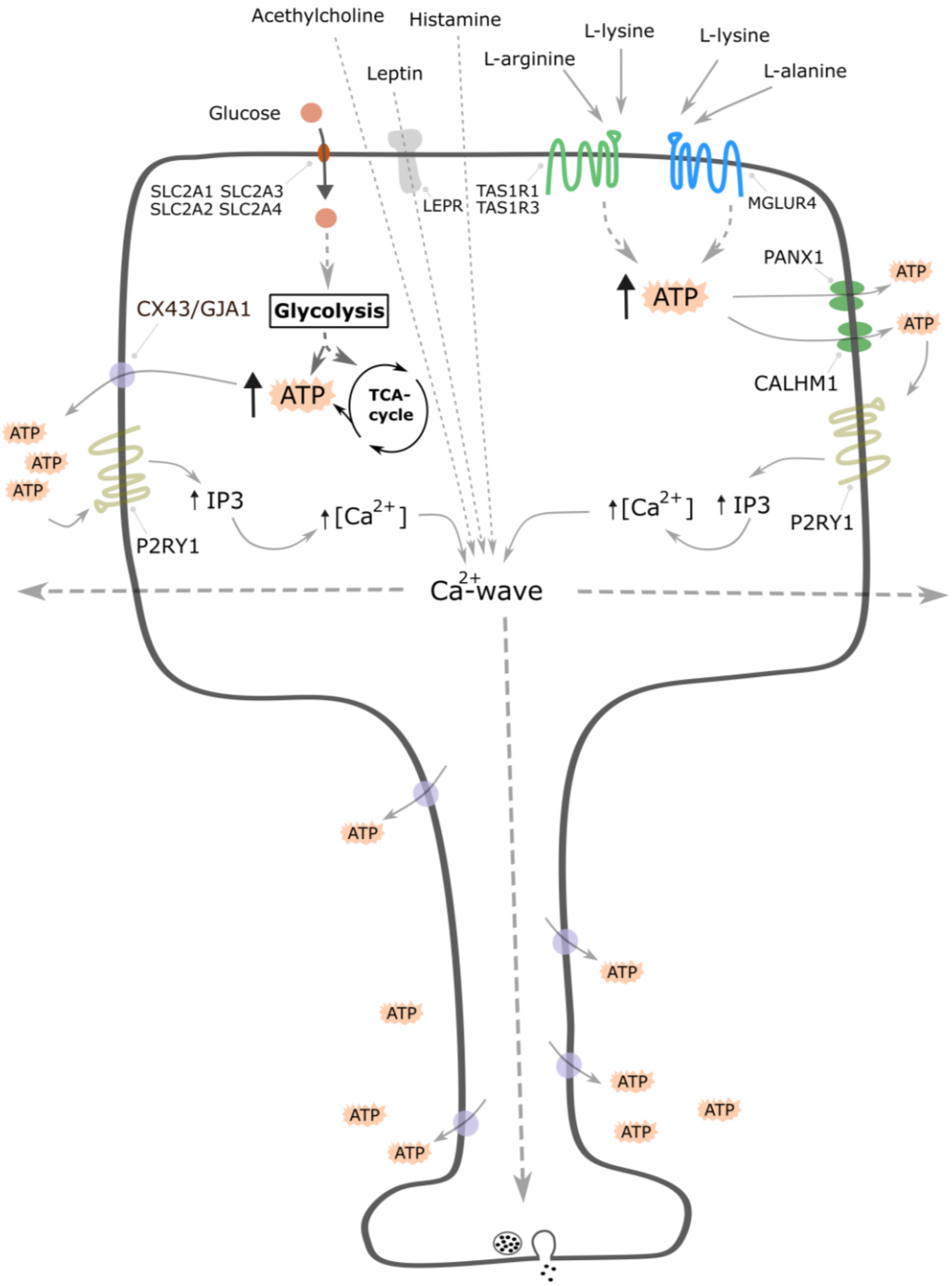

Figure 7 Tanycytes relay metabolic signals in CSF, through ATP-dependant calcium-waves, to hypothalamic neurons. (Legend continues on next page)

Tanycytes transport glucose into the cell by glucose transporters (solute carrier transporter family 2 members 1 to 4 (SLC1-4)) also known as glucose transporters (GLUT1-4). Glucose is then used in the glycolysis to produce adenosine triphosphate (ATP), the cellular energy currency. An increase in cellular ATP concentrations, leads to extracellular transport of ATP through connexin hemichannel 43 (CX43) also known as gap junction protein alpha 1 (GJA1). Further, an increase in extracellular ATP concentration increases the binding affinity to purinergic receptor P2Y, G-protein coupled 1 (P2RY1/P2Y1) leading to subsequent intracellular increases of inositol trisphosphate (IP_3)-dependent release of internal calcium (Ca^{2+}) stores. If the ATP concentration is high enough, the release of calcium will propagate as a calcium wave along the tanycytic process, signalling to brain parenchyma. A similar mechanism of calcium-wave signalling is proposed if amino acids such as histamine, L-alanin, L-arginin and L-lysine binds to the heterodimer taste receptor type 1 member 1 (TAS1R1)/TAS1R3 and Metabotropic glutamate receptor 4 (MGLUR4) also known as Glutamate Metabotropic Receptor 4 (GRM4). Here the ATP is released through pannexin 1 (PANX1) and calcium homeostasis modulator 1 (CALHM1). Before a similar signalling to increased extracellular ATP concentrations through P2ry1 occur. Acetylcholine, Leptin, and histamine, metabolic signals implicated in energy homeostasis and wakefulness, are also shown to elicit a calcium wave in vitro, if puffed onto the tanycytic soma, albeit the mechanism remains elusive. Tanycytes are also shown to form vesicles in their endfeet terminal, likely contributing to synaptic signalling with neurons. TCA-cycle, tricarboxylic acid cycle. Illustration by V.J. Melum. Based on (Frayling, Britton and Dale, 2011; Benford *et al.*, 2017; Lazutkaite *et al.*, 2017; Pasquettaz *et al.*, 2020; Duquenne *et al.*, 2021).

Another way tanycytes contribute to the central regulation of food intake and glucose homeostasis is through active transport of glucose from the CSF to glucose sensitive NPY-neurons in the ARC (Figure 8). By uptake of glucose and phosphorylation to glucose-6-phosphate (G6P), tanycytes transport G6P into the ER by glucose-6-phosphate transporter (G6PT). When inside the ER, it is converted back to glucose by glucose-6-phosphate complex 3 (G6PT3), where glucose is transported along the tanycytic process until secreted out of the cell through a GLUT, in close proximity to glucose-sensitive NPY-neurons (Barahona *et al.*, 2024).

1.5.1.4 Lactate

Opposingly, tanycytes can also decrease food intake by converting glucose to lactate and secrete it in close apposition to lactate-responsive POMC-neurons (Lhomme *et al.*, 2021). Glucose in the CSF is taken up by GLUTs expressed by tanycytes (Figure 8). Through the glycolytic pathway, glucose is metabolized to pyruvate, which again through lactate dehydrogenase A (LDHA) can be converted to lactate. This anaerobic end-product of glycolysis have recently been recognised as an important central signalling molecule and not merely a toxic waste product (for review see: (Magistretti and Allaman, 2018). In tanycytes, monocarboxylates such as lactate are transported out of the cell through monocarboxylate transporter 1, (SLC16A1/MCT1) and 4 (SLC16A3/MCT4). An increase in extracellular lactate concentrations increases the neuronal activity of lactate-responsive POMC neurons which contribute to a reduction in food intake (Lhomme *et al.*, 2021). Hence, tanycytes are shown to be modulators of both orexigenic (appetite inducing) AgRP/NPY- and anorexigenic (appetite suppressing) POMC- neurons through active transport of glucose and lactate (Figure 8).

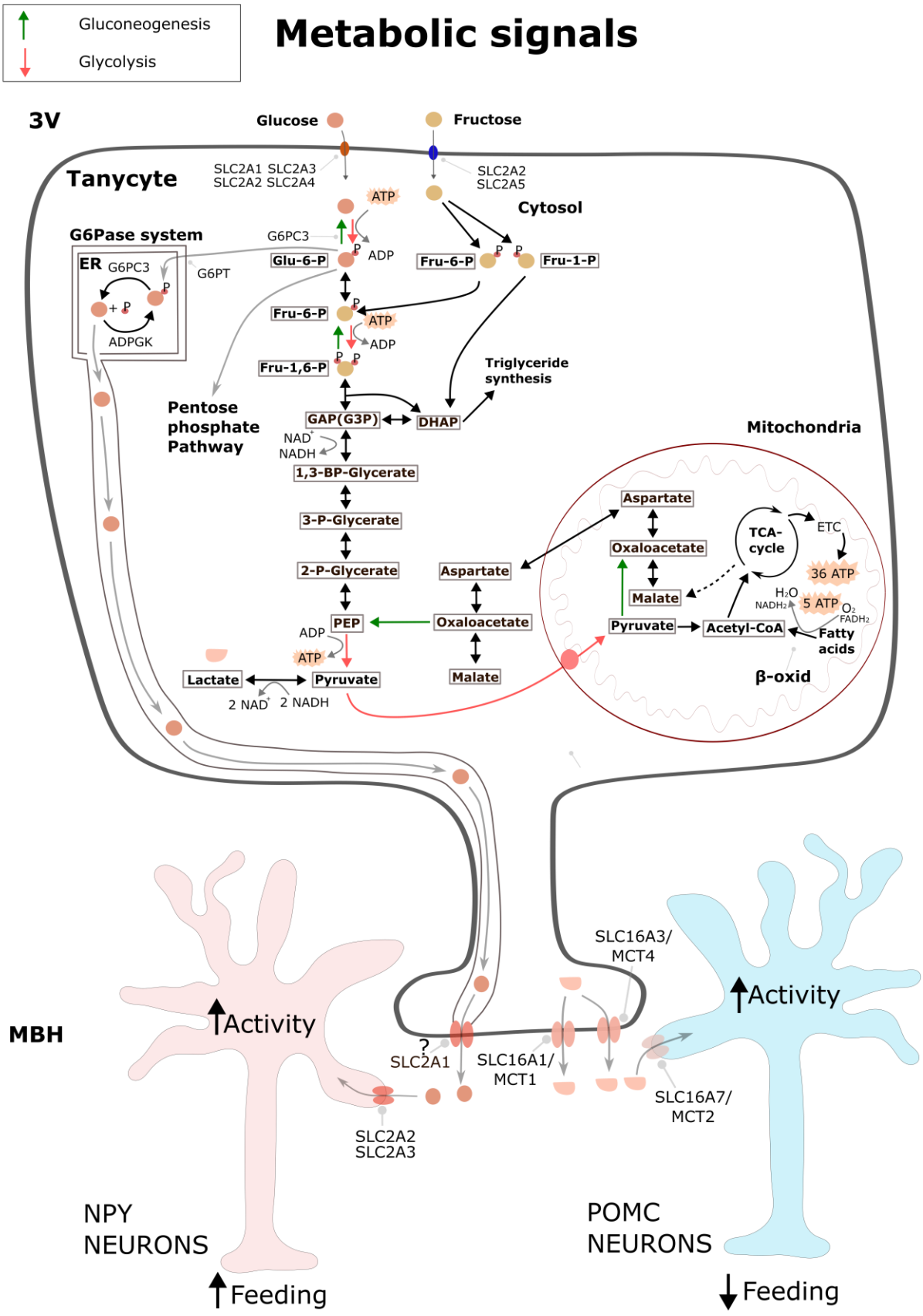

Figure 8 Overview over cellular basis for glucose and lactate signalling in tanycytes, with the proposed influence on hypothalamic neuronal activity. (Legend continue on next page)

Tanycytes transport glucose and fructose into the cell by glucose and fructose transporters (solute carrier transporter family 2 members 1 to 5 (SLC1-5)) also known as glucose transporters (GLUT1-5). Glucose and fructose are then used in the glycolysis to produce adenosine triphosphate (ATP), either anaerobically with lactate as the end-product or aerobically within the mitochondria and the tricarboxylic-cycle (TCA-cycle). Recently, tanycytes have been shown to communicate changes in glucose concentrations of the cerebrospinal fluid to hypothalamic neurons residing in the arcuate nucleus (ARC). First, intracellular glucose is phosphorylated to glucose-6-phosphate (glucose-6-P), but instead of following the normal glycolytic path, the Glucose-6-P is transported into the endoplasmic reticulum (ER) by glucose-6-phospate transporter (G6PT). Here glucose-6-P is dephosphorylated to free glucose by glucose-6-phospate catalytic subunit 3 (G6PC3). This free glucose can travel within the ER until secreted by a glucose transporter. An increase in extracellular glucose is then received by orexigenic neuropeptide Y (NPY) neurons through the SLC2A2 and SLC2A3 and increase the neuronal activity leading to an increased drive to feed. A similar mechanism with opposing effects is proposed for lactate. Here increases in imported tanycytic glucose increases the glycolytic rate and the production of the anaerobic end-product, lactate. Lactate is then shuttled out of the tanycyte through MCT1 and MCT4, increasing the extracellular lactate levels. Anorexigenic proopiomelanocortin (POMC) neurons import lactate through monocarboxylate transporter 2, increasing their neuronal activity which again decrease the drive to feed. Abbreviations: Glu-6-P, Glucose-6-phosphate; Fru-1-P, Fructose-1-Phosphate; Fru-6-P, Fructose-6-Phosphate; Fru-1,6-P, Fructose-1,6-biphosphate; GAP(G3P), Glyceraldehyde 3-phosphate); DHAP, Dihydroxyacetone phosphate;1,3-BP-Glycerate, 1,3-Bisphosphoglycerate; 3-P-Glycerate, 3-Phosphoglycerate; 2-P-Glycerate, 2-Phosphoglycerate; PEP, Phosphoenolpyruvate; TCA-cycle, tricarboxylic acid cycle; β-oxid, β-oxidation; Acetyl-CoA, Acetyl coenzyme A; G6Pase system, Glucose-6-phosphatase system. Illustration by V.J. Melum. Based on (Barahona *et al.*, 2018, 2024; Elizondo-Vega, Recabal and Oyarce, 2019; Lhomme *et al.*, 2021).

1.5.1.5 Fatty acids

To date, there is a limited understanding of how the brain sense and respond to changes in peripheral fatty acid status. However, glial cells, astrocytes and tanycytes are integral in hypothalamic β-oxidation of fatty acids to form ketone bodies and storage of lipids as lipid droplets (Hofmann *et al.*, 2017). Tanycytes are proposed to respond to changes in peripheral circulating fatty acids, palmitate being one of the most abundant in the hypothalamus, through modulation of their secretory activity of Fibroblast growth factor (FGF) 21, a potent metabolic signal regulating energy expenditure and lipolytic activity (Geller *et al.*, 2019). Upon the energetical challenge of fasting, tanycyte alter their metabolism of fatty acids, likely influencing MBH neuronal accessibility and activity (Brunner *et al.*, 2024). More detailed knowledge about tanycytes role in fatty acid sensing, incorporation and response is needed to reveal how hypothalamic fatty acid integration influence energy homeostasis.

1.5.1.6 Sex steroid hormones

Tanycyte morphology has been noted to change with physiological state. Early studies in female rhesus monkeys (*Macaca mulatta*) showed morphological alterations in tanycytes during the menstrual cycle, and a link between morphological changes in tanycytes and a tanycytic modulation of secretory activity of the pars distalis of the pituitary gland was proposed (Anand Kumar and Knowles, 1967; Knowles and Anand Kumar, 1969). More specifically, the size of tanycyte endfeet was observed to have a maximum size in the pre-ovulatory phase and a minimum size during menstruation (Knowles and Anand Kumar, 1969). These morphological changes of tanycytes were, in the female rhesus monkey, experimentally shown to be replicated by gonadectomy and intermuscular injection of oestrogen, demonstrating an endocrine relationship between oestrogen and tanycyte morphology (Knowles and Anand Kumar, 1969). In the year prior, peripheral injections of tritiated oestrogen was shown to be detected in the CSF, enabling CSF to be a window to peripheral gonadal activity (Anand Kumar and Thomas, 1968). Also, in male rhesus monkeys gonadectomy altered tanycyte morphology, and following an injection of testosterone a remodelling towards a gonad-intact male was observed (Knowles and Anand Kumar, 1969). These early observations proposed 3V tanycytes, through CSF sensing properties, to be involved in a hypothalamic-pituitary feedback mechanism involved in regulating reproductive physiology.

More recently, these early observations have been further substantiated. Hypothalamic nerve terminals reside in the ME for neuropeptide release (Figure 6). Once secreted, the neuropeptides follow the hypothalamo-pituitary portal vessels to stimulate or inhibit secretion from endocrine cells in the anterior pituitary gland, regulating gonadal activity. As postulated by Knowles and Anand Kumar, β-tanycytes lining the floor of the 3V interact, through changes in endfeet size and morphology, with the secretory capacity of certain nerve terminals in the ME. Such a function of tanycytes as a physical barrier between the nerve terminal and the fenestrated capillaries in the ME, limiting neuropeptide release, have been reported in both the hypothalamic-pituitary-thyroid axis (Müller-Fielitz *et al.*, 2017) as well as the hypothalamic-pituitary-gonadal axis of both photoperiodic (Yamamura *et al.*, 2004; Wood *et al.*, 2015) and non-photoperiodic species (Prevot *et al.*, 1999; Parkash *et al.*, 2015). Indeed, in female mice, genetical alterations to the molecular mechanism of tanycyte endfeet expansion/retraction is associated with changes in the rhythmicity of the pulsatile release of gonadotropin-releasing hormone (GnRH) neurons in the ME, driving circulatory luteinizing hormone (LH) levels and hence reproductive status (Parkash *et al.*, 2015). In addition, tanycytic relay of peripheral oestrogen status influence the secretory pattern of LH in ovariectomised mice, and a specific deletion of tanycytic oestrogen receptor 1 alpha (ERα) increase body weight, through an increased food intake and decreased energy expenditure (Fernandois *et al.*, 2024). Collectively, tanycytes, through sensing properties, are shown to be dynamic physical barriers regulating neuropeptide release in the ME, constituting a component of a negative feedback loop in hypothalamic-pituitary function.

1.5.2 Evidence for tanycytes of the 3rd ventricle as a stem-cell niche and their contribution to rewiring of neuronal circuits

Neuroepithelial cells form the neural plate in early development. The folding and closing of the neural plate into the neural tube creates the structural characteristics of the central nervous system, with the inside of the tube becoming the ventricular system of the brain and the spinal column (reviewed in: (Stiles and Jernigan, 2010)). During development these neuroepithelial cells elongate and transform into radial glial cells, which have an apical-basal polarity, with their apical part being in contact with the ventricle and basally their long projections are in contact with the pial surface (reviewed in: (Kriegstein and Alvarez-Buylla, 2009)). These radial glial projections are used as guide-wires for newly formed neurons during their migration to destined brain areas (Rakic, 1972). Recent studies have also demonstrated that radial glial cells have stem cell properties (Noctor *et al.*, 2001, 2004).

In early development, radial glial cells undergo symmetric cell division which generates two new radial glial cell, enabling a rapid increase in the pool of radial glial cells. Later on, radial glial cells, through asymmetric cell division, self-renew and produce either a neuronal cell directly, or a progenitor cell. These progenitor cells can differentiate into neurons, astrocytes or oligodendrocytes (Noctor *et al.*, 2001; Noctor, Martínez-cerdeño and Kriegstein, 2008). Towards the end of embryonic development, when the majority of neurons are generated, most radial glial cells detach from the ventricle (apical side) and differentiate into astrocytes and some oligodendrocyte precursor cells. However, a subpopulation of radial glial cells remain attached to the ventricle and retain the ability to divide and produce pluripotent progenitor cells after birth, thereby forming a neural stem cell niche in the sub ventricular zone in the lateral ventricle and in the dentate gyrus of the hippocampus (for review see: (Ihrie and Álvarez-Buylla, 2011; Ming and Song, 2011)). Recently, 3V hypothalamic tanycytes, with their radial glial lineage, have been proposed to be a third site for a stem-cell niche enabling adult neurogenesis (for review see: (Yoo and Blackshaw, 2018)).

In mice, around embryonic day 13, retina and anterior neural fold homeobox (RAX)-expressing radial glial cells lining the tuberal part of the 3V start to differentiate into tanycytes, and by embryonic day 16 the majority of hypothalamic tanycytes are formed (reviewed in: (Placzek *et al.*, 2024)). Coinciding with the neuronal development of the ARC (reviewed in: (Croizier and Bouret, 2022)). After birth, until postnatal day 14, tanycytes in mice apparently retain a limited ability to divide, producing progeny cells that can differentiate into oligodendrocytes, astrocytes or neurons (Yoo *et al.*, 2021). Such ability implies the existence of a tanycytic stem-cell niche, with the potential to generate new cell types, including neurons, beyond the perinatal period. This recent appreciation of a continuous generation of neurons after birth observed in rodents and sheep, challenges the classic neuroscience view of the brain as a static lump of neurons gradually senescing from birth onwards (Kokoeva, Yin and Flier, 2005, 2007; Xu *et al.*, 2005; Hazlerigg *et al.*, 2013; Batailler *et al.*, 2014; Pellegrino *et al.*, 2018). However, it remains

unclear whether adult hypothalamic neurogenesis occurs in primates, including humans, and the topic remains controversial (Eriksson *et al.*, 1998; Bhardwaj *et al.*, 2006; Sorrells *et al.*, 2018; Franjic *et al.*, 2022) reviewed in: (Rakic, 2006; Gould, 2007; Nano and Bhaduri, 2022). Regardless, in rodent species, even if still debated, adult hypothalamic neurogenesis may be a mechanism in which the brain adapt and respond to changing energetic demands.

High fat diet is one environmental factor that has been shown to induce the incorporation of peripheral injected bromodeoxyuridine (BrdU), a marker for cell division (Dolboare 1995, Wojtowicz and Kee 2006), in cells positive for the HuC/D-protein, a neuronal marker (Graus and Ferrer 1990), in the ME of adult (postnatal day 45 and 75) mice (Lee *et al.*, 2012). With the use of a transgenic mouse line nestin-positive cells, a tanycyte marker, were labelled by yellow fluorescent protein (YFP) upon injection of tamoxifen on postnatal day 4 (Lee *et al.*, 2012). At postnatal day 35, these YFP-positive cells co-labelled with markers for HuC/D-protein, indicative of a tanycytic capacity to express neuronal features in the ME (Lee *et al.*, 2012). Further, if the rate of neurogenesis in the whole area was reduced by focused radiation, the animals increase their activity and total energy expenditure (Lee *et al.*, 2012). The disruption of the lower part of the MBH (including PT, ME, ARC, VMH and tanycytes) through radiation is to crude to pin-point that tanycytes is the sole origin of this response, but indicate neurogenesis in the ME as a response to dietary signals.

The FGF family has been suggested as a cue stimulating tanycyte neurogenesis (Robins *et al.*, 2013). This family include 18 different factors (FGF1-10 and FGF 16-23), which are involved in a multitude of developmental processes (for review see: (Beenken and Mohammadi, 2009)). In recombinant adult mice, ICV injection of FGF and BrdU increased α2-tanycyte BrdU incorporation relative to controls, indicative of a higher number of proliferating tanycytes (Robins *et al.*, 2013). Further, in *ex vivo* slice cultures newly formed neurospheres (neural progenitor cells) along the 3V was shown to be derived from α2-tanycytes, making a case for this tanycyte population as the principal site for an adult stem-cell niche, in contrast to Lee et al. 2012 which ascribed this to the β-tanycytic region (Lee *et al.*, 2012; Robins *et al.*, 2013). This discrepancy could be due to the difference in BrdU injection, with peripheral injection being more accessible to the β2-tanycytes, while ICV injection being accessible to all tanycyte subtypes (reviewed in: (Dietrich and Horvath, 2012; Lee and Blackshaw, 2012). In tanycyte cultures, treatment with FGF2 increase tanycyte proliferation (measured as BrdU incorporation), a response attenuated if the function of either P2RY1 or CX43 is blocked (Recabal *et al.*, 2021). However, no *in vivo* increase in tanycytic BrdU incorporation was evident after seven days of ICV FGF infusion, albeit the effect of FGF might have been masked by a small sample size (Recabal *et al.*, 2021). How tanycyte proliferation is linked to FGF and dietary-cues is still incompletely understood. However, previous studies inhibiting the function of FGFR1C have demonstrated decreases in food intake and body weight in mice, rats, hamsters and rhesus monkeys (Sun *et al.*, 2007; Samms *et al.*, 2015).

With the use of genetically engineered models and high-throughput sequencing methods, Yoo et al. recently demonstrated tanycytes capacity to differentiate into neurons (Yoo *et al.*, 2021). As an expansion to their recent work in retinal Müller glia they show that also in tanycytes a similar suppressive action of nuclear factor one family transcription factors (*Nfia/b/x*) on neurogenesis (Clark *et al.*, 2019; Hoang *et al.*, 2020). The selective loss of function of *Nfia/b/x* in tanycytes at postnatal day 3-5 results in increased neurogenesis, through the sonic hedgehog and Wnt signalling pathway, in the ventricular zone and hypothalamus of juvenile mice (postnatal day 17 and postnatal day 45). To understand the identity and the functional role of the tanycyte derived neurons (TDN), the authors used scRNAseq data of control mice and tanycyte *Nfia/b/x*-deficient mice at postnatal day 8, 17 and 45. These data revealed several neuronal clusters/subsets which corresponded to progenitor cells, glutamatergic and GABAergic subtypes. The clusters resemble neuronal subtypes found in the ARC, VMH and DMH. It is worth noting that in the control animals, only modest expressions of these subtypes were present at postnatal day 8, and the importance of *Nfia/b/x* transcription factors in normal regulation of post-natal neurogenesis is unclear.

Further, to nail down the functionality of these TDN, they show them to be able to receive synaptic input and fire action potentials. Albeit the firing pattern seem to plateau after some spikes in both young and adult TDN. At postnatal day 45, a subset of TDNs express leptin receptor (*Lepr*), and respond to intra peritoneal injection of leptin. The phosphorylation of signal transducer and activator of transcription 3 (STAT3) response was evident both in TDNs in the DMH, ARC and the subventricular region, which indicate that the TDNs have a classical neuronal response to leptin, leading to a cascade of down-stream effects involved in regulating energy balance. Further, within the DMH, a four-hour heat stress (38 °C) elicited a comparable response, measured as cFOS, in TDN as in control neurons, highlighting TDN to be functional and responsive to acute environmental conditions influencing energy homeostasis (Yoo *et al.*, 2021). Interestingly, previous laboratory studies have shown neurogenesis in the tanycytic region to be required for an appropriate heat acclimatisation to continuous moderate heat-exposure (32 °C) ((Matsuzaki *et al.*, 2009, 2015, 2017), reviewed in: (Yoo and Blackshaw, 2018)). Together, this shows that TDNs produced by knocking out *Nfia/b/x* in tanycytes have functional capacity to respond to temperature and leptin potentially implicating TDN in hypothalamic energy homeostasis. But conclusive demonstration of the role of TDN in energy homeostasis or in energy status is lacking, and would require cell lineage tracking techniques to be certain.

1.5.3 Summary

Clearly, there are many studies demonstrating a role for tanycytes in hypothalamic control of energy balance. However, specific tanycyte ablation only leads to subtle phenotypic changes in animals that are fed *ad libitum* and within their thermoneutral zone (Yoo *et al.*, 2020). Therefore, the evidence in non-seasonal mice and rats points to the importance of tanycyte function upon energetic challenge (high-fat diet, food restriction or temperature challenge). This emphasises homeostatic energy balance as a major tanycyte function in a non-seasonal animal (Yoo *et al.*, 2020; Porniece Kumar *et al.*, 2021; Rohrbach *et al.*, 2021; Yu *et al.*, 2023; Benevento *et al.*, 2024).

1.6 Tanycytes in a seasonal context

1.6.1 Seasonal TSH-dependent influences of tanycyte conversion of thyroid hormone

The function of tanycytes is modulated on a seasonal scale. As noted in section **1.4**, seasonal changes in TSH secretion by the PT act through TSH receptors on the tanycyte (Figure 5). Tanycytes respond to changes in TSH levels by altering the local bioavailability of thyroid hormone (TH) which in turn has been linked to seasonal reproduction and metabolism (Barrett *et al.*, 2007; Hanon *et al.*, 2008; Sáenz de Miera *et al.*, 2014; Sáenz de Miera *et al.*, 2017) (Figure 9). This is achieved by changes in the expression and hence the activity of the enzymes responsible for the conversion of thyroxine (T4) into active or inactive forms (type II iodothyronine deiodinase (DIO2)/ type III iodothyronine deiodinase (DIO3)) (Hazlerigg and Simonneaux, 2015). Under LP elevated TSH levels promotes increased DIO2 enzymatic activity, which converts T4 into the more biologically active form, triiodothyronine (T3) by outer ring deiodination. Concomitantly, LP exposure induced a reduced expression of DIO3, the enzyme responsible for converting T4 to reverse T3 by inner ring deiodination, and this further increases T3 levels under LP. These enzyme dynamics are reversed when TSH levels are low under SP, creating a low TH environment in the MBH (for review see: (Hazlerigg and Loudon, 2008; Dardente, Hazlerigg and Ebling, 2014)). This TSH-driven reciprocal regulation of tanycytic DIO2/DIO3 enzymatic activity, and hence MBH TH bioavailability is a conserved mechanism underlying seasonal physiology in mammals and birds (Hanon *et al.*, 2008; Nakao *et al.*, 2008).

In sheep, there is direct evidence for a dose dependant *Dio2* RNA expression based on TSH (Hanon *et al.*, 2008). Application of TSH in cell culture of ovine PT/ME cultures, including β2-tanycytes, induced a dose-dependent increase in cAMP as well as increased *Dio2* RNA expression. Since forskolin, a cAMP stimulant, mimicked the same increase in *Dio2* RNA expression, TSH likely alter *Dio2* RNA expression through a cAMP-dependant pathway (Hanon *et al.*, 2008). Further, TSH infusion into the lateral ventricle induce *Dio2* RNA expression in SP adapted sheep, demonstrating TSH to be the link between melatonin responsive PT thyrotrophs and TH modulating tanycytes (Hanon *et al.*, 2008). Also, in SP adapted hamsters, infusion of TSH ICV increase *Dio2* RNA expression in tanycytes (Klosen *et al.*, 2013). This suggests that TSH-signalling is a conserved neuroendocrine relay coupling photoperiod and melatonin, to hypothalamic regulation of metabolic phenotype and reproductive status.

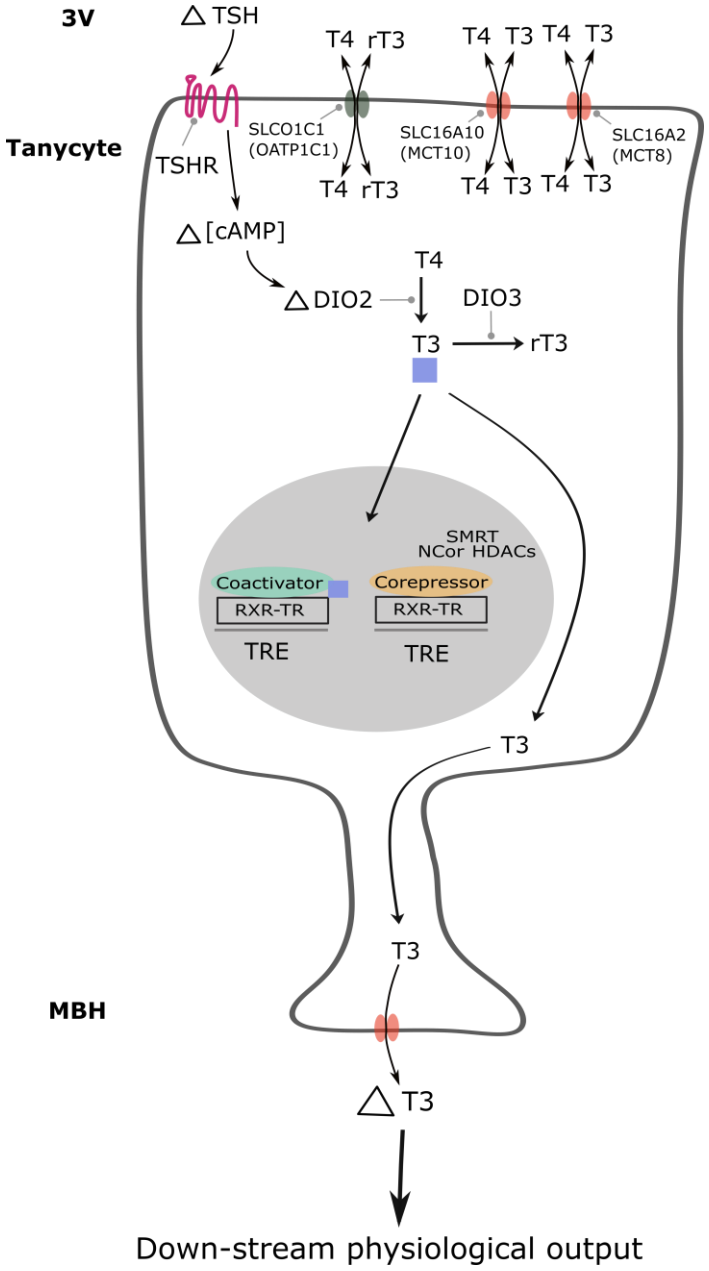

Figure 9 Overview over central regulation of thyroid hormone bioavailability by tanycytic enzymatic activity in the medio-basal hypothalamus (MBH) as a response to thyroid stimulating hormone (TSH). Tanycytes are able to import both inactive (thyroxine (T4) and reverse triiodothyronine (rT3)) and active (triiodothyronine (T3)) forms of thyroid hormone through solute carrier organic anion transporter family member 1C1 (SLCO1C1/OATP1C1), Monocarboxylate transporter 8 (SLC16A2/MCT8) and SLC16A10/MCT10. Within the cell, the enzymatic activity of type Ⅱ iodothyronine deiodinase (DIO2) and type Ⅲ iodothyronine deiodinase (DIO3) regulates the cellular levels of active T3, which binds to thyroid response elements (TRE) in the nucleus and modulate transcription/translation, and hence cellular function. The increase in TSH during long photoperiods binds to TSH-R and increase the cellular concentration of cyclic adenosine monophosphate (cAMP) inducing DIO2 expression. The TSH dependence of DIO3 activity is less known. Tanycytes can also transport T3 out of the cell into the MBH to influence neuronal activity, the details of this transport action in seasonal species remains elusive. Illustration by V.J. Melum.

Since TSH similarly drives tanycyte deiodinase activity in both long- and short-day breeding species, the seasonal regulation of reproduction is likely down-stream of changes in hypothalamic TH (Hanon *et al.*, 2008; Klosen *et al.*, 2013). Recent evidence suggests that kisspeptin and arginine-phenylalanine-amide (RFamide)-related peptide (RFRP) expressing neurons in the MBH may be key to understanding species-specific regulation of seasonal breeding (for review see: (Henningsen, Gauer and Simonneaux, 2016)). In LP-breeders, an increased expression of RFRP-neurons under LP, leads to an activation, either direct or indirect via kisspeptin expressing neurons, of the GnRH neurons which again stimulate increased luteinizing hormone (LH) and follicle stimulating hormone (FSH) secretion from the pituitary, initiating reproductive physiology. Infusion of TSH ICV in SP-adapted hamsters increase the expression of kisspeptin and RFRP expressing neurons, likely following an increase in tanycyte DIO2 activity, which leads to an activation of the reproductive axis (Klosen *et al.*, 2013). In species that breed under SP, RFRP-neurons also show elevated expression during LP, but this does not activate the reproductive axis, and instead decrease in RFRP-expression is associated with reproductive competence in sheep (Clarke *et al.*, 2008; Sari *et al.*, 2009). Hence, it is evident that the down-stream pathways coupling seasonal changes in deiodinase activity to the reproductive axis remain incompletely understood.

The TSH-dependent tanycytic modulation of hypothalamic TH levels also influence metabolism. In Siberian hamsters the SP response with a decrease in body weight, pelage change and daily torpor on-set is blocked in animals given a hypothalamic T3 implant (Barrett *et al.*, 2007; Murphy *et al.*, 2012). Similarly, intrahypothalamic infusion of T3 acutely supresses torpor expression, in SP-acclimated Siberian hamsters, albeit in some animals a shallow torpor episode is observed (Bank *et al.*, 2017). The infusion of T3 results in increased *Dio3* RNA expression, presumably in tanycytes, compared to SP-adapted animals infused with Ringer solution, suggesting that the TSH-driven tanycyte program (High DIO3, low TH) tries to compensate for exogenous delivery of T3 (Bank *et al.*, 2017). Given the observed ability of TH manipulations to modulate the utilization of metabolic depression in Siberian hamsters, it is tempting to speculate that the hypothalamic TH environment influence the thermoregulatory system. In the non-photoperiodic rat, an increase in hypothalamic T3 infusion both ICV and intrahypothalamic to the VMH, increase the thermogenic drive to BAT, and hence modulate energy homeostasis (López *et al.*, 2010; Alvarez-Crespo *et al.*, 2016). Intriguingly, changes in the cellular activity of the tanycyte layer, as assayed by cfos RNA expression, have been shown to precede changes in T_b in hibernating species (Bratincsák *et al.*, 2007; Markussen *et al.*, 2024). Recently, central hypothalamic infusion of T3 was shown to increased food intake in the IBE period of a fat-storing hibernator, however, whether than animal re-entered hibernation was not reported, nor were effects on T_b (Mohr *et al.*, 2024). The evidence for seasonal rheostatic changes in metabolism and reproduction via tanycyte TH conversion in multiple species is strong (reviewed in: (Dardente *et al.*, 2019)), and while there is an indication that acute regulation affects thermoregulatory function, how this links to seasonal rheostatic control is unknown.

1.6.2 Seasonal changes in the retinoic acid pathway

Photoperiodic responses of tanycytes are not limited to changes in the deiodinase enzymes controlling TH conversion, genes related to the retinoic acid (RA) pathway are also altered (reviewed in: (Shearer, Stoney, Morgan, *et al.*, 2012)). Unlike the DIO-TH pathway (**1.6.1**), the TSH-dependence of the RA pathway has not been clearly demonstrated and it has only been reported in rodents (Ross *et al.*, 2004; Barrett *et al.*, 2006; Shearer *et al.*, 2010; Helfer *et al.*, 2012). In both Fischer-344 (F-344) rats (a photoperiodic subspecies of *Rattus norvegicus*) and Siberian hamsters changing photoperiod alters the gene expression of key enzymes involved in RA synthesis (Figure 10) (Ross *et al.*, 2004; Shearer *et al.*, 2010). This suggests photoperiodic changes in RA bioavailability in the hypothalamus controlled by the tanycyte which is the only cell type in the MBH possessing all the key enzymes for the RA pathway (Ross *et al.*, 2004; Shearer *et al.*, 2010; Helfer *et al.*, 2012; Helfer, Barrett and Morgan, 2019). Using a dissociated hypothalami and a RA reporter gene system to assess RA activity, it was demonstrated that LP F-344 rats had a higher RA activity (Helfer *et al.*, 2012).

T3 can induce the expression of genes in the RA pathway potentially enhancing synthesis (*Aldh1a1* and *Cyp26a1*) (Stoney *et al.*, 2016; Olson and Krois, 2019). This suggests a TH dependence on the RA pathway, and therefore an indirect consequence of altered TH environment stimulated by photoperiodically regulated TSH. However, experiments with improved temporal resolution to separate cause and effect are warranted. The actions of TH and RA are linked through receptor interaction and common transcriptional response elements (Umesono *et al.*, 1988; Graupner *et al.*, 1989; Zhang *et al.*, 1992). As with TH there is a large literature on the functions of RA which link it to development, cell division, cell differentiation, and metabolism (reviewed in: (Maden, 2007; Niederreither and Dollé, 2008)). Chemerin has received attention because it is a down-stream target of RA and an adipokine associated with body weight and obesity in humans (Bozaoglu *et al.*, 2007). In a seasonal context both the gene encoding chemerin (Rarres2) and its receptor (*Ccrl2*) are expressed in the tanycytes and have an increased expression on LP (Helfer *et al.*, 2016). Giving chemerin ICV for 2 weeks to SP F-344 rats mimicked LP induced changes in food intake and reduced POMC and AGRP gene expression ((Helfer *et al.*, 2016), (reviewed in: (Helfer and Wu, 2018)). Whereas chemerin administered acutely to animals on 12:12 showed a 1°C change in core body temperature (Helfer *et al.*, 2016). The role of chemerin as a "tanykine" (Bolborea and Langlet, 2021), a secreted product of the tanycyte having a direct effect on energy balance, is an interesting possibility but remains unproven, and in a seasonal context it requires further characterisation.

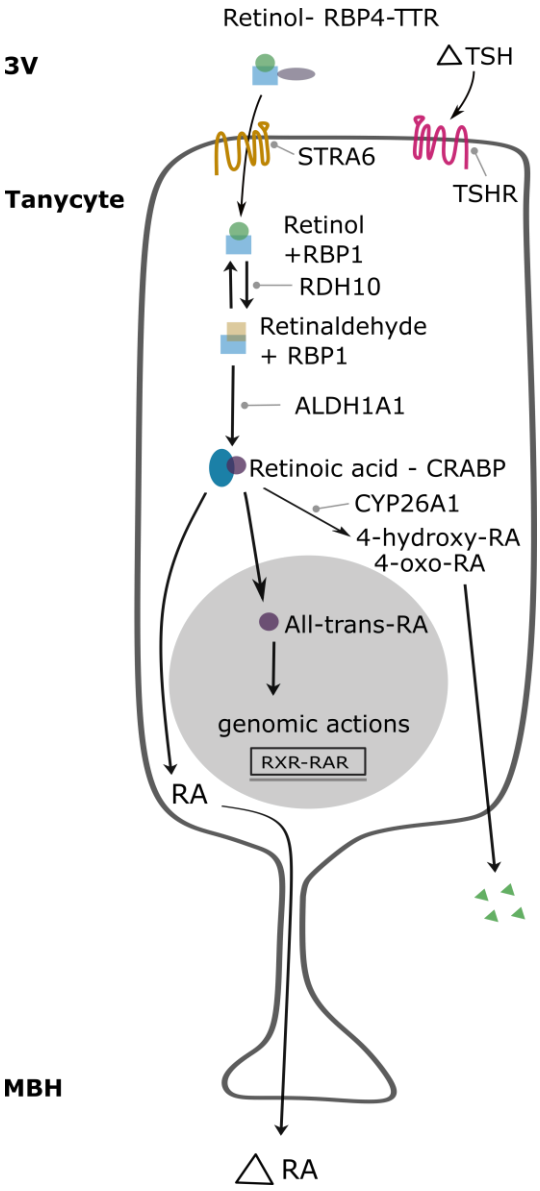

Figure 10 Overview over central regulation of retinoic acid bioavailability by tanycytic enzymatic activity in the medio-basal hypothalamus (MBH). Tanycytes express signalling receptor and transporter of retinol STRA6 (STRA6) which import retinol. Inside the cell, retinol is bound to retinol binding protein 1 (RBP1). Through various retinol dehydrogenases (RDH) retinol is converted to retinaldehyde before aldehyde dehydrogenase 1 family member A1 (ALDH1A1/RALDH1) makes it into retinoic acid (RA), the bioavailable form of retinol. While in the cytoplasm RA is bound to cellular retinoic acid binding protein (CRABP). When translocated to the nucleus RA is undergoing a structural change, before binding to the heterodimer of retinoid-x-receptor (RXR) or retinoid acid receptor (RAR) inducing changes in transcription and translation. RA can in the cytoplasm be degraded by Cytochrome P450 family 26 subfamily A member 1 (CYP26A1) to form polar metabolites such as 4-hydroxy-RA and 4-oxo-RA which can then be transported out of the cell, limiting, the cellular actions of RA. Alternatively, RA, as a lipophilic compound, can exert paracrine signalling if moving out of the cell. Abbreviations: TSH, thyroid stimulating hormone; TSHR, TSH-receptor; TTR, transthyretin. Illustration by V.J. Melum.

1.6.3 Seasonal morphological changes in tanycytes

In addition to the seasonal enzymatic changes, tanycyte morphology depend on photoperiod (reviewed in: (Dardente *et al.*, 2019)). In SP-adapted Siberian hamsters, tanycytes show a reduced expression of intermediate filament proteins (vimentin and nestin) and neural cell adhesion molecule, in their basal bodies and processes, indicative of a photoperiodic change in tanycyte contact with blood vessels and neurons in the MBH (Kameda, Arai and Nishimaki, 2003; Barrett *et al.*, 2006; Bolborea *et al.*, 2011). Further, in both quail and sheep, a retraction of tanycyte endfeet is observed during the breeding season, increasing the pericapillary space for the release of GnRH from nerve terminals (Yamamura *et al.*, 2004; Wood *et al.*, 2015). As mentioned in section **1.5.1.6** Sex steroid hormones, such a remodelling of tanycytes as a physical barrier is observed during the oestrus cycle in rhesus monkeys and laboratory mice and rats (Knowles and Anand Kumar, 1969; Prevot *et al.*, 1999; Parkash *et al.*, 2015), suggesting tanycyte remodelling to be a part of the seasonal gating of reproduction, with the metabolic requirements that follow. Finally, administration of chemerin, as discussed above, has also been shown to lead to hypothalamic remodelling, based on increased vimentin staining (Helfer *et al.*, 2016).

1.6.4 Evidence for seasonal neuro/gliogenesis in the hypothalamus

The so-called "cyclical histogenesis" hypothesis of circannual timing puts forward that circannual rhythms are generated by cycles of cell division, differentiation and cell death (Hazlerigg and Lincoln, 2011). This hypothesis is not exclusive to the brain but as the hypothalamus and pituitary link the photoperiodic signal and the circannual clockwork focusing on "histogenic" regions in the MBH is suggested by the authors (Hazlerigg and Lincoln, 2011). In sheep, an increase in hypothalamic cell proliferation is observed under SP (Migaud *et al.*, 2011; Hazlerigg *et al.*, 2013; Batailler *et al.*, 2018). The cell-type specifics and origin of these increased proliferation levels remains to be determined. Less evidence is available for photoperiodic changes in hypothalamic proliferation levels in rodents, but in golden hamsters an increased BrdU incorporation in the ependymal layer is noted under SP compared to LP (Huang, DeVries and Bittman, 1998). In F-344 rats, the ependymal layer show increased numbers of the proliferation marker Ki67 under SP (Shearer, Stoney, Nanescu, *et al.*, 2012). Collectively, the source and temporal dynamics of hypothalamic cell proliferation awaits further investigation to resolve the importance in seasonal metabolic regulation. But given the literature on tanycytes as a stem cell niche (see section **1.5.2**) and their importance in both the photoperiodic control (see section **1.4**) and circannual processes (Sáenz de Miera *et al.*, 2014) an focus on these cells is warranted.

1.6.5 Seasonal changes in circulating signals potentially sensed by tanycytes

1.6.5.1 Leptin

In the Siberian hamster, circulatory plasma levels of leptin follow the seasonal body weight cycle, with a minimum in SP-adapted hamsters (Atcha *et al.*, 2000; Horton *et al.*, 2000). Albeit the normal acute

homeostatic response to decreased leptin levels (i.e. increased orexigenic drive in the AgRP/NPY- ARC neurons) is not observed, known as the "leptin paradox" ((Rousseau *et al.*, 2002), reviewed in: (Ebling, 2014)). For the golden hamster, with a minimal seasonal change in body weight, the plasma levels of leptin do not differ between LP-adapted and 11 weeks SP-adapted hamsters (Horton et al. 2000). However, in another experiment, with a lower body mass baseline, a tendency for a reduced fat mass was associated with a plasma leptin level decrease in six week SP-adapted golden hamsters (Weitten *et al.*, 2013). Following a neonatally monosodium glutamate deletion of the majority of ARC-neurons (~80%), presumably altering leptin-responsive neurons, male Siberian hamsters still decrease their body weight as a response to SP (Ebling *et al.*, 1998). Recently, thirteen-lined ground squirrels were shown to have a reduced leptin signalling (measured as phosphorylated STAT3 expression) during hibernation, despite increased circulating leptin levels and comparable *Lepr* in ARC POMC neurons (Mohr *et al.*, 2024). Given tanycytes role in leptin entry into the ARC (Duquenne *et al.*, 2021), the importance of tanycytes in the rheostatic control of food intake and body weight regulation needs further exploration.

1.6.5.2 Ghrelin

The current understanding of ghrelin and seasonal changes in food intake and body weight is incomplete. In golden-mantled ground squirrel (*Callospermophilus lateralis*, also named *Citellus lateralis*), an increase in plasma levels of ghrelin is observed during the pre-hibernal fattening period compared to summer and winter measurements (Healy *et al.*, 2010). However, ghrelin in torpor and IBE is comparable to summer measurements (Healy *et al.*, 2010). Absolute plasma levels may not be the key factor as ghrelin resistance in the hibernation period has been demonstrated in thirteen lined ground squirrels (Mohr *et al.*, 2024). Given the attenuated hyperphagic response to peripheral ghrelin in transgenic mice with a defect tanycytic insulin receptor (Porniece Kumar *et al.*, 2021), tanycytes role in the observed seasonal ghrelin resistance awaits further investigation.

1.6.5.3 Glucose

In photoperiodic species, changes in plasma glucose relates to the seasonal metabolic strategy used. For instance, in Siberian hamsters no photoperiodic difference in blood glucose levels is observed, and the induction and termination of both spontaneous and food restricted daily torpor seems not to be driven by changes in glycemia (Diedrich *et al.*, 2023). But in golden hamsters, a food-storing hibernator, glucose levels increase after six weeks under SP prior to hibernation on-set (Weitten *et al.*, 2013). During hibernation, golden hamster plasma glucose levels fluctuate with the T-A cycle, relating to re-feeding in the IBE ((Weitten *et al.*, 2013), reviewed in: (Giroud *et al.*, 2021)). In fat-storing hibernators, such as the thirteen-lined ground squirrel, the whole hibernation period is considered to be in a fasting state, and an decrease in plasma glucose levels is observed (Mohr *et al.*, 2024). These differences in metabolic strategy all require a tight regulation of glycemia, and how this is achieved at different levels at different seasonal states is still incompletely understood. Given tanycytes seasonal change in enzymatic activity and subsequent change in hypothalamic TH availability (section **1.6.1**), and the demonstration that

infusion of T3 ICV in rats increase blood glucose levels (Klieverik *et al.*, 2009), an improved characterization of tanycytes role in seasonal glucose homeostasis or rheostasis is needed.

1.6.5.4 Fatty acids

In species that display a pronounced seasonal cycle of feeding and body weight, it is expected to be changes in plasma levels of fatty acids. Early on, tissues of hibernators were shown to increase in unsaturated fatty acid composition prior to the hibernation period (Lyman *et al.*, 1982). Manipulation of the composition of fatty acids in the diet of chipmunks (*Eutamias amoenus*) is noted to influence minimal T_b and torpor bout duration (Geiser and Kenagy, 1987). In the heart of golden hamster, unsaturated fatty acid composition is noted to correlate with sarcoplasmic reticulum calcium activity and minimal T_b (Giroud *et al.*, 2013). These studies indicate the importance of fatty acids composition in the cellular lipid membrane layer for an appropriate function at low temperature in hibernators (reviewed in: (Arnold *et al.*, 2015)). Fatty acids as an energy substrate vary with metabolic state in golden hamsters, with high levels of free fatty acids in torpor, and reduced upon euthermia, inverse to that of triglycerides (Weitten *et al.*, 2013). How and if tanycytes sense and respond to these changes in circulating fatty acids in photoperiodic species is to my knowledge unknown.

1.6.5.5 Neuromedin U

Neuromedin U (NMU) is a neuropeptide found in the brain whose function is not well known. However, fasting in laboratory mice, increase nmu expression in the DMH (Graham *et al.*, 2003). And infusion of NMU ICV into fasted Male Sprague Dawley rats decreases food intake and body mass, while increasing T_b and energy expenditure (Ivanov *et al.*, 2002). Under LP NMU protein levels in the PT in photoperiodic F-344 rats are increased (Helfer *et al.*, 2012). Importantly, the receptor of neuromedin U (NMUR2) is expressed on tanycytes and also shows higher expression on LP (Helfer *et al.*, 2012; Helfer, Ross and Morgan, 2013). LP housed F-344 rats show increased body mass which appears to contradict the results from the non-photoperiodic laboratory rats with ICV NMU infusion. The discrepancy between observed expression levels and expected expression levels given metabolic state echoes the “leptin paradox” observed in seasonal species (reviewed in: (Ebling, 2014; Appenroth and Cázarez-Márquez, 2024), and may indicate an altered tanycyte receptor sensitivity to NMU. Interestingly, ICV infusion of NMU in SP-adapted F-344 rats leads to a decrease in food intake, body weight and an increase in T_b, concomitantly with an upregulation of *Dio2* RNA expression potentially linking back to TH availability.

1.6.5.6 Sex steroid hormones

Photoperiodic species confine reproduction to favourable times of the year. This seasonal gating of reproductive activity, makes a seasonal profile of circulating sex steroid hormones (Hoffman, Hester and Towns, 1965; Darrow, Yogev and Goldman, 1987; Darrow *et al.*, 1988). In sheep, oestradiol and progesterone influence the RNA expression of certain tanycytic genes, indicative of a role for sex steroid

feedback on tanycyte function (Lomet *et al.*, 2020). How tanycytes sense and respond to these seasonal changes in circulating sex steroid hormones is incompletely understood.

1.7 Current knowledge gaps

Tanycytes are emerging as acute sensors of metabolic feedback and potentially important regulators of hypothalamic control of physiology. This hypothalamic control of physiology is best demonstrated in seasonal animals, where tanycytic conversion of thyroid hormone drives seasonal changes in reproduction and metabolism. Despite the strongest phenotype being in seasonal animals, most research into the mechanisms underlying tanycyte function has been conducted in non-seasonal models (i.e. laboratory mice and rats), because of the better availability of methodological tools in these species.

Consequently, while number of interesting mechanisms of action have been implicated by non-seasonal studies (e.g. nutrient sensing, neurogenic regulation and control of blood-CSF barrier permeability), it is unclear to what extent these contribute to the rheostatic changes seen in the seasonal context. Therefore, I will in this thesis investigate tanycytes in seasonal animals to better understand how they can modulate metabolic feedback, and potentially act as a rheostat.

2 Research aims

To understand the functional role of tanycytes as mediators for changes in metabolic state, it is first necessary to characterise changes in tanycyte biology in animals as they undergo such metabolic changes. During my doctoral studies I did this by utilizing two different seasonal paradigms that shift energy metabolism: maternal photoperiodic programming (Siberian hamster) and hibernation (Golden hamster). In combining these animal models with LASER capture microdissection (LCMD) RNAseq and physiological measurements at various timepoints throughout the seasonal life cycle of the animals. In this thesis I aimed to:

1) Synthesise the current knowledge on the phenomenon of maternal photoperiodic programming, specifically relating to the role of tanycytes in this phenomenon;
2) Characterise the molecular signature of tanycytes during a maternal photoperiodic programming paradigm;
3) Set up a hibernation paradigm and research tools for physiological monitoring;
4) Characterise the tanycytic transcriptome during a hibernation paradigm;

The first objective is achieved in **Paper I**, where we collated the relevant literature on maternal photoperiodic programming in a mini-review. Next, the second objective is addressed in **Paper II**; here we utilised a maternal photoperiodic programming protocol to reveal how the *in utero* programming of the pups results in different sensory characteristics of the tanycytes when the pups have committed to distinct metabolic strategies. The third objective is met in **Paper III**, by use of a photoperiod and temperature manipulation protocol to induce hibernation, with refined telemetric monitoring of physiological status. Further, the fourth objective is addressed in **Paper IV**, where the tanycytic transcriptional profile was studied in distinct metabolic states prior, during and after the hibernation season of golden hamsters.

3 Results

3.1 Paper I: Maternal Photoperiodic Programming: Melatonin and Seasonal Synchronization Before Birth

Paper I is a review published in "Frontiers in Endocrinology" (doi: 10.3389/fendo.2019.00901). The objective of the review was to synthesise the current knowledge of tanycytes role in the phenomenon of MPP.

In brief, MPP is a phenomenon where, during gestation, offspring are metabolically programmed to match their post-natal development to predicted, forthcoming environmental conditions. The offspring is programmed to follow either an accelerated or decelerated developmental trajectory, with differing time of pubertal onset. This phenomenon is seen in some rodent species living in habitat with seasonally fluctuating food availability and thermal demand, and is thought to ensure offspring survival, and increase chances of reproductive success (Negus, Berger and Forslund, 1977; Negus, Berger and Pinter, 1992; Lee, 1993; Gower, Nagy and Stetson, 1994). However, for the programming to be correct, one is to be initiated during spring and summer with favourable times ahead, where growth and sexual maturation is ramped up. While the other is to be initiated during autumn and winter when the cost of living is high, where growth is slowed down and sexual maturation delayed until next spring. To match these two distinct developmental trajectories with the appropriate season, requires precise information about the forthcoming time period. Earlier studies demonstrated that the mother's exposure to daylength changes, is mirrored in her melatonin profile. The melatonin crosses the placental barrier and acts on the developing foetal brain (reviewed in: (Horton and Stetson, 1992; Horton, 2005)). Since the foetus does not synthesise its own melatonin but has functional melatonin receptors, the mother's melatonin acts as a window to the external world to indicate direction of seasonal change. A recent study showed that this change in melatonin duration, via TSH secretion, programs the tanycyte layer *in utero* to initiate a fast or slow developmental trajectory (Sáenz de Miera *et al.*, 2017). The programming that occurs during gestation, determines how the tanycytes, and the offspring respond to changes in daylength after weaning through altering the sensitivity to the TSH signal. The review summarises the evidence that this changing sensitivity of tanycytes to TSH gives photoperiodic history-dependence to the MPP phenomenon.

3.2 Paper II: Hypothalamic tanycytes as mediators of maternally programmed seasonal plasticity

Paper II is published in "Current Biology" (doi: 10.1016/j.cub.2023.12.042) and sought to better understand how MPP of tanycytes changes their molecular signature after birth.

We aimed to characterise the molecular signature of tanycytes during a MPP paradigm. We used the well-established MPP model in the Siberian hamster (*Phodopus sungorus*), and experimentally manipulated the photoperiod to which mothers were exposed during gestation, placing them on either a long photoperiod (LP: 16h of light per 24h) or on a short photoperiod (SP: 8h of light per 24h). The resulting pups remained on the gestational photoperiod until weaning (postnatal day 21). At weaning a cohort from each group was moved to an intermediate photoperiod (IP: 14h of light per 24h). This resulted in four distinct groups when sampled at postnatal day 50: LP, kept at LP throughout the experiment. LPIP, gestated under LP and at weaning moved to IP. SPIP, gestated under SP and at weaning moved to IP. SP, kept at SP throughout the experiment. In line with previous experiments, we observed that the LP and SPIP groups had an accelerated developmental trajectory with an active reproductive status (increased testicular weights), while the SP and LPIP groups showed a slowed and decelerated developmental trajectory with ceased reproductive activity. For each individual, hypothalamic cryosections were used to perform LCMD of the vimentin-positive tanycytic region around the 3V. The tanycyte specificity of the LCMD approach were confirmed by mapping the transcriptome to a single-cell RNAseq dataset with known cellular markers (Campbell *et al.*, 2017).

We observed 6053 genes changing in the tanycytes according to photoperiod. Specifically, tanycytes of LP animals showed an enrichment of genes related to cilia when compared to SP animals. To test if this was evident at the protein level, we used immune-histochemistry (IHC) to look at the anchoring structure of cilium, basal bodies (γ-tubulin), and their ciliary projections (α-tubulin). This revealed an increase in ciliary basal bodies and ciliary projections in LP animals compared to SP animals. Furthermore, an increase in post-weaning photoperiod (SPIP) increased the expression of ciliogenesis markers.

The cilium is the cytological structure serving as a docking station for multiple G-protein coupled receptors (GPCR) and other signalling receptors, including TSH-R (Gerdes, Davis and Katsanis, 2009; Yang, Hong and Kim, 2021). Photoperiodic regulation of ciliation may therefore alter the sensory capacity of tanycytes to metabolic feedback signals, such as TSH. Furthermore, ciliary dysfunction in humans and mice results in various detrimental metabolic phenotypes (Badano *et al.*, 2006; Loktev *et al.*, 2013; Lee *et al.*, 2020).

Collectively, our findings led us to propose a model that links the *in utero* and early life photoperiod to changes in tanycyte sensory function, manifested as number of sensory cilia. These changes in cilia

could influence the excitatory drive from tanycytes on the hypothalamic areas governing growth and development, leading to seasonally appropriate phenotypic output.

3.3 Paper III: A refined method to monitor arousal from hibernation in the European hamster

Paper III is published in "BMC Veterinary Research" (doi: 10.1186/s12917-020-02723-7). The aim of this paper was to set up a hibernation paradigm, and develop monitoring tools.

Studying hibernation requires patience, warm clothes and good colleagues. The aim of **Paper III** was to gain experience in setting up a hibernation paradigm and the research tools for physiological monitoring of hibernation. Specifically, **Paper III** used the European hamster (*Cricetus cricetus*), as our hibernation model. To initiate the preparatory program prior to hibernation, the hamsters were transferred from a long photoperiod (LP: 14h of light per 24h) and 22 °C to a short photoperiod (SP: 10h of light per 24h) and 22 °C. After 8 weeks, the temperature was lowered to 10 °C. We instrumented the hamsters to record T_b with an iButton temperature recorder in the abdominal cavity and an IPTT tag (BMDS IPTT-300®) onto the BAT (T_{BAT}) in the interscapular area. These two sites were chosen to increase the monitoring precision and to be able to detect the early events of natural arousal when the BAT start to increase in temperature.

Within 4 weeks at 10 °C, all animals initiated a hibernation phenotype with a cyclical pattern of dropping their core temperature close to ambient temperature for multiple days (torpor), before spontaneously rewarming back to euthermic levels (arousal), a phenomenon called T-Acycling. A key phenomenon of a lowering of T_b prior to initiation of hibernation was observed and served as an important indicator we use in **Paper IV**.

After 2 weeks of T-A cycling, we started to closely monitor the T_{BAT} of the animals when they aroused from torpor. We show that rewarming of BAT precedes core body rewarming with 48.6 minutes (CI: 45.4-51.7 min). While temperature recordings from both sites follow the same sigmoidal curve trajectories until they reach euthermia. The shivering onset of muscles in the BAT area was noted to be around 15 °C (14.2-16.8 ºC). During arousal there was an increase in ventilation frequency, and peak levels were reached just prior to reaching euthermia. In essence, we show how an additional live temperature recording from the classical BAT can inform us about the earliest initiation of arousal in a hibernator. A refined version of this technique was applied in a separate study not included in this thesis (Markussen *et al.*, 2024).

In the context of this thesis, **Paper III** set up the necessary skills and tools to study tanycytes in hibernation.

3.4 Paper IV: Altered fuel utilisation and sensory capacity in tanycytes throughout the hibernation season in the golden hamster

Paper IV is an accepted manuscript in the "Canadian Journal of Zoology" designed to describe transcriptional changes in tanycytes throughout the hibernation season of golden hamsters.

We sought to characterise the tanycytes using LCMD RNAseq in an adult seasonal hibernation model. Despite using the European hamster in **Paper III** we choose to use the golden hamster (*Mesocricetus auratus*) for this experiment. This is because they are freely available from an approved supplier and are highly photoperiodic and have a good hibernation phenotype, with a clearly defined progression through a photoperiodically regulated preparation for hibernation and a spontaneous termination of hibernation (refractory).

To initiate hibernation, golden hamsters were shifted from long photoperiod (LP: 14h of light per 24h) and 22 ºC to short photoperiod (SP: 10h of light per 24h) and 8 ºC. This initiates a shut-down of the reproductive axis, lowering of T_b set-point and an increase in BAT, all of which are key preparatory events prior to hibernation onset (Lyman *et al.*, 1982; Markussen *et al.*, 2024), a photoperiodic response known to involve tanycytes (Milesi, Simonneaux and Klosen, 2017). After 8-12 weeks in SP 8 ºC the hamsters initiate T-A cycling, shown by multi-day bouts of torpor with a T_b approaching T_a, interrupted by a spontaneous rapid revival back to euthermic temperatures (IBE). Tanycytes have been proposed to play a hitherto unknown part in the regulation of the TA-cycle (Bratincsák *et al.*, 2007; Markussen *et al.*, 2024). This cyclic pattern continues until approximately 20 weeks in SP, were the hamsters suddenly, after no changes in external factors, stop T-A cycling, remain euthermic and start to re-grow their testes (Refractory). As in **Paper II** we collected brains for LCMD and performed RNAseq, but this time we defined our timepoints using telemetric recording of T_b to capture the pre-hibernation phase, IBE, torpor, and the development of the refractory state.

Our results showed that the pre-hibernation and hibernation state showed a signature of gene expression relating to a catabolic state with the break-down of glycogen and upregulation of glycolysis. During torpor we saw an enrichment for pathways related to hypoxia and RNA splicing, while IBE tanycytes showed upregulation of genes related to gene silencing and protein degradation. The tanycytes of the refractory and LP group, both reproductively active (increased testes weight), showed an upregulation of genes related to GPCR ligand binding and ciliation. Collectively, our results suggest an alteration of tanycyte fuel utilisation and sensory capacity as a result of photoperiod manipulation.

These results echo our findings in **Paper II**, where gestational and early life exposure to LP in juvenile Siberian hamsters increased ciliary gene expression and the number of cilia present on tanycytes (Melum

et al., 2024). **Paper IV** and **Paper II** combined suggests that increased expression of ciliary genes in the tanycytic layer may be a general seasonal adaptation to enhance the sensitivity to metabolic feedback signals, such as TSH, and induce the initiation to a spring/summer program.

3.5 Extension to Paper II & Paper IV: Contrasting the photoperiodic responses of tanycytes in the Siberian and Golden hamster

3.5.1 Developmental vs adult photoperiodic paradigm

In this thesis two paradigms have been used. In the first paradigm changes in photoperiod during gestation and early life leads to changes in development and growth of Siberian hamsters to match the opposing energetic demands in summer and winter (Figure 11A). In the second paradigm, adult golden hamsters respond to decreases in photoperiod and temperature to initiate their winter survival strategy, hibernation (Figure 11B).

The two paradigms are distinctive in terms of age, with the Siberian hamster receiving photoperiodic treatment during gestation and early life (until postnatal day 50) while the golden hamster received photoperiodic treatment when more than 3 months old.

Despite these differences, both paradigms involve expression of metabolic depression strategy for winter survival. To identify the similarity and differences of the tanycyte signature in the two paradigms would aid our understanding of tanycyte function. Therefore, I compared the results of the contrast of LP and SP in the Siberian hamster with the contrast of LP and Pre-hibernation (4 weeks of SP exposure) in the golden hamster. Two time points where animals clearly exhibit a photoperiodic response (sexual quiescence) to SP and no torpor expression had occurred in golden hamsters (not measured in Siberian hamsters), albeit differing in photoperiodic treatment, duration of treatment and T_a (Table 1).

Table 1 Summary of differing experimental conditions in the developmental (Siberian hamster) and hibernation (golden hamster) paradigm.

Species	Siberian hamster	Golden hamster
Paradigm	Developmental	Hibernation
Long photoperiod (hrs of light/24 hrs)	16	14
Short photoperiod (hrs of light/24 hrs)	8	10
Duration of exposure to short photoperiod (days)	Gestation + 50	30
Age at sampling (days)	50	120-150
T_a under long photoperiod	22	22
T_a under short photoperiod	22	8
Number of genes with significant change in expression (FDR<0.05)	6053	2291

The developmental paradigm shows a greater number of differentially expressed genes compared to the adult photoperiodic paradigm (Table 1). While the extent is different, I observe that 38 % of the genes upregulated under LP in the golden hamster are shared with the Siberian hamster. Similarly, under SP conditions 41 % of the upregulated genes are shared (Figure 11E). Contrary, only 10 % of the upregulated genes under LP in the golden hamster are shared with the upregulated genes under SP in the Siberian hamster, indicating that the tanycyte layer of the two species have a shared photoperiodic response.

Enrichment analysis reveal that genes associated with enhanced signalling, hormone secretion, glucose import, glial cell proliferation, plasma bound cell projection assembly and lipid biosynthesis are upregulated in tanycytes during LP in both species. While genes related to reduced signalling capacity, increased cell differentiation, response to hypoxia, regulation of nitrogen compound metabolic process, negative regulation of cell growth and breakdown of cellular lipids are upregulated in SP in both species (Figure 11E).

3.5.2 Cilia & G-protein coupled receptors

Independent analysis for each paradigm, revealed the same characteristics of enhanced sensory capacity of tanycytes in LP through up-regulation of cilia related genes (**Paper II** & **Paper IV**). Consistently, the combined analysis shows plasma membrane bounded cell projection assembly (Cilium) to be enriched in the genes overlapping in both paradigms in LP.

Further, the photoperiodically driven changes in ciliation are accompanied with changes in GPCRs' and other signalling receptors. In this aspect, the most striking difference between the two paradigms is the changes and expression levels of *Gpr50*, with high expression and photoperiodic sensitivity in the Siberian hamster but low expression and modest photoperiodic sensitivity in the golden hamster (Figure 12A & B). For *Tshr* a tendency of upregulated expression in LP is seen in both paradigms, but to a much higher degree in Siberian hamsters (0.0000161 FDR Sib vs 0.0795 FDR Gham, Figure 12A & B). Another GPCR with differing expression levels between the paradigms is gamma-aminobutyric acid type B receptor subunit 1 (*Gabbr1*), a receptor for the key inhibitory neurotransmitter in the mammalian brain, which recently have been shown to be involved in glial cell proliferation and differentiation, is highly expressed in the Siberian hamster, but to a less extent in the golden hamster (Serrano-Regal *et al.*, 2020; Cheng *et al.*, 2023). Collectively, the differences in GPCR expression could indicate important discrepancies in tanycyte function between the two species.

3.5.3 Cell differentiation

In **Paper II** we identified a strong signature of MPP-induced tanycyte differentiation (Figure 12C). An analysis possible by mapping our data to six clusters identified by cell fate mapping and single nuclei

RNAseq that characterize the differentiation of a tanycyte to a tanycyte derived neuron (Yoo *et al.*, 2021). Using the same approach, we found no clear photoperiodic effect on the differentiation of tanycytes in the golden hamster hibernation paradigm (Figure 12D). This suggests that while tanycytes may be important for metabolic regulation in adult animals, this may depend less upon cell fate and differentiation processes than is the case during the juvenile period.

3.5.4 Molecular adaptation to conserve energy

In both paradigms the animals utilize a metabolic depression strategy to survive the winter. By looking at photoperiodic changes in genes involved in glycolysis I wanted to investigate if tanycytes in both paradigms share a cellular molecular adaptation to conserve their cellular energy requirement. Overall, the transcriptome in both species indicate an upregulation of glycolytic genes and suggest an increased glycolytic activity in SP (Figure 13). In both paradigms there is an upregulation of Pfkp, the gene encoding a rate-limiting enzyme in glycolysis. Further, pyruvate dehydrogenase kinase 2 (Pdk2), one of four genes that constitute pyruvate dehydrogenase kinase (PDK), an enzyme that inhibits the pyruvate dehydrogenase complex (PDH) to convert pyruvate to acetyl-coenzyme A. This may indicate that winter adaptation involves an increased cellular reliance on glycolysis and a reduced energy yield from the aerobic tricarboxylic acid (TCA) cycle activity, or a shift in fuel for the TCA-cycle from pyruvate to β-oxidation of fatty acids (Figure 13). The enrichment analysis indicates that there is a lipid biosynthesis in tanycytes in LP, while in SP this is shifted to break-down of lipids (Figure 11E), which could favour an increase in β-oxidation of fatty acids to meet the energy demand of the cell. Together, the ependymal layer of both Siberian and golden hamsters has a transcriptional upregulation of key glycolytic genes, hinting at an increased glycolytic rate as an SP adaptation.

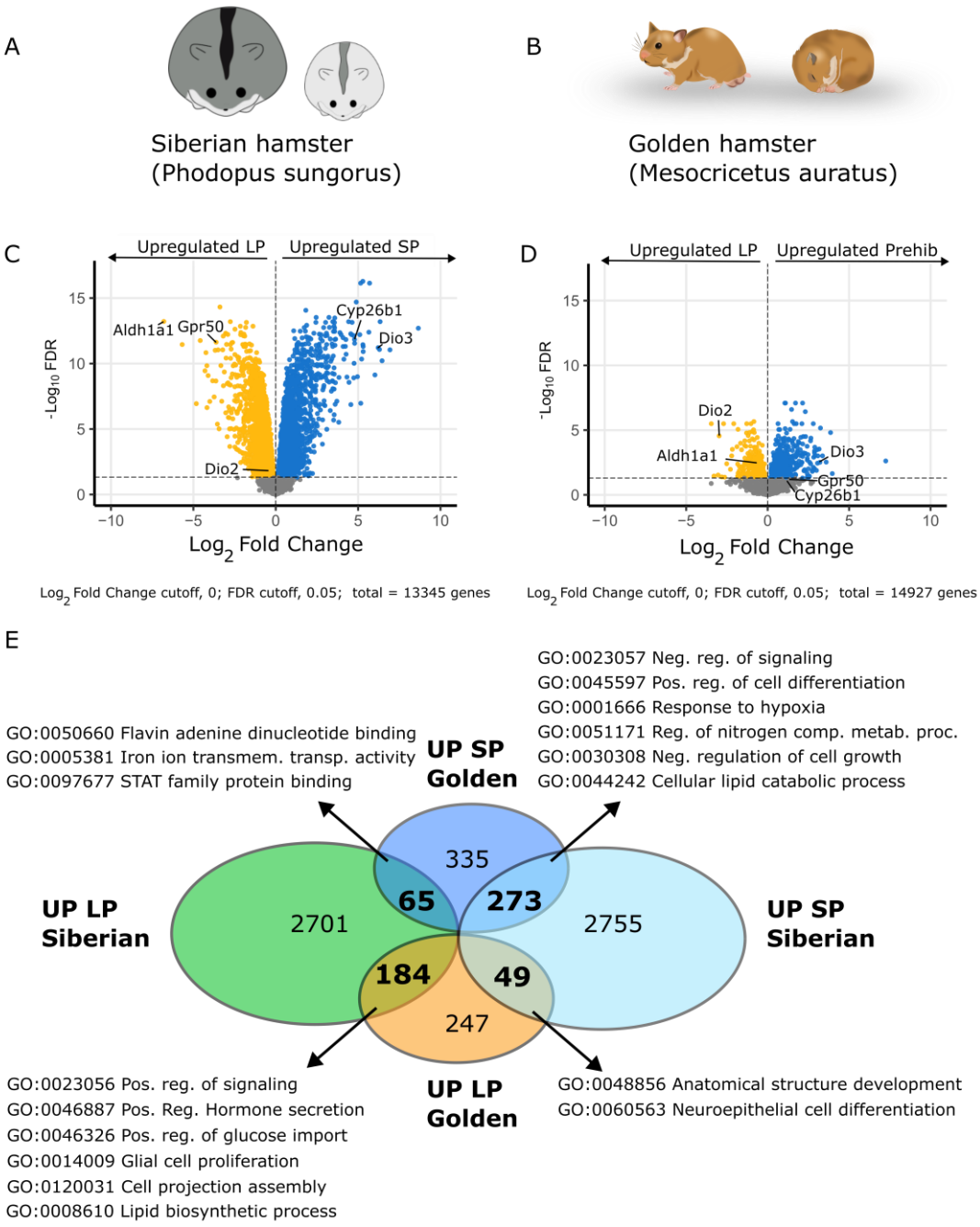

Figure 11 Comparison of the tanycytic transcriptome in two metabolic depression paradigms. A) Juvenile Siberian hamsters (Phodopus sungorus) match their growth, development and reproductive strategy to the environmental energetic demand. B) Adult golden hamster (Mesocricetus auratus) utilize hibernation as a winter survival strategy to reduce their energy requirement when energetic demands are high, and food scarce. C) Volcano plot of the tanycyte transcriptome of Siberian hamster. Orange dots indicate upregulated genes in LP, blue dots indicate upregulated genes in SP. Grey dots indicate genes with no significant change in expression (FDR>0.05). Log2 fold change is shown on the x-axis and -log10FDR on the y-axis. The dashed line indicates FDR=0.05. Total number of genes 13345. D) Volcano plot of the tanycyte transcriptome of adult golden hamster. Prehib = SP 4 wks, colour-coded as in C. Total number of genes 14927. E) Venn diagram analysis that identifies the shared transcriptomic characteristics between the two paradigms/species (571 genes found in both transcriptomes). For each gene set that overlap, the most meaningful results of the enrichment analysis (functional biological process) are indicated with GO term number and description.

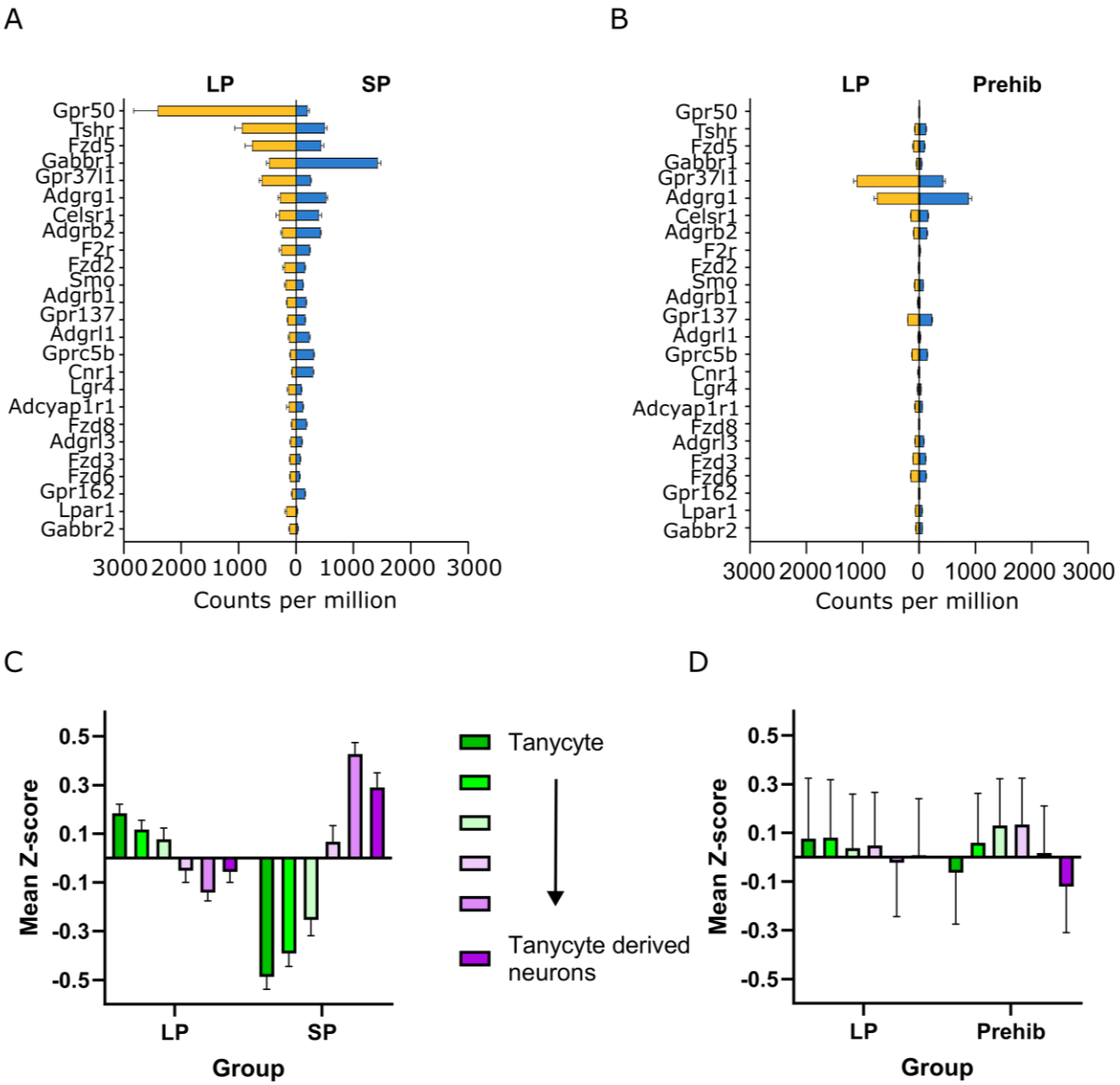

Figure 12 Comparison of G-protein coupled receptor expression and tanycyte differentiation. A) 25 most highly expressed G-protein coupled receptors in the tanycyte transcriptome of Siberian hamsters, with average expression levels for the LP and SP photoperiodic treatment. Shown as average individual counts per million on y-axis and NCBI symbol on x-axis. B) the same list of G-protein coupled receptors in the tanycyte transcriptome of golden hamsters, with average expression levels for the LP and Prehib (SP 4 wks) photoperiodic treatment. Shown as average individual counts per million on y-axis and NCBI symbol on x-axis. Gpr50 is added to allow comparison with panel A. C) Relative expression of genes in clusters defined by snRNAseq (Yoo et al. 2021) to represent different stages of hypothalamic neuronal/glial differentiation. Here shown as mean z-score for the LP and SP photoperiodic treatment of Siberian hamsters in C, and golden hamster in D). Error bars represent the SEM and they are colour-coded as indicated.

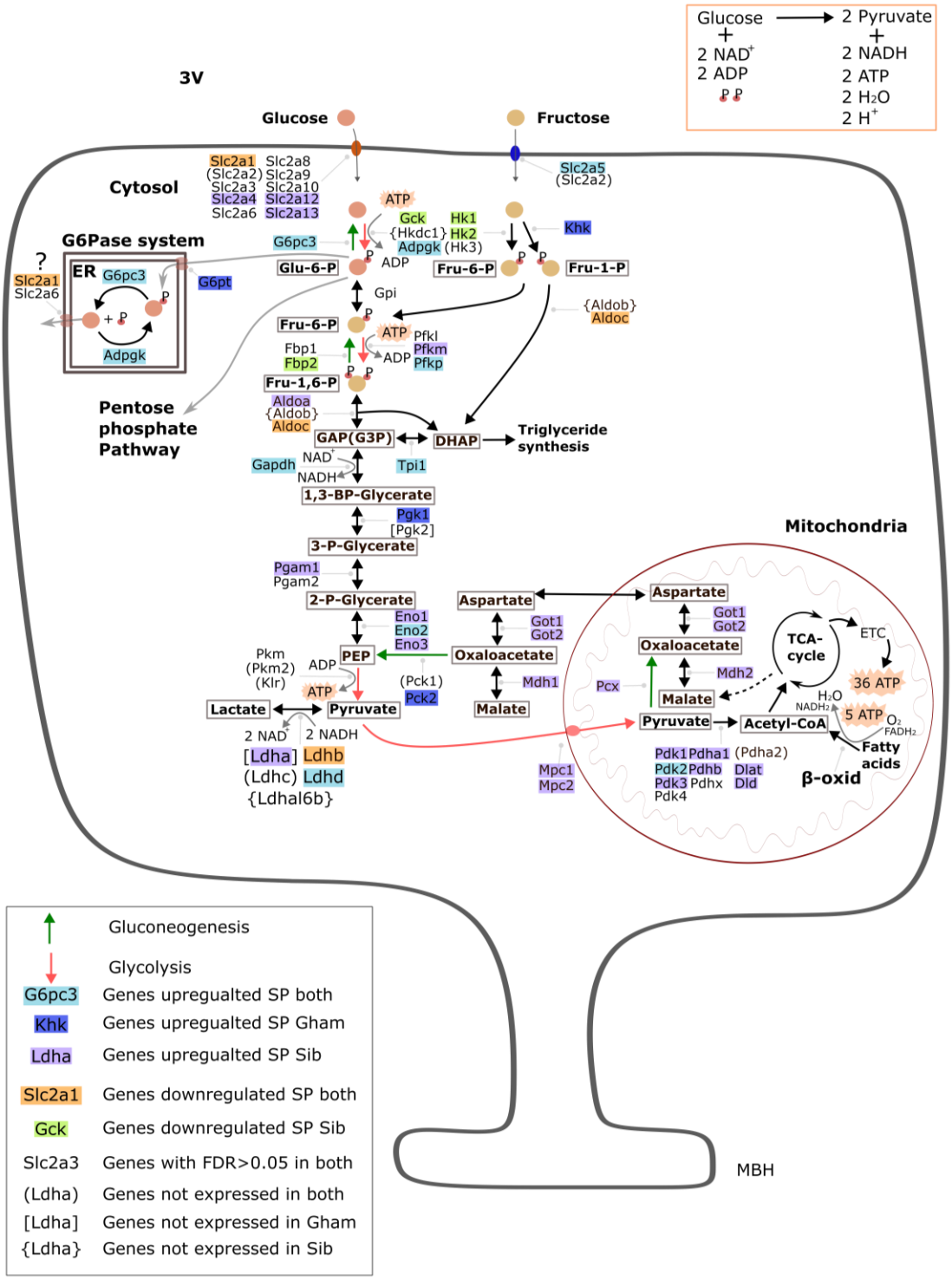

Figure 13 Comparison of transcriptional changes in the glycolytic pathway in the ependymal layer of Siberian and golden hamsters as a potential mechanism to regulate cellular energy consumption in response to short photoperiod. Color-coded as indicated. Abbreviations: Glu-6-P, Glucose-6-phosphate; Fru-1-P, Fructose-1-Phosphate; Fru-6-P, Fructose-6-Phosphate; Fru-1,6-P, Fructose-1,6-biphosphate; GAP(G3P), Glyceraldehyde 3-phosphate); DHAP, Dihydroxyacetone phosphate;1,3-BP-Glycerate, 1,3-Bisphosphoglycerate; 3-P-Glycerate, 3-Phosphoglycerate; 2-P-Glycerate, 2-Phosphoglycerate; PEP, Phosphoenolpyruvate; TCA-cycle, tricarboxylic acid cycle; β-oxid, β-oxidation; Acetyl-CoA, Acetyl coenzyme A; G6Pase system, Glucose-6-phosphatase system, Gham – golden hamster, Sib – Siberian hamster

4 Discussion and Conclusion

My thesis aimed to characterise tanycytes in two seasonal metabolic paradigms to better understand the role of tanycytes in mediating seasonal rheostatic changes in metabolic state. To this end I have characterised the tanycytes in juvenile Siberian hamsters during a MPP paradigm (**Paper II**) and golden hamsters in an adult hibernation paradigm (**Paper IV**). The major finding of my thesis is the increase in cilia-related gene expression in tanycytes in response to lengthening photoperiod in Siberian hamsters (**Paper II**) and during LP and the development of the SP-refractory state in golden hamsters (**Paper IV**). Furthermore, the SP state in both golden and Siberian hamsters shows a gene expression signature relating to enhanced glycolysis (**Paper IV** & thesis section **3.5**). In my discussion of these results, I will first focus on the physiological differences in these paradigms and the apparent similarity in the cellular metabolic gene expression profile. Then I will discuss an interpretation of the cilia result and how this may link to known function of tanycytes and their proposed role in rheostasis. Finally, I will discuss the methodical limitations of my thesis and future avenues for research.

4.1.1 Preparing for winter by reducing metabolic requirements

In both paradigms used in this thesis, at the whole animal physiology level, the response to SP is characterised by energy conservation, though it is achieved in subtly different ways. Whilst both the Siberian and golden hamster shuts off reproduction in response to SP (Hoffman, Hester and Towns, 1965; Gaston and Menaker, 1967; Figala, Hoffmann and Goldau, 1973), in the MPP paradigm this is due to an arrest of reproductive development (Hoffmann, 1978; Sáenz de Miera *et al.*, 2017), whereas in adult golden hamsters this is due to testicular regression due to shut-down of gonadotropin secretion (Turek *et al.*, 1975). Even if we were to compare the response of adult Siberian hamsters to SP with that of golden hamsters we would observe a clear difference, with the adult Siberian hamster loosing substantial amounts of weight, compared to the modest changes in the weight of the golden hamster ((Heldmaier and Steinlechner, 1981a; Chayama *et al.*, 2016), reviewed in: (Bartness and Wade, 1985)). This clear species difference in seasonal body weight regulation, responses associated with the different metabolic depression strategies in response to SP and lower ambient temperature, with Siberian hamsters expressing daily torpor and the golden hamster showing multiday torpor (Ruf and Geiser, 2015). For SP adapted Siberian hamsters a substantial body weight loss is noted prior to onset of spontaneous daily torpor (Heldmaier and Steinlechner, 1981a). By lowering T_a and reducing food availability the body weight loss is accelerated and torpor onset advanced, indicative of a more acute response to energy status than that observed in hibernators (Ruf *et al.*, 1993). Interestingly, if late-born garden dormice (*Eliomys quercinus*) is restricted in feeding opportunities during their pre-hibernal fattening, they utilize daily torpor to counter the decreased caloric intake and ensure an pre-hibernation fat-mass comparable to animals allowed to feed *ad libitum* (Giroud, Turbill and Ruf, 2012; Giroud *et al.*, 2014). Such a compensatory mechanism of daily torpor usage, enables the garden dormice, a fat-

storing hibernator, to have enough fat-reserves to last the whole hibernation period. This shows daily torpor as a flexible mechanism in which animals can maintain a body weight set-point upon periods of food shortage. However, the metabolic "saving" is greater in both the hibernating garden dormice and golden hamster, compared to that of daily torpor in Siberian hamsters. Even though we did not investigate daily torpor in **Paper II**, presumably the overwintering juveniles in our study were prepared to express torpor if exposed to low ambient temperature, and therefore may show similar metabolic adaptations.

This thesis focused on the tanycytes and shows enhanced expression of genes relating to glycolysis under SP (Figure 13). The conserved upregulation of fructose transporter (*Slc2a5*) in both hamster species may indicate a more reliance on fructose as an energy substrate for glycolysis, a shift associated with a cellular energy conserving adaptation to energy shortage (Johnson *et al.*, 2020). Further, the coherent upregulation of *Pdk2* in both hamster species could indicate either that the presumed enhanced glycolytic rate meets the cellular energy requirement of the cell or that β-oxidation of fatty acids rather than pyruvate serves as a substrate for acetyl-CoA synthesis and subsequent TCA-cycling. In fat-storing hibernators, a decrease in glycolytic flux during torpor has been reported previously (Brooks and Storey, 1992), suggesting a reduced reliance on glucose and an increased reliance on β-oxidation of fatty acids to meet the cellular demand during the hibernation period (for review see: (Giroud *et al.*, 2021)). However, in the food-storing Siberian and golden hamsters, the reliance on ingested glucose or fructose as an energy substate under SP is compatible with the observed enhanced glycolytic rate. Potentially, this may highlight a difference at the molecular level between food-hoarding and fat-storing species.

Further, these data are unable to discriminate if enhanced expression of glycolytic related genes are tanycyte-specific or part of a global adaptation in the whole animal in response to SP. However, previous gene expression studies in a hibernator describe differences in the transcriptional responses between different tissues, and between regions within the brain (Andrews, 2004; Schwartz, Hampton and Andrews, 2013; Vermillion *et al.*, 2015). This suggests that there is a physiological need for specific adaptations, depending on cell-types and function. Indeed, our observed changes resonate with previous findings in tanycytes of Siberian hamsters, in which a seasonal upregulation of glycogen and glucose metabolism under SP was reported (Nilaweera *et al.*, 2011). The authors of this earlier study proposed a model in which decreased tanycytic uptake of lactate from the extracellular environment increases neuronal lactate availability. In this thesis, the Siberian hamster, but not golden hamster, shows increased RNA expression levels of *Ldha*, the gene responsible for the enzyme that convert pyruvate to lactate (Figure 13). Linking these insights with the recent demonstration that anorexigenic POMC neurons use lactate as their principal substrate (Figure 8, (Lhomme *et al.*, 2021)), suggests a potential POMC-neuronal excitability based mechanism to explain the drastic reduction in food intake observed in Siberian hamsters under SP. In contrast, the golden hamster, which shows modest body weight changes,

the potentially reduced tanycytic energy usage may enable more transport of limited energy substrates such as glucose. This could be via the G6Pase-system to orexigenic NPY-neurons sustaining the drive to feed and maintain body weight levels even under SP (Figure 8, (Barahona *et al.*, 2024). Such an extrapolation of transcriptomic data alone is speculative, and should only serve as an explanatory working model to generate hypotheses for further experiments.

Both hamster species studied in this thesis utilize a winter survival strategy that consists of recurrent periods of fasting and feeding. For both daily- and multiday torpor the strategy requires tight control over glucose homeostasis. Given the established role of tanycytes as the gateway for glucose' homeostasis through insulin and glucose actions, a seasonal programming of these cells would be of particular interest (Porniece Kumar *et al.*, 2021; Rodríguez-Cortés *et al.*, 2022; Yu *et al.*, 2023). In non-photoperiodic species, one proposed mechanism by which tanycytes contribute to glucose homeostasis is through SCN-driven changes in tanycyte mediated glucose transport, causing a daily fluctuation in accessibility of glucose responsive neurons in the ARC to circulating glucose levels (Rodríguez-Cortés *et al.*, 2022). Such a mechanism seems particularly applicable to participate in daily torpor regulation, which is under circadian control. Indeed, in hypothalamic blocks of SP-adapted torpid Siberian hamsters RNA expression of glucose transporter 3 (*Glut3/Slc2a3*) is upregulated compared to SP-adapted euthermic animals (Haugg *et al.*, 2022). However, the study is unable to resolve the cell-type responsible for the increased *Glut3* RNA expression, and if these increased expression levels lead to an increased capacity for glucose transport into the hypothalamic region. In this thesis I also note an upregulation of certain tanycytic glucose transporters (*Slc2a4, Slc2a12, Slc2a13*) in SP-adapted Siberian hamsters (Figure 13). But, if seasonal changes in tanycyte mediated glucose transport contributes to glucose homeostasis during daily torpor in Siberian hamsters remains to be elucidated.

4.1.2 Cilia, sensing, GPCR signalling and cell division

The major result from my thesis is the change in cilia-related gene expression and cilia number in response to photoperiod. This was an unexpected finding because in the first morphological descriptions of tanycytes, electron microscopy imaging proposed most tanycytes lacked a cilium (Scott and Paull, 1983). However, more recently the β-tanycytes lining the ME are shown to possess one cilium, while the more dorsal α-tanycytes are bi-ciliated (Mirzadeh *et al.*, 2017).

The primary cilium is a hair-like structure found in virtually all vertebrate cells enabling the cell to receive and respond to signalling molecules in the extracellular environment (for review see: (Hilgendorf, Myers and Reiter, 2024)). This complex cellular architecture consists of a modified centriole to form a basal body, the anchoring structure for the ciliary process that protrude out of the cell (reviewed in: (Breslow and Holland, 2019)). The ciliary axoneme consists of a ring of nine microtubule doublets, enabling retrograde and anterograde transport of signalling molecules through intraflagellar

transport with dynein and kinesin microtubule motor proteins (reviewed in: (Anvarian *et al.*, 2019)). Further, this protrusion is ensheathed with the ciliary membrane, that possess cilia specific and general membrane receptors, increasing binding activity through an increased surface area (reviewed in: (Garcia, Raleigh and Reiter, 2018)). In addition to be in more direct access to extracellular metabolic signals, the morphology of the tube-like structure itself enhances signalling capacity in terms of reducing the threshold level to initiate second messenger signalling (reviewed in: (Hilgendorf, Myers and Reiter, 2024)). Ciliary assembly is known to be important for normal development, and abnormalities are linked to metabolic disease (for review see: (Badano *et al.*, 2006; Anvarian *et al.*, 2019)). Defects of the primary cilium within the brain impair normal homeostatic processes and leads to increased food intake and subsequently obesity (Lee *et al.*, 2020; Wang *et al.*, 2021). There are many ways that a change in cilia numbers could affect tanycyte function, which I review below:

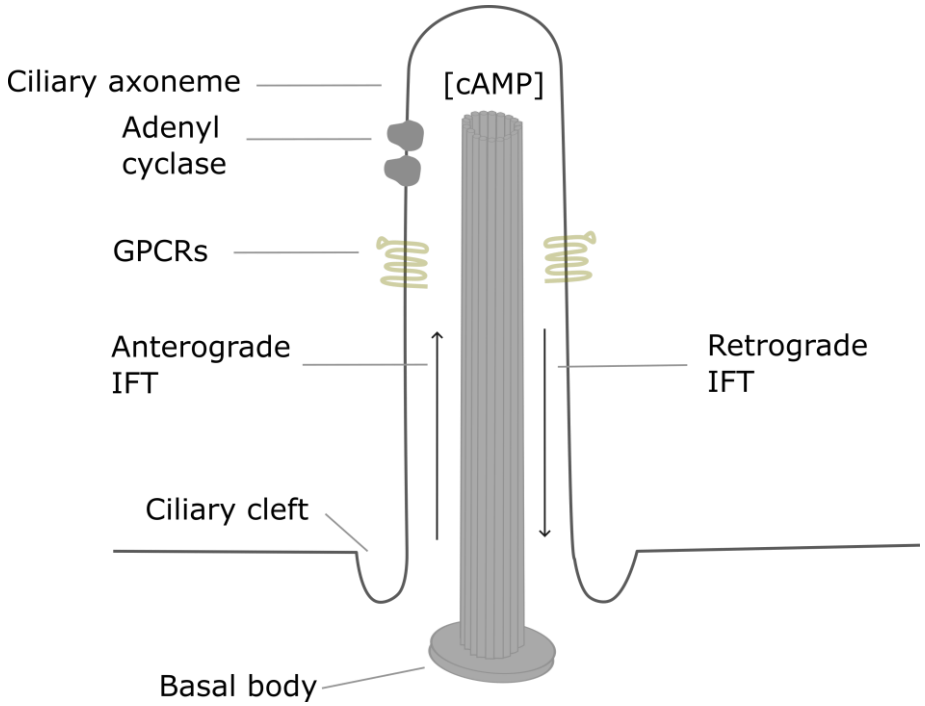

Figure 14 Simplified schematic of key cellular components constituting the primary cilium. A modified centriole, called the basal body creates the anchoring structure for the cellular protrusion. From the basal body, nine microtubule doublets create a ring structure extending outwards from the cell surface. Along the microtubule, there is an intraflagellar transport system (IFT) that can transport cargo, such as receptors, to the ciliary tip. This transport process starts in the ciliary cleft and with the use of the microtubule motor protein kinesin anterograde transport is achieved. Conversely, transport from the tip towards the base, retrograde transport is achieved by dynein motor protein. The ciliary axoneme is endowed with a ciliary membrane that is continuous with the cellular membrane, but distinctive in terms of cellular composition, with high expression of G-protein coupled receptors (GPCRs) and adenyl cyclases, creating a potential for rapid changes in cyclic AMP, amplifying the signal transduction pathway of multiple receptors. Illustration by V.J. Melum. Based on (Anvarian *et al.*, 2019; Hilgendorf, Myers and Reiter, 2024).

4.1.2.1 Cilia and stem cell properties of tanycytes – seasonal timing

In addition to being involved in signalling, the anchoring structure of the cilium, the centriole, is also required to organize the mitotic spindle during cell division. Because, the centriole of the cilium needs to be disassembled prior to cell-division, reduced expression of ciliary genes is predicted in dividing cells (reviewed in: (Breslow and Holland, 2019)). Given the reported role of tanycytes as a stem cell niche we looked into cell division and differentiation.

In **Paper II**, we found no photoperiodic effect on cell-division, (measured as numbers of PCNA and Ki67 positive cells), despite the increased number of cilia in the tanycyte layer under LP. However, we did find a photoperiodic effect on cell differentiation, with the use of established markers for the process of tanycyte differentiation and specialization (**Paper II** & Figure 12C). In fact, the down-regulation of ciliary genes is a feature of tanycytes that initiate the differentiation process (Yoo *et al.*, 2021). Photoperiodically increased tanycyte differentiation was not evident in the golden hamster (Figure 12D). Our result in the Siberian hamster relate to several studies that demonstrate an active neurogenic niche to be within the hypothalamus of both mice and sheep (Migaud *et al.*, 2011; Hazlerigg *et al.*, 2013; Batailler *et al.*, 2014; Pellegrino *et al.*, 2018). During development, hypothalamic histogenesis originate from progenitor cells in the ventricle migrating in to the brain parenchyma (Xie and Dorsky, 2017). This makes tanycytes, which retain some embryonic radial glial characteristics throughout life, an attractive source for hypothalamic neurogenesis (Rodríguez *et al.*, 2005).

In sheep, pinealectomy is shown to influence number of proliferative cells in the hypothalamus and peak proliferation levels correspond to the reproductive phase (Batailler *et al.*, 2018). However, the identity of cells undergoing melatonin dependent cell proliferation remains to be determined. In a recent study in male mice, α-tanycytes were selectively ablated, leading to a reduced reproductive competence, a phenotypic change claimed to be due to reduced α-tanycyte derived neurogenesis (Butruille *et al.*, 2022). However, the ablation procedure influences the overall function of α-tanycytes, and cannot be attributed to the neural stem cell properties of α-tanycytes *per se*. Regardless, these studies start to connect the dots between tanycytes as neuronal stem cells and circannual rhythm generation in tanycytes. In the hypothesis that cyclical histogenesis is the basis for circannual timing, it is stressed that the coordination of the process is of key importance (Hazlerigg and Lincoln, 2011). It is known that: 1) functional primary cilia is important for the cellular reception of signalling molecules, which ensure a coordinated development (reviewed in: (Anvarian *et al.*, 2019)), 2) tanycytes share characteristics with embryonic radial glial cells, key in normal development (reviewed in: (Dardente and Migaud, 2021)), and 3) the cellular architecture of neuronal primary cilia in SCN neurons undergoes a daily cycle of assembly and disassembly correlated to SCN activity (Tu *et al.*, 2023). It is tempting to speculate that our observed changes in cilia expression reflect a similar coordinated ciliary remodelling process operating on a seasonal time frame, underlying tanycyte involvement in seasonal timing.

4.1.2.2 Signalling and sensing in cilia – seasonal rheostasis

Tanycytes have the capacity to modulate hypothalamic areas involved in feeding activity, reproduction and thermoregulation (ARC/LH/VMH/DMH) (Langlet, Levin, *et al.*, 2013; Parkash *et al.*, 2015; Bolborea *et al.*, 2020; Rohrbach *et al.*, 2021; Yoo *et al.*, 2021). Such a tanycytic modulation of hypothalamic function can be achieved in various ways. First, tanycytic morphological changes alter physical barrier properties influencing hypothalamic neuronal populations accessibility to both receive peripheral signalling molecules, and to secrete neuropeptides into the ME (Bolborea *et al.*, 2011; Langlet, Mullier *et al.*, 2013; Parkash *et al.*, 2015; Wood *et al.*, 2015). Second, tanycytic transport of metabolic signals from blood or CSF to hypothalamic regions relay energy status (Duquenne *et al.*, 2021; Barahona *et al.*, 2024). Third, tanycytic enzymatic activity alter hypothalamic bioavailability of T3 (Hanon *et al.*, 2008). Further, tanycytes can divide, producing progeny cells that can differentiate into neurons that integrate in the homeostatic circuits (Yoo *et al.*, 2021). Moreover, tanycytes can sense metabolic signalling molecules and convey the signals to hypothalamic areas through calcium-wave signalling (Bolborea *et al.*, 2020). Given this diverse repertoire of cellular modes of action, specific stimuli probably elicit a distinct tanycytic response. Cilia are a major sensing structure, therefore in a seasonal context, the decrease of sensory cilia in the tanycyte layer would alter the sensory capacity of the tanycytes. In the context of this thesis, I will focus on TSH-R and GPR50.

Tanycytic expression of TSH-R is a fundamental property enabling the relay of photoperiodic time-measurement from the environment through the photoneuroendocrine system resulting in a seasonal change in hypothalamic TH levels, driving seasonal physiology. The importance of the tanycytic encoding of the TSH signal is evident in MPP. Here, gestation of Siberian hamster pups under different photoperiods shifts tanycytic sensitivity to TSH, resulting in distinct metabolic programs (Sáenz de Miera *et al.*, 2017). This was demonstrated with an altered response of deiodinases to the same infusion of TSH, albeit the *Tshr* expression levels were similar. Hence, tanycyte TSH-R sensitivity, not the expression of the receptor, is modulated depending on maternal photoperiodic history. Whether the photoperiodic response of adult hamsters also involves changes in TSH-R sensitivity has not formally been tested, but it is plausible as a mechanism whereby sensitivity changes underlie the on-set of photorefractoriness in adults. Given the specific cellular architecture of the cilium, with its tube-like structure and its ability to traffic GPCRs to the ciliary axoneme to amplify signalling, our finding of changes in ciliation in both MPP and hibernation, could aid explaining this sensitivity difference (**Paper II)**. However, these inferences rely only on *Tshr* RNA expression levels, and a demonstration of protein changes and a presence of TSH-R on the cilium is lacking. Therefore, the link between ciliation and TSH-R sensitivity awaits further investigation.

GPR50 is an orphan receptor, meaning we currently don't know the ligand for it. However, GPR50 is known to show a coherent expression pattern along the 3V in multiple species, and has been used as a

tanycytic marker (Lein *et al.*, 2006; Batailler *et al.*, 2012). Even though the ligand is unknown, GPR50 expression is linked to metabolic phenotype, with GPR50 knock-out (KO) mice displaying resistance to diet-induced obesity, through elevated levels of locomotor activity (Ivanova *et al.*, 2008). If mice are fasted, they initiate daily torpor as an energy conserving mechanism (Hudson and Scott, 1979). This response can be blocked by both peripheral or central administration of leptin (Bechtold *et al.*, 2012). In mice where the *Gpr50* gene has been knocked-out, they more rapidly enter a torpid state and their torpor expression is unaffected by leptin administration (Bechtold *et al.*, 2012). GPR50 KO mice also shown an elevated basal level of *Dio2* expression in the tanycytes, which does not rise further upon fasting, as is evident in wild type rats and mice (Diano *et al.*, 1998; Bechtold *et al.*, 2012). Further, the systemic T3 and glucose levels are decreased in GPR50 KO compared to wild type mice. Together, the interesting phenotype of GPR50 KO mice indicate that GPR50 expression levels may be an important modifier of metabolic feedback signals, influencing tanycytic sensitivity to glucose, leptin and T3. The reported association between decreased levels of *Gpr50* expression and increased torpor expression in Siberian hamsters, leptin deficient (ob/ob) mice and GPR50 KO mice, is also consistent with this interpretation (Barrett *et al.*, 2006; Ivanova *et al.*, 2008). A tanycytic modulation of leptin and glucose sensitivity to adjust the thermal response and hence energy homeostasis, aligns with our results in **Paper II** were we see a drastic reduction of *Gpr50* expression in hamsters under SP. Together, these results put forward GPR50 as a potential important component in torpor regulation. However, we do not see a seasonal regulation of *Gpr50* in the golden hamster, despite this species display multi-day torpor during the hibernation period. The relative expression levels of *Gpr50* are also substantially lower in the golden hamster. Potentially this relates to differences in body weight regulation as another photoperiodic species the sheep with no clear body weight cycle, also does not show photoperiodic regulation of *Gpr50* (Hazlerigg, 2012). So, while the change in TSH sensitivity via a reduction in cilia could be an important regulatory mechanism altering thyroid hormone content in the hypothalamus and therefore the seasonal physiology, the role for tanycytic GPR50 still remains elusive.

4.1.3 Methodological differences, limitations of the work and future studies

The main method I used in this thesis was LCMD followed by RNAseq, this method revealed far greater seasonal changes than previous studies using whole hypothalamic blocks (Lomet *et al.*, 2018; Haugg *et al.*, 2022) demonstrating the strength of the approach and highlighting the importance of tanycytes in seasonal responses. However, a major methodological difference between the LCMD approaches in **Paper II** and **Paper IV** was the rostro-caudal and ventro-dorsal extent of the captured region. In **Paper II** the LCMD sample was guided by vimentin expression in every 10th slide. This created a vimentin roadmap that spatially refined the LCMD sample to contain a high proportion of tanycytes. In contrast to this in **Paper IV** I did not stain for vimentin to preserve brain tissue. Instead, I standardised the

LCMD-sample on a morphologic measure, two times the width of the PT, a choice based on the experience from **Paper II.** This choice led the golden hamster LCMD-samples containing more ependymal cells. However, in both papers the sample is enriched for tanycytes and there are many shared features, including the altered expression of cilia related genes.

The major limitation of my thesis is that I did not validate the gene expression changes in cilia related genes by IHC in **Paper IV** as we did in **Paper II**. This is an essential piece of validation required to confirm this finding. Furthermore, we have presumed that a change in cilia number will alter sensitivity to signals. But if we proceed with this assumption, the emerging question is: which signals need to be rheostatically modulated by changes in tanycytes sensitivity to regulate seasonal physiology?

First, since tanycyte TSH-R sensitivity is driving the down-stream metabolic program in a developmental setting, it is imperative to reveal the involvement of TSH-R sensitivity in the adult seasonal program. A first pass attempt to elucidate this could be to utilize an *in vitro* approach and tanycyte cultures. Here, with the use of bioluminescence resonance energy transfer (BRET), a cyclic AMP measurer, one could indicate the cellular activity to different doses of TSH. Further, one could condition the culture with various concentrations of TSH to see how it impacts the activity to a standardized amount of TSH.

Second, to see if a change in sensitivity of TSH-R underlies the induction of photorefractoriness, an infusion protocol could be utilized. With the use of a photoperiodic species with a characterized photoperiodic response, for instance the golden hamster. Further, there is a need to identify a concentration of TSH in this species that does not, when administered ICV, elicit a physiological response (reproductive on-set) in the mid-period of the SP program. Further, by using the same identified concentration of TSH, at various time points of the seasonal program it is expected to at a certain point induce an activation of the reproductive axis. However, to disentangle the endogenous from external effects on the reproductive axis with such an experiment would be challenging. This experiment, would at best show that the responsiveness to TSH varies with the seasonal program, and that the same concentration of TSH would at parts of the program not elicit a response, and in other parts do. The hypothesis would be that such an application of a low-dose TSH signal, would advance the initiation of the reproductive phase. But that low-doses would only be able to do so after a certain photoperiodic history have elapsed.

Next, to further disentangle the TSH-driven increase in deiodinases and TH state on seasonal phenotype an ICV and intra-hypothalamic implant study is required. More specifically, if golden hamsters adapted to SP are infused ICV with T3 or intra-hypothalamic T3 implants, it would be possible to test the mechanistic link between TH state and seasonal phenotype in a hibernating species, as has proven useful in the Siberian hamster (Murphy *et al.*, 2012; Bank *et al.*, 2015, 2017) . The hypothesis would be that

the enzymatic barrier function of tanycytes, with low DIO2 and high DIO3 expression under SP, would limit the effect of ICV T3 infusion, while a T3 implant circumventing this barrier would induce a long photoperiodic phenotype with no multiday torpor expression and reproductive onset. Such an experiment would mechanistically show the effect of thyroid hormone availability in the MBH in driving seasonal physiology in a hibernator.

There might be other metabolic signals than TSH, that also is subjected to a tanycytic rheostatic modulation. The transcriptomic data from this thesis serves as a resource to elucidate the sensory repertoire of tanycytes in two seasonal hamster species. With the use of Liquid Chromatography with tandem mass spectrometry, circulating metabolites can be identified. The relative abundance profile of these identified metabolites could yield insights into novel metabolites whose levels fluctuate with seasonal state (Wright Muelas *et al.*, 2020). This would give a potential opportunity to link identified metabolic signals to signalling properties of tanycytes, leading to functional tests of rheostatic control (Ewald *et al.*, 2024).

Even though I here highlight the presumed importance of cilia numbers underlying tanycytic sensitivity to metabolic signals, there are other possible explanations. As demonstrated previously, tanycytes undergo morphological changes of their physical barrier in seasonal species, with a retraction of their endfeet during the breeding phase, to ensure GnRH access to the ME (Yamamura *et al.*, 2004; Wood *et al.*, 2015). In this thesis I have not used EM to investigate if such morphological plasticity underlies the observed phenotypic changes. Given the multitude of tanycyte action, and the reported previous literature, it is likely that multiple changes in tanycyte function occur in concert to achieve its effect on down-stream circuitry.

Another mechanism tanycytes could use to seasonally modify the MBH sensitivity to metabolic signals is through alteration of tight-junction proteins, which again will influence the leakiness of the BBB and hence the access of MBH neurons to signalling molecules. Such a seasonal leakiness has been reported in sheep, with unknown physiological consequences (Chevillard *et al.*, 2022). Hence the regulation of a rheostatic mechanism through a seasonal modulation of tight-junction proteins and fenestration cannot be excluded. However, initial descriptions of changes in leakiness, as measured by perfusion of a small biotinylated tracer molecule, prior to and after the on-set of hibernation in both European hamsters and thirteen-lined ground squirrels seems not to favour such a model to be at the core of a rheostatic mechanism (Markussen, 2020; Mohr *et al.*, 2024).

Due to the chosen LCMD-method in this thesis, the subclasses of tanycytes, with known divergent roles were pooled together. This limits understanding of the sub-type specific actions in a seasonal context, known to both underly morphological and barrier-properties. In fact, our IHC data highlights a

difference in the extent of cilia changes between α- and β-tanycytes (**Paper II**), highlighting this limitation of the LCMD-method.

The limited temporal and spatial resolution of the LCMD-samples in this thesis makes it unsuitable to aid in deciphering the importance of tanycyte neural stem cell properties. First, the transcriptomic data represents a snap-shot in time. This is problematic with the known temporal dynamics of cellular proliferation processes. Second, the LCMD-sample consists of a restricted region, if proliferating tanycytes have migrated outside of this region, they would escape the transcriptomic picture. Hence, the LCMD-approach is unsuitable to draw inferences on seasonal changes in tanycyte neuronal stem cell properties. To this end, an experiment with the utilization of cell-fate mapping and high spatial and temporal resolution would be required. By labelling tanycytes (e.g. RAX), and follow the progression of these cells throughout a full cycle of the circannual program would be an important experiment to properly characterize the neural stem cell properties of tanycytes in a seasonal context. Further, by keeping the photoperiodic signal constant, and infuse the animal with melatonin, mimicking a short or long photoperiod, the melatonin-dependence of the neural stem cell properties could be elucidated. It would also be interesting to infuse TSH into the 3V and see how this influences a short photoperiodic animal, and whether neurogenesis precedes the activation of the reproductive axis. Finally, the "killer experiment" would be, if possible, to limit tanycyte differentiation/proliferation, without altering other tanycytic cell properties, and see if this impinges the seasonal program. To further demonstrate the involvement of TSH in this process would aid in establishing a mechanistic link between TSH and neural stem cell properties of tanycytes as a driver behind the seasonal program. Further, this could be tested by ICV infusion of TSH, in a SP-adapted hamster with tanycytes unable to differentiation/proliferate and see if the known reproductive stimulatory effect of TSH is blocked. To utilize technological tools enabling such a repression of neural stem cell properties, while leaving the other cellular properties in tact are closer than ever in non-photoperiodic models, and hopefully these techniques spill-over into the field of seasonal biology.

At last, we are still only starting to grasp the complexity and diversity of tanycytes and through which means they drive seasonal physiologic output. Recent advances in technology and collaborative efforts between researchers working with non-photoperiodic and photoperiodic species would expand our understanding of this peculiar cell-type in years to come.

Conclusion

With the use of two seasonal rodent species, the Siberian and golden hamster, this thesis suggests that the overwintering state of both species are characterised by a reduction in ciliary gene expression and hence a reduced tanycytic sensitivity to signals in the CSF, submerging their apical surface. The thesis does not provide firm evidence for which signals, but presumably, altered TSH sensitivity is of key importance. A model for the various cellular responses underlying this reduced sensory capacity is proposed. Such a model put forward tanycytes, and remodelling of their sensitivity to metabolic feedback signals as a key component in seasonal rodent species rheostatic setpoint of energy metabolism.

Works cited

Alvarez-Crespo, M., Csikasz, R.I., Martínez-Sánchez, N., Diéguez, C., Cannon, B., Nedergaard, J. and López, M. (2016) 'Essential role of UCP1 modulating the central effects of thyroid hormones on energy balance', *Molecular Metabolism*, 5(4), pp. 271–282. Available at: https://doi.org/10.1016/j.molmet.2016.01.008.

Anand Kumar, T.C. and Knowles, S.F. (1967) 'A System linking the Third Ventricle with the Pars Tuberalis of the Rhesus Monkey', *Nature*, 215(5096), pp. 54–55. Available at: https://doi.org/10.1038/215054a0.

Anand Kumar, T.C. and Thomas, G.H. (1968) 'Metabolites of 3H-Oestradiol-17β in the Cerebrospinal Fluid of the Rhesus Monkey', *Nature*, 219(5154), pp. 628–629. Available at: https://doi.org/10.1038/219628a0.

Andrews, M.T. (2004) 'Genes controlling the metabolic switch in hibernating mammals', *Biochemical Society Transactions*, 32(6), pp. 1021–1024. Available at: https://doi.org/10.1042/BST0321021.

Anvarian, Z., Mykytyn, K., Mukhopadhyay, S., Pedersen, L.B. and Christensen, S.T. (2019) 'Cellular signalling by primary cilia in development, organ function and disease', *Nature Reviews Nephrology*, 15(4), pp. 199–219. Available at: https://doi.org/10.1038/s41581-019-0116-9.

Appenroth, D. and Cázarez-Márquez, F. (2024) 'Seasonal food intake and energy balance: Neuronal and non-neuronal control mechanisms', *Neuropharmacology*, 257(June). Available at: https://doi.org/10.1016/j.neuropharm.2024.110050.

Arnold, W., Giroud, S., Valencak, T.G. and Ruf, T. (2015) 'Ecophysiology of omega fatty acids: A lid for every jar', *Physiology*, 30(3), pp. 232–240. Available at: https://doi.org/10.1152/physiol.00047.2014.

Atcha, Z., Cagampang, F.R.A., Stirland, J.A., Morris, I.D., Brooks, A.N., Ebling, F.J.P., Klingenspor, M. and Loudon, A.S.I. (2000) 'Leptin Acts on Metabolism in a Photoperiod-Dependent Manner, But Has No Effect on Reproductive Function in the Seasonally Breeding Siberian Hamster (Phodopus sungorus)', *Endocrinology*, 141(11), pp. 4128–4135. Available at: https://doi.org/10.1210/endo.141.11.7769.

Badano, J.L., Mitsuma, N., Beales, P.L. and Katsanis, N. (2006) 'The Ciliopathies : An Emerging Class of Human Genetic Disorders', pp. 125–148. Available at: https://doi.org/10.1146/annurev.genom.7.080505.115610.

Balland, E., Dam, J., Langlet, F., Caron, E., Steculorum, S., Messina, A., Rasika, S., Falluel-Morel, A., Anouar, Y., Dehouck, B., *et al.* (2014) 'Hypothalamic tanycytes are an ERK-gated conduit for leptin into the brain.', *Cell metabolism*, 19(2), pp. 293–301. Available at: https://doi.org/10.1016/j.cmet.2013.12.015.

Bank, J.H.H., Kemmling, J., Rijntjes, E., Wirth, E.K. and Herwig, A. (2015) 'Thyroid hormone status affects expression of daily torpor and gene transcription in Djungarian hamsters (Phodopus sungorus)', *Hormones and Behavior*, 75, pp. 120–129. Available at: https://doi.org/10.1016/j.yhbeh.2015.09.006.

Bank, J.H.H., Cubuk, C., Wilson, D., Rijntjes, E., Kemmling, J., Markovsky, H., Barrett, P. and Herwig, A. (2017) 'Gene expression analysis and microdialysis suggest hypothalamic triiodothyronine (T3) gates daily torpor in Djungarian hamsters (Phodopus sungorus)', *Journal of Comparative Physiology B: Biochemical, Systemic, and Environmental Physiology*, 187(5–6), pp. 857–868. Available at: https://doi.org/10.1007/s00360-017-1086-5.

Barahona, M.J., Llanos, P., Recabal, A., Escobar-Acuña, K., Elizondo-Vega, R., Salgado, M., Ordenes, P., Uribe, E., Sepúlveda, F.J., Araneda, R.C., *et al.* (2018) 'Glial hypothalamic inhibition of GLUT2 expression alters satiety, impacting eating behavior', *Glia*, 66(3), pp. 592–605. Available at: https://doi.org/10.1002/glia.23267.

Barahona, M.J., Ferrada, L., Vera, M. and Nualart, F. (2024) 'Tanycytes release glucose using the glucose-6-phosphatase system during hypoglycemia to control hypothalamic energy balance', *Molecular Metabolism*, 84(101940). Available at: https://doi.org/10.1016/j.molmet.2024.101940.

Barnes, B.M. (1986) 'Annual cycles of gonadotropins and androgens in the hibernating golden-mantled ground squirrel', *General and Comparative Endocrinology*, 62(1), pp. 13–22. Available at: https://doi.org/10.1016/0016-6480(86)90089-4.

Barnes, B.M., Kretzmann, M., Zucker, I. and Licht, P. (1988) 'Plasma Androgen and Gonadotropin Levels during Hibernation and Testicular Maturation in Golden-Mantled Ground Squirrels', *Biology of Reproduction*, 38(3), pp. 616–622. Available at: https://doi.org/10.1095/BIOLREPROD38.3.616.

Barnes, B.M. (1989) 'Freeze avoidance in a mammal: Body temperatures below 0°C in an arctic hibernator', *Science*, 244(4912), pp. 1593–1595. Available at: https://doi.org/10.1126/science.2740905.

Barrett, P., Ivanova, E., Graham, E.S., Ross, A.W., Wilson, D., Plé, H., Mercer, J.G., Ebling, F.J., Schuhler, S., Dupré, S.M., *et al.* (2006) 'Photoperiodic regulation of cellular retinoic acid-binding protein 1, GPR50 and nestin in tanycytes of the third ventricle ependymal layer of the Siberian hamster', *Journal of Endocrinology*, 191(3), pp. 687–698. Available at: https://doi.org/10.1677/JOE.1.06929.

Barrett, P., Ebling, F.J.P., Schuhler, S., Wilson, D., Ross, A.W., Warner, A., Jethwa, P., Boelen, A., Visser, T.J., Ozanne, D.M., *et al.* (2007) 'Hypothalamic Thyroid Hormone Catabolism Acts as a Gatekeeper for the Seasonal Control of Body Weight and Reproduction', *Endocrinology*, 148(8), pp. 3608–3617. Available at: https://doi.org/10.1210/en.2007-0316.

Bartness, T.J., Powers, J.B., Hastings, M.H., Bittman, E.L. and Goldman, B.D. (1993) 'The timed infusion paradigm for melatonin delivery: What has it taught us about the melatonin signal, its reception, and the photoperiodic control of seasonal responses?', *Journal of Pineal Research*, 15(4), pp. 161–190. Available at: https://doi.org/10.1111/j.1600-079X.1993.tb00903.x.

Bartness, T.J. and Wade, G.N. (1985) 'Photoperiodic control of seasonal body weight cycles in hamsters', *Neuroscience & Biobehavioral Reviews*, 9(4), pp. 599–612. Available at: https://doi.org/10.1016/0149-7634(85)90006-5.

Batailler, M., Mullier, A., Sidibe, A., Delagrange, P., Prévot, V., Jockers, R. and Migaud, M. (2012) 'Neuroanatomical distribution of the orphan GPR50 receptor in adult sheep and rodent brains', *Journal of Neuroendocrinology*, 24(5), pp. 798–808. Available at: https://doi.org/10.1111/j.1365-2826.2012.02274.x.

Batailler, M., Droguerre, M., Baroncini, M., Fontaine, C., Prevot, V. and Migaud, M. (2014) 'DCX-expressing cells in the vicinity of the hypothalamic neurogenic niche: A comparative study between mouse, sheep, and human tissues', *Journal of Comparative Neurology*, 522(8), pp. 1966–1985. Available at: https://doi.org/10.1002/cne.23514.

Batailler, M., Chesneau, D., Derouet, L., Butruille, L., Segura, S., Cognié, J., Dupont, J., Pillon, D. and Migaud, M. (2018) 'Pineal-dependent increase of hypothalamic neurogenesis contributes to the timing of seasonal reproduction in sheep', *Scientific Reports 2018 8:1*, 8(1), pp. 1–13. Available at: https://doi.org/10.1038/s41598-018-24381-4.

Bechtold, D.A., Sidibe, A., Saer, B.R.C., Li, J., Hand, L.E., Ivanova, E.A., Darras, V.M., Dam, J., Jockers, R., Luckman, S.M., *et al.* (2012) 'A role for the melatonin-related receptor GPR50 in leptin signaling, adaptive thermogenesis, and torpor', *Current Biology*, 22(1), pp. 70–77. Available at: https://doi.org/10.1016/j.cub.2011.11.043.

Beenken, A. and Mohammadi, M. (2009) 'The FGF family: biology, pathophysiology and therapy', *Nature Reviews Drug Discovery 2009 8:3*, 8(3), pp. 235–253. Available at: https://doi.org/10.1038/nrd2792.

Benevento, M., Alpár, A., Gundacker, A., Afjehi, L., Balueva, K., Hevesi, Z., Hanics, J., Rehman, S., Pollak, D.D., Lubec, G., *et al.* (2024) *A brainstem–hypothalamus neuronal circuit reduces feeding upon heat exposure*, *Nature*. Springer US. Available at: https://doi.org/10.1038/s41586-024-07232-3.

Benford, H., Bolborea, M., Pollatzek, E., Lossow, K., Hermans-Borgmeyer, I., Liu, B., Meyerhof, W., Kasparov, S. and Dale, N. (2017) 'A sweet taste receptor-dependent mechanism of glucosensing in hypothalamic tanycytes', *Glia*, 65(5), pp. 773–789. Available at: https://doi.org/10.1002/GLIA.23125.

Bhardwaj, R.D., Curtis, M.A., Spalding, K.L., Buchholz, B.A., Fink, D., Björk-Eriksson, T., Nordborg, C., Gage, F.H., Druid, H., Eriksson, P.S., *et al.* (2006) 'Neocortical neurogenesis in humans is restricted to development', *Proc. Natl Acad. Sci. USA*, 103(33), pp. 12564–12568. Available at: https://doi.org/10.1073/pnas.0605177103.

Bolborea, M., Laran-Chich, M.P., Rasri, K., Hildebrandt, H., Govitrapong, P., Simonneaux, V.R., Pévet, P., Steinlechner, S. and Klosen, P. (2011) 'Melatonin controls photoperiodic changes in tanycyte vimentin and neural cell adhesion molecule expression in the Djungarian hamster (Phodopus sungorus)', *Endocrinology*, 152(10), pp. 3871–3883. Available at: https://doi.org/10.1210/en.2011-1039.

Bolborea, M., Pollatzek, E., Benford, H., Sotelo-Hitschfeld, T. and Dale, N. (2020) 'Hypothalamic tanycytes generate acute hyperphagia through activation of the arcuate neuronal network', *Proceedings of the National Academy of Sciences of the United States of America*, 117(25), pp. 14473–14481. Available at: https://doi.org/10.1073/pnas.1919887117.

Bolborea, M. and Langlet, F. (2021) 'What is the physiological role of hypothalamic tanycytes in metabolism?', *American Journal of Physiology-Regulatory, Integrative and Comparative Physiology* [Preprint]. Available at: https://doi.org/10.1152/ajpregu.00296.2020.

Bozaoglu, K., Bolton, K., McMillan, J., Zimmet, P., Jowett, J., Collier, G., Walder, K. and Segal, D. (2007) 'Chemerin Is a Novel Adipokine Associated with Obesity and Metabolic Syndrome', *Endocrinology*, 148(10), pp. 4687–4694. Available at: https://doi.org/10.1210/EN.2007-0175.

Bratincsák, A., McMullen, D., Miyake, S., Tóth, Z.E., Hallenbeck, J.M. and Palkovits, M. (2007) 'Spatial and temporal activation of brain regions in hibernation: c-fos expression during the hibernation bout in thirteen-lined ground squirrel', *Journal of Comparative Neurology*, 505(4). Available at: https://doi.org/10.1002/cne.21507.

Breslow, D.K. and Holland, A.J. (2019) 'Mechanism and Regulation of Centriole and Cilium Biogenesis', *Annual Review of Biochemistry*, 88(June), pp. 691–724. Available at: https://doi.org/10.1146/annurev-biochem-013118-111153.

van Breukelen, F. and Martin, S.L. (2015) 'The hibernation continuum: Physiological and molecular aspects of metabolic plasticity in mammals', *Physiology*, 30(4), pp. 273–281. Available at: https://doi.org/10.1152/physiol.00010.2015.

Bronson, F.H. (1988) ‘Mammalian reproductive strategies: Genes, photoperiod and latitude’, *Reproduction Nutrition Developpement*, 28(2 B), pp. 335–347. Available at: https://doi.org/10.1051/rnd:19880301.

Bronson, F.H. (1989) *Mammalian reproductive biology*. University of Chicago Press.

Brooks, S.P.J. and Storey, K.B. (1992) ‘Mechanisms of glycolytic control during hibernation in the ground squirrel Spermophilus lateralis’, *Journal of Comparative Physiology B*, 162(1), pp. 23–28. Available at: https://doi.org/10.1007/BF00257932.

Brunner, M., Lopez-rodriguez, D., Estrada-meza, J., Rohrbach, A., Deglise, T., Messina, A., Thorens, B., Santoni, F. and Langlet, F. (2024) ‘Fasting induces metabolic switches and spatial redistributions of lipid processing and neuronal interactions in tanycytes’, pp. 1–19. Available at: https://doi.org/10.1038/s41467-024-50913-w.

Bünning, E. (1960) ‘Circadian Rhythms and the Time Measurement in Photoperiodism’, *Cold Spring Harbor Symposia on Quantitative Biology*, 25(0), pp. 249–256. Available at: https://doi.org/10.1101/SQB.1960.025.01.026.

Butruille, L., Batailler, M., Cateau, M.-L., Sharif, A., Leysen, V., Prévot, V., Vaudin, P., Pillon, D. and Migaud, M. (2022) ‘Selective Depletion of Adult GFAP-Expressing Tanycytes Leads to Hypogonadotropic Hypogonadism in Males’, *Frontiers in Endocrinology*, 13(869019). Available at: https://doi.org/10.3389/fendo.2022.869019.

Campbell, J.N., Macosko, E.Z., Fenselau, H., Pers, T.H., Lyubetskaya, A., Tenen, D., Goldman, M., Verstegen, A.M.J., Resch, J.M., McCarroll, S.A., *et al.* (2017) ‘A molecular census of arcuate hypothalamus and median eminence cell types’, *Nature Neuroscience*, 20(3), pp. 484–496. Available at: https://doi.org/10.1038/nn.4495.

Cannon, B. and Nedergaard, J. (2004) ‘Brown Adipose Tissue: Function and Physiological Significance’, *Physiological Reviews*, 84(1), pp. 277–359. Available at: https://doi.org/10.1152/physrev.00015.2003.

Carey, H. V., Andrews, M.T. and Martin, S.L. (2003) ‘Mammalian hibernation: Cellular and molecular responses to depressed metabolism and low temperature’, *Physiological Reviews*, 83(4), pp. 1153–1181. Available at: https://doi.org/10.1152/physrev.00008.2003.

Chayama, Y., Ando, L., Tamura, Y., Miura, M. and Yamaguchi, Y. (2016) ‘Decreases in body temperature and body mass constitute pre-hibernation remodelling in the Syrian golden hamster, a facultative mammalian hibernator’, *Royal Society Open Science*, 3(160002). Available at: https://doi.org/10.1098/rsos.160002.

Cheng, Y.T., Luna-Figueroa, E., Woo, J., Chen, H.C., Lee, Z.F., Harmanci, A.S. and Deneen, B. (2023) ‘Inhibitory input directs astrocyte morphogenesis through glial GABABR’, *Nature*, 617(7960), pp. 369–376. Available at: https://doi.org/10.1038/s41586-023-06010-x.

Chevillard, P.-M., Batailler, M., Piégu, B., Estienne, A., Blache, M.-C., Dubois, J.-P., Pillon, D., Vaudin, P., Dupont, J., Just, N., *et al.* (2022) ‘Seasonal vascular plasticity in the mediobasal hypothalamus of the adult ewe’, *Histochemistry and Cell Biology*, 157(5), pp. 581–593. Available at: https://doi.org/10.1007/s00418-022-02079-z.

Clark, B.S., Stein-O'Brien, G.L., Shiau, F., Cannon, G.H., Davis-Marcisak, E., Sherman, T., Santiago, C.P., Hoang, T. V., Rajaii, F., James-Esposito, R.E., *et al.* (2019) 'Single-Cell RNA-Seq Analysis of Retinal Development Identifies NFI Factors as Regulating Mitotic Exit and Late-Born Cell Specification', *Neuron*, 102(6), pp. 1111-1126.e5. Available at: https://doi.org/10.1016/J.NEURON.2019.04.010.

Clarke, I.J., Sari, I.P., Qi, Y., Smith, J.T., Parkington, H.C., Ubuka, T., Iqbal, J., Li, Q., Tilbrook, A., Morgan, K., *et al.* (2008) 'Potent Action of RFamide-Related Peptide-3 on Pituitary Gonadotropes Indicative of a Hypophysiotropic Role in the Negative Regulation of Gonadotropin Secretion', *Endocrinology*, 149(11), pp. 5811–5821. Available at: https://doi.org/10.1210/en.2008-0575.

Cohen, J. (2022) 'Fauci looks back-and ahead.', *Science (New York, N.Y.)*. United States, pp. 1137–1138. Available at: https://doi.org/10.1126/science.ade7664.

Collden, G., Balland, E., Parkash, J., Caron, E., Langlet, F., Prevot, V. and Bouret, S.G. (2015) 'Neonatal overnutrition causes early alterations in the central response to peripheral ghrelin', *Molecular Metabolism*, 4(1), pp. 15–24. Available at: https://doi.org/10.1016/j.molmet.2014.10.003.

Cowley, M.A., Pronchuk, N., Fan, W., Dinulescu, D.M., Colmers, W.F. and Cone, R.D. (1999) 'Integration of NPY, AGRP, and Melanocortin Signals in the Hypothalamic Paraventricular Nucleus: Evidence of a Cellular Basis for the Adipostat', *Neuron*, 24(1), pp. 155–163. Available at: https://doi.org/10.1016/S0896-6273(00)80829-6.

Cowley, M.A., Smart, J.L., Rubinstein, M., Cerdán, M.G., Diano, S., Horvath, T.L., Cone, R.D. and Low, M.J. (2001) 'Leptin activates anorexigenic POMC neurons through a neural network in the arcuate nucleus', *Nature*, 411(6836), pp. 480–484. Available at: https://doi.org/10.1038/35078085.

Cowley, M.A., Smith, R.G., Diano, S., Tschöp, M., Pronchuk, N., Grove, K.L., Strasburger, C.J., Bidlingmaier, M., Esterman, M., Heiman, M.L., *et al.* (2003) 'The distribution and mechanism of action of ghrelin in the CNS demonstrates a novel hypothalamic circuit regulating energy homeostasis', *Neuron*, 37(4), pp. 649–661. Available at: https://doi.org/10.1016/S0896-6273(03)00063-1.

Croizier, S. and Bouret, S.G. (2022) 'Molecular control of the development of hypothalamic neurons involved in metabolic regulation', *Journal of Chemical Neuroanatomy*, 123, p. 102117. Available at: https://doi.org/10.1016/J.JCHEMNEU.2022.102117.

Cubuk, C., Bank, J.H.H. and Herwig, A. (2016) 'The Chemistry of Cold: Mechanisms of Torpor Regulation in the Siberian Hamster', *Physiology*, 31(1), pp. 51–59. Available at: https://doi.org/10.1152/physiol.00028.2015.

Dali, R., Estrada-Meza, J. and Langlet, F. (2023) 'Tanycyte, the neuron whisperer', *Physiology and Behavior*, 263, p. 114108. Available at: https://doi.org/10.1016/j.physbeh.2023.114108.

Dardente, H., Klosen, P., Pévet, P. and Masson-Pévet, M. (2003) 'MT1 melatonin receptor mRNA expressing cells in the pars tuberalis of the European hamster: Effect of photoperiod', *Journal of Neuroendocrinology*, 15(8), pp. 778–786. Available at: https://doi.org/10.1046/j.1365-2826.2003.01060.x.

Dardente, H., Wyse, C.A., Birnie, M.J., Dupré, S.M., Loudon, A.S.I., Lincoln, G.A. and Hazlerigg, D.G. (2010) 'A molecular switch for photoperiod responsiveness in mammals', *Current Biology*, 20(24), pp. 2193–2198. Available at: https://doi.org/10.1016/j.cub.2010.10.048.

Dardente, H., Wood, S., Ebling, F. and Sáenz de Miera, C. (2019) ‘An integrative view of mammalian seasonal neuroendocrinology’, *Journal of Neuroendocrinology*, 31(5), p. e12729. Available at: https://doi.org/10.1111/jne.12729.

Dardente, H., Hazlerigg, D.G. and Ebling, F.J.P. (2014) ‘Thyroid Hormone and Seasonal Rhythmicity’, *Frontiers in Endocrinology*, 5(19). Available at: https://doi.org/10.3389/fendo.2014.00019.

Dardente, H. and Migaud, M. (2021) ‘Thyroid hormone and hypothalamic stem cells in seasonal functions’, in G. Litwack (ed.) *Vitamins and Hormones*. 1st edn. Elsevier Inc., pp. 91–131. Available at: https://doi.org/10.1016/bs.vh.2021.02.005.

Darrow, J.M., Duncan, M.J., Bartke, A., Bona-Gallo, A. and Goldman, B.D. (1988) ‘Influence of photoperiod and gonadal steroids on hibernation in the European hamster’, *Journal of Comparative Physiology A*, 163(3), pp. 339–348. Available at: https://doi.org/10.1007/BF00604009.

Darrow, J.M., Yogev, L. and Goldman, B.D. (1987) ‘Patterns of reproductive hormone secretion in hibernating Turkish hamsters’, *American Journal of Physiology-Regulatory, Integrative and Comparative Physiology*, 253(2), pp. R329-36. Available at: https://doi.org/10.1152/ajpregu.1987.253.2.R329.

Diano, S., Naftolin, F., Goglia, F. and Horvath, T.L. (1998) ‘Fasting-induced increase in type II iodothyronine deiodinase activity and messenger ribonucleic acid levels is not reversed by thyroxine in the rat hypothalamus’, *Endocrinology*, 139(6), pp. 2879–2884. Available at: https://doi.org/10.1210/endo.139.6.6062.

Diedrich, V., Haugg, E., Van Hee, J. and Herwig, A. (2023) ‘Role of glucose in daily torpor of Djungarian hamsters (Phodopus sungorus): challenge of continuous in vivo blood glucose measurements’, *American Journal of Physiology - Regulatory Integrative and Comparative Physiology*, 325(4), pp. R359–R379. Available at: https://doi.org/10.1152/ajpregu.00040.2023.

Diedrich, V., Kumstel, S. and Steinlechner, S. (2015) ‘Spontaneous daily torpor and fasting-induced torpor in Djungarian hamsters are characterized by distinct patterns of metabolic rate’, *Journal of Comparative Physiology B*, 185(3), pp. 355–366. Available at: https://doi.org/10.1007/s00360-014-0882-4.

Dietrich, M.O. and Horvath, T.L. (2012) ‘Fat incites tanycytes to neurogenesis’, *Nature Neuroscience*, 15(5). Available at: https://doi.org/10.1038/nn.3091.

Dietrich, M.O. and Horvath, T.L. (2013) ‘Hypothalamic control of energy balance : insights into the role of synaptic plasticity’, *Trends in Neurosciences*, 36(2), pp. 65–73. Available at: https://doi.org/10.1016/j.tins.2012.12.005.

Dunlap, J.C., Loros, J.J. and DeCoursey, P.J. (2004) *Chronobiology: Biological timekeeping*. Sunderland, MA, US: Sinauer Associates.

Duquenne, M., Folgueira, C., Bourouh, C., Millet, M., Silva, A., Clasadonte, J., Imbernon, M., Fernandois, D., Martinez-Corral, I., Kusumakshi, S., *et al.* (2021) ‘Leptin brain entry via a tanycytic LepR–EGFR shuttle controls lipid metabolism and pancreas function’, *Nature Metabolism*, 3(8), pp. 1071–1090. Available at: https://doi.org/10.1038/s42255-021-00432-5.

Ebling, F.J.P.P. (2014) ‘On the value of seasonal mammals for identifying mechanisms underlying the control of food intake and body weight’, *Hormones and Behavior*, 66(1), pp. 56–65. Available at: https://doi.org/10.1016/j.yhbeh.2014.03.009.

Ebling, F.P., Arthurs, O.J., Turney, B.W. and Cronin, A.S. (1998) 'Seasonal Neuroendocrine Rhythms in the Male Siberian Hamster Persist After Monosodium Glutamate-Induced Lesions of the Arcuate Nucleus in the Neonatal Period', *Journal of Neuroendocrinology*, 10(9), pp. 701–712. Available at: https://doi.org/10.1046/j.1365-2826.1998.00253.x.

Elizondo-Vega, R.J., Recabal, A. and Oyarce, K. (2019) 'Nutrient Sensing by Hypothalamic Tanycytes', *Frontiers in Endocrinology*, 10(244). Available at: https://doi.org/10.3389/fendo.2019.00244.

Elliott, J.A., Stetson, M.H. and Menaker, M. (1972) 'Regulation of Testis Function in Golden Hamsters: A Circadian Clock Measures Photoperiodic Time', *Science*, 178(4062), pp. 771–3. Available at: https://doi.org/10.1126/science.178.4062.771.

Elmquist, J.K., Coppari, R., Balthasar, N., Ichinose, M. and Lowell, B.B. (2005) 'Identifying Hypothalamic Pathways Controlling Food Intake , Body Weight , and Glucose Homeostasis', *The Journal of Comparative Neurology*, 493, pp. 63–71. Available at: https://doi.org/10.1002/cne.20786.

Eriksson, P.S., Perfilieva, E., Björk-Eriksson, T., Alborn, A.-M., Nordborg, C., Peterson, D.A. and Gage, F.H. (1998) 'Neurogenesis in the adult human hippocampus', *Nature Medicine*, 4(11), pp. 1313–1317. Available at: https://doi.org/10.1038/3305.

Ewald, J.D., Zhou, G., Lu, Y., Kolic, J., Ellis, C., Johnson, J.D., Macdonald, P.E. and Xia, J. (2024) 'Web-based multi-omics integration using the Analyst software suite', *Nature Protocols 2024*, pp. 1–31. Available at: https://doi.org/10.1038/s41596-023-00950-4.

Faouzi, M., Leshan, R., Björnholm, M., Hennessey, T., Jones, J. and Münzberg, H. (2007) 'Differential Accessibility of Circulating Leptin to Individual Hypothalamic Sites', *Endocrinology*, 148(11), pp. 5414–5423. Available at: https://doi.org/10.1210/EN.2007-0655.

Fernandois, D., Rusidzé, M., Mueller-Fielitz, H., Sauve, F., Deligia, E., Silva, M.S.B., Evrard, F., Franco-García, A., Mazur, D., Martinez-Corral, I., *et al.* (2024) 'Estrogen receptor-α signaling in tanycytes lies at the crossroads of fertility and metabolism', *Metabolism: Clinical and Experimental*, 158(March). Available at: https://doi.org/10.1016/j.metabol.2024.155976.

Figala, J., Hoffmann, K. and Goldau, G. (1973) 'Zur Jahresperiodik beim Dsungarischen Zwerghamster Phodopus sungorus Pallas', *Oecologia*, 12(2), pp. 89–118. Available at: https://doi.org/10.1007/BF00345511.

Franjic, D., Skarica, M., Ma, S., Arellano, J.I., Tebbenkamp, A.T.N., Choi, J., Xu, C., Li, Q., Morozov, Y.M., Andrijevic, D., *et al.* (2022) 'Transcriptomic taxonomy and neurogenic trajectories of adult human, macaque, and pig hippocampal and entorhinal cells', *Neuron*, 110(3), pp. 452-469.e14. Available at: https://doi.org/10.1016/J.NEURON.2021.10.036.

Frayling, C., Britton, R. and Dale, N. (2011) 'ATP-mediated glucosensing by hypothalamic tanycytes', *The Journal of Physiology*, 589(9), pp. 2275–2286. Available at: https://doi.org/10.1113/jphysiol.2010.202051.

García-Cáceres, C., Balland, E., Prevot, V., Luquet, S., Woods, S.C., Koch, M., Horvath, T.L., Yi, C.X., Chowen, J.A., Verkhratsky, A., *et al.* (2019) 'Role of astrocytes, microglia, and tanycytes in brain control of systemic metabolism', *Nature Neuroscience*, pp. 7–14. Available at: https://doi.org/10.1038/s41593-018-0286-y.

Garcia, G., Raleigh, D.R. and Reiter, J.F. (2018) 'Review How the Ciliary Membrane Is Organized Inside-Out to Communicate Outside-In', *Current Biology*, 28(8), pp. R421–R434. Available at: https://doi.org/10.1016/j.cub.2018.03.010.

Gaston, S. and Menaker, M. (1967) 'Photoperiodic Control of Hamster Testis', *Science*, 158(3803), pp. 925–928. Available at: https://doi.org/10.1126/SCIENCE.158.3803.925.

Geiser, F. (2021) 'Patterns and Expression of Torpor', in *Ecological Physiology of Daily Torpor and Hibernation*. Cham, Switzerland: Springer International Publishing (Fascinating Life Sciences), pp. 93–108. Available at: https://doi.org/10.1007/978-3-030-75525-6.

Geiser, F. and Kenagy, G.J. (1987) 'Polyunsaturated lipid diet lengthens torpor and reduces body temperature in a hibernator', *American Journal of Physiology - Regulatory Integrative and Comparative Physiology*, 252(5 (21/5)). Available at: https://doi.org/10.1152/ajpregu.1987.252.5.r897.

Geller, S., Arribat, Y., Netzahualcoyotzi, C., Lagarrigue, S., Carneiro, L., Zhang, L., Amati, F., Lopez-Mejia, I.C. and Pellerin, L. (2019) 'Tanycytes Regulate Lipid Homeostasis by Sensing Free Fatty Acids and Signaling to Key Hypothalamic Neuronal Populations via FGF21 Secretion', *Cell Metabolism*, 30(4), pp. 833-844.e7. Available at: https://doi.org/10.1016/j.cmet.2019.08.004.

Gerdes, J.M., Davis, E.E. and Katsanis, N. (2009) 'The Vertebrate Primary Cilium in Development, Homeostasis, and Disease', *Cell*, 137(1), pp. 32–45. Available at: https://doi.org/10.1016/j.cell.2009.03.023.

Giroud, S., Frare, C., Strijkstra, A., Boerema, A., Arnold, W. and Ruf, T. (2013) 'Membrane Phospholipid Fatty Acid Composition Regulates Cardiac SERCA Activity in a Hibernator, the Syrian Hamster (Mesocricetus auratus)', *PLoS ONE*, 8(5). Available at: https://doi.org/10.1371/journal.pone.0063111.

Giroud, S., Zahn, S., Criscuolo, F., Chery, I., Blanc, S., Turbill, C. and Ruf, T. (2014) 'Late-born intermittently fasted juvenile garden dormice use torpor to grow and fatten prior to hibernation: consequences for ageing processes', *Proceedings of the Royal Society B: Biological Sciences*, 281, p. 20141131. Available at: https://doi.org/10.1098/rspb.2014.1131.

Giroud, S., Habold, C., Nespolo, R.F., Mejías, C., Terrien, J., Logan, S.M., Henning, R.H. and Storey, K.B. (2021) 'The Torpid State: Recent Advances in Metabolic Adaptations and Protective Mechanisms†', *Frontiers in Physiology*, 11, p. 623665. Available at: https://doi.org/10.3389/fphys.2020.623665.

Giroud, S., Turbill, C. and Ruf, T. (2012) 'Torpor Use and Body Mass Gain During Pre-Hibernation in Late-Born Juvenile Garden Dormice Exposed to Food Shortage', in T. Ruf et al. (eds) *Living in a Seasonal World*. Berlin, Germany: Springer, pp. 481–491. Available at: https://doi.org/10.1007/978-3-642-28678-0_42.

Goldman, B.D. (2001) 'Mammalian photoperiodic system: Formal properties and neuroendocrine mechanisms of photoperiodic time measurement', *Journal of Biological Rhythms*, 16(4), pp. 283–301. Available at: https://doi.org/10.1177/074873001129001980.

Gould, E. (2007) 'How widespread is adult neurogenesis in mammals?', *Nature Reviews Neuroscience*, 8(June), pp. 481–488. Available at: https://doi.org/https://doi.org/10.1038/nrn2147.

Gower, B.A., Nagy, T.R. and Stetson, M.H. (1994) 'Pre- and postnatal effects of photoperiod on collared lemmings (Dicrostonyx groenlandicus)', *The American journal of physiology*, 267(4 Pt 2), pp. 879–887. Available at: https://doi.org/10.1152/AJPREGU.1994.267.4.R879.

Graham, E.S., Turnbull, Y., Fotheringham, P., Nilaweera, K., Mercer, J.G., Morgan, P.J. and Barrett, P. (2003) 'Neuromedin U and Neuromedin U receptor-2 expression in the mouse and rat hypothalamus: Effects of nutritional status', *Journal of Neurochemistry*, 87(5), pp. 1165–1173. Available at: https://doi.org/10.1046/j.1471-4159.2003.02079.x.

Graupner, G., Wills, K.N., Tzukerman, M., Zhang, X.K. and Pfahl, M. (1989) 'Dual regulatory role for thyroid-hormone receptors allows control of retinoic-acid receptor activity', *Nature*, 340(6235), pp. 653–656. Available at: https://doi.org/10.1038/340653a0.

Gwinner, E. (1986) *Circannual rhythms*. Berlin Heidelberg: Springer Verlag.

Hall, V. and Goldman, B. (1980) 'Effects of gonadal steroid hormones on hibernation in the Turkish hamster (Mesocricetus brandti)', *Journal of Comparative Physiology B*, 135(2), pp. 107–114. Available at: https://doi.org/10.1007/BF00691200.

Hanon, E.A., Lincoln, G.A., Fustin, J.M., Dardente, H., Masson-Pévet, M., Morgan, P.J. and Hazlerigg, D.G. (2008) 'Ancestral TSH Mechanism Signals Summer in a Photoperiodic Mammal', *Current Biology*, 18(15), pp. 1147–1152. Available at: https://doi.org/10.1016/j.cub.2008.06.076.

Hastings, M.H., Maywood, E.S. and Brancaccio, M. (2018) 'Generation of circadian rhythms in the suprachiasmatic nucleus', *Nature Reviews Neuroscience*, 19(8), pp. 453–469. Available at: https://doi.org/10.1038/s41583-018-0026-z.

Haugg, E., Borner, J., Diedrich, V. and Herwig, A. (2022) 'Comparative transcriptomics of the Djungarian hamster hypothalamus during short photoperiod acclimation and spontaneous torpor', *FEBS Open Bio*, 12(2), pp. 443–459. Available at: https://doi.org/10.1002/2211-5463.13350.

Hazlerigg, D. (2012) 'The evolutionary physiology of photoperiodism in vertebrates', in A. Kalsbeek et al. (eds) *Progress in Brain Research*, pp. 413–422. Available at: https://doi.org/10.1016/B978-0-444-59427-3.00023-X.

Hazlerigg, D. and Loudon, A. (2008) 'New Insights into Ancient Seasonal Life Timers', *Current Biology*, 18(17), pp. R795–R804. Available at: https://doi.org/10.1016/J.CUB.2008.07.040.

Hazlerigg, D. and Simonneaux, V. (2015) 'Seasonal Regulation of Reproduction in Mammals', in *Knobil and Neill's Physiology of Reproduction*. Fourth Edi. Elsevier, pp. 1575–1604. Available at: https://doi.org/10.1016/B978-0-12-397175-3.00034-X.

Hazlerigg, D.G., Wyse, C.A., Dardente, H., Hanon, E.A. and Lincoln, G.A. (2013) 'Photoperiodic Variation in CD45-Positive Cells and Cell Proliferation in the Mediobasal Hypothalamus of the Soay Sheep', *Chronobiology International*, 30(4), pp. 548–558. Available at: https://doi.org/10.3109/07420528.2012.754450.

Hazlerigg, D.G., Appenroth, D., Tomotani, B.M., West, A.C. and Wood, S.H. (2023) 'Biological timekeeping in polar environments : lessons from terrestrial vertebrates'. Available at: https://doi.org/10.1242/jeb.246308.

Hazlerigg, D.G. and Lincoln, G.A. (2011) 'Hypothesis: Cyclical Histogenesis Is the Basis of Circannual Timing', *Journal of Biological Rhythms*, 26(6), pp. 471–485. Available at: https://doi.org/10.1177/0748730411420812.

Healy, J.E., Ostrom, C.E., Wilkerson, G.K. and Florant, G.L. (2010) 'Plasma ghrelin concentrations change with physiological state in a sciurid hibernator (Spermophilus lateralis)', *General and Comparative Endocrinology*, 166(2), pp. 372–378. Available at: https://doi.org/10.1016/j.ygcen.2009.12.006.

Heldmaier, G., Ortmann, S. and Elvert, R. (2004) 'Natural hypometabolism during hibernation and daily torpor in mammals', *Respiratory Physiology and Neurobiology*, 141(3), pp. 317–329. Available at: https://doi.org/10.1016/j.resp.2004.03.014.

Heldmaier, G. and Steinlechner, S. (1981a) ‘Seasonal control of energy requirements for thermoregulation in the djungarian hamster (Phodopus sungorus), living in natural photoperiod’, *Journal of Comparative Physiology B*, 142(4), pp. 429–437. Available at: https://doi.org/10.1007/BF00688972.

Heldmaier, G. and Steinlechner, S. (1981b) ‘Seasonal pattern and energetics of short daily torpor in the Djungarian hamster, Phodopus sungorus’, *Oecologia*, 48(2), pp. 265–270. Available at: https://doi.org/10.1007/BF00347975.

Helfer, G., Ross, A.W., Russell, L., Thomson, L.M., Shearer, K.D., Goodman, T.H., McCaffery, P.J. and Morgan, P.J. (2012) ‘Photoperiod Regulates Vitamin A and Wnt/β-Catenin Signaling in F344 Rats’, *Endocrinology*, 153(2), pp. 815–824. Available at: https://doi.org/10.1210/en.2011-1792.

Helfer, G., Ross, A.W., Thomson, L.M., Mayer, C.D., Stoney, P.N., McCaffery, P.J. and Morgan, P.J. (2016) ‘A neuroendocrine role for chemerin in hypothalamic remodelling and photoperiodic control of energy balance’, *Scientific Reports*, 6(May), pp. 1–12. Available at: https://doi.org/10.1038/srep26830.

Helfer, G., Barrett, P. and Morgan, P.J. (2019) ‘A unifying hypothesis for control of body weight and reproduction in seasonally breeding mammals’, *Journal of Neuroendocrinology*. Blackwell Publishing Ltd. Available at: https://doi.org/10.1111/jne.12680.

Helfer, G., Ross, A.W. and Morgan, P.J. (2013) ‘Neuromedin U Partly Mimics Thyroid-Stimulating Hormone and Triggers Wnt/β-Catenin Signalling in the Photoperiodic Response of F344 Rats’, *Journal of Neuroendocrinology*, 25(12), pp. 1264–1272. Available at: https://doi.org/10.1111/JNE.12116.

Helfer, G. and Wu, Q.F. (2018) ‘Chemerin: A multifaceted adipokine involved in metabolic disorders’, *Journal of Endocrinology*. BioScientifica Ltd., pp. R79–R94. Available at: https://doi.org/10.1530/JOE-18-0174.

Heller, H.C., Crawshaw, L.I., Hammel, H.T., Heller, H.C., Crawshaw, L.I. and Hammel, H.T. (1978) ‘The Thermostat of Vertebrate Aninamals’, 239(2), pp. 102–115.

Heller, H.C. and Hammel, H.T. (1972) ‘CNS control of body temperature during hibernation’, *Comparative Biochemistry And Physiology*, 41, pp. 349–359.

Henningsen, J.B., Gauer, F. and Simonneaux, V. (2016) ‘RFRP neurons - the doorway to understanding seasonal reproduction in mammals’, *Frontiers in Endocrinology*, 7(36). Available at: https://doi.org/10.3389/fendo.2016.00036.

Hilgendorf, K.I., Myers, B.R. and Reiter, J.F. (2024) ‘Emerging mechanistic understanding of cilia function in cellular signalling’, *Nature Reviews Molecular Cell Biology*, 25(7), pp. 555–573. Available at: https://doi.org/10.1038/s41580-023-00698-5.

Hoang, T., Wang, J., Boyd, P., Wang, F., Santiago, C., Jiang, L., Yoo, S., Lahne, M., Todd, L.J., Jia, M., *et al.* (2020) ‘Gene regulatory networks controlling vertebrate retinal regeneration’, *Science*, 370(6519). Available at: https://doi.org/10.1126/science.abb8598.

Hoffman, R.A., Hester, R.J. and Towns, C. (1965) ‘Effect of light and temperature on the endocrine system of the golden hamster (Mesocricetus auratus waterhouse)’, *Comparative Biochemistry And Physiology*, 15(4), pp. 525–533. Available at: https://doi.org/10.1016/0010-406X(65)90152-0.

Hoffman, R.A. and Reiter, R.J. (1965) ‘Pineal Gland: Influence on Gonads of Male Hamsters’, *Science*, 148(3677), pp. 1609–1611. Available at: https://doi.org/10.1126/science.148.3677.1609.

Hoffmann, K. (1978) ‘Effects of short photoperiod on puberty, growth and moult in the Djungarian hamster (Phodopus sungorus)’, *J. Reprod. Fert.*, 54, pp. 29–35. Available at: https://doi.org/10.1007/BF00345511.

Hofmann, K., Lamberz, C., Piotrowitz, K., Offermann, N., But, D., Scheller, A., Al-Amoudi, A. and Kuerschner, L. (2017) ‘Tanycytes and a differential fatty acid metabolism in the hypothalamus’, *GLIA*, 65(2), pp. 231–249. Available at: https://doi.org/10.1002/glia.23088.

Horton, T.H. (1984a) ‘Growth and maturation in Microtus montanus : effects of photoperiods before and after weaning’, *Canadian Journal of Zoology*, 62(9), pp. 1741–1746. Available at: https://doi.org/10.1139/z84-256.

Horton, T.H. (1984b) ‘Growth and reproductive development of male Microtus montanus is affected by the prenatal photoperiod.’, *Biology of reproduction*, 31(3), pp. 499–504. Available at: https://doi.org/10.1095/biolreprod31.3.499.

Horton, T.H. (1985) ‘Cross-fostering of Voles Demonstrates in Utero Effect of Photoperiod’, *Biology of Reproduction*, 33(4), pp. 934–939. Available at: https://doi.org/10.1095/BIOLREPROD33.4.934.

Horton, T.H., Ray, S.L., Rollag, M.D., Yellon, S.M. and Stetson, M.H. (1992) ‘Maternal transfer of photoperiodic information in Siberian hamsters. V. Effects of melatonin implants are dependent on photoperiod’, *Biology of Reproduction*, 47(2), pp. 291–296. Available at: https://doi.org/10.1095/biolreprod47.2.291.

Horton, T.H., Buxton, O.M., Losee-Olson, S. and Turek, F.W. (2000) ‘Twenty-four-hour profiles of serum leptin in siberian and golden hamsters: photoperiodic and diurnal variations’, *Hormones and behavior*, 37(4), pp. 388–398. Available at: https://doi.org/10.1006/HBEH.2000.1592.

Horton, T.H. (2005) ‘Fetal origins of developmental plasticity: Animal models of induced life history variation’, *American Journal of Human Biology*, 17(1), pp. 34–43. Available at: https://doi.org/10.1002/ajhb.20092.

Horton, T.H., Ray, S.L. and Stetson, M.H. (1989) ‘Maternal transfer of photoperiodic information in Siberian hamsters. III. Melatonin injections program postnatal reproductive development expressed in constant light’, *Biology of Reproduction*, 41(1), pp. 34–39. Available at: https://doi.org/10.1095/biolreprod41.1.34.

Horton, T.H., Stachecki, S.A. and Stetson, M.H. (1990) ‘Maternal transfer of photoperiodic information in Siberian hamsters. IV. Peripubertal reproductive development in the absence of maternal photoperiodic signals during gestation’, *Biology of Reproduction*, 42(3), pp. 441–449. Available at: https://doi.org/10.1095/biolreprod42.3.441.

Horton, T.H. and Stetson, M.H. (1992) ‘Maternal transfer of photoperiodic information in rodents’, *Animal Reproduction Science*, 30(1–3), pp. 29–44. Available at: https://doi.org/10.1016/0378-4320(92)90004-W.

Huang, L., DeVries, G.J. and Bittman, E.L. (1998) ‘Photoperiod regulates neuronal bromodeoxyuridine labeling in the brain of a seasonally breeding mammal’, *Journal of Neurobiology*, 36(3), pp. 410–420. Available at: https://doi.org/10.1002/(SICI)1097-4695(19980905)36:3<410::AID-NEU8>3.0.CO;2-Z.

Hudson, J.W. and Scott, I.M. (1979) ‘Daily Torpor in the Laboratory Mouse, Mus musculus Var. Albino’, *https://doi.org/10.1086/physzool.52.2.30152564*, 52(2), pp. 205–218. Available at: https://doi.org/10.1086/PHYSZOOL.52.2.30152564.

Hut, R.A., Kronfeld-Schor, N., van der Vinne, V. and De la Iglesia, H. (2012) 'In search of a temporal niche: Environmental factors', *Progress in Brain Research*, 199, pp. 281–304. Available at: https://doi.org/10.1016/B978-0-444-59427-3.00017-4.

Hut, R.A., Paolucci, S., Dor, R., Kyriacou, C.P. and Daan, S. (2013) 'Latitudinal clines: An evolutionary view on biological rhythms', *Proceedings of the Royal Society B: Biological Sciences*, 280(1765). Available at: https://doi.org/10.1098/rspb.2013.0433.

Ihrie, R.A. and Álvarez-Buylla, A. (2011) 'Lake-Front Property : A Unique Germinal Niche by the Lateral Ventricles of the Adult Brain', *Neuron*, 70(4), pp. 674–686. Available at: https://doi.org/10.1016/j.neuron.2011.05.004.

Ivanov, T.R., Lawrence, C.B., Stanley, P.J. and Luckman, S.M. (2002) 'Evaluation of neuromedin U actions in energy homeostasis and pituitary function', *Endocrinology*, 143(10), pp. 3813–3821. Available at: https://doi.org/10.1210/en.2002-220121.

Ivanova, E.A., Bechtold, D.A., Dupré, S.M., Brennand, J., Barrett, P., Luckman, S.M. and Loudon, A.S.I. (2008) 'Altered metabolism in the melatonin-related receptor (GPR50) knockout mouse', *American Journal of Physiology - Endocrinology and Metabolism*, 294(1).

James, G. and Butt, A.M. (2002) 'P2Y and P2X purinoceptor mediated Ca2+ signalling in glial cell pathology in the central nervous system', *European Journal of Pharmacology*, 447(2–3), pp. 247–260. Available at: https://doi.org/10.1016/S0014-2999(02)01756-9.

Jansen, H.T., Popiela, C.L., Jackson, G.L. and Iwamoto, G.A. (1993) 'A re-evaluation of the effects of gonadal steroids on neuronal activity in the male rat', *Brain Research Bulletin*, 31(1–2), pp. 217–223. Available at: https://doi.org/10.1016/0361-9230(93)90028-A.

Johnson, R.J., Stenvinkel, P., Andrews, P., Sánchez-Lozada, L.G., Nakagawa, T., Gaucher, E., Andres-Hernando, A., Rodriguez-Iturbe, B., Jimenez, C.R., Garcia, G., *et al.* (2020) 'Fructose metabolism as a common evolutionary pathway of survival associated with climate change, food shortage and droughts', *Journal of Internal Medicine*, 287(3), pp. 252–262. Available at: https://doi.org/10.1111/joim.12993.

Johnston, J.D., Messager, S., Barrett, P. and Hazlerigg, D.G. (2003) 'Melatonin action in the pituitary: Neuroendocrine synchronizer and developmental modulator?', *Journal of Neuroendocrinology*, 15(4), pp. 405–408. Available at: https://doi.org/10.1046/j.1365-2826.2003.00972.x.

Kameda, Y., Arai, Y. and Nishimaki, T. (2003) 'Ultrastructural localization of vimentin immunoreactivity and gene expression in tanycytes and their alterations in hamsters kept under different photoperiods', *Cell Tissue Res*, 314, pp. 251–262. Available at: https://doi.org/10.1007/s00441-003-0789-y.

Karpovich, S.A., Tøien, Æ.Ø., Buck, C.L. and Barnes, Æ.B.M. (2009) 'Energetics of arousal episodes in hibernating arctic ground squirrels', pp. 691–700. Available at: https://doi.org/10.1007/s00360-009-0350-8.

Klieverik, L.P., Janssen, S.F., Van Riel, A., Foppen, E., Bisschop, P.H., Serlie, M.J., Boelen, A., Ackermans, M.T., Sauerwein, H.P., Fliers, E., *et al.* (2009) 'Thyroid hormone modulates glucose production via a sympathetic pathway from the hypothalamic paraventricular nucleus to the liver', *Proceedings of the National Academy of Sciences of the United States of America*, 106(14), pp. 5966–5971. Available at: https://doi.org/10.1073/pnas.0805355106.

Klosen, P., Bienvenu, C., Demarteau, O., Dardente, H., Guerrero, H., Pévet, P. and Masson-Pévet, M. (2002) 'The mt1 Melatonin Receptor and RORβ Receptor Are Co-localized in Specific TSH-immunoreactive Cells in the Pars Tuberalis of the Rat Pituitary', *Journal of Histochemistry & Cytochemistry*, 50(12), pp. 1647–1657. Available at: https://doi.org/10.1177/002215540205001209.

Klosen, P., Sébert, M.-E., Rasri, K., Laran-Chich, M.-P. and Simonneaux, V. (2013) 'TSH restores a summer phenotype in photoinhibited mammals via the RF-amides RFRP3 and kisspeptin', *The FASEB Journal*, 27(7), pp. 2677–2686. Available at: https://doi.org/10.1096/fj.13-229559.

Knowles, S.F. and Anand Kumar, T.C. (1969) 'Structural changes, related to reproduction, in the hypothalamus and in the pars tuberalis of the rhesus monkey: Part I. The hypothalamus. Part II. The pars tuberalis', *Philosophical Transactions of the Royal Society of London. B, Biological Sciences*, 256(809), pp. 357–375. Available at: https://doi.org/10.1098/rstb.1969.0045.

Kokoeva, M. V., Yin, H. and Flier, J.S. (2005) 'Neurogenesis in the hypothalamus of adult mice: Potential role in energy balance', *Science*, 310(5748), pp. 679–683. Available at: https://doi.org/10.1126/science.1115360.

Kokoeva, M. V., Yin, H. and Flier, J.S. (2007) 'Evidence for constitutive neural cell proliferation in the adult murine hypothalamus', *Journal of Comparative Neurology*, 505(2), pp. 209–220. Available at: https://doi.org/10.1002/CNE.21492.

Kriegstein, A. and Alvarez-Buylla, A. (2009) 'The glial nature of embryonic and adult neural stem cells', *Annual Review of Neuroscience*, pp. 149–184. Available at: https://doi.org/10.1146/annurev.neuro.051508.135600.

Langlet, F., Mullier, A., Bouret, Sebastien G, Prevot, V. and Dehouck, B. (2013) 'Tanycyte-like cells form a blood-cerebrospinal fluid barrier in the circumventricular organs of the mouse brain.', *The Journal of comparative neurology*, 521(15), pp. 3389–405. Available at: https://doi.org/10.1002/cne.23355.

Langlet, F., Mullier, A., Bouret, Sebastien G., Prevot, V. and Dehouck, B. (2013) 'Tanycyte-like cells form a blood–cerebrospinal fluid barrier in the circumventricular organs of the mouse brain', *Journal of Comparative Neurology*, 521(15), pp. 3389–3405. Available at: https://doi.org/10.1002/cne.23355.

Langlet, F., Levin, B.E., Luquet, S., Mazzone, M., Messina, A., Dunn-Meynell, A.A., Balland, E., Lacombe, A., Mazur, D., Carmeliet, P., *et al.* (2013) 'Tanycytic VEGF-A boosts blood-hypothalamus barrier plasticity and access of metabolic signals to the arcuate nucleus in response to fasting', *Cell Metabolism*, 17(4), pp. 607–617. Available at: https://doi.org/10.1016/j.cmet.2013.03.004.

Lazutkaite, G., Soldà, A., Lossow, K., Meyerhof, W. and Dale, N. (2017) 'Amino acid sensing in hypothalamic tanycytes via umami taste receptors', *Molecular Metabolism*, 6(11), pp. 1480–1492. Available at: https://doi.org/10.1016/J.MOLMET.2017.08.015.

Lee, C.H., Song, D.K., Park, C.B., Choi, J., Kang, G.M., Shin, S.H., Kwon, I., Park, S., Kim, S., Kim, J.Y., *et al.* (2020) 'Primary cilia mediate early life programming of adiposity through lysosomal regulation in the developing mouse hypothalamus', *Nature Communications 2020 11:1*, 11(1), pp. 1–19. Available at: https://doi.org/10.1038/s41467-020-19638-4.

Lee, D.A., Bedont, J.L., Pak, T., Wang, H., Song, J., Miranda-Angulo, A., Takiar, V., Charubhumi, V., Balordi, F., Takebayashi, H., *et al.* (2012) 'Tanycytes of the hypothalamic median eminence form a diet-responsive neurogenic niche', *Nature Neuroscience*, 15(5), pp. 700–702. Available at: https://doi.org/10.1038/nn.3079.

Lee, D.A. and Blackshaw, S. (2012) 'Functional implications of hypothalamic neurogenesis in the adult mammalian brain', *International Journal of Developmental Neuroscience*, 30(8), pp. 615–621. Available at: https://doi.org/10.1016/j.ijdevneu.2012.07.003.

Lee, T.M., Spears, N., Tuthill, C.R. and Zucker, I. (1989) 'Maternal Melatonin Treatment Influences Rates of Neonatal Development of Meadow Vole Pups', *Biology of Reproduction*, 40(3), pp. 495–502. Available at: https://doi.org/10.1095/biolreprod40.3.495.

Lee, T.M., Pelz, K., Licht, P. and Zucker, I. (1990) 'Testosterone influences hibernation in golden-mantled ground squirrels', *Am J Physiol Regul Integr Comp Physiol*, 259(28), pp. 760–767.

Lee, T.M. (1993) 'Development of meadow voles is influenced postnatally by maternal photoperiodic history', *American Journal of Physiology - Regulatory Integrative and Comparative Physiology*, 265(4 34-4). Available at: https://doi.org/10.1152/ajpregu.1993.265.4.r749.

Lein, E.S., Hawrylycz, M.J., Ao, N., Ayres, M., Bensinger, A., Bernard, A., Boe, A.F., Boguski, M.S., Brockway, K.S., Byrnes, E.J., *et al.* (2006) 'Genome-wide atlas of gene expression in the adult mouse brain', *Nature 2006 445:7124*, 445(7124), pp. 168–176. Available at: https://doi.org/10.1038/nature05453.

Lhomme, T., Clasadonte, J., Imbernon, M., Fernandois, D., Sauve, F., Caron, E., da Silva Lima, N., Heras, V., Martinez-Corral, I., Mueller-Fielitz, H., *et al.* (2021) 'Tanycytic networks mediate energy balance by feeding lactate to glucose-insensitive POMC neurons', *Journal of Clinical Investigation*, 131(18). Available at: https://doi.org/10.1172/JCI140521.

Loktev, A. V., Jackson, P.K., Way, D.N.A. and Francisco, S.S. (2013) 'Neuropeptide Y Family Receptors Traffic via the Bardet-Biedl Syndrome Pathway to Signal in Neuronal Primary Cilia', *CellReports*, 5(5), pp. 1316–1329. Available at: https://doi.org/10.1016/j.celrep.2013.11.011.

Lomet, D., Cognié, J., Chesneau, D., Dubois, E., Hazlerigg, D. and Dardente, H. (2018) 'The impact of thyroid hormone in seasonal breeding has a restricted transcriptional signature', *Cellular and Molecular Life Sciences*, 75(5), pp. 905–919. Available at: https://doi.org/10.1007/s00018-017-2667-x.

Lomet, D., Druart, X., Hazlerigg, D., Beltramo, M. and Dardente, H. (2020) 'Circuit-level analysis identifies target genes of sex steroids in ewe seasonal breeding', *Molecular and Cellular Endocrinology*, 512(110825). Available at: https://doi.org/10.1016/j.mce.2020.110825.

López, M., Varela, L., Vázquez, M.J., Rodríguez-Cuenca, S., González, C.R., Velagapudi, V.R., Morgan, D.A., Schoenmakers, E., Agassandian, K., Lage, R., *et al.* (2010) 'Hypothalamic AMPK and fatty acid metabolism mediate thyroid regulation of energy balance', *Nature Medicine*, 16(9), pp. 1001–1008. Available at: https://doi.org/10.1038/nm.2207.

Lyman, C.P. (1948) 'The oxygen consumption and temperature regulation of hibernating hamsters', *Journal of Experimental Zoology*, 109(1), pp. 55–78. Available at: https://doi.org/10.1002/jez.1401090105.

Lyman, C.P. (1954) 'Activity, Food Consumption and Hoarding in Hibernators', *Journal of Mammalogy*, 35(4), p. 545. Available at: https://doi.org/10.2307/1375580.

Lyman, C.P., Willis, J.S., Malan, A. and Wang, L.C.H. (1982) *Hibernation and Torpor in Mammals and Birds, Physiological ecology*. Edited by C.P. Lyman. New York: Academic Press. Available at: https://doi.org/10.2307/3808208.

Lyman, C.P. and Chatfield, P.O. (1955) ‘Physiology of Hibernation in Mammals’, *Physiological Reviews*, 35(2), pp. 403–425. Available at: https://doi.org/10.1152/physrev.1955.35.2.403.

Maden, M. (2007) ‘Retinoic acid in the development, regeneration and maintenance of the nervous system’, *Nature Reviews Neuroscience*, 8(10), pp. 755–765. Available at: https://doi.org/10.1038/nrn2212.

Magistretti, P.J. and Allaman, I. (2018) ‘Lactate in the brain: from metabolic end-product to signalling molecule’, *Nature Reviews Neuroscience 2018 19:4*, 19(4), pp. 235–249. Available at: https://doi.org/10.1038/nrn.2018.19.

Malan, A., Ciocca, D., Challet, E. and Pévet, P. (2018) ‘Implicating a Temperature-Dependent Clock in the Regulation of Torpor Bout Duration in Classic Hibernation’, *Journal of Biological Rhythms*, 33(6), pp. 626–636. Available at: https://doi.org/10.1177/0748730418797820.

Markussen, F.A.F. (2020) *Hibernation in European Hamsters (Cricetus crisetus): An assessment of brain permeability during torpor-arousal cycling*. UiT-The Arctic University of Norway.

Markussen, F.A.F., Cázarez-Márquez, F., Melum, V.J., Hazlerigg, D.G. and Wood, S.H. (2024) ‘C-Fos Induction in the Choroid Plexus, Tanycytes and Pars Tuberalis Is an Early Indicator of Spontaneous Arousal From Torpor in a Deep Hibernator’, *Journal of Experimental Biology*, 227(10). Available at: https://doi.org/10.1242/jeb.247224.

Masumoto, K.H., Ukai-Tadenuma, M., Kasukawa, T., Nagano, M., Uno, K.D., Tsujino, K., Horikawa, K., Shigeyoshi, Y. and Ueda, H.R. (2010) ‘Acute induction of Eya3 by late-night light stimulation triggers TSHβ expression in photoperiodism’, *Current Biology*, 20(24), pp. 2199–2206. Available at: https://doi.org/10.1016/j.cub.2010.11.038.

Matsuzaki, K., Katakura, M., Hara, T., Li, G., Hashimoto, M. and Shido, O. (2009) ‘Proliferation of neuronal progenitor cells and neuronal differentiation in the hypothalamus are enhanced in heat-acclimated rats’, *Pflugers Archiv European Journal of Physiology*, 458(4), pp. 661–673. Available at: https://doi.org/10.1007/S00424-009-0654-2/FIGURES/10.

Matsuzaki, K., Katakura, M., Inoue, T., Hara, T., Hashimoto, M. and Shido, O. (2015) ‘Aging attenuates acquired heat tolerance and hypothalamic neurogenesis in rats’, *Journal of Comparative Neurology*, 523(8), pp. 1190–1201. Available at: https://doi.org/10.1002/CNE.23732.

Matsuzaki, K., Katakura, M., Sugimoto, N., Hara, T., Hashimoto, M. and Shido, O. (2017) ‘Neural progenitor cell proliferation in the hypothalamus is involved in acquired heat tolerance in long-term heat-acclimated rats’, *PLOS ONE*, 12(6), p. e0178787. Available at: https://doi.org/10.1371/JOURNAL.PONE.0178787.

Melum, V.J., Sáenz de Miera, C., Markussen, F.A.F., Cázarez-Márquez, F., Jaeger, C., Sandve, S.R., Simonneaux, V., Hazlerigg, D.G. and Wood, S.H. (2024) ‘Hypothalamic tanycytes as mediators of maternally programmed seasonal plasticity’, *Current Biology*, 34(3), pp. 632-640.e6. Available at: https://doi.org/10.1016/J.CUB.2023.12.042.

Migaud, M., Batailler, M., Pillon, D., Franceschini, I. and Malpaux, B. (2011) ‘Seasonal changes in cell proliferation in the adult sheep brain and pars tuberalis’, *Journal of Biological Rhythms*, 26(6), pp. 486–496. Available at: https://doi.org/10.1177/0748730411420062.

Milesi, S., Simonneaux, V. and Klosen, P. (2017) ‘Downregulation of Deiodinase 3 is the earliest event in photoperiodic and photorefractory activation of the gonadotropic axis in seasonal hamsters’, *Scientific Reports*, 7(1), p. 17739. Available at: https://doi.org/10.1038/s41598-017-17920-y.

Ming, G. li and Song, H. (2011) ‘Adult neurogenesis in the mammalian brain: significant answers and significant questions’, *Neuron*, 70(4), pp. 687–702. Available at: https://doi.org/10.1016/J.NEURON.2011.05.001.

Mirzadeh, Z., Kusne, Y., Duran-Moreno, M., Cabrales, E., Gil-Perotin, S., Ortiz, C., Chen, B., Garcia-Verdugo, J.M., Sanai, N. and Alvarez-Buylla, A. (2017) ‘Bi- and uniciliated ependymal cells define continuous floor-plate-derived tanycytic territories’, *Nature Communications*, 8, pp. 1–12. Available at: https://doi.org/10.1038/ncomms13759.

Mohr, S.M., Dai Pra, R., Platt, M.P., Feketa, V. V., Shanabrough, M., Varela, L., Kristant, A., Cao, H., Merriman, D.K., Horvath, T.L., *et al.* (2024) ‘Hypothalamic hormone deficiency enables physiological anorexia in ground squirrels during hibernation’, *Nature Communications*, 15(1). Available at: https://doi.org/10.1038/s41467-024-49996-2.

Mrosovsky, N. (1971) *Hibernation and the Hypothalamus*. Edited by A. Towe. Boston, MA: Springer US. Available at: https://doi.org/10.1007/978-1-4684-7176-2.

Mrosovsky, N. (1990) *Rheostasis: The Physiology of Change*. New York: Oxford University Press.

Mrosovsky, N. and Fisher, K.C. (1970) ‘Sliding set points for body weight in ground squirrels during the hibernation season.’, *Canadian journal of zoology*, 48(2), pp. 241–247. Available at: https://doi.org/10.1139/z70-040.

Müller-Fielitz, H., Stahr, M., Bernau, M., Richter, M., Abele, S., Krajka, V., Benzin, A., Wenzel, J., Kalies, K., Mittag, J., *et al.* (2017) ‘Tanycytes control the hormonal output of the hypothalamic-pituitary-thyroid axis’, *Nature Communications*, 8(1). Available at: https://doi.org/10.1038/s41467-017-00604-6.

Mullier, A., Bouret, S.G., Prevot, V. and Dehouck, B. (2010) ‘Differential distribution of tight junction proteins suggests a role for tanycytes in blood-hypothalamus barrier regulation in the adult mouse brain’, *Journal of Comparative Neurology*, 518(7), pp. 943–962. Available at: https://doi.org/10.1002/cne.22273.

Murphy, M., Jethwa, P.H., Warner, A., Barrett, P., Nilaweera, K.N., Brameld, J.M. and Ebling, F.J.P. (2012) ‘Effects of Manipulating Hypothalamic Triiodothyronine Concentrations on Seasonal Body Weight and Torpor Cycles in Siberian Hamsters’, *Endocrinology*, 153(1), pp. 101–112. Available at: https://doi.org/10.1210/en.2011-1249.

Nakao, N., Ono, H., Yamamura, T., Anraku, T., Takagi, T., Higashi, K., Yasuo, S., Katou, Y., Kageyama, S., Uno, Y., *et al.* (2008) ‘Thyrotrophin in the pars tuberalis triggers photoperiodic response’, *Nature*, 452(7185), pp. 317–322. Available at: https://doi.org/10.1038/nature06738.

Nano, P.R. and Bhaduri, A. (2022) ‘Mounting evidence suggests human adult neurogenesis is unlikely’, *Neuron*, 110(3), pp. 353–355. Available at: https://doi.org/10.1016/J.NEURON.2022.01.004.

Nedergaard, J. and Cannon, B. (1990) ‘Mammalian hibernation’, *Philosophical Transactions - Royal Society of London, B*, 326(1237), pp. 669–686. Available at: https://doi.org/10.1098/rstb.1990.0038.

Negus, N.C., Berger, P.J. and Brown, B.W. (1986) ‘Microtine population dynamics in a predictable environment’, *Canadian Journal of Zoology*, 64(3), pp. 785–792. Available at: https://doi.org/10.1139/z86-117.

Negus, N.C., Berger, P.J. and Forslund, L.G. (1977) 'Reproductive Strategy of Microtus montanus', *Journal of Mammalogy*, 58(3), pp. 347–353. Available at: https://doi.org/10.2307/1379333.

Negus, N.C., Berger, P.J. and Pinter, A.J. (1992) 'Phenotypic plasticity of the montane vole (Microtus montanus) in unpredictable environments', *Canadian Journal of Zoology*, 70(11), pp. 2121–2124. Available at: https://doi.org/10.1139/z92-285.

Niederreither, K. and Dollé, P. (2008) 'Retinoic acid in development: towards an integrated view', *Nature Reviews Genetics 2008 9:7*, 9(7), pp. 541–553. Available at: https://doi.org/10.1038/nrg2340.

Nilaweera, K., Herwig, A., Bolborea, M., Campbell, G., Mayer, C.D., Morgan, P.J., Ebling, F.J.P. and Barrett, P. (2011) 'Photoperiodic regulation of glycogen metabolism, glycolysis, and glutamine synthesis in tanycytes of the Siberian hamster suggests novel roles of tanycytes in hypothalamic function', *Glia*, 59(11), pp. 1695–1705. Available at: https://doi.org/10.1002/glia.21216.

Noctor, S.C., Flint, A.C., Weissman, T.A., Dammerman, R.S. and Kriegstein, A.R. (2001) 'Neurons derived from radial glial cells establish radial units in neocortex', *Nature*, 409(6821), pp. 714–720. Available at: https://doi.org/10.1038/35055553.

Noctor, S.C., Martínez-cerdeño, V., Ivic, L. and Kriegstein, A.R. (2004) 'Cortical neurons arise in symmetric and asymmetric division zones and migrate through specific phases', *Nat Neurosci*, 7(2), pp. 136–144. Available at: https://doi.org/10.1038/nn1172.

Noctor, S.C., Martínez-cerdeño, V. and Kriegstein, A.R. (2008) 'Distinct Behaviors of Neural Stem and Progenitor Cells Underlie Cortical', *The Journal of Comparative Neurology*, 508, pp. 28–44. Available at: https://doi.org/10.1002/cne.21669.

Olson, C.J.H. and Krois, C.R. (2019) 'Thyroid hormone regulation of retinoic acid synthesis in brown adipose tissue', *The FASEB Journal*, 33(S1), pp. 485.8-485.8. Available at: https://doi.org/10.1096/FASEBJ.2019.33.1_SUPPLEMENT.485.8.

Ono, H., Hoshino, Y., Yasuo, S., Watanabe, M., Nakane, Y., Murai, A., Ebihara, S., Korf, H.-W. and Yoshimura, T. (2008) 'Involvement of thyrotropin in photoperiodic signal transduction in mice.', *Proceedings of the National Academy of Sciences of the United States of America*, 105(47), pp. 18238–42. Available at: https://doi.org/10.1073/pnas.0808952105.

Orellana, J.A., Sáez, P.J., Cortés-Campos, C., Elizondo, R.J., Shoji, K.F., Contreras-Duarte, S., Figueroa, V., Velarde, V., Jiang, J.X., Nualart, F., *et al.* (2012) 'Glucose increases intracellular free Ca(2+) in tanycytes via ATP released through connexin 43 hemichannels.', *Glia*, 60(1), pp. 53–68. Available at: https://doi.org/10.1002/glia.21246.

Parkash, J., Messina, A., Langlet, F., Cimino, I., Loyens, A., Mazur, D., Gallet, S., Balland, E., Malone, S.A., Pralong, F., *et al.* (2015) 'Semaphorin7A regulates neuroglial plasticity in the adult hypothalamic median eminence', *Nature Communications*, 6. Available at: https://doi.org/10.1038/ncomms7385.

Pasquettaz, R., Kolotuev, I., Rohrbach, A., Gouelle, C., Pellerin, L. and Langlet, F. (2020) 'Peculiar protrusions along tanycyte processes face diverse neural and nonneural cell types in the hypothalamic parenchyma', *Journal of Comparative Neurology*, 529(3), pp. 553–575. Available at: https://doi.org/10.1002/cne.24965.

Pellegrino, G., Trubert, C., Terrien, J., Pifferi, F., Leroy, D., Loyens, A., Migaud, M., Baroncini, M., Maurage, C.A., Fontaine, C., *et al.* (2018) 'A comparative study of the neural stem cell niche in the adult hypothalamus of human, mouse, rat and gray mouse lemur (Microcebus murinus)', *Journal of Comparative Neurology*, 526(9), pp. 1419–1443. Available at: https://doi.org/10.1002/cne.24376.

Perrigo, G. and Bronson, F.H. (1983) ‘Foraging effort, food intake, fat deposition and puberty in female mice’, *Biology of Reproduction*, 29(2), pp. 455–463. Available at: https://doi.org/10.1095/BIOLREPROD29.2.455.

Placzek, M., Chinnaiya, K., Kim, D.W. and Blackshaw, S. (2024) ‘Control of tuberal hypothalamic development and its implications in metabolic disorders’, *Nature Reviews Endocrinology* [Preprint]. Available at: https://doi.org/10.1038/s41574-024-01036-1.

Porniece Kumar, M., Cremer, A.L., Klemm, P., Steuernagel, L., Sundaram, S., Jais, A., Hausen, A.C., Tao, J., Secher, A., Pedersen, T.Å., *et al.* (2021) ‘Insulin signalling in tanycytes gates hypothalamic insulin uptake and regulation of AgRP neuron activity’, *Nature Metabolism*, 3(12), pp. 1662–1679. Available at: https://doi.org/10.1038/s42255-021-00499-0.

Prevot, V., Croix, D., Bouret, S., Dutoit, S., Tramu, G., Stefano, G.B. and Beauvillain, J.C. (1999) ‘Definitive evidence for the existence of morphological plasticity in the external zone of the median eminence during the rat estrous cycle: implication of neuro-glio-endothelial interactions in gonadotropin-releasing hormone release’, *Neuroscience*, 94(3), pp. 809–819. Available at: https://doi.org/10.1016/S0306-4522(99)00383-8.

Prevot, V., Dehouck, B., Sharif, A., Ciofi, P., Giacobini, P. and Clasadonte, J. (2018) ‘The Versatile Tanycyte: A Hypothalamic Integrator of Reproduction and Energy Metabolism’, *Endocrine Reviews*, 39(3), pp. 333–368. Available at: https://doi.org/10.1210/er.2017-00235.

Rakic, P. (1972) ‘Mode of cell migration to the superficial layers of fetal monkey neocortex’, *Journal of Comparative Neurology*, 145(1), pp. 61–83. Available at: https://doi.org/10.1002/CNE.901450105.

Rakic, P. (2006) ‘No More Cortical Neurons for You’, *Science*, 313(5789), pp. 928–929. Available at: https://doi.org/10.1126/science.1131713.

Ramón y Cajal, S. (1909) *Histologie du système nerveux de l’homme & des vertébrés*, *Histologie du système nerveux de l’homme & des vertébrés*. Paris: Maloine. Available at: https://doi.org/10.5962/bhl.title.48637.

Ravault, J.-P. and Ortavant, R. (1977) ‘Light control of prolactin secretion in sheep. Evidence for a photoinducible phase during a diurnal rhythm’, *Ann. Biol. Anim. Bioch. Biophys*, 17(3B), pp. 459–473.

Recabal, A., Elizondo-Vega, R., Philippot, C., Salgado, M., López, S., Palma, A., Tarifeño-Saldivia, E., Timmermann, A., Seifert, G., Caprile, T., *et al.* (2018) ‘Connexin-43 Gap Junctions Are Responsible for the Hypothalamic Tanycyte-Coupled Network’, *Frontiers in Cellular Neuroscience*, 12(406). Available at: https://doi.org/10.3389/fncel.2018.00406.

Recabal, A., Fernández, P., López, S., Barahona, M.J., Ordenes, P., Palma, A., Carlos, R.E., Uribe, A., Caprile, T., Sáez, J.C., *et al.* (2021) ‘The FGF2-induced tanycyte proliferation involves a connexin 43 hemichannel / purinergic-dependent pathway’, (June 2020), pp. 182–199. Available at: https://doi.org/10.1111/jnc.15188.

Robins, S.C., Stewart, I., McNay, D.E., Taylor, V., Giachino, C., Goetz, M., Ninkovic, J., Briancon, N., Maratos-Flier, E., Flier, J.S., *et al.* (2013) ‘α-Tanycytes of the adult hypothalamic third ventricle include distinct populations of FGF-responsive neural progenitors’, *Nature Communications*, 4(May), pp. 1–13. Available at: https://doi.org/10.1038/ncomms3049.

Rodríguez-Cortés, B., Hurtado-Alvarado, G., Martínez-Gómez, R., León-Mercado, L.A., Prager-Khoutorsky, M. and Buijs, Ruud M. (2022) ‘Suprachiasmatic nucleus-mediated glucose entry into the arcuate nucleus determines the daily rhythm in blood glycemia’, *Current Biology*, 32(4), pp. 796-805.e4. Available at: https://doi.org/10.1016/j.cub.2021.12.039.

Rodríguez, E., Guerra, M., Peruzzo, B. and Blázquez, J.L. (2019) 'Tanycytes: A rich morphological history to underpin future molecular and physiological investigations', *Journal of Neuroendocrinology*, 31(3), pp. 1–29. Available at: https://doi.org/10.1111/jne.12690.

Rodríguez, E.M., Blázquez, J.L., Pastor, F.E., Peláez, B., Peña, P., Peruzzo, B. and Amat, P. (2005) 'Hypothalamic Tanycytes: A Key Component of Brain–Endocrine Interaction', *International Review of Cytology*, 247, pp. 89–164. Available at: https://doi.org/10.1016/S0074-7696(05)47003-5.

Rodríguez, E.M., Blázquez, J.L. and Guerra, M. (2010) 'The design of barriers in the hypothalamus allows the median eminence and the arcuate nucleus to enjoy private milieus: The former opens to the portal blood and the latter to the cerebrospinal fluid', *Peptides*, 31(4), pp. 757–776. Available at: https://doi.org/10.1016/j.peptides.2010.01.003.

Rohrbach, A., Caron, E., Dali, R., Brunner, M., Pasquettaz, R., Kolotuev, I., Santoni, F., Thorens, B. and Langlet, F. (2021) 'Ablation of glucokinase-expressing tanycytes impacts energy balance and increases adiposity in mice', *Molecular Metabolism*, 53(July), pp. 1–17. Available at: https://doi.org/10.1016/j.molmet.2021.101311.

Ross, A.W., Webster, C.A., Mercer, J.G., Moar, K.M., Ebling, F.J., Schuhler, S., Barrett, P. and Morgan, P.J. (2004) 'Photoperiodic Regulation of Hypothalamic Retinoid Signaling: Association of Retinoid X Receptor γ with Body Weight', *Endocrinology*, 145(1), pp. 13–20. Available at: https://doi.org/10.1210/en.2003-0838.

Rousseau, K., Atcha, Z., Cagampang, F.R.A., Le Rouzic, P., Stirland, J.A., Ivanov, T.R., Ebling, F.J.P., Klingenspor, M. and Loudon, A.S.I. (2002) 'Photoperiodic Regulation of Leptin Resistance in the Seasonally Breeding Siberian Hamster (Phodopus sungorus)', *Endocrinology*, 143(8), pp. 3083–3095. Available at: https://doi.org/10.1210/endo.143.8.8967.

Ruf, T., Stieglitz, A., Steinlechner, S., Blank, J.L. and Heldmaier, G. (1993) 'Cold exposure and food restriction facilitate physiological responses to short photoperiod in Djungarian hamsters (Phodopus sungorus)', *Journal of Experimental Zoology*, 267(2), pp. 104–112. Available at: https://doi.org/10.1002/JEZ.1402670203.

Ruf, T. and Geiser, F. (2015) 'Daily torpor and hibernation in birds and mammals', *Biological Reviews*, 90(3), pp. 891–926. Available at: https://doi.org/10.1111/brv.12137.

Sáenz de Miera, C., Monecke, S., Bartzen-Sprauer, J., Laran-Chich, M.-P., Pévet, P., Hazlerigg, D.G. and Simonneaux, V. (2014) 'A Circannual Clock Drives Expression of Genes Central for Seasonal Reproduction', *Current Biology*, 24(13), pp. 1500–1506. Available at: https://doi.org/10.1016/J.CUB.2014.05.024.

Sáenz de Miera, C., Bothorel, B., Jaeger, C., Simonneaux, V. and Hazlerigg, D. (2017) 'Maternal photoperiod programs hypothalamic thyroid status via the fetal pituitary gland', *Proceedings of the National Academy of Sciences of the United States of America*, 114(31), pp. 8408–8413. Available at: https://doi.org/10.1073/pnas.1702943114.

Sáenz de Miera, C. (2019) 'Maternal photoperiodic programming enlightens the internal regulation of thyroid-hormone deiodinases in tanycytes', *Journal of Neuroendocrinology*, 31(1), p. e12679. Available at: https://doi.org/10.1111/jne.12679.

Sáenz De Miera, C., Monecke, S., Bartzen-Sprauer, J., Laran-Chich, M.P., Pévet, P., Hazlerigg, D.G. and Simonneaux, V. (2014) 'A circannual clock drives expression of genes central for seasonal reproduction', *Current Biology*, 24(13), pp. 1500–1506. Available at: https://doi.org/10.1016/j.cub.2014.05.024.

Samms, R.J., Lewis, J.E., Lory, A., Fowler, M.J., Cooper, S., Warner, A., Emmerson, P., Adams, A.C., Luckett, J.C., Perkins, A.C., *et al.* (2015) 'Antibody-Mediated Inhibition of the FGFR1c Isoform Induces a Catabolic Lean State in Siberian Hamsters', *Current Biology*, 25(22), pp. 2997–3003. Available at: https://doi.org/10.1016/j.cub.2015.10.010.

Sari, I.P., Rao, A., Smith, J.T., Tilbrook, A.J. and Clarke, I.J. (2009) 'Effect of RF-Amide-Related Peptide-3 on Luteinizing Hormone and Follicle-Stimulating Hormone Synthesis and Secretion in Ovine Pituitary Gonadotropes', *Endocrinology*, 150(12), pp. 5549–5556. Available at: https://doi.org/10.1210/EN.2009-0775.

Saunders, N.R., Dziegielewska, K.M., Møllgård, K. and Habgood, M.D. (2018) 'Physiology and molecular biology of barrier mechanisms in the fetal and neonatal brain', *Journal of Physiology*, 596(23), pp. 5723–5756. Available at: https://doi.org/10.1113/JP275376.

Scholander, P.F., Hock, R., Walters, V., Johnson, F. and Irving, L. (1950) 'HEAT REGULATION IN SOME ARCTIC AND TROPICAL MAMMALS AND BIRDS', *The Biological Bulletin*, 99(2), pp. 237–258. Available at: https://doi.org/10.2307/1538741.

Schwartz, C., Hampton, M. and Andrews, M.T. (2013) 'Seasonal and Regional Differences in Gene Expression in the Brain of a Hibernating Mammal', *PLoS ONE*, 8(3). Available at: https://doi.org/10.1371/journal.pone.0058427.

Schwartz, M.W., Woods, S.C., Porte, D., Seeley, R.J. and Baskin, D.G. (2000) 'Central nervous system control of food intake', *Nature 2000 404:6778*, 404(6778), pp. 661–671. Available at: https://doi.org/10.1038/35007534.

Scott, D.E. and Paull, W.K. (1983) 'Scanning electron microscopy of the mammalian cerebral-ventricular system', *Micron (1969)*, 14(2), pp. 165–186. Available at: https://doi.org/10.1016/0047-7206(83)90018-3.

Serrano-Regal, M.P., Luengas-Escuza, I., Bayón-Cordero, L., Ibarra-Aizpurua, N., Alberdi, E., Pérez-Samartín, A., Matute, C. and Sánchez-Gómez, M.V. (2020) 'Oligodendrocyte Differentiation and Myelination Is Potentiated via GABAB Receptor Activation', *Neuroscience*, 439, pp. 163–180. Available at: https://doi.org/10.1016/j.neuroscience.2019.07.014.

Shearer, K.D., Goodman, T.H., Ross, A.W., Reilly, L., Morgan, P.J. and McCaffery, P.J. (2010) 'Photoperiodic regulation of retinoic acid signaling in the hypothalamus', *Journal of Neurochemistry*, 112(1), pp. 246–257. Available at: https://doi.org/10.1111/j.1471-4159.2009.06455.x.

Shearer, K.D., Stoney, P.N., Morgan, P.J. and McCaffery, P.J. (2012) 'A vitamin for the brain', *Trends in Neurosciences*, 35(12), pp. 733–741. Available at: https://doi.org/10.1016/j.tins.2012.08.005.

Shearer, K.D., Stoney, P.N., Nanescu, S.E., Helfer, G., Barrett, P., Ross, A.W., Morgan, P.J. and McCaffery, P. (2012) 'Photoperiodic expression of two RALDH enzymes and the regulation of cell proliferation by retinoic acid in the rat hypothalamus', *Journal of Neurochemistry*, 122(4), pp. 789–799. Available at: https://doi.org/10.1111/j.1471-4159.2012.07824.x.

Sheriff, M.J., Williams, C.T., Kenagy, G.J., Buck, C.L. and Barnes, B.M. (2012) 'Thermoregulatory changes anticipate hibernation onset by 45 days: Data from free-living arctic ground squirrels', *Journal of Comparative Physiology B: Biochemical, Systemic, and Environmental Physiology*, 182(6), pp. 841–847. Available at: https://doi.org/10.1007/s00360-012-0661-z.

Smith, R.E. and Hock, R.J. (1963) 'Brown Fat: Thermogenic Effector of Arousal in Hibernators', *Science*, 140(3563), pp. 199–200. Available at: https://doi.org/10.1126/SCIENCE.140.3563.199.

Sorrells, S.F., Paredes, M.F., Cebrian-Silla, A., Sandoval, K., Qi, D., Kelley, K.W., James, D., Mayer, S., Chang, J., Auguste, K.I., *et al.* (2018) 'Human hippocampal neurogenesis drops sharply in children to undetectable levels in adults', *Nature 2018 555:7696*, 555(7696), pp. 377–381. Available at: https://doi.org/10.1038/nature25975.

Steinlechner, S., Heldmaier, G. and Becker, H. (1983) 'The seasonal cycle of body weight in the Djungarian hamster: photoperiodic control and the influence of starvation and melatonin', *Oecologia*, 60(3), pp. 401–405. Available at: https://doi.org/10.1007/BF00376859.

Stetson, M.H., Ray, S.L., Creyaufmiller, N. and Horton, T.H. (1989) 'Maternal transfer of photoperiodic information in Siberian hamsters. II. The nature of the maternal signal, time of signal transfer, and the effect of the maternal signal on peripubertal reproductive development in the absence of photoperiodic input.', *Biology of reproduction*, 40(3), pp. 458–465. Available at: https://doi.org/10.1095/biolreprod40.3.458.

Stetson, M.H., Elliott, J.A. and Goldman, B.D. (1986) 'Maternal Transfer of Photoperiodic Information Influences the Photoperiodic Response of Prepubertal Djungarian Hamsters (Phodopus Sungorus Sungorus)', *Biology of Reproduction*, 34(4), pp. 664–669. Available at: https://doi.org/10.1095/biolreprod34.4.664.

Stiles, J. and Jernigan, T.L. (2010) 'The basics of brain development', *Neuropsychology Review*, 20(4), pp. 327–348. Available at: https://doi.org/10.1007/s11065-010-9148-4.

Stoney, P.N., Helfer, G., Rodrigues, D., Morgan, P.J. and Mccaffery, P. (2016) 'Thyroid hormone activation of retinoic acid synthesis in hypothalamic tanycytes', *Glia*, 64(3), pp. 425–439. Available at: https://doi.org/10.1002/glia.22938.

Sullivan, A.I., Potthoff, M.J. and Flippo, K.H. (2022) 'Tany-Seq: Integrated Analysis of the Mouse Tanycyte Transcriptome', *Cells*, 11(9), pp. 1–10. Available at: https://doi.org/10.3390/cells11091565.

Sun, H.D., Malabunga, M., Tonra, J.R., DiRenzo, R., Carrick, F.E., Zheng, H., Berthoud, H.R., McGuinness, O.P., Shen, J., Bohlen, P., *et al.* (2007) 'Monoclonal antibody antagonists of hypothalamic FGFR1 cause potent but reversible hypophagia and weight loss in rodents and monkeys', *American Journal of Physiology - Endocrinology and Metabolism*, 292(3), pp. 964–976. Available at: https://doi.org/10.1152/ajpendo.00089.2006.

Tu, H.Q., Li, S., Xu, Y.L., Zhang, Y.C., Li, P.Y., Liang, L.Y., Song, G.P., Jian, X.X., Wu, M., Song, Z.Q., *et al.* (2023) 'Rhythmic cilia changes support SCN neuron coherence in circadian clock', *Science*, 380(6648), pp. 972–979. Available at: https://doi.org/10.1126/science.abm1962.

Turek, F.W., Elliott, J.A., Alvis, J.D. and Menaker, M. (1975) 'The Interaction of Castration and Photoperiod in the Regulation of Hypophyseal and Serum Gonadotropin Levels in Male Golden Hamsters', *Endocrinology*, 96(4), pp. 854–860.

Umesono, K., Giguere, V., Glass, C.K., Rosenfeld, M.G. and Evans, R.M. (1988) 'Retinoic acid and thyroid hormone induce gene expression through a common responsive element', *Nature*, 336(6196), pp. 262–5. Available at: https://doi.org/10.1038/336262a0.

Uriarte, M., De Francesco, P.N., Fernandez, G., Cabral, A., Castrogiovanni, D., Lalonde, T., Luyt, L.G., Trejo, S. and Perello, M. (2019) 'Evidence Supporting a Role for the Blood-Cerebrospinal Fluid Barrier Transporting Circulating Ghrelin into the Brain', *Molecular Neurobiology*, 56(6), pp. 4120–4134. Available at: https://doi.org/10.1007/s12035-018-1362-8.

Vanecek, J. (1998) 'Cellular mechanisms of melatonin action', *Physiological Reviews*, 78(3), pp. 687–721. Available at: https://doi.org/10.1152/physrev.1998.78.3.687.

Vermillion, K.L., Anderson, K.J., Hampton, M. and Andrews, M.T. (2015) 'Gene expression changes controlling distinct adaptations in the heart and skeletal muscle of a hibernating mammal', *Physiological Genomics*, 47(3), pp. 58–74. Available at: https://doi.org/10.1152/physiolgenomics.00108.2014.

van der Vinne, V., Tachinardi, P., Riede, S.J., Akkerman, J., Scheepe, J., Daan, S. and Hut, R.A. (2019) 'Maximising survival by shifting the daily timing of activity', *Ecology Letters*, 22(12), pp. 2097–2102. Available at: https://doi.org/10.1111/ele.13404.

Van Der Vinne, V., Riede, S.J., Gorter, J.A., Eijer, W.G., Sellix, M.T., Menaker, M., Daan, S., Pilorz, V. and Hut, R.A. (2014) 'Cold and hunger induce diurnality in a nocturnal mammal', *Proceedings of the National Academy of Sciences of the United States of America*, 111(42), pp. 15256–15260. Available at: https://doi.org/https://doi.org/10.1073/pnas.1413135111.

Wang, L.C.H. (1979) 'Time patterns and metabolic rates of natural torpor in the Richardson's ground squirrel', *Canadian Journal of Zoology*, 57(1), pp. 149–155. Available at: https://doi.org/10.1139/z79-012.

Wang, Y., Bernard, A., Comblain, F., Yue, X., Paillart, C., Zhang, S., Reiter, J.F. and Vaisse, C. (2021) 'Melanocortin 4 receptor signals at the neuronal primary cilium to control food intake and body weight', *Journal of Clinical Investigation*, 131(9). Available at: https://doi.org/10.1172/JCI142064.

Weitten, M., Robin, J.P., Oudart, H., Pévet, P. and Habold, C. (2013) 'Hormonal changes and energy substrate availability during the hibernation cycle of Syrian hamsters', *Hormones and Behavior*, 64(4), pp. 611–617. Available at: https://doi.org/10.1016/j.yhbeh.2013.08.015.

Wells, L.J. (1935) 'Seasonal sexual rhythm and its experimental modification in the male of the thirteen-lined ground squirrel (citellus tridecemlineatus)', *The Anatomical Record*, 62(4), pp. 409–447. Available at: https://doi.org/10.1002/ar.1090620406.

Wood, S.H., Christian, H.C., Miedzinska, K., Saer, B.R.C., Johnson, M., Paton, B., Yu, L., McNeilly, J., Davis, J.R.E., McNeilly, A.S., *et al.* (2015) 'Binary Switching of Calendar Cells in the Pituitary Defines the Phase of the Circannual Cycle in Mammals', *Current Biology*, 25(20), pp. 2651–2662. Available at: https://doi.org/10.1016/J.CUB.2015.09.014.

Wood, S.H., Hindle, M.M., Mizoro, Y., Cheng, Y., Saer, B.R.C., Miedzinska, K., Christian, H.C., Begley, N., McNeilly, J., McNeilly, A.S., *et al.* (2020) 'Circadian clock mechanism driving mammalian photoperiodism', *Nature Communications*, 11(1). Available at: https://doi.org/10.1038/s41467-020-18061-z.

Woodfill, C.J.I., Robinson, J.E., Malpaux, B. and Karsch, F.J. (1991) 'Synchronization of the Circannual Reproductive Rhythm of the Ewe by Discrete Photoperiodic Signals1', *Biology of Reproduction*, 45(1), pp. 110–121. Available at: https://doi.org/10.1095/biolreprod45.1.110.

Woodfill, C.J.I., Wayne, N.L., Moenter, S.M. and Karsch, F.J. (1994) 'Photoperiodic Synchronization of a Circannual Reproductive Rhythm in Sheep: Identification of Season-Specific Time Cues1', *Biology of Reproduction*, 50(4), pp. 965–976. Available at:https://doi.org/10.1095/biolreprod50.4.965.

Wright Muelas, M., Roberts, I., Mughal, F., O'Hagan, S., Day, P.J. and Kell, D.B. (2020) 'An untargeted metabolomics strategy to measure differences in metabolite uptake and excretion by mammalian cell lines', *Metabolomics*, 16(10), pp. 1–12. Available at: https://doi.org/10.1007/s11306-020-01725-8.

Xie, Y. and Dorsky, R.I. (2017) 'Development of the hypothalamus: conservation, modification and innovation', *Development*, 144(9), pp. 1588–1599. Available at: https://doi.org/10.1242/DEV.139055.

Xu, Y., Tamamaki, N., Noda, T., Kimura, K., Itokazu, Y., Matsumoto, N., Dezawa, M. and Ide, C. (2005) 'Neurogenesis in the ependymal layer of the adult rat 3rd ventricle', *Experimental Neurology*, 192(2), pp. 251–264. Available at: https://doi.org/10.1016/J.EXPNEUROL.2004.12.021.

Yamamura, T., Hirunagi, K., Ebihara, S. and Yoshimura, T. (2004) 'Seasonal Morphological Changes in the Neuro-Glial Interaction between Gonadotropin-Releasing Hormone Nerve Terminals and Glial Endfeet in Japanese Quail', *Endocrinology*, 145(9), pp. 4264–4267. Available at: https://doi.org/10.1210/EN.2004-0366.

Yang, D.J., Hong, J. and Kim, K.W. (2021) 'Hypothalamic primary cilium: A hub for metabolic homeostasis', *Experimental and Molecular Medicine*, 53(7), pp. 1109–1115. Available at: https://doi.org/10.1038/s12276-021-00644-5.

Yoo, S., Cha, D., Kim, D.W., Hoang, T. V. and Blackshaw, S. (2019) 'Tanycyte-Independent Control of Hypothalamic Leptin Signaling', *Frontiers in Neuroscience*, 13, p. 240. Available at: https://doi.org/10.3389/fnins.2019.00240.

Yoo, S., Cha, D., Kim, S., Jiang, L., Cooke, P., Adebesin, M., Wolfe, A., Riddle, R., Aja, S. and Blackshaw, S. (2020) 'Tanycyte ablation in the arcuate nucleus and median eminence increases obesity susceptibility by increasing body fat content in male mice', *Glia*, 68(10), pp. 1987–2000. Available at: https://doi.org/10.1002/glia.23817.

Yoo, S., Kim, J., Lyu, P., Hoang, T. V., Ma, A., Trinh, V., Dai, W., Jiang, L., Leavey, P., Duncan, L., *et al.* (2021) 'Control of neurogenic competence in mammalian hypothalamic tanycytes', *Science Advances*, 7(22), pp. 1–21. Available at: https://doi.org/10.1126/sciadv.abg3777.

Yoo, S. and Blackshaw, S. (2018) 'Regulation and function of neurogenesis in the adult mammalian hypothalamus', *Progress in Neurobiology*, 170, pp. 53–66. Available at: https://doi.org/10.1016/j.pneurobio.2018.04.001.

Yousef, M.K., Robertson, D. and Johnson, H.D. (1967) 'Effect of hibernation on oxygen consumption and thyroidal I131 release rate mf mesocricetus auratus', *Life Sciences*, 6(11), pp. 1185–1194. Available at: https://doi.org/10.1016/0024-3205(67)90201-9.

Yu, Q., Gamayun, I., Wartenberg, P., Zhang, Q., Qiao, S., Kusumakshi, S., Candlish, S., Götz, V., Wen, S., Das, D., *et al.* (2023) 'Bitter taste cells in the ventricular walls of the murine brain regulate glucose homeostasis', *Nature Communications*, 14(1). Available at: https://doi.org/10.1038/s41467-023-37099-3.

Zhang, X.-K., Hoffmann, B., Tran, P.B.-V., Graupner, G. and Pfahl, M. (1992) 'Retinoid X receptor is an auxiliary protein for thyroid hormone and retinoic acid receptors', *Nature*, 355(6359), pp. 441–446. Available at: https://doi.org/10.1038/355441a0.

Papers

Paper I

frontiers in Endocrinology

REVIEW
published: 10 January 2020
doi: 10.3389/fendo.2019.00901

Maternal Photoperiodic Programming: Melatonin and Seasonal Synchronization Before Birth

*Jayme van Dalum†, Vebjørn J. Melum†, Shona H. Wood and David G. Hazlerigg**

Department of Arctic and Marine Biology, UiT – the Arctic University of Norway, Tromsø, Norway

This mini-review considers the phenomenon of maternal photoperiodic programming (MPP). In order to match neonatal development to environmental conditions at the time of birth, mammals use melatonin produced by the maternal pineal gland as a transplacental signal representing ambient photoperiod. Melatonin acts via receptors in the fetal pituitary gland, exerting actions on the developing medio-basal hypothalamus. Within this structure, a central role for specialized ependymal cells known as tanycytes has emerged, linking melatonin to control of hypothalamic thyroid metabolism and in turn to pup development. This review summarizes current knowledge of this programming mechanism, and its relevance in an eco-evolutionary context. Maternal photoperiodic programming emerges as a useful paradigm for understanding how *in utero* programing of hypothalamic function leads to life-long effects on growth, reproduction, health and disease in mammals, including humans.

Keywords: melatonin, pars tuberalis, tanycyte, fetal programming, thyrotropin (TSH—thyroid-stimulating hormone), photoperiodic history, deiodinase, thyroid hormone (T3)

OPEN ACCESS

Edited by:
Claudia Torres-Farfan, Austral University of Chile, Chile

Reviewed by:
Chandana Haldar, Banaras Hindu University, India
Laura Bennet, The University of Auckland, New Zealand

***Correspondence:**
David G. Hazlerigg
david.hazlerigg@uit.no

† These authors share joint first authorship

Specialty section:
This article was submitted to Translational Endocrinology, a section of the journal Frontiers in Endocrinology

Received: *30 September 2019*
Accepted: *10 December 2019*
Published: *10 January 2020*

Citation:
van Dalum J, Melum VJ, Wood SH and Hazlerigg DG (2020) Maternal Photoperiodic Programming: Melatonin and Seasonal Synchronization Before Birth. Front. Endocrinol. 10:901. doi: 10.3389/fendo.2019.00901

INTRODUCTION

Life on a rotating planet brings predictable daily and seasonal environmental challenges to the balancing of energy budgets for biological fitness. Because thermo-energetic challenges are inversely related to body size, the capacity to predict the cyclical environmental changes is of special importance for small animals (1), presumably this is crucial in the neonatal/juvenile period. The light-dark cycle and annually changing day lengths (photoperiod), are the most predictable information sources regarding the time of the day and time of the year. Adult mammals are in direct contact with the photic environment, and translate this signal via the hormone melatonin, to time their own changes in physiology and behavior. Contrastingly, the fetus is isolated from photoperiodic information both because light levels *in utero* are much lower than in the surrounding environment, and light sensing pathways are not fully developed until after birth in many cases (2, 3). To deal with this challenge, mammals use maternal melatonin as a transplacental signal (4), through which the fetus gains information about time of day [for review see (5, 6), and references therein], and about time of year [for review see (7), and references therein]. Several articles in this review series deal with the former aspect, and so we focus here on the latter, which we describe as maternal photoperiodic programming (MPP). We first discuss

the eco-evolutionary importance of MPP; then we go on to review current understanding of how MPP takes place, focussing on the sites of action of melatonin during the fetal and neonatal period.

THE EVOLUTIONARY DRIVERS FOR MPP

While seasonal conditions at any given point in the annual cycle may vary considerably from year to year, photoperiod is the most reliable cue for position in the annual cycle, and hence is a predictor of forthcoming environmental challenges. This in essence is the ultimate evolutionary reason for the evolution of melatonin-based photoperiodic synchronization in mammals. It is also important to appreciate that absolute day length alone is insufficient as a synchronizing signal because all variations in day length, except the solsticial maxima and minima, occur twice in every solar year. Hence the use of photoperiod as a cue must be dependent on prior history of photoperiodic exposure: intermediate photoperiods preceded by the long days of summer presage autumn and winter, whereas intermediate photoperiods preceded by the short days of winter presage spring and summer (**Figure 1A**) [for review see (8)].

This importance of integrating photoperiodic history into the use of photoperiod as a cue is made abundantly clear by a consideration of reproductive development and life-history strategy in short lived rodent species including voles and hamsters (9–11). In such animals the time from conception to reproductive maturity is potentially <2 months, and so multiple generations are typically born within a single annual breeding season. Nonetheless, the optimal life-history strategy for individuals born in the spring is entirely different from that for individuals born late in the breeding season (**Figure 1A**). For the former a "live fast, die young" strategy with fitness success based on producing progeny within the same summer season is appropriate because within the same season there will continue to be sufficient resources for lactation and rearing young. Contrastingly, young born later in the season do not have time for breeding and rearing of young before the autumn decline in resources and increased thermo-energetic demand occurs. As consequence these late born pups delay reproduction until the following year, conserving resources for investment in overwintering survival. In the field, the use of these two alternate life-history strategies as a function of time of birth reveals itself as a bimodal age distribution in wild caught individuals (9–11).

CHARACTERIZATION OF MPP IN THE LABORATORY

In the laboratory it is possible to reveal these alternate strategies simply by manipulation of artificial photoperiod. In the Montane vole (*Microtus montanus*), pups gestated and raised under long photoperiods (16L:8D) delay growth and maturation when exposed to shorter, intermediate photoperiods (14L:10D) at weaning, whereas pups gestated under short photoperiods (8L:16D) undergo accelerated growth and maturation when exposed to the same intermediate photoperiod (12, 13). The use of intermediate photoperiods is a powerful paradigm to show that weaned offspring have a "memory" of prior photoperiodic history. Determining if this "memory" is encoded *in utero* or neonatally, was a challenge addressed by a series of elegant studies by Milton Stetson, Teresa Horton and colleagues, which dissected the origins of this photoperiodic history, both through cross-fostering experiments and by resolving photoperiodic manipulation into gestational, neonatal and post-weaning phases [(12, 14, 15), reviewed in (7, 16)].

Cross fostering experiments in Montane voles demonstrate that the *in utero* environment is where the programming of developmental trajectories occurs (14). Pregnant mothers were kept under long (16L:8D) or short (8L:16D) photoperiods. At birth, half of the young were given to a foster mother who had experienced the same photoperiod as the birth-mother and the other half of the young went to a foster mother who had experienced the opposite photoperiod during pregnancy, compared to the birth-mother. All young were raised under intermediate (14L:10D) photoperiods after birth. The accelerated growth and sexual maturation of short-day gestated voles compared to long-day gestated voles clearly demonstrated the *in utero* transfer of photoperiodic information by the actual birth-mother. The foster mother's photoperiodic history had no effect on the offspring after birth, which excludes the effect of maternal signals transferred through milk. Similar effects of maternal photoperiodic programming have been shown in Siberian hamsters (*Phodopus sungorus*) (15, 17), collared lemmings (*Dicrostonyx groenlandicus*) (18), and meadow voles (*Microtus pennsylvanicus*) (19, 20).

The clear conclusion from these studies is that photoperiod influences reproductive development in a manner dependent on the interaction between photoperiod exposure *in utero* and photoperiod exposure post-weaning. Photoperiod exposure in the intervening neonatal period has little influence, and constitutes a "dead zone" for MPP, probably because at this stage the photo-neuroendocrine system (PNS) is not fully light-responsive and pups typically remain in subterranean nests (21).

MPP IN NON-RODENT SPECIES

Longer-lived, larger mammals also show evidence of MPP. Sexual maturity of red deer gestated under short photoperiods is advanced compared to long photoperiods (22). The effect of gestation is also evident in the prolactin levels of sheep lambs at the time of birth, with levels being lower in short-day gestated lambs than in long-day gestated lambs (23). Moreover, subsequent responses to intermediate (LD12:12) photoperiods after birth were quite different, with prolactin levels rapidly increased in short-day gestated lambs but decreased in long-day gestated lambs. Under natural conditions sheep and other ungulates have a single round of reproduction in a given year,

Abbreviations: Dio2, type 2 deiodinase; Dio3, type 3 deiodinase; MBH, medio basal hypothalamus; MPP, maternal photoperiodic programing; MT1, type 1 melatonin receptor; 3V, 3rd ventricle; PNS, photoneuroendocrine system; PD, pars distalis; PT, pars tuberalis; Px, pinealectomy; SCN, suprachiasmatic nucleus; SCG, superior cervical ganglion; T3, triiodothyronine; T4, thyroxine; TSH, thyroid stimulating hormone.

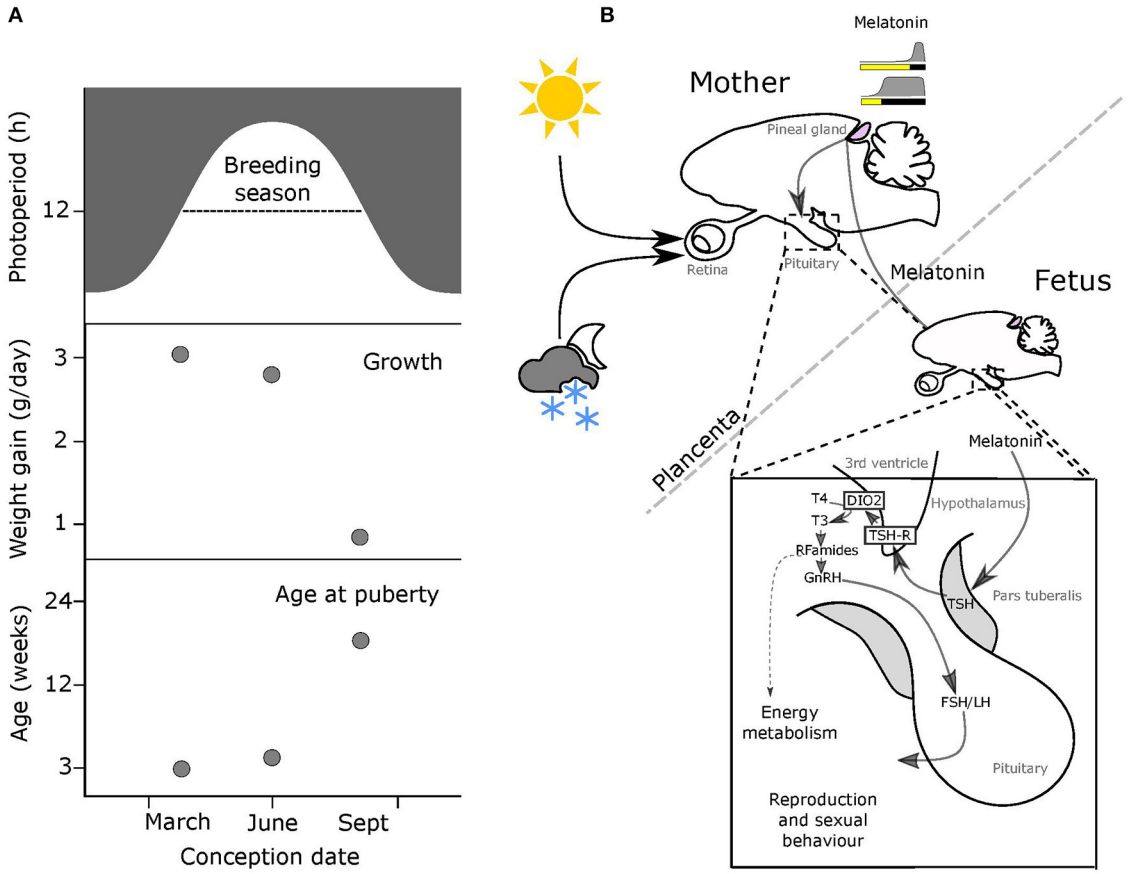

FIGURE 1 | Melatonin-mediated transplacental relay of photoperiodic information. **(A)** The breeding season for small rodents runs from spring through to early autumn (top panel, dashed line). Middle & bottom panels: offspring born early in the breeding season on increasing photoperiods grow fast and breed in the same season, while pups born later on declining photoperiods grow slowly and delay breeding to the following year. **(B)** Actions of maternal melatonin via the pars tuberalis (PT). In both the mother and the fetus, thyrotrophs in the *pars tuberalis* (PT) contain melatonin receptors (MT1), and in response to shorter melatonin signals representing intermediate to long photoperiods these cells secrete thyroid stimulating hormone (TSH). Tanycytes lining the 3rd ventricle, express TSH receptors, and respond to changing levels of PT TSH secretion by modulating relative levels of expression of two thyroid hormone deiodinase enzymes (dio2 and dio3). This affects the local thyroid environment in the MBH, with relatively increased dio2 expresison causing a relative increase in levels of T3 (the active form of TH). This in turn determines the reproductive behavior and energy metabolism of the adult animal.

and this is tightly constrained to an autumn period to ensure that young are born in the spring. Hence in contrast to voles and hamsters, an evolutionary narrative based on alternate life-history strategies cannot apply. Rather it is likely that *in utero* programming establishes the phase for calendar timer mechanisms from birth which then continue throughout life.

ROLE OF MELATONIN IN MPP

Except in early development, the pineal gland of mammals secretes melatonin in a light responsive fashion. The photic input pathway from the retina to the suprachiasmatic nucleus (SCN) drives rhythmic melatonin production from the pineal gland and this melatonin signal is sculpted by photoperiod to provide an internal endocrine representation for external photoperiod, this is the PNS (**Figure 1B**) [for review see (8, 24)]. Through this means, short (winter) photoperiods are represented by increased duration of nocturnally elevated plasma melatonin titers and long (summer) photoperiods by shorter duration for nocturnally elevated titers (**Figure 1B**).

The pivotal role of maternal pineal melatonin production in MPP was first demonstrated by a series of studies in Siberian hamsters (*P. sungorus*) [(17, 25–27), for review see (28)]. Injection of melatonin to pineal-intact mothers caused a suppression of pup testicular growth, dependent on the phase of melatonin injection relative to the light dark cycle. Specifically, injections in afternoon were most effective, because melatonin delivered at this phase extended the endogenous maternal melatonin signal to give it a profile mimicking a short photoperiod (25). Complete removal of the maternal melatonin signal by pinealectomy (px) blocked the effect of *in utero* photoperiod manipulations on pup development (26), as did fitting of pineal-intact mothers with continuous release

melatonin implants (27). Collectively, these studies reveal that maternal pineal melatonin production relays information about ambient photoperiod to the developing fetus.

MELATONIN SITES OF ACTION IN THE DEVELOPING FETUS

The use of the radio-analog of melatonin, 2-iodo-melatonin (29), led to the identification of melatonin binding sites in a range of central and peripheral fetal tissues (30). In fetal rodents, melatonin binding sites representing high affinity G–protein coupled receptors are consistently observed in the pars tuberalis (PT) and pars distalis (PD) of the pituitary and in the SCN [(31–33), for review see (30, 34)]. While type 1 melatonin receptor (mt1) expression disappears from the PD within a few days of birth (35), expression in the PT persists, and this site has emerged as the key site for the seasonal actions of melatonin in adult mammals [for review see (8, 30, 36–38)].

The PT shows the highest concentration of melatonin receptors of all mammalian tissues, and these mediate photoperiodic control of TSH production by the PT through a circadian-based "coincidence timer" mechanism (39, 40). TSH produced by the PT acts locally on the TSH receptors (TSHR) expressed in tanycyte cells lining the third ventricle of the hypothalamus (41, 42). Ligand binding to TSHR regulates the expression of deiodinase seleno-enzymes (Dio2 and Dio3), which in turn controls the local metabolism of thyroid hormone within the mediobasal hypothalamus (MBH), driving seasonal adaptations (**Figure 1B**) [(41, 42), for review see (24, 43)].

FETAL PT AS A TARGET FOR THE MATERNAL MELATONIN SIGNAL

Based on the paradigm emerging in adult mammals, Sáenz de Miera and colleagues have explored the involvement of the PT and MBH in MPP (44). This study demonstrates that in the Siberian hamster, expression of *TSH* in the fetal PT at the time of birth depends on maternal photoperiod, with high expression in pups gestated on LP but low expression in pups gestated on SP. These effects on PT *TSH* gene expression persisted through the perinatal period. As in adult mammals, *TSHR* expression is found in the ependymal region, and corresponding effects of photoperiod on the expression of dio2 and dio3 were observed (i.e., high *dio2* and low *dio3* in LP gestated pups and the converse in SP gestated pups). These studies provide evidence that the fetal PT mediates seasonal programming effects of maternal melatonin.

MPP ESTABLISHES PHOTOPERIODIC HISTORY-DEPENDENCE AT THE LEVEL OF THE TANYCYTES

Maternal photoperiod not only sets neonatal levels of TSH and deiodinase gene expression, associated with different trajectories for gonadal development, it also influences the sensitivity of MBH deiodinase gene expression to photoperiod exposure post-weaning. Specifically SP-gestation was associated with more dio2 and less dio3 expression in response to intermediate photoperiods than was the case for LP-gestated pups (**Figure 2**). Hence MPP is seen in hypothalamic expression of the key enzymes controlling thyroid status in the developing hypothalamus.

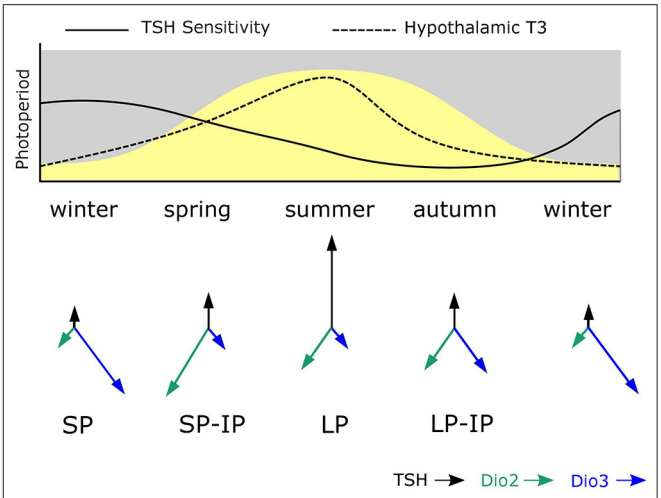

FIGURE 2 | Model for photoperiodic history-dependence through shifting tanycyte sensitivity to TSH. The solid line in the upper panel shows how tanycyte sensitivity to TSH is presumed to change during the course of the year. During winter PT TSH secretion is photoperiodically inhibited and TSH-sensitivity becomes heightened. In spring increased TSH production is a potent stimulus for increased dio2 expression due to high TSH sensitivity established in the winter phase. As spring becomes summer, sensitivity to TSH in the tanycytes declines and so high dio2 expression is not maintained despite continued exposure to long photoperiods. Then in autumn, the combination of declining TSH secretion and reduced sensitivity to TSH established in the summer phase leads to loss of dio2 expression and increased dio3 expression. The system then resets to the winter. The predicted consequences of this for hypothalamic T3 levels is shown as a dashed line—the asymmetry of this relative to the curve for photoperiod represents photoperiodic history-dependence. The lower panel shows the predicted consequences of this process for TSH, dio2 and dio3 expression—where arrow lengths represent strength of expression.

This effect does not seem to derive from downstream programming of both melatonin synthesis in the weaned pups, and sensitivity to melatonin at the level of the pup PT, but rather, it derives from history-dependent differences in sensitivity to TSH produced by the pup PT. This was demonstrated by icv injection of exogenous TSH which had a bigger inductive effect on *dio2* expression in SP- than in LP-gestated pups (**Figure 2**). Since no overt changes in *TSHR* expression in the MBH were seen in these experiments (44), other causes for this apparent shift in TSH sensitivity must be sought.

The identification of tanycytes as the site at which MPP generates photoperiodic history dependence echoes data from studies in the Soay sheep (45). Here, the onset of refractoriness to SP-exposure, i.e., another example of photoperiodic history-dependence, also appears at the level of *dio2/dio3* expression in tanycytes independently of changes in *TSH* expression in the PT.

FUNCTIONAL ROLES FOR HYPOTHALAMIC TANYCYTES

If the significance of these programming phenomena are to be properly understood it is imperative that attention focuses on tanycyte function. Tanycytes are a specialized form of ependymal cell derived from a glial cell lineage shared with microglial cells—for review see (46–49). They differ morphologically from the cuboidal epithelial cells that line most of the ventricular walls in that they have a bipolar morphology with extensive processes projecting into the parenchymal tissue surrounding the ependymal zone. Detailed analysis suggests that hypothalamic tanycytes may be subclassified based upon their anatomical location and upon their expression profiles (50)—but how these differences relate to differences in function remains uncertain. Much has been written on the possible functions of these cells, and at least three broad classes of cellular process have emerged: metabolic sensing (48, 51–53) regulation of blood/CSF/brain interfaces (50) and neurogenesis (54). The regulation of deiodinase gene expression and consequent effects on the local thyroid environment is but one molecular function of tanycytes, and may impact on any or all of the above cellular processes. At one level dio2/dio3 are regulators of uptake of active thyroid hormone into the circumventricular environment, and so serve a role as enzymatic "gatekeepers" (55). At another level, because T3 levels in the hypothalamus interact with the AMP-kinase dependent energy sensing pathways (56), shifts in deiodinase expression may be linked to metabolic sensing and responses. Thirdly, because T3 is strongly implicated in neurogenic pathways (57–59), shifts in T3 status dependent on photoperiodic history may impact in neurogenesis-dependent neural plasticity in the basal hypothalamus (54, 60, 61). Much remains to be done to establish an integrated view on the consequences of photoperiodic programming of tanycyte function.

MPP IN THE WIDER CONTEXT OF PROGRAMMING BY EARLY LIFE EXPERIENCE

The life-long consequences of early life experience is a topic of major biomedical importance. Epidemiological studies in humans demonstrate a positive correlation between low birthweight and susceptibility to obesity and cardiovascular health problems in adult life (62–66). Attempts to understand the mechanisms behind this phenomenon have led to studies in rats, in which maternal undernutrition leads to a chronic increase in susceptibility to weight gain when fed a "cafeteria" diet (67). Remarkably, this effect is completely reversed by treatment with the lipostatic hormone, leptin, in a narrow window in the neonatal period, which has closed by 10 days post-partum [(67), for review see (68)]. The mechanisms behind this effect of leptin remain unclear, it is probably not a coincidence that the ependymal zone of the MBH expresses high levels of leptin receptor at post-natal day 4, which then decline rapidly over the following week (69). This pattern is the inverse of that seen in the arcuate nuclei, and points to a transient role for leptin in establishing energy regulatory circuits in the neonatal period. The mapping of leptin receptor expression to the region encompassing the tanycytes involved in MPP suggests that this region is at the crux of mechanisms through which hypothalamic control circuits are established in early life. For this reason, we suggest that MPP, which relies on a harmless and non-invasive environmental perturbation (i.e., light) and acts through a well-defined pharmacological pathway (i.e., MT1 receptors in the PT), is a useful experimental paradigm for investigating the mechanisms through which early life experience establishes long term patterns of hypothalamic regulation.

AUTHOR CONTRIBUTIONS

All authors listed have made a substantial, direct and intellectual contribution to the work, and approved it for publication.

FUNDING

VM was supported by the Tromsø forskningsstiftelse (TFS) starter grant TFS2016SW, fonds Paul-Mandel pour les neurosciences, and the Norwegian research council Aurora travel grant, awarded to SW. JD was supported by HFSP program grant RGP0030/2015-C301 Evolution of seasonal timers, awarded to DH. The publication charges for this article have been funded by a grant from the publication fund of UiT The Arctic University of Norway.

REFERENCES

1. Hazlerigg DG, Tyler NJC. Activity patterns in mammals: circadian dominance challenged. *PLoS Biol.* (2019) 17:e3000360.doi: 10.1371/journal.pbio.3000360
2. Moore RY. Development of the suprachiasmatic nucleus. In: Klein DC, Moore RY, Reppert SM, editors. *Reppert Suprachiasmatic Nucleus: The Mind's Clock*. Oxford: University Press (1991). p. 391–404.
3. Ribelayga C, Gauer F, Pévet P, Simonneaux V. Ontogenesis of hydroxyindole-O-methyltransferase gene expression and activity in the rat pineal gland. *Dev Brain Res.* (1998) 110:235–9.doi: 10.1016/S0165-3806(98)00114-X
4. Yellon SM, Longo LD. Melatonin rhythms in fetal and maternal circulation during pregnancy in sheep. *Am J Physiol.* (1987) 252:E799–802.doi: 10.1152/ajpendo.1987.252.6.E799
5. Davis FC. Melatonin: role in development. *J Biol Rhythms.* (1997) 12:498–508.doi: 10.1177/074873049701200603
6. Hassell KJ, Reiter RJ, Robertson NJ. Melatonin and its role in neurodevelopment during the perinatal period: a review. *Fetal Matern Med Rev.* (2013) 24:76–107.doi: 10.1017/S0965539513000089
7. Horton TH. Fetal origins of developmental plasticity: animal models of induced life history variation. *Am J Hum Biol.* (2005) 17:34–43.doi: 10.1002/ajhb.20092
8. West AC, Wood SH. Seasonal physiology: making the future a thing of the past. *Curr Opin Physiol.* (2018) 5:1–8.doi: 10.1016/j.cophys.2018.04.006
9. Negus NC, Berger PJ, Forslund LG. Reproductive strategy of microtus montanus. *J Mammal.* (1977) 58:347–53.doi: 10.2307/1379333

10. Negus NC, Berger PJ, Brown BW. Microtine population dynamics in a predictable environment. *Can J Zool.* (1986) 64:785–92.doi: 10.1139/z86-117
11. Negus NC, Berger PJ, Pinter AJ. Phenotypic plasticity of the montane vole (*Microtus montanus*) in unpredictable environments. *Can J Zool.* (1992) 70:2121–4.doi: 10.1139/z92-285
12. Horton TH. Growth and reproductive development of male microtus montanus is affected by the prenatal photoperiod. *Biol Reprod.* (1984) 31:499–504.doi: 10.1095/biolreprod31.3.499
13. Horton TH. Growth and maturation in *Microtus montanus* : effects of photoperiods before and after weaning. *Can J Zool.* (1984) 62:1741–6.doi: 10.1139/z84-256
14. Horton TH. Cross-fostering of voles demonstrates *in utero* effect of photoperiod. *Biol Reprod.* (1985) 33:934–9.doi: 10.1095/biolreprod33.4.934
15. Stetson MH, Elliott JA, Goldman BD. Maternal transfer of photoperiodic information influences the photoperiodic response of prepubertal djungarian hamsters (Phodopus Sungorus Sungorus)1. *Biol Reprod.* (1986) 34:664–9.doi: 10.1095/biolreprod34.4.664
16. Horton TH, Stetson MH. Maternal transfer of photoperiodic information in rodents. *Anim Reprod Sci.* (1992) 30:29–44.doi: 10.1016/0378-4320(92)90004-W
17. Stetson MH, Ray SL, Creyaufmiller N, Horton TH. Maternal transfer of photoperiodic information in Siberian hamsters. II. the nature of the maternal signal, time of signal transfer, and the effect of the maternal signal on peripubertal reproductive development in the absence of photoperiodic input1. *Biol Reprod.* (1989) 40:458–65.doi: 10.1095/biolreprod40.3.458
18. Gower BA, Nagy TR, Stetson MH. Pre- and postnatal effects of photoperiod on collared lemmings (*Dicrostonyx groenlandicus*). *Am J Physiol.* (1994) 267:R879–87.doi: 10.1152/ajpregu.1994.267.4.R879
19. Lee TM, Spears N, Tuthill CR, Zucker I. Maternal melatonin treatment influences rates of neonatal development of meadow vole pups1. *Biol Reprod.* (1989) 40:495–502.doi: 10.1095/biolreprod40.3.495
20. Lee TM. Development of meadow voles is influenced postnatally by maternal photoperiodic history. *Am J Physiol.* (1993) 265:R749–55.doi: 10.1152/ajpregu.1993.265.4.R749
21. Gruder-Adams S, Getz LL. Comparison of the mating system and paternal behavior in microtus ochrogaster and *M. pennsylvanicus*. *J Mammal.* (1985) 66:165–7.doi: 10.2307/1380976
22. Adam CL, Kyle CE, Young P. Influence of prenatal photoperiod on postnatal reproductive development in male red deer (*Cervus elaphus*). *J Reprod Fertil.* (1994) 100:607–11.doi: 10.1530/jrf.0.1000607
23. Ebling FJP, Wood RI, Suttie JM, Adel TE, Foster DL. Prenatal photoperiod influences neonatal prolactin secretion in the sheep. *Endocrinology.* (1989) 125:384–91.doi: 10.1210/endo-125-1-384
24. Dardente H, Wood S, Ebling F, Sáenz de Miera C. An integrative view of mammalian seasonal neuroendocrinology. *J Neuroendocrinol.* (2019) 31:e12729.doi: 10.1111/jne.12729
25. Horton TH, Lynn Ray S, Stetson MH. Maternal transfer of photoperiodic information in Siberian hamsters. III. Melatonin injections program postnatal reproductive development expressed in constant lights1. *Biol Reprod.* (1989) 41:34–9.doi: 10.1095/biolreprod41.1.34
26. Horton TH, Stachecki SA, Stetson MH. Maternal transfer of photoperiodic information in Siberian hamsters. IV. Peripubertal reproductive development in the absence of maternal photoperiodic signals during gestation1. *Biol Reprod.* (1990) 42:441–9.doi: 10.1095/biolreprod42.3.441
27. Horton TH, Lynn Ray S, Rollag MD, Yellon SM, Stetson MH. Maternal transfer of photoperiodic information in Siberian hamsters. V. Effects of melatonin implants are dependent on photoperiod. *Biol Reprod.* (1992) 47:291–6.doi: 10.1095/biolreprod47.2.291
28. Horton TH, Stetson MH. Maternal programming of the fetal brain dictates the response of juvenile Siberian hamsters to photoperiod: dissecting the information transfer system. *J Exp Zool.* (1990) 256:200–2.doi: 10.1002/jez.1402560443
29. Vakkuri O, Lämsä E, Rahkamaa E, Ruotsalainen H, Leppäluoto J. Iodinated melatonin: preparation and characterization of the molecular structure by mass and 1H NMR spectroscopy. *Anal Biochem.* (1984) 142:284–9.doi: 10.1016/0003-2697(84)90466-4
30. Morgan PJ, Barrett P, Howell HE, Helliwell R. Melatonin receptors: localization, molecular pharmacology and physiological significance. *Neurochem Int.* (1994) 24:101–46.doi: 10.1016/0197-0186(94)90100-7
31. Rivkees SA, Reppert SM. Appearance of melatonin receptors during embryonic life in Siberian hamsters (*Phodopus sungorous*). *Brain Res.* (1991) 568:345–9.doi: 10.1016/0006-8993(91)91424-Y
32. Vanecek J. The melatonin receptors in rat ontogenesis. *Neuroendocrinology.* (1988) 48:201–3.doi: 10.1159/000125008
33. Williams LM, Martinoli MG, Titchener LT, Pelletier G. The ontogeny of central melatonin binding sites in the rat. *Endocrinology.* (1991) 128:2083–90.doi: 10.1210/endo-128-4-2083
34. Vanecek J. Cellular mechanisms of melatonin action. *Physiol Rev.* (1998) 78:687–721.doi: 10.1152/physrev.1998.78.3.687
35. Johnston JD, Messager S, Ebling FJP, Williams LM, Barrett P, Hazlerigg DG. Gonadotrophin-releasing hormone drives melatonin receptor down-regulation in the developing pituitary gland. *Proc Natl Acad Sci USA.* (2003) 100:2831–5.doi: 10.1073/pnas.0436184100
36. Dardente H. Does a melatonin-dependent circadian oscillator in the pars tuberalis drive prolactin seasonal rhythmicity? *J Neuroendocrinol.* (2007) 19:657–66.doi: 10.1111/j.1365-2826.2007.01564.x
37. Wood S, Loudon A. Clocks for all seasons: unwinding the roles and mechanisms of circadian and interval timers in the hypothalamus and pituitary. *J Endocrinol.* (2014) 222:R39–59.doi: 10.1530/JOE-14-0141
38. Wood SH. How can a binary switch within the pars tuberalis control seasonal timing of reproduction? *J Endocrinol.* (2018) 239:R13–25.doi: 10.1530/JOE-18-0177
39. Dardente H, Wyse CA, Birnie MJ, Dupré SM, Loudon ASI, Lincoln GA, et al. A molecular switch for photoperiod responsiveness in mammals. *Curr Biol.* (2010) 20:2193–8.doi: 10.1016/j.cub.2010.10.048
40. Masumoto K, Ukai-Tadenuma M, Kasukawa T, Nagano M, Uno KD, Tsujino K, et al. Acute induction of Eya3 by late-night light stimulation triggers TSHβ expression in photoperiodism. *Curr Biol.* (2010) 20:2199–206.doi: 10.1016/j.cub.2010.11.038
41. Hanon EA, Lincoln GA, Fustin J-M, Dardente H, Masson-Pévet M, Morgan PJ, et al. Ancestral TSH mechanism signals summer in a photoperiodic mammal. *Curr Biol.* (2008) 18:1147–52.doi: 10.1016/j.cub.2008.06.076
42. Ono H, Hoshino Y, Yasuo S, Watanabe M, Nakane Y, Murai A, et al. Involvement of thyrotropin in photoperiodic signal transduction in mice. *Proc Natl Acad Sci USA.* (2008) 105:18238–42.doi: 10.1073/pnas.0808952105
43. Dardente H, Hazlerigg DG, Ebling FJP. Thyroid hormone and seasonal rhythmicity. *Front Endocrinol.* (2014) 5:19.doi: 10.3389/fendo.2014.00019
44. Sáenz de Miera C, Bothorel B, Jaeger C, Simonneaux V, Hazlerigg D. Maternal photoperiod programs hypothalamic thyroid status via the fetal pituitary gland. *Proc Natl Acad Sci USA.* (2017) 114:8408–13.doi: 10.1073/pnas.1702943114
45. Sáenz de Miera C, Hanon EA, Dardente H, Birnie M, Simonneaux V, Lincoln GA, et al. Circannual variation in thyroid hormone deiodinases in a short-day breeder. *J Neuroendocrinol.* (2013) 25:412–21.doi: 10.1111/jne.12013
46. Rodríguez EM, Blázquez JL, Pastor FE, Peláez B, Peña P, Peruzzo B, Amat P. Hypothalamic tanycytes: a key component of brain–endocrine interaction. *Int Rev Cytol.* (2005) 247:89–164.doi: 10.1016/S0074-7696(05)47003-5
47. Rodríguez EM, Blá Zquez B JL, Guerra M. The design of barriers in the hypothalamus allows the median eminence and the arcuate nucleus to enjoy private milieus: the former opens to the portal blood and the latter to the cerebrospinal fluid. *Peptides.* (2010) 31:757–76.doi: 10.1016/j.peptides.2010.01.003
48. Bolborea M, Dale N. Hypothalamic tanycytes: potential roles in the control of feeding and energy balance. *Trends Neurosci.* (2013) 36:91–100.doi: 10.1016/j.tins.2012.12.008
49. Lewis JE, Ebling FJP. Tanycytes as regulators of seasonal cycles in neuroendocrine function. *Front Neurol.* (2017) 8:79.doi: 10.3389/fneur.2017.00079
50. Prevot V, Dehouck B, Sharif A, Ciofi P, Giacobini P, Clasadonte J. The versatile tanycyte: a hypothalamic integrator of reproduction and energy metabolism. *Endocr Rev.* (2018) 39:333–68.doi: 10.1210/er.2017-00235
51. Frayling C, Britton R, Dale N. ATP-mediated glucosensing by hypothalamic tanycytes. *J Physiol.* (2011) 589:2275–86.doi: 10.1113/jphysiol.2010.202051

52. Lazutkaite G, Soldà A, Lossow K, Meyerhof W, Dale N. Amino acid sensing in hypothalamic tanycytes via umami taste receptors. *Mol Metab.* (2017) 6:1480–92.doi: 10.1016/j.molmet.2017.08.015
53. Balland E, Dam J, Langlet F, Caron E, Steculorum S, Messina A, et al. Hypothalamic tanycytes are an ERK-gated conduit for leptin into the brain. *Cell Metab.* (2014) 19:293–301.doi: 10.1016/j.cmet.2013.12.015
54. Rizzoti K, Lovell-Badge R. Pivotal role of median eminence tanycytes for hypothalamic function and neurogenesis. *Mol Cell Endocrinol.* (2017) 445:7–13.doi: 10.1016/j.mce.2016.08.020
55. Barrett P, Ebling FJP, Schuhler S, Wilson D, Ross AW, Warner A, et al. Hypothalamic thyroid hormone catabolism acts as a gatekeeper for the seasonal control of body weight and reproduction. *Endocrinology.* (2007) 148:3608–17.doi: 10.1210/en.2007-0316
56. López M, Varela L, Vázquez MJ, Rodríguez-Cuenca S, González CR, Velagapudi VR, et al. Hypothalamic AMPK and fatty acid metabolism mediate thyroid regulation of energy balance. *Nat Med.* (2010) 16:1001–8.doi: 10.1038/nm.2207
57. Lezoualc'h F, Seugnet I, Monnier AL, Ghysdael J, Behr JP, Demeneix BA. Inhibition of neurogenic precursor proliferation by antisense alpha thyroid hormone receptor oligonucleotides. *J Biol Chem.* (1995) 270:12100–8.doi: 10.1074/jbc.270.20.12100
58. López-Juárez A, Remaud S, Hassani Z, Jolivet P, Pierre Simons J, Sontag T, et al. Thyroid hormone signaling acts as a neurogenic switch by repressing sox2 in the adult neural stem cell niche. *Cell Stem Cell.* (2012) 10:531–43.doi: 10.1016/j.stem.2012.04.008
59. Remaud S, Gothié JD, Morvan-Dubois G, Demeneix BA. Thyroid hormone signaling and adult neurogenesis in mammals. *Front Endocrinol.* (2014) 5:62.doi: 10.3389/fendo.2014.00062
60. Migaud M, Batailler M, Segura S, Duittoz A, Franceschini I, Pillon D. Emerging new sites for adult neurogenesis in the mammalian brain: a comparative study between the hypothalamus and the classical neurogenic zones. *Eur J Neurosci.* (2010) 32:2042–52.doi: 10.1111/j.1460-9568.2010.07521.x
61. Migaud M, Batailler M, Pillon D, Franceschini I, Malpaux B. Seasonal changes in cell proliferation in the adult sheep brain and pars tuberalis. *J Biol Rhythms.* (2011) 26:486–96.doi: 10.1177/0748730411420062
62. Barker DJ, Godfrey K, Gluckman P, Harding J, Owens J, Robinson J. Fetal nutrition and cardiovascular disease in adult life. *Lancet.* (1993) 341:938–41.doi: 10.1016/0140-6736(93)91224-A
63. Barker D, Eriksson J, Forsén T, Osmond C. Fetal origins of adult disease: strength of effects and biological basis. *Int J Epidemiol.* (2002) 31:1235–9.doi: 10.1093/ije/31.6.1235
64. Bateson P, Barker D, Clutton-Brock T, Deb D, D'Udine B, Foley RA, et al. Developmental plasticity and human health. *Nature.* (2004) 430:419–21.doi: 10.1038/nature02725
65. Gluckman PD, Hanson MA. Living with the past: evolution, development, and patterns of disease. *Science.* (2004) 305:1733–6.doi: 10.1126/science.1095292
66. Roseboom T, de Rooij S, Painter R. The dutch famine and its long-term consequences for adult health. *Early Hum Dev.* (2006) 82:485–91.doi: 10.1016/j.earlhumdev.2006.07.001
67. Vickers MH, Gluckman PD, Coveny AH, Hofman PL, Cutfield WS, Gertler A, et al. Neonatal leptin treatment reverses developmental programming. *Endocrinology.* (2005) 146:4211–6.doi: 10.1210/en.2005-0581
68. Vickers MH. Developmental programming and adult obesity: the role of leptin. *Curr Opin Endocrinol Diabetes Obes.* (2007) 14:17–22.doi: 10.1097/MED.0b013e328013da48
69. Cottrell EC, Cripps RL, Duncan JS, Barrett P, Mercer JG, Herwig A, et al. Developmental changes in hypothalamic leptin receptor: relationship with the postnatal leptin surge and energy balance neuropeptides in the postnatal rat. *Am J Physiol Integr Comp Physiol.* (2009) 296:R631–9.doi: 10.1152/ajpregu.90690.2008

Conflict of Interest: The authors declare that the research was conducted in the absence of any commercial or financial relationships that could be construed as a potential conflict of interest.

Paper II

Report

Current Biology

Hypothalamic tanycytes as mediators of maternally programmed seasonal plasticity

Graphical abstract

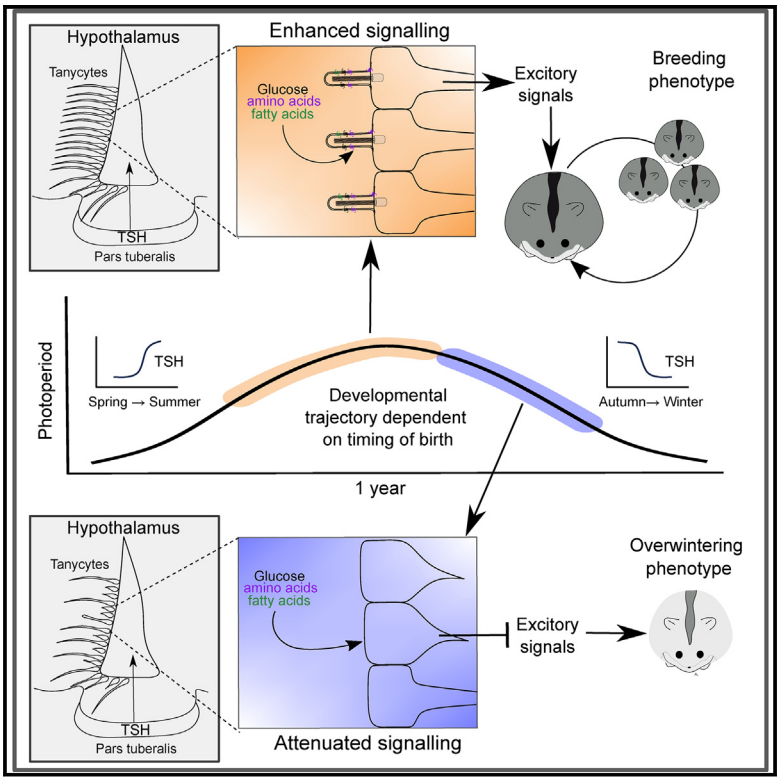

Highlights

- Siberian hamster development depends on pre- and post-natal photoperiod experience
- Tanycyte transcriptome is highly photoperiod sensitive
- Tanycytes have fewer sensory cilia in short photoperiod-raised hamsters
- Increasing photoperiod post-weaning stimulates ciliogenesis

Authors

Vebjørn J. Melum,
Cristina Sáenz de Miera,
Fredrik A.F. Markussen, ...,
Valérie Simonneaux,
David G. Hazlerigg, Shona H. Wood

Correspondence

david.hazlerigg@uit.no (D.G.H.),
shona.wood@uit.no (S.H.W.)

In brief

Hypothalamic tanycytes are glial cells implicated in hypothalamic sensing of metabolic status. Melum et al. show that, in Siberian hamsters, tanycyte sensory attributes are highly sensitive to early life programming by light exposure *in utero* and post-natally. A model linking this phenomenon to seasonal programming of life history is proposed.

Melum et al., 2024, Current Biology *34*, 632–640
February 5, 2024
https://doi.org/10.1016/j.cub.2023.12.042

CellPress

CellPress
OPEN ACCESS

Current Biology

Report

Hypothalamic tanycytes as mediators of maternally programmed seasonal plasticity

Vebjørn J. Melum,[1,4] Cristina Sáenz de Miera,[2] Fredrik A.F. Markussen,[1] Fernando Cázarez-Márquez,[1] Catherine Jaeger,[4] Simen R. Sandve,[3] Valérie Simonneaux,[4] David G. Hazlerigg,[1,5,7,*] and Shona H. Wood[1,5,6,7,8,*]

[1]Arctic seasonal timekeeping initiative (ASTI), UiT—The Arctic University of Norway, Department of Arctic and Marine Biology, Arctic Chronobiology and Physiology Research Group, NO-9037 Tromsø, Norway
[2]University of Michigan Medical School, Department of Molecular and Integrative Physiology, Ann Arbor, MI 48109, USA
[3]Faculty of Biosciences, Norwegian University of Life Sciences (NMBU), NO-1432 Ås, Norway
[4]University of Strasbourg, Institute of Cellular and Integrative Neurosciences, Strasbourg 67000, France
[5]X (formerly Twitter): @ArcticSeasonal
[6]X (formerly Twitter): @WoodLab_Arctic
[7]These authors contributed equally
[8]Lead contact
*Correspondence: david.hazlerigg@uit.no (D.G.H.), shona.wood@uit.no (S.H.W.)
https://doi.org/10.1016/j.cub.2023.12.042

SUMMARY

In mammals, maternal photoperiodic programming (MPP) provides a means whereby juvenile development can be matched to forthcoming seasonal environmental conditions.[1–4] This phenomenon is driven by *in utero* effects of maternal melatonin[5–7] on the production of thyrotropin (TSH) in the fetal *pars tuberalis* (PT) and consequent TSH receptor-mediated effects on tanycytes lining the 3rd ventricle of the mediobasal hypothalamus (MBH).[8–10] Here we use LASER capture microdissection and transcriptomic profiling to show that TSH-dependent MPP controls the attributes of the ependymal region of the MBH in juvenile animals. In Siberian hamster pups gestated and raised on a long photoperiod (LP) and thereby committed to a fast trajectory for growth and reproductive maturation, the ependymal region is enriched for tanycytes bearing sensory cilia and receptors implicated in metabolic sensing. Contrastingly, in pups gestated and raised on short photoperiod (SP) and therefore following an over-wintering developmental trajectory with delayed sexual maturation, the ependymal region has fewer sensory tanycytes. Post-weaning transfer of SP-gestated pups to an intermediate photoperiod (IP), which accelerates reproductive maturation, results in a pronounced shift toward a ciliated tanycytic profile and formation of tanycytic processes. We suggest that tanycytic plasticity constitutes a mechanism to tailor metabolic development for extended survival in variable overwintering environments.

RESULTS AND DISCUSSION

Maternal photoperiod profoundly affects offspring developmental trajectory and the tanycytic transcriptome

Wild Siberian hamsters (*Phodopus sungorus*) and other short-lived rodents use both the duration and direction of change of photoperiod to determine whether juveniles follow a fast, breeding or a slow, overwintering trajectory[1–4] (Figure 1A). To mimic this in the lab, we used a breeding protocol (Figure 1B) in which conception on long photoperiods (LPs, 16-h light/24 h) is followed by exposure to either LP or short photoperiod (SP, 8-h light/24 h) through pregnancy to weaning at postnatal day (pn) 21, followed by a continuation on these photoperiods or transfer to an intermediate photoperiod (IP, 14-h light/24 h) to the end of the study (pn50). This produced 4 distinctive trajectories of early-life photoperiodic history: steady-state long photoperiod (LP), declining photoperiod (LPIP), steady-state short photoperiod (SP), and increasing photoperiod (SPIP) (Figure 1B). In line with previously published work,[8] the response to these regimes revealed the interactive effects of photoperiod exposure pre- and post-weaning. Steady-state LP animals reached the largest size and had the largest testes, and steady-state SP animals the smallest, reflecting the pre- and post-weaning photoperiodic experience (Figures 1C and 1D). Transfer of LP-gestated pups to IP arrested growth and reproductive maturation, whereas transfer of SP-gestated pups to IP had the opposite effect, stimulating gonadal development and increased somatic growth (Figures 1C and 1D). Hence the developmental trajectory in the juvenile period depends on the interactive effects of photoperiod during gestation and post-weaning.

Previous work demonstrates that this photoperiodic programming is a melatonin-dependent phenomenon involving transplacental actions of melatonin *in utero*, which then modulate pup sensitivity to photoperiod in the post-weaning phase.[5–7] Melatonin acts via MT1 receptors in the pup *pars tuberalis* (PT) to control photoperiod-dependent production of the glycoprotein

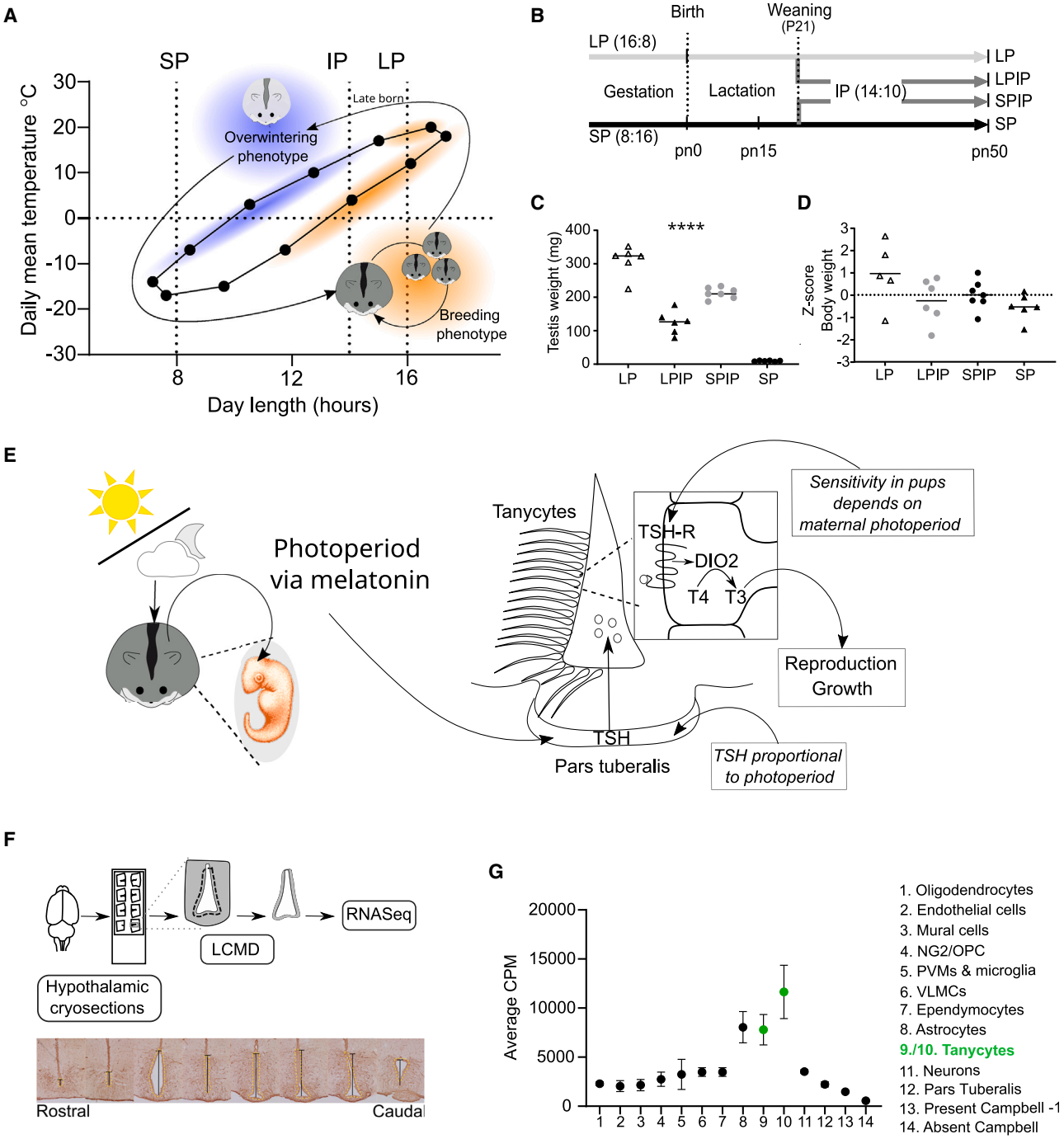

Figure 1. History-dependent effects of photoperiod on early-life developmental trajectory in Siberian hamsters (*Phodopus sungorus*)

(A) Elliptical relationship between the annual cycles of photoperiod and temperature in the natural habitat (55°N, Kazakhstan) and the influence on pup developmental trajectories. Pups born in spring to mid-summer are exposed to increasing/long photoperiods from conception and develop rapidly, allowing a further round of reproduction in the same year. Pups born in the late summer to autumn develop an overwintering phenotype (including white fur and expression of daily torpor) and delay breeding until the following spring.

(B) Experimental photoperiod manipulation paradigm to generate pups following divergent developmental trajectories mimicking the natural phenomenon. Adult females were gestated on a long (16-h light, 8-h dark [16:8]) or short photoperiod (8:16). At birth the mothers and pups were maintained on the gestation photoperiod. At weaning/postnatal day 21 (pn21), the pups were either maintained on the gestational photoperiods or transferred to an intermediate photoperiod (IP; 14:10). Animals were sampled at pn50.

(C) Testis weights in milligrams for each individual in each experimental group: long photoperiod (LP), long photoperiod transferred to intermediate photoperiod (LPIP), short photoperiod transferred to intermediate photoperiod (SPIP), and short photoperiod (SP). ****$p < 0.0001$ using a one-way ANOVA.

(D) Distribution of body weights of individual pups normalized to the pooled mean body mass (expressed as *Z* score).

(legend continued on next page)

hormone, thyrotropin (TSH), which in turn acts on TSH receptor (TSH-R)-expressing tanycytes lining the 3rd ventricle (3v) of the neighboring mediobasal hypothalamus (MBH) (Figure 1E).[8–10] Since we found previously that the level of TSH expression in the PT of hamster pups directly reflects current photoperiod, while tanycytic sensitivity to central injections of TSH at 50 days of age depends on photoperiodic history,[8] we hypothesized that the encoding of seasonal time depends on maternal photoperiodic effects on the development of tanycytes.

We performed RNA sequencing (RNA-seq) on LASER capture microdissected tissue from the tanycytic periventricular region, defined by expression of the intermediate filament protein vimentin (Figures 1F and S1). Using a single-cell RNA-seq[11] dataset, we confirmed that our approach yielded a tanycyte-enriched transcriptome (Figure 1G). Photoperiod treatment had a profound effect on the tanycytic transcriptome, with over 30% of all detectable transcripts showing significant changes in expression (FDR < 0.01). Nearly 60% of transcriptome-wide, between-sample variation in gene expression was accounted for by a single principal component, resolving samples according to photoperiod treatment (Figure 2A). These transcriptomic changes are far more pronounced than those reported in previous studies performed on whole hypothalamic blocks from Siberian hamsters or seasonally breeding sheep,[12–14] suggesting that photoperiodic effects on the tanycyte phenotype are the originators of seasonal neuroendocrine responses.

LP-gestated and -raised animals have more sensory ciliated tanycytes

We found 1,553 genes with increased expression under LP compared to SP (FDR < 0.001) (Figure 2B; Data S1B). Among these, strong enrichment for genes linked to the GO term "Cilium" (GO:0005929, FDR 2.86 × 10^{-12}) and to the GO process "Cilium assembly" (GO:0060271, FDR 9.21 × 10^{-4}) (Figure 2C; Table S1) suggests that the tanycytic presentation of cilia into the lumen of the 3rd ventricle is a photoperiod-dependent phenotype. Since ciliary function depends heavily on ciliary membrane lipids,[15] the heightened expression of genes including apolipoprotein E under LP, giving rise to strong enrichment for the GO term "High-Density Lipoprotein" (GO:0034364, FDR 9.57 × 10^{-3}), is also consistent with this interpretation.

To test whether photoperiod altered the abundance of cilia, we used immunological markers for cilia projections (acetylated α-tubulin) and basal bodies (γ-tubulin) to stain coronal and ventricular face hypothalamic sections from LP- and SP-reared hamsters (Figures 2D–2F and S2). In the putative α-tanycyte region, we found on average 4 times more basal bodies in LP-reared compared to SP-reared animals (Figures 2D and 2E; p = 0.002 by unpaired t test). The ventricular face sections confirm these findings showing an increased intensity in cilia projection staining and more distinct basal bodies in LP animals compared to SP animals (Figure 2F). The same trend was observed in the putative β-tanycyte region, albeit to a lesser extent (Figures S2C and S2D; 2-fold difference, p < 0.05 by unpaired t test). Collectively, these data demonstrate a profound effect of early life photoperiod on ciliary assembly in the tanycytic region.

Variable presence of sensory cilia on the apical surfaces of tanycytes likely leads to differences in sensory function through altered presentation of cell surface receptors and coupling to signal transduction machinery,[16–19] and this has been linked to the function of several G protein-coupled receptors (GPCRs).[18,20] This may account for the photoperiodic history-dependent differences in tanycyte TSH sensitivity between LP- and SP-gestated hamsters,[8] and may also be linked to the expression of a wide repertoire of GPCRs in the tanycytic transcriptome, many of which show photoperiod-dependent changes in RNA expression (Figure 2G). Of these, *gpr50*, the most abundantly expressed GPCR in the tanycyte transcriptome, shows the largest photoperiodic response, with expression levels an order of magnitude higher under LP. Along with previous metabolic studies in *gpr50* null mice,[21] this result implicates *gpr50* signaling in the photoperiodic programming of metabolic phenotype in juvenile hamsters. While cilia also provide a scaffold for sonic hedgehog (SHH) signaling (reviewed in Wheway et al., Anvarian et al., and Schou et al.[16,17,22]), and the expression of *shh* in the MBH of sheep varies with seasonal status,[13,14,23] we only saw modest effects on SHH pathway genes in the present study (Figures S3A and S3B). Overall, these profound effects on ciliation and expression of GPCRs suggest that early-life photoperiod modulates tanycytic sensitivity to metabolic feedback signals in the cerebrospinal fluid (CSF).

Plasticity of tanycytic phenotype in response to post-weaning photoperiodic change

Transferring animals to IP at weaning has opposite effects on the developmental trajectories of LP- and SP-reared animals: testis growth is arrested in the former and accelerated in the latter (Figure 1B).[8] As a result, by pn50, mean testes and body weights in LPIP animals were lower than those in SPIP animals. On the premise that this photoperiodic history-dependent modulation of post-weaning pup development stems from effects at the level of tanycytes, we explored the effects of post-weaning changes in photoperiod on the tanycyte transcriptome.

Transfer to IP has highly asymmetric effects on the transcriptional profile of the tanycytic region (Figure 3A; Data S1C–S1E), with a post-weaning increase in photoperiod (SPIP versus SP contrast) producing almost an order of magnitude more differentially expressed genes (DEGs) than is the case for a post-weaning decrease in photoperiod (LPIP versus LP contrast). Previously we showed that post-weaning suppression of gonadal growth and FSH secretion occurs in LPIP animals within 3 days following transfer to IP whereas activation of gonadal growth in SP-gestated pups emerges over the following month.[8]

(E) Melatonin-based photoperiodic relay mechanism operative in gestation interacts with direct perception of photoperiod by weaned pups. Maternal melatonin and pup melatonin engage sequentially with neuroendocrine control of pup development via the *pars tuberalis* and the tanycytes of the pups.
(F) Workflow to generate photoperiod-dependent tanycyte transcriptomes: Siberian hamster brains were sampled at pn50 and cryosectioned, and the vimentin-positive region surrounding the 3rd ventricle was LASER capture microdissected and processed for Illumina RNA-seq. See also Figure S1.
(G) Average counts per million (cpm) across all samples for all genes defined by Campbell et al.[11] as cell-type-specific cluster markers. Error bars indicate the SEM.

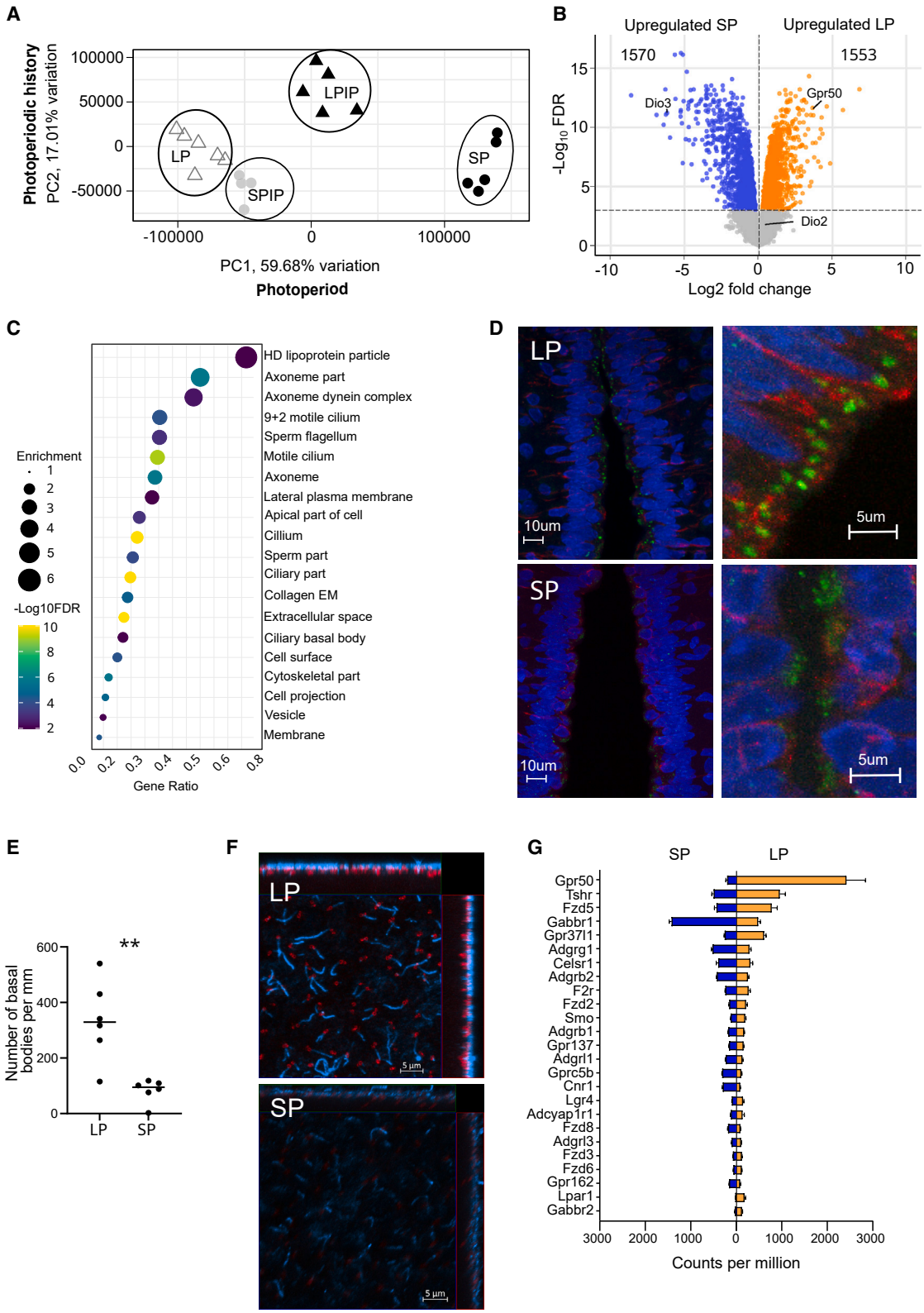

Figure 2. Photoperiodic effects on the tanycytic transcriptome and ciliary assembly

(A) Principal component analysis (PCA) plot showing the variation on the first two principal components for the entire transcriptome for all samples. Black circles, SP animals; gray circles, SPIP; black triangles, LPIP; white triangles, LP.

(legend continued on next page)

These findings suggest that a process of developmental remodeling of the ependymal region of the MBH precedes overt phenotypic changes in SPIP animals, whereas shutdown of reproductive development in LPIP animals reflects acute changes in the function of established feedback control circuits.

To characterize mechanisms involved in remodeling of the tanycytic region in SPIP animals, we looked for DEGs particularly associated with increasing photoperiod. Hence, we identified 109 DEGs for the SP versus SPIP contrast, which were not present in the SP versus LP contrast (FDR < 0.001 cut-off). This short list includes 4 upregulated genes linked to ciliogenesis (*ttc30a*, *kiz*, *rimbp3b*, and *ptpdc1*) and 4 key elements of FGF-signaling pathways implicated in migration of neural progenitors (*fgf18*, *cspg5*, *htra1*, and *chst11*)[25–28] (Figure 3B).

In the most common laboratory mouse strains (i.e., photoperiod-insensitive laboratory rodent models[29]), the cell-division phase of hypothalamic neurogenesis is essentially complete by the end of the neonatal period, and the juvenile period is a phase of establishment of neuronal connectivity.[30–32] Consistent with this model, while we see considerable numbers of MBH cells staining positively for the cell division markers PCNA and Ki67 in neonatal hamsters, this staining has disappeared almost completely by pn50 (Figures 3C and S3C). Furthermore, we see no effects of photoperiod treatment on the very limited numbers of positively stained cells beyond pn15 (Figure S3C). This suggests a model in which post-weaning photoperiodic remodeling in SPIP animals does not stem from effects on cell division per se, but rather on differentiation or migration of post-mitotic cells.

Recently, Yoo and colleagues combined cell fate mapping and single-nucleus (sn)RNA-seq to define a set of 6 clusters characterizing the differentiation of tanycytes into tanycyte-derived neurons, each defined by approximately 1,000 to 2,000 cluster marker genes.[24] While we were able to identify approximately 90% of these markers in our RNA-seq dataset (9,141 genes), the relative levels of cluster marker gene expression differed profoundly between LP- and SP-reared animals (Figure 3D). Expression of cluster markers for differentiated tanycytes (i.e., ciliated cells, staining positively for the intermediate filament protein vimentin[32,33,34]) was markedly higher in LP-reared animals, while markers for tanycyte-derived neurons were increased in SP-reared animals.

Strikingly, cluster marker expression in SP-gestated animals was profoundly affected by post-weaning transfer to IP but was almost completely unaffected by transfer from LP to IP (Figure 3D). In support of this picture of remodeling and changing tanycyte phenotype, we observed clear photoperiodic effects on the extent and intensity of vimentin staining (Figures 3E and S3D).

The accepted model for relay of photoperiodic information in seasonal mammals sees TSH production by the PT driving a flip-flop switch between tanycytic states of high active thyroid hormone (T_3), high retinoic acid (RA) (LP, summer state) and low T_3, low RA (SP, winter state) (Figure 1E).[35–37] This is mediated through reciprocal effects on the expression of thyroid hormone deiodinases (*dio2* versus *dio3*) and retinol-metabolizing enzymes (*aldh1a1* versus *cyp26b1*), for which we see clear inverse regulation in hamster pups undergoing SPIP and LPIP transitions (Figure 3F). Hence the model predicts that transcriptomic responses to photoperiod in the tanycytic region stem from interactive effects of RA-/T_3-dependent nuclear hormone receptor signaling, mediated by ligand-dependent heterodimeric interactions between nuclear thyroid hormone receptors (TRα/β), retinoic acid receptors (RARα/β), and retinoid X receptors (RXR).[38] Consistent with this model, we found strong statistical enrichment for thyroid response elements (TREs) and retinoic acid response elements (RAREs) in genes induced or repressed by the SP to IP transition, and to a lesser extent following the LP to IP transition (Table S2). Among the SPIP-induced genes, the most enriched in terms of the combined total of TREs and RAREs is *arrb1* (β-arrestin), which is a key mediator of GPCR de-/re-sensitization[39–41] (Figure 3G). Our analysis also revealed many other enriched response elements in the sets of genes responsive to transfer to IP (Table S2), suggesting that T_3/RA signals initiate a complex cascade response to photoperiodic change.

A hypothalamic substrate for phenological plasticity

Pathologies that impair ciliary assembly are associated with increased fat deposition in mice,[20] and transgenic targeting of ciliary assembly in hypothalamic neurons leads to obesity through insensitivity to metabolic feedback signals.[42] We speculate that by suppressing tanycytic assembly of sensory cilia, SP limits relay of positive metabolic feedback signals in the CSF to the hypothalamus of juvenile hamsters and thereby establishes a "rheostatic"[43] shift to a metabolic phenotype suited to overwintering survival. Our data demonstrate that the process by which

(B) Volcano plot for the LP versus SP comparison. Orange dots are genes upregulated in LP and blue dots are genes upregulated in SP (FDR < 0.001). The x axis is the $\log_2$ fold change and the y axis is the $-\log_{10}$ transformed FDR value. Cut-off line is at FDR = 0.001. The number of upregulated genes in SP and LP is represented. Labels show the responses of well-known photoperiodically regulated genes: *dio3*, *dio2*, and *gpr50*. See also Data S1A.

(C) Dot plot of non-redundant GO terms for genes upregulated in LP. The size of the dot represents the enrichment calculated using GOrilla analysis. The color of the dot represents the $-\log_{10}$ transformed FDR value for the enrichment. The x axis is the gene ratio (number of genes present in the input list and GO term divided by total number of genes within the GO term). See also Table S1.

(D) Immunohistochemistry for basal bodies of cilia (γ-tubulin, green), vimentin (red), and nuclei (DAPI, blue) on coronal sections. Images are z stack maximum projections. Scale bars are 10 or 5 μm, as indicated on the image. LP, long photoperiod; SP, short photoperiod. The region shown is 400–600 μm from the bottom of the median eminence, corresponding to the alpha tanycyte region. See also Figure S2A.

(E) Quantification of the number of basal bodies per millimeter of ventricular surface for 6 individuals per group. Statistical differences were assessed by two-tailed unpaired t test, **p = 0.0022. See also Figures S2C and S2D.

(F) Immunohistochemistry of the face of the 3rd ventricle. Basal bodies of the cilia (γ-tubulin, red) and ciliary projections (α-tubulin, blue). Images shown are z stack maximal projections. The images show the area of the ventricle face compatible with the coronal images shown in (D). The outer edges of the image show a side-on view of the z stack. Scale bars represent 5 μm. See also Figure S2B.

(G) GPCR expression in the tanycytic transcriptomes of SP- (blue) and LP- (orange) reared hamsters, ranked in descending order of mean abundance across all individual samples. Error bars represent the SEM. See also Figures S3A and S3B.

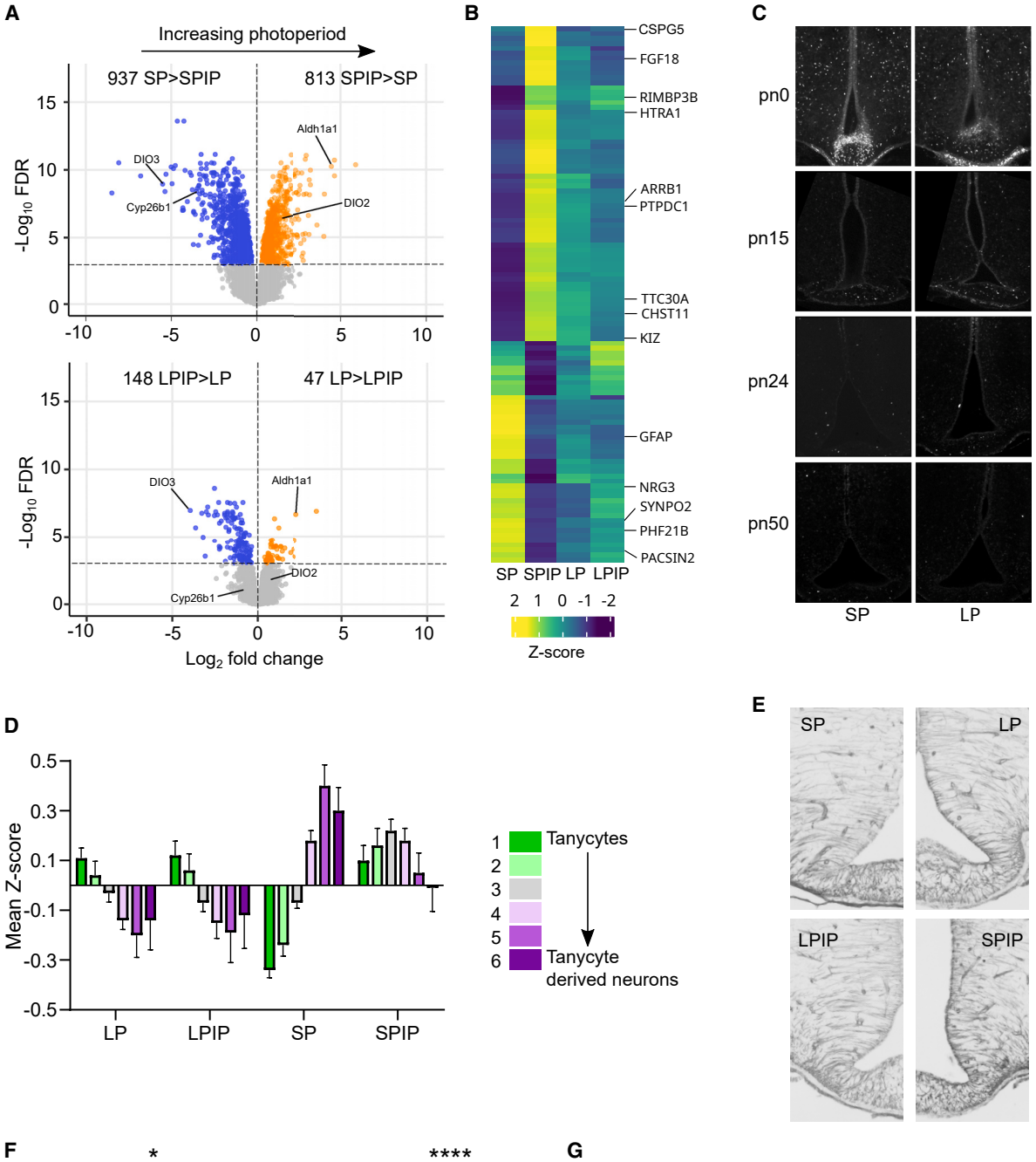

(legend on next page)

overwintering juveniles switch to a spring/summer phenotype following exposure to increasing photoperiod involves reorganization of the ependymal layer to establish a population of sensory tanycytes. Contrastingly, tissue reorganization appears less important for arrest of reproductive development by exposure to declining photoperiod. Along with our recent findings that gonadal development and tanycytic gene expression are more temperature sensitive in voles reared on an autumn photoperiodic regime than on a spring regime,[44,45] these data lead us to propose that the tanycytic region is the key hypothalamic substrate for phenological plasticity in mammals.

STAR★METHODS

Detailed methods are provided in the online version of this paper and include the following:

- KEY RESOURCES TABLE
- RESOURCE AVAILABILITY
  - Lead contact
  - Materials availability
  - Data and code availability
- EXPERIMENTAL MODEL AND SUBJECT DETAILS
  - Siberian hamsters
- METHOD DETAILS
  - *Phodopus sungorus* genome sequencing
  - LASER capture microdissection of tanycytes
  - LCMD-RNA-seq, mapping and counts
  - Gene expression analysis
  - Transcription factor binding site analysis
  - Immunohistochemistry
  - Third ventricle face whole mounts for cilia
  - PCNA & Ki67 staining
- QUANTIFICATION AND STATISTICAL ANALYSIS

SUPPLEMENTAL INFORMATION

Supplemental information can be found online at https://doi.org/10.1016/j.cub.2023.12.042.

ACKNOWLEDGMENTS

The work was supported by grants from the Tromsø Forskningsstiftelse (TFS) starter grant (TFS2016SW) and the TFS infrastructure grant (IS3_17_SW) awarded to S.H.W., Research Council of Norway Overseas research grant (Hypothalamic tanycytes as epigenetic calendars) awarded to S.H.W., Fonds Paul Mandel pour les recherches en neurosciences (Hypothalamic tanycytes as epigenetic calendars) awarded to S.H.W. and V.S., and University of Strasbourg Institute for Advanced Studies fellowship (project: Epigenetic light) awarded to D.G.H. The Arctic Seasonal Timekeeping Initiative (ASTI) grant and UiT strategic funds support D.G.H., S.H.W., F.A.F.M., and F.C.-M. The authors would like to acknowledge the National Infrastructure for Research Data (NIRD) project number nn9893k for use of the computing cluster SAGA to complete the bioinformatic analysis. In addition, we acknowledge the assistance of the Elixir-Norway project (https://elixir.no) (Elixir3, 322392) and, specifically, Lars Grønvold and Thu-Hien To for their assistance with the transcription factor binding site analysis. We thank Cristina Sandu for help in setting up and performing the initial microdissection tests and validation. Finally, we acknowledge the UiT core microscopy facility for the use of the confocal microscope.

AUTHOR CONTRIBUTIONS

Conceptualization, D.G.H., S.H.W., V.S., and C.S.d.M.; methodology, V.J.M., C.S.d.M., C.J., F.A.F.M., F.C.-M., S.R.S., and S.H.W.; software, S.R.S.; validation, C.J., C.S.d.M., F.A.F.M., and F.C.-M.; formal analysis, V.J.M., S.H.W., S.R.S., and D.G.H.; investigation, V.J.M., C.S.d.M., V.S., C.J., F.C.-M., F.A.F.M., and S.H.W.; resources, V.S. and S.H.W.; data curation, S.H.W., S.R.S., and V.J.M.; writing – original draft, S.H.W., D.G.H., and V.J.M.; writing – review & editing, all authors; visualization, S.H.W. and D.G.H.; supervision, S.H.W., D.G.H., and V.S.; project administration, V.S. and S.H.W.; funding acquisition, S.H.W., D.G.H., and V.S.

DECLARATION OF INTERESTS

The authors declare no competing interests.

Received: April 22, 2023
Revised: November 7, 2023
Accepted: December 13, 2023
Published: January 12, 2024

REFERENCES

1. Horton, T.H. (1984). Growth and maturation in Microtus montanus: effects of photoperiods before and after weaning. Can. J. Zool. *62*, 1741–1746.
2. Horton, T.H. (1984). Growth and reproductive development of male Microtus montanus is affected by the prenatal photoperiod. Biol. Reprod. *31*, 499–504.
3. Negus, N.C., Berger, P.J., and Brown, B.W. (1986). Microtine population dynamics in a predictable environment. Can. J. Zool. *64*, 785–792.
4. Negus, N.C., Berger, P.J., and Forslund, L.G. (1977). Reproductive strategy of Microtus montanus. J. Mammal. *58*, 347–353.

Figure 3. Increasing photoperiod post-weaning promotes tissue reorganization in the tanycytic region

(A) Volcano plots for post-weaning photoperiodic increase (SP to IP transition, upper panel) and decrease (LP to IP transition, lower panel); the dotted horizontal line indicates the FDR = 0.001 threshold. Data are presented as $\log_2$ fold change, upregulated in long photoperiod (LP) in orange, downregulated in short photoperiod (SP) in blue. See also Data S1B.

(B) Heatmap of differential gene expression for 109 genes passing the significance threshold for the SP to IP transition, but not for the LP versus SP contrast. The group mean *Z* score is color-coded as indicated. See also Data S1B and S1E.

(C) Dark field micrographs of PCNA staining in the mediobasal hypothalamus of hamsters between birth (pn0) and 50 days of age (pn50). See also Figure S3C.

(D) Relative abundances of genes in clusters representing different stages of hypothalamic neural/glial differentiation defined by snRNA-seq.[24] The mean *Z* score for expression of marker genes within each cluster is shown for each of the 4 photoperiod treatments. Error bars represent the SEM. The bars are color-coded as indicated.

(E) Vimentin staining in the MBH of hamsters raised to pn50 on the indicated photoperiod regimes. Note increased staining at ependymal surface and in processes projecting from tanycytes into the parenchyma in LP and SPIP animals. See also Figure S3D.

(F) Reciprocal effects of photoperiod treatment on tanycytic expression of enzymes determining local production of T_3 and RA in the MBH, presented as ratios between enzymes governing synthesis (*dio2* for T_3 and *aldh1a1* for RA) and degradation (*dio3* for T_3 and *cyp26* for RA). Results of one-way ANOVA are shown: *$p < 0.01$, ****$p < 0.0001$.

(G) Detection of putative TREs and RAREs in the promoter region of *aarb1* (β-arrrestin). The figure shows the position of putative sites identified for JASPAR matrices in the 2 kb region upstream of the predicted transcription start site (TSS). See also Table S2.

5. Weaver, D.R., and Reppert, S.M. (1986). Maternal melatonin communicates day length to the fetus in djungarian hamsters. Endocrinology *119*, 2861–2863.
6. Horton, T.H., Stachecki, S.A., and Stetson, M.H. (1990). Maternal transfer of photoperiodic information in Siberian hamsters. IV. Peripubertal reproductive development in the absence of maternal photoperiodic signals during gestation. Biol. Reprod. *42*, 441–449.
7. Lee, T.M., Spears, N., Tuthill, C.R., and Zucker, I. (1989). Maternal melatonin treatment influences rates of neonatal development of meadow vole pups. Biol. Reprod. *40*, 495–502.
8. Saenz de Miera, C., Bothorel, B., Jaeger, C., Simonneaux, V., and Hazlerigg, D. (2017). Maternal photoperiod programs hypothalamic thyroid status via the fetal pituitary gland. Proc. Natl. Acad. Sci. USA *114*, 201702943.
9. Sáenz de Miera, C., Beymer, M., Routledge, K., Król, E., Selman, C., Hazlerigg, D.G., and Simonneaux, V. (2020). Photoperiodic regulation in a wild-derived mouse strain. J. Exp. Biol. *223*, jeb217687.
10. van Dalum, J., Melum, V.J., Wood, S.H., and Hazlerigg, D.G. (2019). Maternal photoperiodic programming: melatonin and seasonal synchronization before birth. Front. Endocrinol. *10*, 901.
11. Campbell, J.N., Macosko, E.Z., Fenselau, H., Pers, T.H., Lyubetskaya, A., Tenen, D., Goldman, M., Verstegen, A.M.J., Resch, J.M., McCarroll, S.A., et al. (2017). A molecular census of arcuate hypothalamus and median eminence cell types. Nat. Neurosci. *20*, 484–496.
12. Haugg, E., Borner, J., Diedrich, V., and Herwig, A. (2022). Comparative transcriptomics of the Djungarian hamster hypothalamus during short photoperiod acclimation and spontaneous torpor. FEBS Open Bio *12*, 443–459.
13. Lomet, D., Cognié, J., Chesneau, D., Dubois, E., Hazlerigg, D., and Dardente, H. (2018). The impact of thyroid hormone in seasonal breeding has a restricted transcriptional signature. Cell. Mol. Life Sci. *75*, 905–919.
14. Lomet, D., Druart, X., Hazlerigg, D., Beltramo, M., and Dardente, H. (2020). Circuit-level analysis identifies target genes of sex steroids in ewe seasonal breeding. Mol. Cell. Endocrinol. *512*, 110825.
15. Nechipurenko, I.V. (2020). The enigmatic role of lipids in cilia signaling. Front. Cell Dev. Biol. *8*, 777.
16. Wheway, G., Nazlamova, L., and Hancock, J.T. (2018). Signaling through the primary cilium. Front. Cell Dev. Biol. *6*, 8.
17. Anvarian, Z., Mykytyn, K., Mukhopadhyay, S., Pedersen, L.B., and Christensen, S.T. (2019). Cellular signalling by primary cilia in development, organ function and disease. Nat. Rev. Nephrol. *15*, 199–219.
18. Mykytyn, K., and Askwith, C. (2017). G-protein-coupled receptor signaling in cilia. Cold Spring Harb. Perspect. Biol. *9*, a028183.
19. Gerdes, J.M., Davis, E.E., and Katsanis, N. (2009). The vertebrate primary cilium in development, homeostasis, and disease. Cell *137*, 32–45.
20. Loktev, A.V., and Jackson, P.K. (2013). Neuropeptide Y family receptors traffic via the Bardet-Biedl syndrome pathway to signal in neuronal primary cilia. Cell Rep. *5*, 1316–1329.
21. Ivanova, E.A., Bechtold, D.A., Dupré, S.M., Brennand, J., Barrett, P., Luckman, S.M., and Loudon, A.S.I. (2008). Altered metabolism in the melatonin-related receptor (GPR50) knockout mouse. Am. J. Physiol. Endocrinol. Metab. *294*, E176–E182.
22. Schou, K.B., Pedersen, L.B., and Christensen, S.T. (2015). Ins and outs of GPCR signaling in primary cilia. EMBO Rep. *16*, 1099–1113.
23. Wood, S.H., Christian, H.C., Miedzinska, K., Saer, B.R.C., Johnson, M., Paton, B., Yu, L., McNeilly, J., Davis, J.R.E., McNeilly, A.S., et al. (2015). Binary switching of calendar cells in the pituitary defines the phase of the circannual cycle in mammals. Curr. Biol. *25*, 2651–2662.
24. Yoo, S., Kim, J., Lyu, P., Hoang, T.V., Ma, A., Trinh, V., Dai, W., Jiang, L., Leavey, P., Duncan, L., et al. (2021). Control of neurogenic competence in mammalian hypothalamic tanycytes. Sci. Adv. *7*, eabg3777.
25. Bernfield, M., Götte, M., Park, P.W., Reizes, O., Fitzgerald, M.L., Lincecum, J., and Zako, M. (1999). Functions of cell surface heparan sulfate proteoglycans. Annu. Rev. Biochem. *68*, 729–777.
26. Sirko, S., von Holst, A., Weber, A., Wizenmann, A., Theocharidis, U., Götz, M., and Faissner, A. (2010). Chondroitin sulfates are required for fibroblast growth factor-2-dependent proliferation and maintenance in neural stem cells and for epidermal growth factor-dependent migration of their progeny. Stem Cell. *28*, 775–787.
27. Cortes, M., Baria, A.T., and Schwartz, N.B. (2009). Sulfation of chondroitin sulfate proteoglycans is necessary for proper Indian hedgehog signaling in the developing growth plate. Development *136*, 1697–1706.
28. Kim, G.-Y., Kim, H.-Y., Kim, H.-T., Moon, J.-M., Kim, C.-H., Kang, S., and Rhim, H. (2012). HtrA1 is a novel antagonist controlling fibroblast growth factor (FGF) signaling via cleavage of FGF8. Mol. Cell Biol. *32*, 4482–4492.
29. Kasahara, T., Abe, K., Mekada, K., Yoshiki, A., and Kato, T. (2010). Genetic variation of melatonin productivity in laboratory mice under domestication. Proc. Natl. Acad. Sci. USA *107*, 6412–6417.
30. Bouret, S.G., and Simerly, R.B. (2006). Developmental programming of hypothalamic feeding circuits. Clin. Genet. *70*, 295–301.
31. Bouret, S.G. (2022). Developmental programming of hypothalamic melanocortin circuits. Exp. Mol. Med. *54*, 403–413.
32. Altman, J., and Bayer, S.A. (1978). Development of the diencephalon in the rat. III. Ontogeny of the specialized ventricular linings of the hypothalamic third ventricle. J. Comp. Neurol. *182*, 995–1015.
33. Mirzadeh, Z., Kusne, Y., Duran-Moreno, M., Cabrales, E., Gil-Perotin, S., Ortiz, C., Chen, B., Garcia-Verdugo, J.M., Sanai, N., and Alvarez-Buylla, A. (2017). Bi- and uniciliated ependymal cells define continuous floor-plate-derived tanycytic territories. Nat. Commun. *8*, 13759.
34. Rodríguez, E.M., Blázquez, J.L., Pastor, F.E., Peláez, B., Peña, P., Peruzzo, B., and Amat, P. (2005). Hypothalamic tanycytes: a key component of brain–endocrine interaction. Int. Rev. Cytol. *247*, 89–164.
35. Hazlerigg, D., and Simonneaux, V. (2015). Seasonal regulation of reproduction in mammals. In Knobil and Neill's Physiology of Reproduction (Elsevier), pp. 1575–1604.
36. West, A.C., and Wood, S.H. (2018). Seasonal physiology: making the future a thing of the past. Curr. Opin. Physiol. *5*, 1–8.
37. Shearer, K.D., Goodman, T.H., Ross, A.W., Reilly, L., Morgan, P.J., and McCaffery, P.J. (2010). Photoperiodic regulation of retinoic acid signaling in the hypothalamus. J. Neurochem. *112*, 246–257.
38. Evans, R.M., and Mangelsdorf, D.J. (2014). Nuclear receptors, RXR, and the Big Bang. Cell *157*, 255–266.
39. Gurevich, V.V., and Gurevich, E.V. (2019). GPCR signaling regulation: the role of GRKs and Arrestins. Front. Pharmacol. *10*, 125.
40. Jean-Charles, P.-Y., Kaur, S., and Shenoy, S.K. (2017). G protein–coupled receptor signaling through β-arrestin–dependent mechanisms. J. Cardiovasc. Pharmacol. *70*, 142–158.
41. Thomsen, A.R.B., Plouffe, B., Cahill, T.J., Shukla, A.K., Tarrasch, J.T., Dosey, A.M., Kahsai, A.W., Strachan, R.T., Pani, B., Mahoney, J.P., et al. (2016). GPCR-G protein-β-arrestin super-complex mediates sustained G protein signaling. Cell *166*, 907–919.
42. Volta, F., and Gerdes, J.M. (2017). The role of primary cilia in obesity and diabetes. Ann. N. Y. Acad. Sci. *1391*, 71–84.
43. Mrosovsky, N. (1990). Rheostasis: The Physiology of Change, 1st ed. (Oxford University Press).
44. van Rosmalen, L., van Dalum, J., Appenroth, D., Roodenrijs, R.T.M., de Wit, L., Hazlerigg, D.G., Hut, R.A., van Rosmalen, L., van Dalum, J., Appenroth, D., et al. (2021). Mechanisms of temperature modulation in mammalian seasonal timing. FASEB J *35*, e21605.
45. van Dalum, M.J., van Rosmalen, L., Appenroth, D., Cazarez Marquez, F., Roodenrijs, R.T.M., de Wit, L., Hut, R.A., and Hazlerigg, D.G. (2023). Ambient temperature effects on the spring and autumn somatic growth trajectory show plasticity in the photoneuroendocrine response pathway in the tundra vole. J. Biol. Rhythms *38*, 586–600.
46. Castro-Mondragon, J.A., Riudavets-Puig, R., Rauluseviciute, I., Lemma, R.B., Turchi, L., Blanc-Mathieu, R., Lucas, J., Boddie, P., Khan, A., Manosalva Pérez, N., et al. (2022). JASPAR 2022: the 9th release of the

open-access database of transcription factor binding profiles. Nucleic Acids Res. *50*, D165–D173.

47. Chen, S., Zhou, Y., Chen, Y., and Gu, J. (2018). fastp: an ultra-fast all-in-one FASTQ preprocessor. Bioinformatics *34*, i884–i890.
48. Kolmogorov, M., Yuan, J., Lin, Y., and Pevzner, P.A. (2019). Assembly of long, error-prone reads using repeat graphs. Nat. Biotechnol. *37*, 540–546.
49. Li, H. (2018). Minimap2: pairwise alignment for nucleotide sequences. Bioinformatics *34*, 3094–3100.
50. Shafin, K., Pesout, T., Chang, P.-C., Nattestad, M., Kolesnikov, A., Goel, S., Baid, G., Kolmogorov, M., Eizenga, J.M., Miga, K.H., et al. (2021). Haplotype-aware variant calling with PEPPER-Margin-DeepVariant enables high accuracy in nanopore long-reads. Nat. Methods *18*, 1322–1332.
51. Li, H., Handsaker, B., Wysoker, A., Fennell, T., Ruan, J., Homer, N., Marth, G., Abecasis, G., and Durbin, R.; 1000 Genome Project Data Processing Subgroup (2009). The Sequence Alignment/Map format and SAMtools. Bioinformatics *25*, 2078–2079.
52. Earl, D., Bradnam, K., St. John, J., Darling, A., Lin, D., Fass, J., Yu, H.O.K., Buffalo, V., Zerbino, D.R., Diekhans, M., et al. (2011). Assemblathon 1: a competitive assessment of de novo short read assembly methods. Genome Res. *21*, 2224–2241.
53. Manni, M., Berkeley, M.R., Seppey, M., and Zdobnov, E.M. (2021). BUSCO: assessing genomic data quality and beyond. Curr. Protoc. *1*, e323.
54. Shumate, A., and Salzberg, S.L. (2021). Liftoff: accurate mapping of gene annotations. Bioinformatics *37*, 1639–1643.
55. Langmead, B., and Salzberg, S.L. (2012). Fast gapped-read alignment with Bowtie 2. Nat. Methods *9*, 357–359.
56. Robinson, M.D., McCarthy, D.J., and Smyth, G.K. (2010). edgeR: a Bioconductor package for differential expression analysis of digital gene expression data. Bioinformatics *26*, 139–140.
57. Harding, S.D., Armstrong, J.F., Faccenda, E., Southan, C., Alexander, S.P.H., Davenport, A.P., Pawson, A.J., Spedding, M., and Davies, J.A.; NC-IUPHAR (2022). The IUPHAR/BPS guide to PHARMACOLOGY in 2022: curating pharmacology for COVID-19, malaria and antibacterials. Nucleic Acids Res. *50*, D1282–D1294.
58. Walker, B.J., Abeel, T., Shea, T., Priest, M., Abouelliel, A., Sakthikumar, S., Cuomo, C.A., Zeng, Q., Wortman, J., Young, S.K., and Earl, A.M. (2014). Pilon: an integrated tool for comprehensive microbial variant detection and genome assembly improvement. PLoS One *9*, e112963.
59. Butler, A.E., Matveyenko, A.V., Kirakossian, D., Park, J., Gurlo, T., and Butler, P.C. (2016). Recovery of high-quality RNA from laser capture microdissected human and rodent pancreas. J. Histotechnol. *39*, 59–65.
60. Wood, S.H., Craig, T., Li, Y., Merry, B., and de Magalhães, J.P. (2013). Whole transcriptome sequencing of the aging rat brain reveals dynamic RNA changes in the dark matter of the genome. Age *35*, 763–776.
61. Eden, E., Navon, R., Steinfeld, I., Lipson, D., and Yakhini, Z. (2009). GOrilla: a tool for discovery and visualization of enriched GO terms in ranked gene lists. BMC Bioinf. *10*, 48.
62. Wickham, H. (2016). ggplot2: Elegant Graphics for Data Analysis (Use R! Ser.).
63. Grant, C.E., Bailey, T.L., and Noble, W.S. (2011). FIMO: scanning for occurrences of a given motif. Bioinformatics *27*, 1017–1018.
64. Robinson, J.T., Thorvaldsdóttir, H., Winckler, W., Guttman, M., Lander, E.S., Getz, G., and Mesirov, J.P. (2011). Integrative genomics viewer. Nat. Biotechnol. *29*, 24–26.
65. Mclean, I.W., and Nakane, P.K. (1974). Periodate-lysine-paraformaldehyde fixative. A new fixation for immunoelectron microscopy. J. Histochem. Cytochem. *22*, 1077–1083.
66. Klosen, P., Maessen, X., and van den Bosch de Aguilar, P. (1993). PEG embedding for immunocytochemistry: application to the analysis of immunoreactivity loss during histological processing. J. Histochem. Cytochem. *41*, 455–463.
67. Morin, L.P., and Wood, R.I. (2001). A Stereotaxic Atlas of the Golden Hamster Brain (Elsevier Science).

STAR★METHODS

KEY RESOURCES TABLE

REAGENT or RESOURCE	SOURCE	IDENTIFIER
Antibodies		
Mouse anti-Vimentin	ThermoFisher	Cat# MA5-11883; RRID:AB_10985392
Rabbit anti γ-tubulin	Sigma-Aldrich	Cat# T5192; RRID:AB_261690
Goat anti-mouse Alexa Fluor 647	Abcam	Cat# ab150115; RRID:AB_2687948
Donkey anti-rabbit Alexa Fluor 488	Abcam	Cat# ab150073; RRID:AB_2636877
Mouse anti α-tubulin	Sigma-Aldrich	Cat# T6793; RRID:AB_477585
Goat Anti-Mouse Brilliant Violet 42	Jackson Immuno research	Cat# 115-675-166; RRID:AB_2651087
Rabbit anti-Ki67	Abcam	Cat# ab15580; RRID:AB_443209
Monoclonal anti-PCNA made in mouse	Abcam	Cat# ab29; RRID:AB_303394
Chemicals, peptides, and recombinant proteins		
Rnase inhibitor ProtectRNA 500x	Sigma-Aldrich	R7397
cold water fish skin gelatine	Sigma-Aldrich	G7041
bovine serum albumin	Sigma-Aldrich	A2153
tween 20	Sigma-Aldrich	P9416
TrueBlack lipofuscin autofluorescence quencher	Biotium	23007
Hoechst 33342 solution	ThermoFisher	62249
Dabco 33-LV reagent	Sigma-Aldrich	290734
Triton X-100	Sigma-Aldrich	T8787
SYTOX green	Thermo Fisher	S7020
Crystal Mount Aqueous Mounting Medium	Sigma-Aldrich	C0612
Normal horse serum	NHS; Vector Labs., Burlingame, CA, USA	S-2000-20
niquel-3,3-diaminobenzidine (Ni-DAB)	Sigma-Aldrich	D7304
Critical commercial assays		
Nanobind Tissue Big DNA Kit	Circulomics	102-302-100
SQK-LSK109 kit	Nanopore	SQK-LSK109
Qiagen all prep DNA/RNA micro kit	Qiagen	80284
Short Read Elimination Kit	Circulomics	EXP-SFE001
Vectastain Universal Elite ABC kit	Vector Labs.	PK-6200
Deposited data		
nanopore long read genome sequencing, illumina genome sequencing	This paper & Sequence read archive (SRA)	SRA: PRJNA839344
RNA-seq data	This paper & GEO	SRA: PRJNA842667; GEO: GSE204883
Genome assembly project	This paper & DDBJ/ENA/GenBank	GenBank: JANBXA000000000
Genome assembly statistics	This paper	DataverseNO: https://doi.org/10.18710/1IHNDD
Number of transcription factor binding sites in *Phodopus sungorus* genome	This paper	DAtaverseNO: https://doi.org/10.18710/1IHNDD
Comparative analysis between pseudotime clusters from mouse single RNAseq pseudotime analysis and our RNAseq dataset	This paper	DataverseNO: https://doi.org/10.18710/1IHNDD
Body and testis weight	This paper	DataverseNO: https://doi.org/10.18710/1IHNDD
Pseudotime clusters from snRNAseq in mice	Yoo et al.[24]	https://doi.org/10.1126/sciadv.abg3777
SnRNAseq data from the hypothalamus of mice	Campbell et al.[11]	https://doi.org/10.1038/nn.4495
Mouse GRCm39 ensembl release 104	Ensembl	Ensembl: https://www.ensembl.org/Mus_musculus/Info/Annotation

(*Continued on next page*)

Continued		
REAGENT or RESOURCE	SOURCE	IDENTIFIER
JASPAR (JASPAR2022_CORE_non-redundant)	Castro-Mondragon et al.[46]	JASPAR: https://jaspar.elixir.no/
Curated list of GPCRs	IUPHAR	IUPHAR: https://www.guidetopharmacology.org/GRAC/ReceptorFamiliesForward?type=GPCR
Experimental models: Organisms/strains		
Siberian hamsters (*Phodopus sungorus*)	Chronobiotron UMS 3415	N/A
Software and algorithms		
R scripts for transcription factor binding site analysis	This paper	Github: https://doi.org/10.5281/zenodo.10285435
R scripts for differential expression analysis	This paper	Github: https://doi.org/10.5281/zenodo.10285435
Porechop ONT and fastp (genome assembly)	Chen et al.[47]	https://doi.org/10.1093/bioinformatics/bty560
Flye v2.8	Kolmogorov et al.[48]	https://doi.org/10.1038/s41587-019-0072-8
Minimap2	Li et al.[49]	https://doi.org/10.1093/bioinformatics/bty191
PEPPER	Shafin et al.[50]	https://doi.org/10.1038/s41592-021-01299-w
samtools	Li et al.[51]	https://doi.org/10.1093/bioinformatics/btp352
Assembly statistics script (assemblathon-stats.pl)	Earl et al.[52]	https://doi.org/10.1101/gr.126599.111
Busco v5.1	Berkeley et al.[53]	https://doi.org/10.1002/cpz1.323
Liftoff tool	Shumate et al.[54]	https://doi.org/10.1093/bioinformatics/btaa1016
Bowtie2	Langmead et al.[55]	https://doi.org/10.1038/nmeth.1923
R	R project	https://www.r-project.org/
EdgeR	Robinson et al.[56]	https://doi.org/10.1093/bioinformatics/btp616
GoRilla	Eden et al.[57]	https://doi.org/10.1186/1471-2105-10-48
FIMO tool (MEME suite) v. 5.4.1	Grant et al.[46]	https://doi.org/10.1093/bioinformatics/btr064
Zeiss zen	Zeiss	https://www.zeiss.com/microscopy/en/products/software/zeiss-zen.html#zenversions
Qupath	Qupath	https://qupath.github.io/
ImageJ	Wayne Rasband	https://ImageJ.nih.gov/ij/
Pilon v1.23	Walker et al.[58]	https://doi.org/10.1371/journal.pone.0112963
Graphpad prism	Graphpad software	https://www.graphpad.com/

RESOURCE AVAILABILITY

Lead contact

Further information and requests for resources and reagents should be directed to and will be fulfilled by the lead contact, Shona Wood (shona.wood@uit.no).

Materials availability

This study did not generate new unique reagents.

Data and code availability

- RNA-seq data from LASER captured tanycytes are available at SRA: PRJNA842667 and GEO: GSE204883 and are publicly available as of the date of publication. key resources table The nanopore long read genome sequencing and illumina genome sequencing used to generate the *Phodopus sungorus* genome have been deposited in the SRA: PRJNA839344 and are publicly available as of the date of publication. key resources table The genome assembly for *Phodopus sungorus* has been deposited in GenBank: JANBXA000000000 and are publicly available as of the date of publication. key resources table Genome assembly statistics for the *Phodopus sungorus* genome, the number of transcription factor binding site motifs identified in the *Phodopus sungorus* genome and the genes present in our dataset and the corresponding tanycyte cluster from the pseudotime analysis of Yoo et al.[24] have all been deposited as tables in DataverseNO: https://doi.org/10.18710/1IHNDD key resources table. All other analyzed data and confocal images reported in this paper will be shared by the lead contact upon request.
- R scripts and related files for differential gene expression and transcription factor binding site analysis are available on key resources table Github: https://doi.org/10.5281/zenodo.10285435
- Any additional information required to reanalyze the data reported in this paper is available from the lead contact upon request.

EXPERIMENTAL MODEL AND SUBJECT DETAILS

Siberian hamsters

Experiments were conducted in accordance with French National Law implementing the European Communities Council Directive 2010/63/EU and the French Directive 2013-118. All procedures were validated by the Animal Welfare Committee of the Animal Resource and Experimentation platform (Chronobiotron UMS 3415) of the Strasbourg Institute of Neuroscience.

Siberian hamsters (*Phodopus sungorus*) were mated on long photoperiod (LP — 16 h light:8 h dark (16:8)), before transfer of half of the pregnant females to SP (8:16). Dams and pups remained on the same photoperiod until weaning. From weaning, half of the animals in each litter remained on the same photoperiod and half were transferred to IP (14:10) (Figure 1A). All sample groups contained offspring from at least three different litters. Males were killed at postnatal day (pn) 0, 15, 24, and 50 in the mid-light phase. All animals were weighed before harvesting of tissues. Testis weight and body weight were recorded.

METHOD DETAILS

Phodopus sungorus genome sequencing

Livers collected for genome sequencing were snap frozen on chilled isopentane over liquid nitrogen and stored at -80°C. High molecular weight DNA was isolated from 27mg frozen liver using Nanobind Tissue Big DNA Kit from Circulomics. Extracted DNA was sheared using a 27G blunt end needle. The resulting DNA was sequenced using both long read nanopore sequencing and short read illumina sequencing for assembly polishing. For the long-read sequencing, size selection was performed by using the Short Read Elimination Kit from Circulomics. A sequencing library was made using the SQK-LSK109 kit, following the Genomic DNA by Ligation Nanopore Protocol. Library was sequenced on one Promethion flow cell (FLO-PRO002). Illumina sequencing of paired-end 150bp reads was performed by Novogene Fastq files used for genome assembly are available on SRA:PRJNA839344.

Figure S1A shows the bioinformatic pipeline for genome assembly. In brief, the long-read sequences were quality filtered and trimmed using porechop ONT and fastp.[47] The following parameters were used in fastp: -disable_trim_poly_g , -disable_adapter_trimming , -q 7, -l 4000, -f 50. This produced a total of 72,6 Gb porechop filtered data with an average read N50 of 50.5kb.

The *Phodopus sungorus* genome was assembled using flye v2.8[48] with three different overlap sizes (7k, 15k, 20k). We chose to continue with the 15k overlap assembly.

For error correction of the long reads sequences we first mapped raw long reads to the 15k overlap assembly using minimap2.[49] We then used PEPPER[50] to correct base errors in assembly using nanopore reads themselves, using the base calling model parameters: –model_path pepper_r941_guppy305_human.pkl. Finally, we performed a second round of assembly error correction using pilon v 1.23.[58] Here, the Illumina short reads were mapped to genome assembly using 'bwa mem' with default parameters. The resulting bam file was sorted using 'samtools sort'[51] command and then pilon v 1.23 was used with default parameters to correct remaining errors. This resulted in our final assembly; Psun-UiT-1 (Figure S1A) available in Genbank:JANBXA010000000. A script for summarizing the statistics for the assembly was used[52] (see key resources table), the results are found on DataverseNO: https://doi.org/10.18710/1IHNDD .

To check the quality of our assembly we used busco v5.1[53] with the vertebrata_odb10 conserved gene set to estimate gene space contiguity. Our assembly had a gene contiguity of 98.1%.

We annotated Psun-UiT-1 using the liftoff tool[54] and the mouse genome (Mouse GRCm39, Ensembl release 104) (Figure S1A). 21882 genes were annotated in our new genome.

LASER capture microdissection of tanycytes

The brains (6 per group) were snap frozen on chilled isopentane over liquid nitrogen and sectioned on the cryostat (-20°C; Leica CM3000) at 25μm. The brains were cut in series to allow the whole medio-basal hypothalamic region to be covered on one slide (Figure 1F). For LASER capture microdissection (LCMD) each animal had 5 – 6 PEN membrane frame slides (Arcturus, Thermo Fisher) slides of 12 sections and every 7th section was stained for vimentin (see immunohistochemistry subsection) to measure the ventral-dorsal length of vimentin expression, as a marker for tanycyte location. This measurement was used when microdissecting each series, to enrich for tanycytes. Slides were individually placed in pre-cooled 50 mL centrifuge tubes (Corning) on dry ice and stored at -80°C.

Immediately before LCMD the membrane frame slides were stained using cresyl violet and dehydrated based on Butler et al.[59] Unless stated all solutions contained Rnase inhibitor (ProtectRNA 500x, Sigma). In brief, frozen slides were rapidly defrosted at room temperature and placed in 0.2% cresyl violet in 70% ethanol for 1 min 30 s, then 30 s each of: 75% ethanol (twice), 95% ethanol and 100% ethanol. The final step was 2 min in 100% ethanol without Rnase inhibitor. From here the slides were air-dried for 5 min at room temperature and directly transferred to the laser microdissector (Veritas Microdissection Instrument, Model 704, Arcturus Bioscience) and microdissection was completed within 30 min to minimize RNA degradation. LCMD was carried out at x10. IR laser power of 70-100 mW and 2500 μsec of pulse (1 hit) were used to capture the tanycytes on the transfer film of the microdissection caps (Capsure Macro LCM caps, Arcturus) followed by UV laser power of 18 mW and 2 μm of spot size for cutting around the captured tissue.

We microdissected the tanycytic region of the 3rd ventricle within two to three cell bodies of the ventricle wall (Figure S1B) and limited to the dorsal length indicated by the vimentin staining. The microdissected tissues were collected in Rnase-free DNA low-

bind tubes, snap frozen on dry ice and stored at -80°C. RNA was extracted from the microdissected tissue using the Qiagen all prep DNA/RNA micro kit according to the manufacturer's instructions. The RNA integrity numbers were determined by TapeStation high sensitivity RNA analysis and all were between 8.5 and 9.

LCMD-RNA-seq, mapping and counts

RNA-seq library construction was performed by BGI using their standard RNA-seq protocol and paired-end sequenced on an Illumina high seq 4000. Quality control checks and barcode removal were performed according to BGI protocol. Approximately 40 to 50 million reads were generated per sample. Mapping was performed on the Sigma2 national infrastructure for research data (NIRD) supercomputer SAGA. FASTQ files were mapped using bowtie2[55] and these parameters: bowtie2 -q —phred33 —fr -t -p 8 -x. Psun-UiT-1 genome assembly and Psun annotation we generated were used for the mapping (Figure S1C). This approach mapped un-spliced reads (as previously[23,60]) and gave a mapping rate which averaged 83%. Feature counts was used to count the mapped reads to genes, using these parameters: featureCounts -p -t exon -g gene_id (Figure S1C), on average 72% of alignments were assigned to an annotated feature.

FASTQ files and count files were deposited in key resources table GEO: GSE204883

Gene expression analysis

Differential expression analyses were performed using using Rstudio, and the package EdgeR.[56] We determined the median counts per million (CPM) across the whole experiment for each gene and applied a cut off of 10 raw counts (0.5 CPM in our study), removing genes with a median of less than one CPM from the analysis. 13346 genes remained representing our LCMD transcriptome, this dataset was used in all subsequent analysis.

In brief, a GLM analysis according to the EdgeR manual was conducted to determine which genes were differentially expressed between the groups (Data S1). Volcano plots of these data were generated using the enhanced volcano package. Throughout the analysis we used a FDR cut off of 0.001 and no log 2-fold change cut off.

A single nuclei RNA-seq dataset generated by Campbell et al.[11] determined cell type specific markers for genes in the hypothalamus. This list was used to categorize the genes expressed in our dataset into cell types. We averaged the counts per million across the experiment for the genes in those specific cell type clusters and plotted the data to show cell type enrichment in our dataset (Figure 1G).

The list of G-protein coupled receptors used in our analysis was from IUPHAR which has a curated list of all GPCR (7TMs) excluding olfactory receptors (n = 411).[57]

GO term enrichment analysis was performed using GORilla,[61] the expressed transcriptome was used as a background for the analysis. The enriched terms were filtered manually for redundancy and data were visualized using R and ggplot2[62] to create dot plots (Table S1; Figure 2C).

A single nuclei RNA-seq dataset generated by Yoo et al.[24] determined specific markers for the transition between alpha tanycytes and tanycyte derived neurons using pseudo time analysis. This identified 6 distinct cell type clusters. Using the genes listed within each cluster an individual *Z* score was calculated across the genes by taking the counts per million for each gene and each individual in our dataset. Then individual *Z* score within each cluster was used to create the mean *Z* score and standard deviation for each experimental group. The data were plotted using Graphpad prism 8 (Figure 3D).

Transcription factor binding site analysis

We downloaded TFBS motifs from the JASPAR database (JASPAR2022_CORE_non-redundant)[46] and scanned the entire genome for individual matches of all motifs using the FIMO tool from the MEME Suite (ver 5.4.1).[63] The FIMO tool was run with default settings, except for the parameter ''—max-stored-scores'', which was set to 1000000. Only motifs in the CORE_vertebrates database were used for downstream analyses.

For each gene promoter in the Psun genome (-2000/+200 bp from TSS) significant TFBS motif matches from FIMO were counted. The numbers of identified motifs in each gene found in our Psun assembly are available on DataverseNO: https://doi.org/10.18710/1IHNDD .

For each TFBS motif, a 2x2 contingency table was constructed summarizing the number of promoters with ≥ 1 and no matches in the SPIP unique DEGs or LPIP DEGs and in all other genes. These contingency tables were then used to tests for enrichment of TFBS motifs in promoters in genes either the SPIP unique DEGs or LPIP DEGs using the fisher.test function in R. Correction for multiple testing was carried out using the p.adjust function in R with the false discovery rate method. The odds ratios were calculated for each motif; (number of genes with motif ''A'' in the gene set of interest divided by number of genes with non ''A'' motif in the gene set of interest) divided by (number of genes with motif ''A'' in background divided by number of genes with non ''A'' motif in the background) (Table S2).

IGV browser[64] was used to view the position of the significant RARE and TRE motif matrixes in the promoter region of *arrb1*, a simplified representation is in Figure 3G.

Immunohistochemistry

Vimentin staining for LCMD

The slides were oven dried at 45°C for 5 min, fixed for 10 min with ice-cold paraformaldehyde 4% in phosphate buffer (PB), and then rinsed 3 times 5 min with Tris buffered saline (TBS). Blocking was performed with non-fat milk powder for 1 h and primary antibody incubation occurred overnight at 4°C with mouse anti-vimentin antibody (1:1000, ThermoFisher MA5-11883) in TBS-tween 20 (TBS-T20) containing 1% donkey serum and 0.1% NaN_3. The slides were then rinsed 3 times 10 min in TBS-T20 and incubated for 1-h with biotinylated donkey anti-mouse secondary antibody (1:1000) in TBS-T20 containing 1% donkey serum. After 3 times 10-min rinses in TBS-T20 and an additional 10-min rinse in TBS, the slides were stained for 5-10 min with DAB 1:100 in TBS. The slides were finally rinsed twice 5 min with tap water and covered with Crystal Mount Aqueous Mounting Medium (Sigma-Aldrich C0612). After overnight air drying, the slides were washed twice for 5 min in toluene, mounted with Eukitt Mounting Medium and imaged with a x5 objective.

Coronal sections for cilia

For immunohistochemistry, transcardiac perfusion was performed with periodate-lysine-paraformaldehyde.[65] The brain was dissected out and embedded in polyethylene glycol (PEG).[66] 10 μm coronal sections were obtained using a rotary microtome (Leitz 1512). PEG sections were rehydrated in a water bath and mounted on glass slides (Superfrost ultra plus gold, fisher scientific) dried at 50°C for 15 min and stored at -80°C until staining. Sections were rehydrated in distilled water and then 95°C trisodium citrate pH 6.0 for 60 min for antigen retrieval. Slides were cooled at room temperature for 45-60 min in antigen retrieval solution. Sections were rinsed in tris buffered saline (TBS pH 7.4). Non-specific binding and hydrophobic interactions were blocked by 1 h incubation at room temperature in 0.5% cold water fish skin gelatine (Sigma-Aldrich G7041) and 0.5% bovine serum albumin (Sigma-Aldrich A2153) in TBS pH 7.4 containing 0.05% tween 20 (Sigma-Aldrich P9416). Incubation of primary antibodies followed, with mouse anti vimentin (1:1000, ThermoFisher MA5-11883) and rabbit anti γ-tubulin (1:1000, Sigma-Aldrich T5192) in blocking solution for 48-h at 4°C. Sections were washed in TBS-tween and then incubated with the secondary antibody mix (goat anti-mouse Alexa Fluor 647 Abcam ab150115, Donkey anti-rabbit Alexa Fluor 488 ab150073) for 2 h at room temperature, followed by repeated rinses with PBS pH 7.4 and 1 min of treatment with TrueBlack lipofuscin autofluorescence quencher (Biotium 23007). The quencher was washed off with PBS pH 7.4 followed by counterstain for 10 min with Hoechst 33342 solution (1 μg/mL, ThermoFisher 62249) in PBS pH 7.4. Slides were mounted in 90% glycerol in PBS pH7.4 containing 2.5% Dabco 33-LV reagent (Sigma-Aldrich 290734), cover-slipped and sealed with nail polish. Sections were imaged using a Zeiss LSM 780 confocal microscope. Regions were selected on basis of section morphology to correspond to bregma -2.3 to bregma -2.9 in golden hamster brain atlas.[67] An overview image was taken at x10 objective using the counterstain followed by a 27 slice (10.18 μm thickness total) z stack with x63 magnification objective at either 400-600 μm distance from the median eminence outer boarder, to correspond to the alpha tanycyte region, or at the area by the 3rd ventricle floor (Median eminence), corresponding to the beta tanycyte region (Figure S2A). The capture settings with x63 objective were; ExHoechst: 405 nm, EmHoechst: 410-483 nm, ExAF488: 488nm, EmAF488: 514-630 nm, ExAF647: 633 nm, EmAF647:638-755 nm.

Six LP- and six SP-gestated animals were included in the analysis. Zeiss zen software was used to create maximum intensity projections from the z stack. The images were exported into QuPath for analysis. The area around the ventricle wall was selected for analysis, an intensity threshold of 20 and a size threshold of 260nm (average size of a basal body) was used to identify and count basal bodies. The number of identified basal bodies was normalized by the length of the ventricle included in the analysis to give the number of basal bodies per millimeter (mm).

Third ventricle face whole mounts for cilia

Three LP- and Three SP- gestated animals PEG embedded brains were dewaxed overnight in PBS pH 7.4 at room temperature with gentle shaking. In brief, under a stereoscope the wall of the 3rd ventricle was dissected out in PBS pH 7.4 using a scalpel and tweezers. Making a sagittal cut with a scalpel, an approximate 500 μm section containing the 3rd ventricle wall was then separated from the remaining hemisphere and stored in 12-well plate in PBS pH 7.4.

Antigen retrieval was performed with a 95°C trisodium citrate bath pH 6.0 for 1 h and left to cool for 1 h to room temperature before permeabilization for 10 min using PBS pH7.4 containing 0.2% Triton X-100 (Sigma-Aldrich T8787) and 0.05% Tween 20. The sections were blocked as described above. Primary incubation in blocking solution was done with a mix of mouse anti α-tubulin (1:1000 Sigma-Aldrich T6793) and rabbit anti γ-tubulin (1:500, Sigma-Aldrich T5192) at 4°C with gentle shaking. The sections were washed four times 20 min with gentle shaking in PBS pH 7.4 containing 0.05% tween 20. To minimize staining α-tubulin inside the cell, secondary antibodies were incubated for 1 h with 1:500 Goat Anti-Mouse Brilliant Violet 421 (Jackson Immuno research 115-675-166) and 1:500 goat anti rabbit Alexa flour 647 (Abcam ab150115) in blocking solution then washed again four time 20 min in PBS 0.05% tween 20 with gentle shaking. Sections were counterstained for 10 min with 1 μM SYTOX green (Thermo Fisher S7020) followed by three times 10 min washes before storage in PBS pH7.4 until imaging.

The sections were imaged on a Zeiss LSM800 confocal microscope by placing the sections ventricle side down in a Mattek dish (Mattek P35G-1.5-14-C) and fixed in place with a small circle of Twinsil (Picodent #13001000). A drop of antifade mounting medium and a coverslip were added to prevent section from drying out during imaging. Using the counterstain, an overview image was created by tiling 3-4 images containing 3-4 z-positions. Regions for high magnification were selected between 400 and 600 μm distance dorsally from the Median Eminence outer border (alpha tanycyte region) and 0-400 μm anteriorly from the most dorsal point of the pars tuberalis (beta tanycyte region) (Figure S2B). A 40 × 40 μm area was imaged with a x63 objective by taking a z stack consisting of 55-60 slices, starting above the ciliated wall, and ending 8-10 μm into the tissue. Capture settings with x63 objective used

was ExBV421: 465 nm, EmBV421: 400-530 nm, ExSYTOXG: 504nm, EmSYTOXG: 517-565nm, ExAF647: 633 nm, EmAF647:450-700 nm.

The images were visualized using Zeiss Zen software and maximum intensity projections were created. The same display settings were applied to all images for each color channel. Representative images from an LP and SP-gestated animal from the alpha tanycyte region are shown (Figure 2F).

PCNA & Ki67 staining

The slides were taken from 4°C and rinsed in distilled water. Antigen reactivation was performed by submerging the slides in Citrate buffer (0.1M sodium monophosphate, 0.1M citric acid, pH 6) and autoclaving them. After cooling for 30 min at room temperature, slides were washed twice for 5 min in Tris buffer 0.1M (TB) and once in TB with 0.3% Triton X (TBX). Endogenous peroxidase expression was blocked with TB containing 0.3% H2O2 for 30 min (1.5% for 15 min for Ki67). After rinsing in TB and TBX, saturation of non-specific binding sites was performed by incubation in 5% normal horse serum (NHS; Vector Labs., Burlingame, CA, USA) in TBX for 1h. Incubation with primary antibodies took place overnight at room temperature. All antibodies were diluted in TBX, 2% NHS. The following primary antibodies were used: rabbit anti-Ki67 at 1:1000 (ab15580, Abcam) and monoclonal anti-PCNA made in mouse: PC10 at 1:10000 (ab29, Abcam). For negative controls, the slides were incubated in the same buffer in the absence of primary antibody. The next morning, slides were washed in TB and TBX. Then, slides were incubated for 1h using the secondary biotinylated rabbit universal antibody of the Vectastain Universal Elite ABC kit (Vector Labs.) at 1:400 in TBX, 2% NHS. Excess antibody was washed away with TB and TBX followed by 1 h incubation with the avidin-peroxidase complex (ABC) from the Universal Elite ABC kit (Vector Labs.) at 1:20 in TBX. The excess of ABC complex was washed away with TB and peroxidase activity was detected using niquel-3,3-diaminobenzidine (Ni-DAB) (0.5 mg/ml DAB (Sigma-Aldrich), 0.1M sodium acetate, 0.04% ammonium chloride, 2.5% nickel sulphate). After detection, slides were dehydrated in serial alcohols in distilled H2O (70%, 95%, 100%, and 100%), cleared in Histoclear (National diagnostics) and permanently mounted using Eukitt (Sigma-Aldrich).

Photographs were taken using a Zeiss Axioskop microscope fitted with a Zeiss Axiocam Icc1 camera (Carl Zeiss). Positive PCNA and Ki67 cell numbers were evaluated in ependymal layer up to 600μm from the base of the ventricle wall using Qupath. ImageJ was used to invert the PCNA images to aid visualization (Figure 3C).

QUANTIFICATION AND STATISTICAL ANALYSIS

The differential gene expression analysis was done using Rstudio, and the package EdgeR.[56] Three samples failed library construction and one sample from the SPIP group was excluded from the RNA-seq analysis because it had low read counts therefore it was an outlier in the PCA analysis. The final RNA-seq analysis the numbers of animals for each group analysis were LP = 5, SP = 5, SPIP = 4 and LPIP = 6. Significance in this study was defined as a false discovery rate below 0.001.

Graphpad prism was used to analyze body weight and testis weight (6 per group). Details of the statistical test and significances are given in the figure legend. One-way ANOVA and a Tukey test for multiple comparisons was used. Significance for these data were defined as an adjusted p value less than 0.05.

Graphpad prism was also used to test for statistical differences in the cilia (6 per group), as there were only two groups in this analysis an unpaired t-test was used. Significance for these data were defined as an p value less than 0.05.

Graphpad prism was used for the statistics to assess the age and photoperiod effects on cell division markers (ki67 and PCNA), details are given in the legends. In all cases either a one-way or two-way ANOVA and a Tukey test for multiple comparisons was used. Significance for these data were defined as an adjusted p value less than 0.05.

Paper III

Markussen et al. BMC Veterinary Research (2021) 17:14
https://doi.org/10.1186/s12917-020-02723-7

BMC Veterinary Research

RESEARCH ARTICLE Open Access

A refined method to monitor arousal from hibernation in the European hamster

Fredrik A. F. Markussen[1†], Vebjørn J. Melum[1†], Béatrice Bothorel[2], David G. Hazlerigg[1], Valérie Simonneaux[2] and Shona H. Wood[1*]

Abstract

Background: Hibernation is a physiological and behavioural adaptation that permits survival during periods of reduced food availability and extreme environmental temperatures. This is achieved through cycles of metabolic depression and reduced body temperature (torpor) and rewarming (arousal). Rewarming from torpor is achieved through the activation of brown adipose tissue (BAT) associated with a rapid increase in ventilation frequency. Here, we studied the rate of rewarming in the European hamster (*Cricetus cricetus*) by measuring both BAT temperature, core body temperature and ventilation frequency.

Results: Temperature was monitored in parallel in the BAT (IPTT tags) and peritoneal cavity (iButtons) during hibernation torpor-arousal cycling. We found that increases in brown fat temperature preceded core body temperature rises by approximately 48 min, with a maximum re-warming rate of 20.9℃*h^{-1}. Re-warming was accompanied by a significant increase in ventilation frequency. The rate of rewarming was slowed by the presence of a spontaneous thoracic mass in one of our animals. Core body temperature re-warming was reduced by 6.2℃*h^{-1} and BAT rewarming by 12℃*h^{-1}. Ventilation frequency was increased by 77% during re-warming in the affected animal compared to a healthy animal. Inspection of the position and size of the mass indicated it was obstructing the lungs and heart.

Conclusions: We have used a minimally invasive method to monitor BAT temperature during arousal from hibernation illustrating BAT re-warming significantly precedes core body temperature re-warming, informing future study design on arousal from hibernation. We also showed compromised re-warming from hibernation in an animal with a mass obstructing the lungs and heart, likely leading to inefficient ventilation and circulation.

Keywords: Brown fat, Hibernation, Torpor, Arousal

Background

Hibernation is a physiological and behavioural adaptation that permits survival during periods of reduced food availability and extreme environmental temperatures. This is achieved through cycles of metabolic depression characterised by reduced body temperature (torpor) and rewarming (arousal). Entrance into torpor precisely is controlled by decreases in heart rate, ventilation frequency and oxygen consumption [1, 2]. Arousal occurs in a coordinated manner with increased ventilation frequency and oxygen consumption subsequently followed by heart rate, blood pressure and core body temperature rise [1]. Rewarming from torpor is achieved through the activation of subcutaneous brown fat reserves on top of the scapulae (classical BAT) and within the intra-scapular region (intra-scapular BAT) [3]. The primary function of brown fat is heat generation through non shivering thermogenesis [4], which has a high energy (oxygen) demand [5, 6]. During arousal from torpor

* Correspondence: shona.wood@uit.no
†Fredrik A. F. Markussen and Vebjørn J. Melum these authors contributed equally.
[1]Arctic Chronobiology and Physiology Research Group, Department of Arctic and Marine Biology, UiT – The Arctic University of Norway, NO-9037 Tromsø, Norway
Full list of author information is available at the end of the article

temperature increases in brown fat correlate with increased oxygen consumption (respiration rate) in the brown bat (*Eptesicus fuscus*) and the golden-mantled ground squirrel (*Callospermophilus lateralis*), and precede rectal or muscle temperature increases [7–10].

Activation of brown fat is thought to originate in the thermo-sensing regions in the hypothalamus coupled to a sympathetic nervous pathway, which activates beta adrenergic receptors and in turn the brown fat mitochondria [11]. The thermogenic capacity of brown fat comes from the use of proton leak (uncoupling) in mitochrondria as opposed to the coupled oxidative phosphorylation pathway which produces ATP [12]. The uncoupled pathway depends on the BAT-specific expression of the uncoupling protein, UCP1 transporter in the mitochondrial membrane. Initiation of this process requires good oxygen/energy supply to the BAT, and a marked increase in ventilation is an early event in the rewarming process [13]. The heat generated from BAT rewarms the anterior of the animal first, and then increases in heart rate and circulation are required to warm the rest of the animal and raise core body temperature (Tb). Subsequently, shivering thermogenesis is initiated to help the animal to reach normal body temperature (euthermy) quickly [5, 6, 14]. In Syrian hamsters (*Mesocricetus auratus*) the initiation of shivering thermogenesis can only occur once the body temperature is above 16℃ [5] and in the marmot (*Marmota marmota*) shivering is only observed when the subcutaneous BAT temperature reaches 16℃ [4]. These data highlight the importance of non-shivering thermogenesis by BAT in the initial stages of the re-warming process.

Tb monitoring by iButtons implanted into the intraperitoneal cavity is the standard method used to monitor torpor arousal cycling during hibernation [15–18], and while it is known that BAT activation is the first stage in the re-warming process it is rarely monitored and good characterisation of the relationship between BAT and core body temperature during hibernation is lacking. Here, we use a minimally invasive method to monitor both BAT temperature (T_{BAT}) and Tb in a well-established hibernation model, the European hamster (*Cricetus cricetus*) [19–21]. We demonstrate that increases in T_{BAT} precede increases in Tb and that the ventilation frequency correlates with the rate of T_{BAT} re-warming. Furthermore, one animal with a thoracic mass showed impaired ventilation which led to a marked slowing of the re-warming process.

Results

Re-warming in brown fat compared to the core body

We placed Implantable Programmable Temperature Transponder (IPTT) tags subcutaneously to measure the T_{BAT}. In the same animals we surgically implanted iButtons into the intraperitoneal cavity to monitor Tb. To initiate the preparation for hibernation we transferred animals from long photoperiod (14L:10D, 14 h of light per 24 h) and 22℃ (LP22), to short photoperiod (10L:14D, 10 h of light per 24 h) and 22℃ (SP22). After 8 weeks, we reduced the room temperature to 10℃ (SP10, Fig. 1a). All animals showed a hibernation phenotype within 4 weeks of transfer to SP10, which was preceded by "test drops" in Tb of approximately 10 to 15℃ below euthermy before initiating the multi-day torpor-arousal cycling characteristic of the hibernation season (Fig. 1b). Once hibernating, the European hamster drops its Tb to near ambient room temperature for multiple days (approximately 25℃ below euthermy) and arouses at intervals returning to euthermy (Fig. 1b).

We confirmed the initiation of the hibernation season and torpor-arousal cycling for at least 2 weeks before we started monitoring T_{BAT} during the periodic arousals. These data were time matched with Tb from the iButtons. Arousal events were recorded from five individuals (3 females, 2 males). We observed that both T_{BAT} and Tb show similar sigmoidal curve trajectories until euthermy is reached (Fig. 2a, non-linear asymmetric sigmoidal model, T_{BAT}: $r^2 = 0.9778$; Tb: $r^2 = 0.9878$). We show that BAT re-warming precedes subsequent core body re-warming by 48.6 min (CI: 45.4–51.7 min) (Fig. 2a). The mean ventilation frequency (VF) for the 5 individuals was calculated for each quartile of re-warming showing a clear linear increase in VF during re-warming which correlated with T_{BAT} (Fig. 2a, one-way ANOVA $p < 0.0001$, $R^2 = 0.86$). Using visual assessment, the onset of shivering in muscles adjacent to the BAT during arousal was noted, an average BAT temperature of 15℃ (CI: 14.2–16.8℃) was recorded at the onset of shivering (Fig. 2b).

We calculated the maximum re-warming rate (RWR_{MAX}) by analysing the linear phase of the sigmoidal curve and fitting a best fit regression line (Fig. 2c). We found that RWR_{MAX} was similar for BAT (RWR_{MAX} = 20.9℃*h^{-1}; 95% confidence interval (CI): 20.3℃ to 21.5℃) and core body (RWR_{MAX} = 21.0℃*h^{-1}; CI: 15.4℃ – 26.5℃) (Fig. 2c), however Tb RWR_{MAX} showed more individual variance. We then calculated the rate of change in re-warming (acceleration), or how fast RWR_{MAX} is achieved, by using the derivatives of the sigmoidal curve in the exponential and asymptotic phases (Fig. 2c). We found the initiation of re-warming (exponential phase) is delayed by 66 min in the core body compared to the BAT. However, the time to reach RWR_{MAX} is less in the core body (59 min) compared to the BAT (83 min) (Fig. 3c).

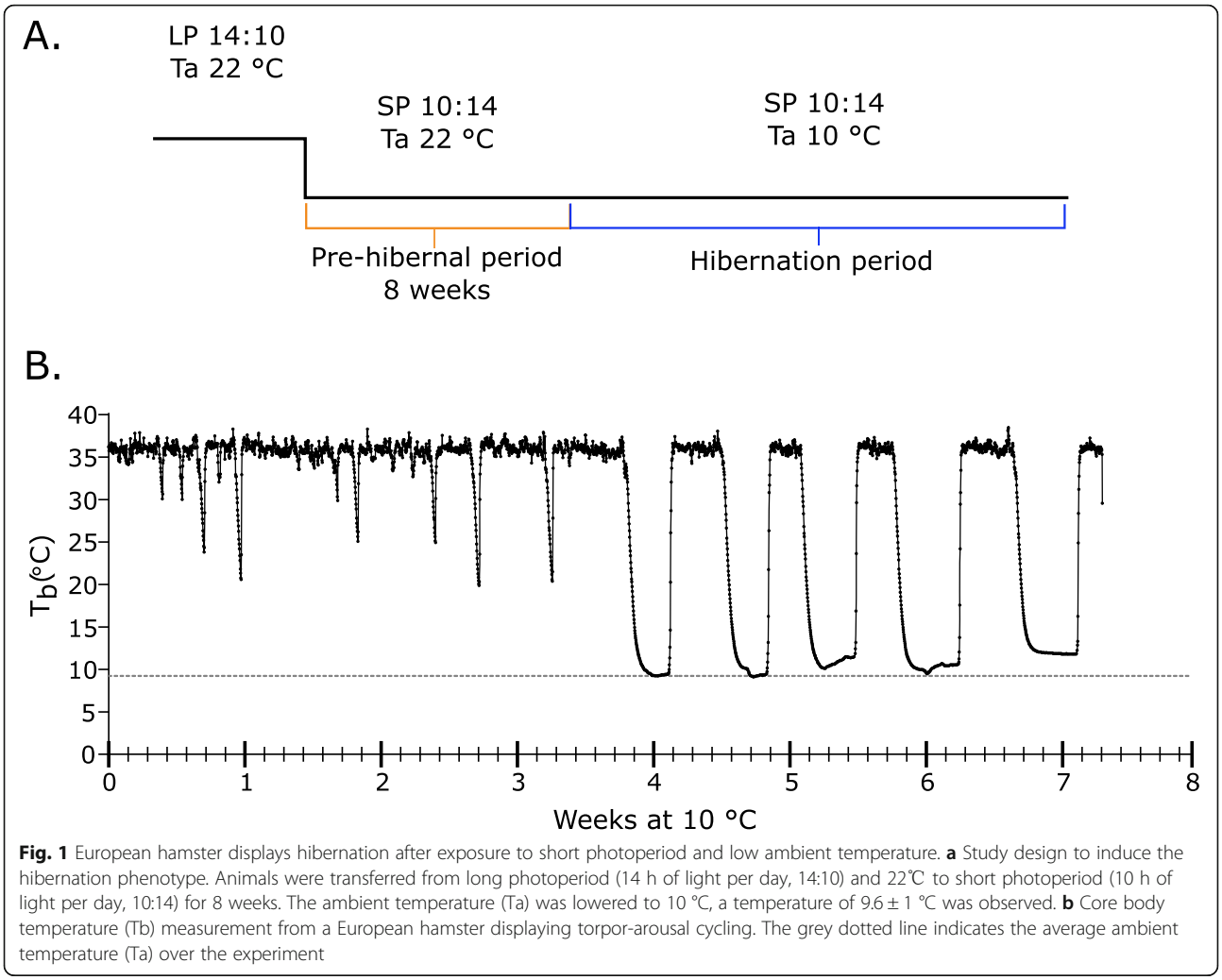

Fig. 1 European hamster displays hibernation after exposure to short photoperiod and low ambient temperature. **a** Study design to induce the hibernation phenotype. Animals were transferred from long photoperiod (14 h of light per day, 14:10) and 22℃ to short photoperiod (10 h of light per day, 10:14) for 8 weeks. The ambient temperature (Ta) was lowered to 10 °C, a temperature of 9.6 ± 1 °C was observed. **b** Core body temperature (Tb) measurement from a European hamster displaying torpor-arousal cycling. The grey dotted line indicates the average ambient temperature (Ta) over the experiment

Brown fat re-warming is compromised by the presence of a spontaneous thoracic mass

We identified one individual in our study with a spontaneous thoracic mass (Fig. 3a). When comparing the amount of time spent torpid or aroused the affected animal spent 63.5% aroused and 14.5% torpid, compared to an average of 25.9% aroused and 54.6% torpid for the healthy animals (Fig. 3b). The RWR_{max} of brown fat was reduced by 12℃*h^{-1} relative to a representative healthy animal (Fig. 3c). The RWR_{max} of the core body was less compromised showing a reduction of 6.2℃*h^{-1}. Ventilation frequency increases still correlated with T_{BAT} (Healthy: pearson $r = 0.899$, p-value = 0.002, affected: pearson $r = 0.873$, p-value = 0.002) but the affected animal showed a 77% higher maximum ventilation frequency compared to a healthy animal (Fig. 3c). BAT re-warming precedes core body re-warming by 53.9 min in the affected animal, this is outside the confidence intervals for the healthy animals, suggesting that the efficiency of BAT re-warming of the core is compromised.

Discussion

Our study has used a minimally invasive method to measure BAT temperature during hibernation. We show that there is a significant correlation between T_{BAT} and Tb, with T_{BAT} increases preceding that of Tb. Compared to intraperitoneal implantation of iButtons the IPTT tags offer a minimally invasive method to monitor temperature. Furthermore there is a significant advantage to monitoring BAT temperature in hibernation studies instead of core body temperature because the earliest arousal events can be detected almost immediately.

The increases in T_{BAT} and Tb are both correlated with increased ventilation frequency. Hyperventilation has been previously observed in the thirteen-lined ground squirrel but BAT temperature was not studied [13]. Our Tb RWR_{max} are similar to previous observations in rodents and European hamsters [22] but no data on BAT temperature is available.

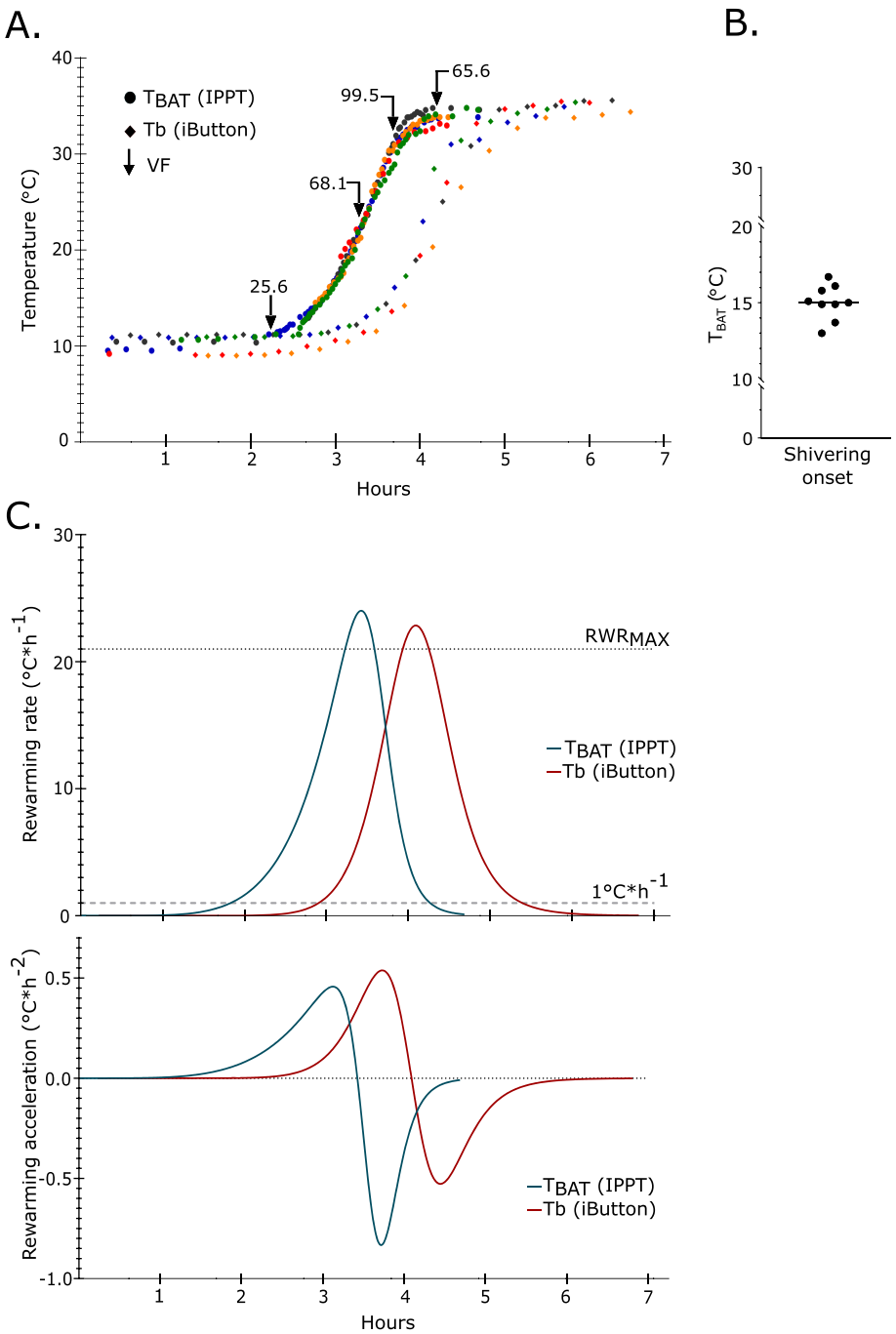

Fig. 2 Brown adipose tissue re-warming precedes core body temperature increases. **a** Core body temperature (Tb – iButton, diamond symbol) and BAT temperature recordings (T_{BAT} - IPTT tag, circle symbol) from 5 individuals during an arousal from torpor (each individual represented by a different colour). The mean ventilation frequency (VF) at each quartile of arousal, as defined by a non-linear curve fit for all individuals, is indicated by black arrows. **b** BAT temperature recording corresponding to onset of BAT adjacent skeletal muscle shivering. Observations and recordings were done in 9 separate arousal events in 5 different animals. **c** Five arousal events synchronised in time at 23.5 °C showing the modelled 1st and 2nd derivatives. First derivate graph describes rewarming rate (RWR) and second derivate graph the rewarming acceleration. Mean maximum rewarming rate (RWRmax, best fit linear regression) is similar for both Tb and TBAT at 21.0 C∗h − 1 (CI: 15.4–26.5 °C∗h − 1) and 20.9 °C∗h − 1 (CI: 20.3–21.4 °C∗h − 1), respectively

Re-warming efficiency of the BAT in the affected animal was only 38% of that in the healthy animal, whereas the rewarming efficiency of the core body was 67% of that in the healthy animal. We also observed a greatly increased ventilation frequency compared to a healthy animal. We suggest that the size and position of the

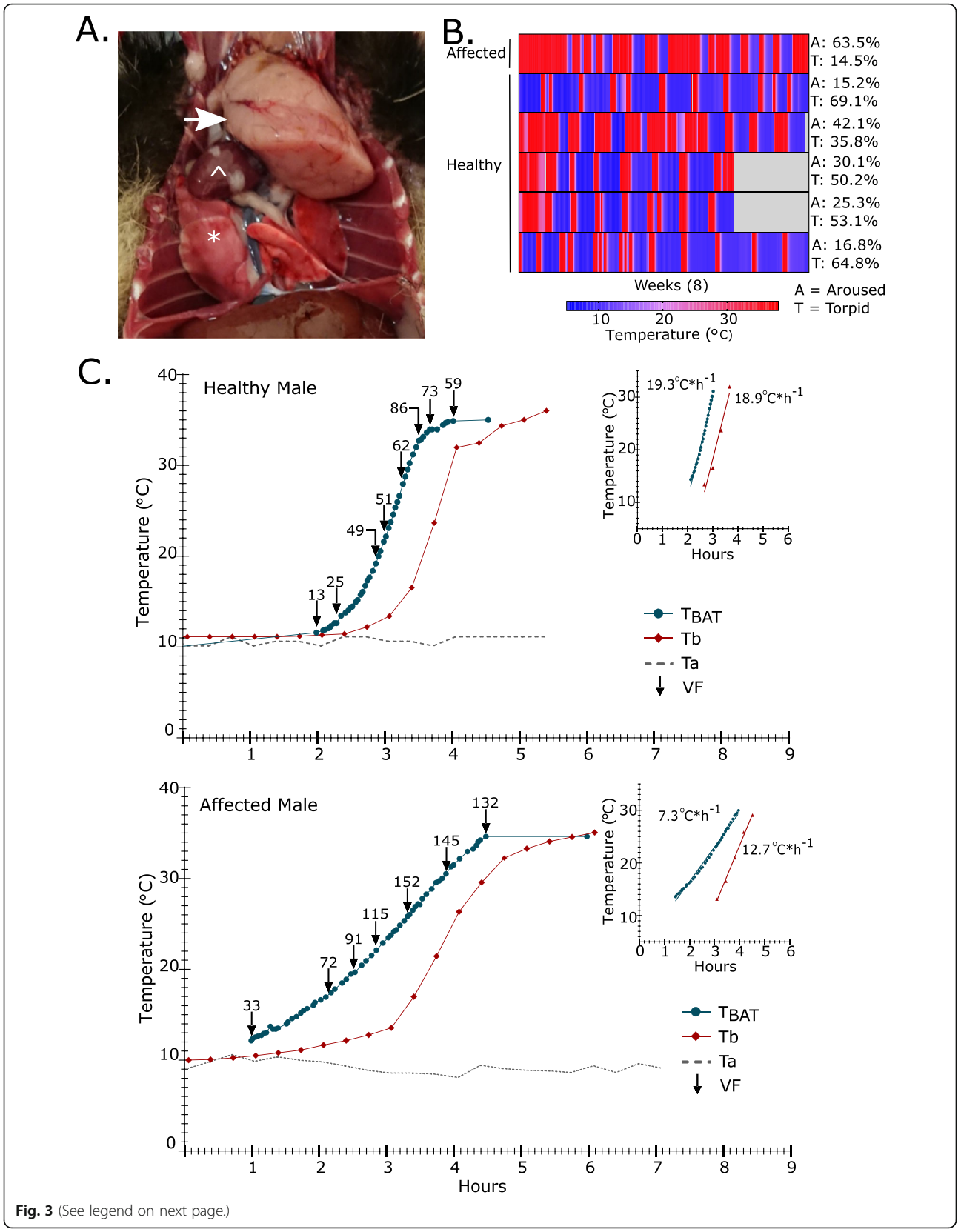

Fig. 3 (See legend on next page.)

(See figure on previous page.)
Fig. 3 Rewarming from torpor is compromised in an animal with a thoracic mass. **a** Post-mortem image of exposed thoracic cavity of a European hamster with a thoracic mass (indicated by the white arrow). For reference, white * is placed on lungs and ^ on heart. **b** Heat-map of core body temperature recorded by iButtons over the course of the experiment. Each line is an individual animal, the first animal has the thoracic mass. The percentage time spent above 35.5℃ (Euthermic – aroused) and below 12℃ (Torpid) is indicated, the remainder is time spent between 35 to 12 ℃ (entering or arousing from torpor) for each individual. Grey indicates no data was recorded in this period. **c** Core body temperature (Tb), BAT temperature (T_{BAT}) and ventilation frequency (VF) changes during arousal from torpor in a healthy male and an affected male with a thoracic mass. Grey dotted line shows room temperature (Ta). Inset graph shows the linear portion of the arousal that was used to calculate maximum re-warming rate (RWR_{max}) in ℃ per hour

thoracic mass obstructed the lungs, reducing ventilation volume, thereby compromising the animal's ability to deliver the necessary oxygen to support the activity of BAT. This probably resulted in increased ventilation frequency in an attempt to meet tissue demands. It has been observed that the early arousal events show a reliance on increased ventilation frequency and that increases in heart rate occur later as peripheral circulation increases [13]. The generally lower re-warming efficiency in both BAT and core body might be interpreted as evidence for compromised cardiac function leading to reduced circulation efficiency. In support of a decreased rate of re-warming of the BAT and core body due to decreased circulation we see re-warming rates in the affected animal are comparable to that of the much larger Marmot (5000 g compared to 500 g) [22].

The discrepancy between BAT re-warming efficiency and core body re-warming is intriguing, and possibly relates to complicated relationship and order of events in arousal which start with increased ventilation to increase oxygen availability, followed by vasodilation, and increased heart rate, to re-perfuse the circulation and rewarm the whole animal. Low oxygen availability increases vasodilation [23] therefore in the affected animal lower oxygen availability may have increased vasodilation leading to a compensated re-warming efficiency of the core body. Vasodilation would also benefit the BAT by supplying more oxygen in the blood. In support of this the affected animal in the initial stages of BAT rewarming from 10 to 15℃ appears to show a gentler slope compared to 20 to 30℃ (Fig. 3c), indicating a lower efficiency in the early arousal stage which would not benefit from vasodilation, this distinction is not seen in the healthy animals. Another explanation for the discrepancy between BAT and core body re-warming efficiency may be the additional contribution of shivering thermogenesis to core body temperature increases.

We propose that the thoracic mass observed in this study is a thymus tumour, and whilst, thymus tumours are rare they are reported in domestic, laboratory and wild contexts [24]. The thymus is a lymphoid organ involved in T-cell maturation, it is located in front of the heart and found in all vertebrates (reviewed in: [25]). However, without histology we cannot ascertain whether the observed thoracic mass is a neoplasia, granuloma or an abscess, nevertheless thymus tumours have been previously histologically characterised in this laboratory colony of European hamsters, the size, position and incidence we observe closely matches previous observations [26]. This previous characterisation also noted a close match human thymic epithelial tumours [26]. Human thymus tumour cases often present with tumours that obstruct the heart and lungs, similar to our observations. Also in humans, an association of thymus tumour with hypothermia/defective re-warming has been reported twice [27, 28]. Impressively in one of the cases the patient experienced a body temperature between 32.8℃ to 35℃ (Ambient room temperature: 22℃) [27]. However, the cause of hypothermia in these cases is unknown.

Conclusions

In conclusion we have used temperature logging in BAT and intraperitoneal cavity to study progression of arousal in hibernating hamsters. We also showed compromised re-warming from hibernation in an animal with a mass obstructing the lungs and heart, likely leading to inefficient ventilation and circulation.

Methods

Animals and ethics statement

European hamsters were bred from stock animals at the Chronobiotron, an animal facility dedicated to the study of biological rhythms. Animals were housed in an environment controlled room in separate cages according to legislations provided in European Commission directive 2010/63/EU. Specifically, animals were housed individually due to aggressive behavior in static type 3H Makrolon® cages (Zoonlab, Castrop-Rauxel, Germany). The bedding material was SAFE® select poplar wood granulate. Environmental enrichment was provided by cardboard nesting material and gnawing sticks. Daily visual checks are made to monitor individual animal health throughout the experiment. The general health of the colony is monitored twice a year, according to the FELASA recommendations for health monitoring of hamsters [29]. PCR tests on biological samples taken from animals in the colony are performed to indicate the presence of the following pathogens: *helicobacter hepaticus,*

pasteurella pneumotropica, corynebacterium kutscheri, demodex sp. No clinical signs that could be attributed to these pathogens has been observed in the colony of European Hamsters bred at the Chronobiotron, Strasbourg, France.

Animals were provided with *ad libitum* access to food (Safe®105 diet, Safe, Augy, France) and water throughout the study period. The animals were kept under a long photoperiod (14L:10D) and at 22℃ (LP22) until the start of the experiment. All animals were 1.5 years old at the start of the experiment. To initiate the preparation for hibernation (pre-hibernal period) the animals were transferred to a short photoperiod (10L:14D) at 22℃ (SP22). After 8 weeks, the temperature was lowered to 10℃ (SP10), all animals exhibited torpor-arousal cycling, and were kept in this condition to the end of the experiment (10 weeks, Fig. 1a). 48 animals (22 male, 26 female) underwent hibernation. Post hoc analysis of temperature data from six hamsters (3 male and 3 female) are included in this study, the remaining hamsters are part of another study. This is a longitudinal study design monitoring individual animals over 8 weeks during torpor arousal cycling. All hamsters were euthanized at the end of the study by a combination of isoflourane, Zoletil/Xlyazine and decapitation. The experimental procedure was validated by a local ethical committee and further validated by the Ministry of Higher Education, Research and Innovation (APAFIS#21424-2019070219421923 v3).

Calibration of IPTT tags

The accuracy of each IPTT tag (BMDS IPTT-300®) was verified from manufacturer to be ± 1℃ of actual temperature in the range between 21 and 30℃. During torpor-arousal the tags would measure between 10–38℃ therefore to ensure accuracy between the iButtons and IPTT tags we created an individual calibration curve for each IPTT tag allowing for *post hoc* correction at a 0.1℃ resolution. A similar method was used by Wacker et al. [30]. Each tag was calibrated using a water bath containing two iButtons (thermochron DS1922L, Maxim integrated) set to 16-bit resolution (0.0625℃) and sampling rate of 2 s, the IPTT tag was scanned every 2–3 s. The water bath was then placed on a heating plate with a magnetic stirrer and heated, the temperature range recorded was 5℃ to 39℃. The resulting data was plotted in Graphpad Prism v8.0 and a regression analysis was done to allow for calibration of the IPTT tag recordings.

iButton and IPTT tag surgery

Surgeries were performed on each animal to implant iButtons and IPTT tags. Each animal was anesthetized by 3% isoflurane, surgery was performed under 3% isoflurane and 95% oxygen. The IPTT-tag was implanted subcutaneously into the classical brown adipose tissue (BAT) depot, using a standard IPTT-tag injector (supplied by the manufacturer). Post-mortem verification ensured the tag was in contact with the BAT. The iButton was implanted in the abdominal cavity with the use of laparotomy. At the site of laparotomy a subcutaneous injection of lidocaine mixture (lurocaine/bupivacaine, 2.5 mg/kg each) was administered. Subcutaneous inject of AINS meloxicam (2 mg/kg) was performed while the animal is anesthetised, and following surgery meloxicam (metacam® buvable 1.5 mg / ml, dose 1 mg / kg) was added to drinking water 3 days post-surgery. Drinking was monitored in the animals post-surgery establishing that they were drinking normally. The reason for administration in the drinking water is that the European hamster is an extremely aggressive therefore subcutaneous administration without anaesthesia was not an option. The animals were extensively monitored after surgery and allowed to recover for two weeks.

Behaviour and temperature monitoring

To keep track of individual torpor-arousal patterns, behavioural recordings were made twice per day; 1 to 2 h after lights on and 9–10 h after lights on. We defined torpid as a ventilation frequency (VF) < 10 per min, curled up position in hibernacula, immobile, unresponsive and an IPTT reading < 13.5℃. Signs of arousal were; increased IPTT tag temperature and increased ventilation frequency, at which point we began IPTT monitoring until the animal was fully awake, mobile and a euthermic body temperature was achieved, duration of monitoring varied but on average was approximately 5 h. From the beginning of arousal IPTT tag temperatures were taken every two minutes, and ventilation frequency was counted at regular intervals for 1 min. Shivering was defined as the first muscle contractions observed from the beginning of arousal monitoring. The contractions are usually observed in the scapular region, as soon as a contraction was observed we manually scanned the IPPT tag to note the BAT temperature. IButton core temperature recordings were collected post-mortem and time matched with the calibrated IPTT measurements. Graphpad Prism v8.0 was used for statistical analysis and data plotting.

Statistical analyses

Graphpad Prism v8.0 was used for statistical analysis and data plotting. Assymetrical sigmoid curve fitting was used to analysis the temperature data from both the BAT and core body. We defined a mean baseline temperature as 0% aroused (9.8℃) and euthermy as 100% aroused (37℃), allowing us to establish 23.5℃ as the 50% mark around which all arousal events could be synchronised and

therefore plotted together to fit a best fit regression line to the linear phase of the sigmoid curve determine mean maximum re-warming rate (RWR_{MAX}), and the acceleration by analysing the derivatives of the exponential and asymptotic phases of the sigmoid curve. The exponential phase and the asymptotic phase can be defined as $1 \leq y\ 0 \leq RWR_{MAX}$, i.e. the period of time where rewarming rate is faster or equal to 1 °C ∗h − 1 but slower or equal to RWR_{MAX}. This can be used as a measure of how fast RWR_{MAX} is achieved after initiation of arousal. One way ANVOVA was used to determine significant increases in ventilation rate over the arousal event. Person correlation was used to determine the correlation between ventilation and T_{BAT}. Confidence intervals (CI) are given were appropriate.

Abbreviations

BAT: Brown fat; UCP1: Uncoupled protein 1; ATP: Adenosine triphosphate; T_{BAT}: Brown fat temperature; Tb: Core body temperature; IPTT: Implantable Programmable Temperature Transponder; VF: Ventilation frequency; RWR_{MAX}: Maximum re-warming rate

Acknowledgements

The authors thank all of the animal staff at the Chronobiotron facility, especially Dominique Ciocca and Nicolas Lethenet, for their expert care of their research animals and technical assistance.

Authors' contributions

FM - Experimental design, analysed the data, collected samples, prepared figures, and revised manuscript. VJM – Experimental design, analysed the data, collected samples, prepared manuscript. BB – performed surgeries, technical expertise, revised the manuscript. DGH - conceived and designed the experiments, supervised, and revised the manuscript. VS - conceived and designed the experiments, supervised, provided funding and revised the manuscript. SHW– conceived and designed the experiments, supervised, provided funding and prepared the manuscript. All authors read and approved the manuscript.

Funding

This work was supported by grants from the Tromsø forskningsstiftelse (TFS) starter grant TFS2016SW (awarded to SHW), the fonds Paul-Mandel pour les neurosciences, and the Norwegian research council Aurora travel grant (awarded to SHW & VS). The funding bodies took no part in the design of the study, collection, analysis, interpretation of data, or writing of the manuscript. Funds supported travel, experiments, and salary of SHW and VJM. The publication charges for this article have been funded by a grant from the publication fund of UiT: The Arctic University of Norway.

Availability of data and materials

The datasets used and/or analysed during the current study are available from the corresponding author on reasonable request.

Ethics approval and consent to participate

The experimental procedure was validated by a local ethical committee at the University of Strasbourg and further validated by the Ministry of Higher Education, Research and Innovation in France (APAFIS#21424-2019070219421923 v3).

Consent for publication

Not applicable.

Competing interests

No competing interests to declare.

Author details

[1]Arctic Chronobiology and Physiology Research Group, Department of Arctic and Marine Biology, UiT – The Arctic University of Norway, NO-9037 Tromsø, Norway. [2]Institute of Cellular and Integrative Neurosciences, CNRS UPR 3212, University of Strasbourg, Strasbourg, France.

Received: 23 April 2020 Accepted: 10 December 2020
Published online: 07 January 2021

References

1. Fishman AP, Lyman CP. Hibernation in Mammals. Circulation. 1961;24:434–45. doi:https://doi.org/10.1161/01.CIR.24.2.434.
2. Snapp BD, Heller HC. Suppression of Metabolism during Hibernation in Ground Squirrels (Citellus lateralis). Physiol Zool. 1981;54:297–307. doi:https://doi.org/10.1086/physzool.54.3.30159944.
3. Zhang F, Hao G, Shao M, Nham K, An Y, Wang Q, et al. An Adipose Tissue Atlas: An Image-Guided Identification of Human-like BAT and Beige Depots in Rodents. Cell Metab. 2018;27:252–62.e3. doi:https://doi.org/10.1016/j.cmet.2017.12.004.
4. Smith RE, Hock RJ. Brown Fat: Thermogenic Effector of Arousal in Hibernators. Science. 1963;140:199–200. doi:https://doi.org/10.1126/science.140.3563.199.
5. Cannon B, Nedergaard J. Brown Adipose Tissue: Function and Physiological Significance. Physiol Rev. 2004;84:277–359. doi:https://doi.org/10.1152/physrev.00015.2003.
6. Nedergaard J, Cannon B, Lindberg O. Microcalorimetry of isolated mammalian cells. Nature. 1977;267:518–20. doi:https://doi.org/10.1038/267518a0.
7. Hayward JS, Ball EG. Quantitative aspects of brown adipose tissue thermogenesis during arousal from hibernation. Biol Bull. 1966;131:94–103. doi:https://doi.org/10.2307/1539650.
8. Horwitz B, Smith R, Pengelley E. Estimated heat contribution of brown fat in arousing ground squirrels (Citellus lateralis). Am J Physiol Content. 1968;214:115–21. doi:https://doi.org/10.1152/ajplegacy.1968.214.1.115.
9. Smalley RL, Dryer RL. Brown Fat: Thermogenic Effect during Arousal from Hibernation in the Bat. Science (80-). 1963;140:1333–4. doi:https://doi.org/10.1126/science.140.3573.1333.
10. Rauch JC. Sequential changes in regional distribution of blood in Eptesicus fuscus (big brown bat) daring arousal from hibernation. Can J Zool. 1973;51:973–81. doi:https://doi.org/10.1139/z73-141.
11. Morrison SF, Madden CJ, Tupone D. Central Neural Regulation of Brown Adipose Tissue Thermogenesis and Energy Expenditure. Cell Metab. 2014;19:741–56. doi:https://doi.org/10.1016/j.cmet.2014.02.007.
12. Staples JF. Metabolic suppression in mammalian hibernation: the role of mitochondria. J Exp Biol. 2014;217:2032–6. doi:https://doi.org/10.1242/jeb.092973.
13. Landau BR, Dawe AR. Respiration in the Hibernation of the 13-Lined Ground Squirrel. Am J Physiol Content. 1958;194:75–82. doi:https://doi.org/10.1152/ajplegacy.1958.194.1.75.
14. Hayward JS, Lyman CP. Mammalian hibernation III. 3rd. New York: Elsevier; 1967.
15. Sáenz de Miera C, Monecke S, Bartzen-Sprauer J, Laran-Chich M-P, Pévet P, Hazlerigg DG, et al. A Circannual Clock Drives Expression of Genes Central for Seasonal Reproduction. Curr Biol. 2014;24:1500–6. https://doi.org/10.1016/j.cub.2014.05.024.
16. Revel FG, Herwig A, Garidou M-L, Dardente H, Menet JS, Masson-Pévet M, et al. The circadian clock stops ticking during deep hibernation in the European hamster. Proc Natl Acad Sci U S A. 2007;104:13816–20. doi:https://doi.org/10.1073/pnas.0704699104.
17. Chayama Y, Ando L, Tamura Y, Miura M, Yamaguchi Y. Decreases in body temperature and body mass constitute pre-hibernation remodelling in the Syrian golden hamster, a facultative mammalian hibernator. R Soc Open Sci. 2016;3:160002. doi:https://doi.org/10.1098/rsos.160002.
18. Williams CT, Barnes BM, Richter M, Buck CL. Hibernation and Circadian Rhythms of Body Temperature in Free-Living Arctic Ground Squirrels. Physiol Biochem Zool. 2012;85:397–404. doi:https://doi.org/10.1086/666509.
19. Fenyk-Melody J. The European Hamster. In: The Laboratory Rabbit, Guinea Pig, Hamster, and Other Rodents. Elsevier; 2012. p. 923–33. doi:https://doi.org/10.1016/B978-0-12-380920-9.00036-5.
20. Canguilhem B, Vaultier J-P, Pevet P, Coumaros G, Masson-Pevet M, Bentz I. Photoperiodic regulation of body mass, food intake, hibernation, and reproduction in intact and castrated male European hamsters,Cricetus cricetus. J Comp Physiol A. 1988;163:549–57. doi:https://doi.org/10.1007/BF00604908.

21. Gautier C, Bothorel B, Ciocca D, Valour D, Gaudeau A, Dupré C, et al. Gene expression profiling during hibernation in the European hamster. Sci Rep. 2018;8:13167. doi:https://doi.org/10.1038/s41598-018-31506-2.
22. Geiser F, Baudinette RV. The relationship between body mass and rate of rewarming from hibernation and daily torpor in mammals. J Exp Biol. 1990; 151:349–59. http://www.ncbi.nlm.nih.gov/pubmed/2380659.
23. Umbrello M, Dyson A, Feelisch M, Singer M. The Key Role of Nitric Oxide in Hypoxia: Hypoxic Vasodilation and Energy Supply–Demand Matching. Antioxid Redox Signal. 2013;19:1690–710. doi:https://doi.org/10.1089/ars.2012.4979.
24. Ghadially FN, Illman O. Naturally occurring thymomas in the European hamster. J Pathol Bacteriol. 1965;90:465–9. doi:https://doi.org/10.1002/path.1700900214.
25. Miller JFAP. The golden anniversary of the thymus. Nat Rev Immunol. 2011; 11:489–95. doi:https://doi.org/10.1038/nri2993.
26. Brandes K, Fend F, Monecke S, Teifke JP, Breuer W, Hermanns W. Comparative Morphologic and Immunohistochemical Investigation of Spontaneously Occurring Thymomas in a Colony of European Hamsters. Vet Pathol. 2004;41:346–52. doi:https://doi.org/10.1354/vp.41-4-346.
27. Johns RH, Reinhardt AK. Association between thymoma and persistent hypothermia: a case report. J Med Case Rep. 2009;3:73. doi:https://doi.org/10.1186/1752-1947-3-73.
28. Ho WKW, Wilson JD. Hypothermia, hyperhidrosis, myokymia and increased urinary excretion of catecholamines associated with a thymoma. Med J Aust. 1993;158:787–8. doi:https://doi.org/10.5694/j.1326-5377.1993.tb121967.x.
29. Mähler M, Berard M, Feinstein R, Gallagher A, Illgen-Wilcke B, Pritchett-Corning K, et al. FELASA recommendations for the health monitoring of mouse, rat, hamster, guinea pig and rabbit colonies in breeding and experimental units. Lab Anim. 2014;48:178–92. doi:https://doi.org/10.1177/0023677213516312.
30. Wacker CB, Daniella Rojas A, Geiser F. The use of small subcutaneous transponders for quantifying thermal biology and torpor in small mammals. J Therm Biol. 2012;37:250–4. doi:https://doi.org/10.1016/j.jtherbio.2011.11.007.

Publisher's Note

Paper IV

Altered fuel utilisation and sensory capacity in tanycytes throughout the hibernation season in the golden hamster

Vebjørn. J. Melum[1,2], Béatrice Bothorel[2], Marie-Azélie Moralia[2], Valérie Simonneaux[2], David G. Hazlerigg[1], Shona H. Wood[1]

1 Arctic Seasonal Timekeeping Initiative (ASTI), Arctic Chronobiology and Physiology research group, Department of Arctic and Marine Biology, UiT — The Arctic University of Norway, Tromsø

2 University of Strasbourg, Institute of Cellular and Integrative Neurosciences, Strasbourg, France

Abstract

Hibernation is a physiological and behavioural adaptation that permits survival during periods of reduced food availability and extreme environmental temperatures. This is achieved through episodes of metabolic depression and body cooling (torpor), and subsequent rewarming (arousal), cycling between which is presumed to stem from changes in hypothalamic metabolic control. Several recent lines of evidence implicate the hypothalamic tanycytes in this phenomenon.

To investigate tanycytic changes over the hibernation season, golden hamsters (*Mesocricetus auratus*), were transferred from long photoperiod 22°C to short photoperiod (SP) 8°C, sampling animals at physiologically defined points across the hibernation season for LASER capture microdissection and RNAseq of the tanycytic region.

Our analysis revealed a marked reduction in the expression of genes linked to ciliary assembly and GPCR-signalling during the hibernation season, as well as evidence for a shift towards increased glycolytic metabolism. These aspects were all reversed in refractory animals which spontaneously ceased to express torpor after extended exposure to SP 8°C. Tanycytes sampled mid-torpor show increased expression of immediate-early genes compared to the interbout euthermic state, while genes linked to RNA processing and translation show the reverse effect. The implications of these findings for the putative involvement of tanycytes in hibernation control mechanisms are discussed.

Keywords: Tanycyte, hibernation, torpor, seasonal, photoperiod, refractory, hamster

Introduction

Hibernation is a physiological and behavioural adaptation that permits survival during seasonal periods of energy shortage *via* a combination of pre-hibernal energy storage and hibernal metabolic depression (torpor). Ground squirrels, dormice and golden/European hamsters are examples of deep hibernators, all requiring a seasonal preparative phase to express the hibernation phenotype. Torpor during deep hibernation can reduce metabolic rate to 1% of the active state (reviewed in:(Ruf and Geiser 2015)). Animals undergoing deep hibernation repeatedly cycle between the hibernating (torpid) and the active (aroused) states for the entire hibernation season (T-A cycling). Seasonal changes in photoperiod are the primary cue used to initiate the suite of seasonal physiological adaptations to permit the expression of the hibernation phenotype. In a lab setting, it is possible to induce the physiological preparations for deep hibernation in hamsters by transferring them from long (LP) to short photoperiods (SP). Exposure to SP results in sexual quiescence, brown adipose tissue recruitment, moderate fattening and food caching over a period of 8 weeks (Lyman et al. 1982; Markussen et al. 2024). SP-adapted animals exposed to a reduced ambient temperature (8°C) express T-A cycling for several months (Lyman et al. 1982; Markussen et al. 2024). Finally, there is a spontaneous termination of T-A cycling concomitant with physiological preparations for the coming spring including reactivation of the gonads. This is referred to as the refractory state (Sáenz de Miera et al. 2014). Importantly, the refractory state occurs spontaneously, independent of changes in ambient temperature or photoperiod, signifying the existence of an internal timing mechanism, which would be an advantage to an animal isolated in a hibernaculum (Gwinner 1986; Hut et al. 2014; Sáenz de Miera et al. 2014). Hence, we may in summary identify 3 key regulatory aspects governing the hibernation season: (i) The regulation of the preparative events to allow entry into torpor and

subsequent rounds of T-A cycling, (ii) the regulation of the T-A cycle itself, and (iii) the termination of the hibernation season through the development of the refractory state.

Recent studies in mammals suggest that a specialised glial cell type present in the ependymal region surrounding the third ventricle in the mediobasal hypothalamus, the tanycyte, may play a key role in all the above aspects. Tanycytes sit in a privileged position in the mediobasal hypothalamus, at the interface between the blood brain barrier and the cerebrospinal fluid (CSF)-brain barrier. There, they are believed to act as metabolic sensors controling the access of nutrients and hormones to the brain (Parkash et al. 2015; Bolborea et al. 2020; Duquenne et al. 2021; Lhomme et al. 2021).

It has also become abundantly clear over the last two decades that tanycytes play a key role in driving seasonal photoperiodic changes in metabolic and reproductive physiology through modulation of hypothalamic thyroid hormone (TH) availability (reviewed in:(Dardente et al. 2014, 2019; Hazlerigg and Simonneaux 2015)). This process depends on photoperiod, with melatonin duration as the primary cue used to initiate the programme of seasonally adapted physiological change. Melatonin acts via MT1 receptors in the *pars tuberalis* (PT) to control photoperiod-dependent production of the glycoprotein hormone, thyrotropin (TSH), which in turn acts on TSH receptor (TSH-R)-expressing tanycytes (Hanon et al. 2008, 2010; Sáenz de Miera et al. 2013; Wood et al. 2020). In response to LP, TSH is produced and tanycytes convert inactive T4 to active T3 via a deiodinase enzyme (DIO2). On SP, when TSH synthesis is inhibited, increased DIO3 reduces T3 to T2. Infusion of TSH into the 3rd ventricle of an SP golden hamster (*Mesocricetus auratus*) increases Dio2 expression and restores its summer phenotype within 4-6 weeks (Klosen et al. 2013). Furthermore, experimental manipulation of TH status in Siberian hamsters (*Phodopus sungorus*) revealed that a hypothyroid environment is permissive for the expression of daily torpor and that T3 manipulation can reversibly halt torpor (Murphy et al. 2012; Bank et al. 2015, 2017). Studies manipulating T3 have not been

reported in a deep hibernator, but it is likely that the low TH environment within the hypothalamus and subsequent effects on the reproductive axis are permissive for hibernation (Gaston and Menaker 1967; Morin and Zucker 1978; Darrow et al. 1987).

Analyses of brain c-Fos expression pattern (a marker for cellular activation) demonstrate that in both 13-lined ground squirrels (*Ictidomys tridecemlineatus*) and in golden hamsters tanycytes show dramatic changes in activation over the T-A cycle (Bratincsák et al. 2007; Markussen et al. 2024). We have previously suggested that tanycytes, through their sensitivity to factors in the blood or cerebrospinal fluid, may mediate metabolic feedback-based initiation of the spontaneous arousal process and that the observed cellular activation during T-A cycling relates to this function (Markussen et al. 2024).

Finally, in several seasonal models, including hibernators (European hamster, Arctic ground squirrel and golden hamster), it has become clear that tanycytic changes in deiodinase expression occur spontaneously with the onset of the refractory state (Revel et al. 2006; Sáenz de Miera et al. 2013, 2014; Milesi et al. 2017; Chmura et al. 2022). This suggests that, as well as regulating photoperiod-dependent preparation of winter physiology, tanycytes may also drive innately timed spontaneous termination of the winter hibernating state (Hut et al. 2014; Sáenz de Miera et al. 2014).

Based upon these studies implicating tanycytes in the regulation of hibernation, the aim of this study was to characterise changes in tanycyte characteristics over the course of the hibernation season. For this purpose, we chose the golden hamster as a model, since all three aspects of hibernation regulation (photoperiodic induction, T-A cycling and the refractory state) are strongly expressed in this species. Here, we describe changing characteristics at the transcriptome level based on RNAseq analysis of LASER capture microdissected tissue samples taken before, during and after the hibernation phase as well as from torpid and aroused animals in the middle of the hibernation phase.

Materials and Methods

Animals

Three months old male golden hamsters (*Mesocricetus auratus*) were housed under long photoperiod (LP, 14 hours of light, 10 hours of dark) and an ambient temperature of 22°C. Animals had *ad libitum* access to food and water throughout the experiment and received nesting material and a wooden stick in their home cage. Three weeks prior to the experiment, under isoflurane anesthesia, an iButton (Maxim) was implanted in the abdominal cavity to record body temperature.

At the start of the experiment, six groups (n = 5 to 6 per group) were kept on LP at 22°C. LP groups were sampled immediately prior to the photoperiodic switch and 16 weeks into the experiment. Only data from the second LP group are shown because the two LP groups did not differ physiologically, and the second LP group are better age matched to the SP animals. The remaining animals were transferred to short photoperiod (SP, 10 hours of light/14 hours of dark) at an ambient temperature of 8°C to initiate hibernation. Animals were sampled 4 weeks after transfer to SP (pre-hibernation), after 8 to 12 weeks of SP prior to initiating T-A cycling (late pre-hibernation), or after three T-A cycles either when aroused in interbout euthermic (IBE) or in deep torpor (torpid). The average IBE duration in this experiment was approximately 24 hours, animals were sampled late in their interbout euthermia phase (23 hours). The average torpor duration in this experiment was approximately 26 hours and torpid animals were sampled at their mid-point of torpor. After approximately 20 weeks of SP exposure, animals spontaneously stopped hibernating and were sampled at least 2 weeks after the last torpor bout (refractory).

For sampling, animals were anesthetised with 4% isoflurane and decapitated. The study was conducted at the Chronobiotron (CNRS- UMS 3415) in accordance with the French National

Law implementing the European Communities Council Directive 2010/63/EU and the French Directive 2013-118. Animal procedures were reviewed by the local ethical committee (Comité Régional d'Éthique en Matière d'Expérimentation Animale de Strasbourg, CEEA 35) and the official authorization was given on December 2019 by la Direction Générale de la Recherche et de l'Innovation under the number APAFIS#22534-2019100822522580 v2.

Plasma samples

At euthanasia, blood was collected in tubes with heparin, inverted and wrapped in aluminium foil to protect it from light. The blood was allowed to clot for 20 minutes on ice before moved to a precooled centrifuge at 4 °C and centrifuged for 20 minutes for euthermic animals and 50 minutes for torpid animals at 2000 G. The time span was required to obtain a clear separation of plasma and blood cells in the torpid group. Plasma was collected in aliquots and stored at -80°C until further use.

Testosterone concentration in the plasma sample was measured with a competitive inhibition ELISA kit (MyBioSource, MBS2516160, USA) following manufacturer's instructions, and optical density was measured by a microplate reader (Promega Glomax explorer GM3510) at 450 nm.

Tissue collection

After decapitation, the brain was carefully removed from the skull by one operator, while another placed the animal on its belly and proceeded with tissue collection. The interscapular adipose tissue (iAT), containing both interscapular brown adipose tissue (iBAT) and interscapular subcutaneous white adipose tissue (iWAT) was removed. The iAT was weighed and visible iBAT was dissected, and the remaining iWAT was weighed. iBAT weight = iAT weight - iWAT. Testes were dissected out and weighed to confirm reproductive status.

LASER capture microdissection and RNA extraction

The brains were covered with pre-cooled OCT, snap frozen in chilled isopentane over dry ice and 95% ethanol and stored at -80°C. Each brain was cut, with a cryostat (-20ºC; CM3050 S, Leica Biosystems), in series of 20 µm thick sections covering the whole medio-basal hypothalamic region and mounted on 6-8 membrane slides (415190-9081-000, Carl Zeiss) of 8 sections each. Slides were stored at - 80ºC until further use.

Immediately before LCMD, the membrane slides were stained using cresyl violet as described previously (Melum et al. 2024). When ready, the slides were transferred to the laser micro dissector (PALM MicroBeam system, Zeiss) with the PALMRobo software (V4.8, Zeiss) and microdissection was completed within 45 minutes to minimize RNA degradation. LCMD was carried out at 10x, with the following settings: Cut energy = 42-49; Cut focus = 84; LPC Energy = 58; LPC focus = 84, to capture the tanycytes on the transfer film of the microdissection caps (415190-9211-000, Carl Zeiss). The dorso-ventral extent of the area was determined by two times the PT width for each animal to correct for size differences. The width of the LCMD-sample was strived to be two to three cell bodies. When done, the tube was closed and snap frozen on dry ice and stored at -80ºC. The RNA was extracted from the microdissected tissue using the Qiagen all prep DNA/RNA micro kit (80284) following the supplied instructions. The RNA integrity numbers were determined by TapeStation high sensitivity RNA analysis (5067-5579, 5067-5581, 5067-5580, Agilent) and all used samples had a RNA integrity numbers (RIN) between 7 to 9.

LCMD-RNAseq, mapping and gene counts

RNA-seq library construction was performed by BGI using their standard RNAseq protocol and Illumina high seq 4000. Quality control checks and barcode removal were performed according to the BGI protocol. Approximately 35-40 million reads per sample were generated. Mapping was performed using STARaligner and the standard settings (Dobin et al. 2013).

Reads were mapped to the golden hamster genome (BCM_Maur_2.0, ref.seq: GCF_017639785.1) and the annotation was provided by NCBI (GCF_017639785.1_BCM_Maur_2.0_genomic.gtf). The mapping rate was 88%. Feature counts was used to count the mapped reads to genes, using these parameters: featureCounts -p -t exon -g gene_id, on average 70% of alignments were assigned to an annotated feature.

FASTQ files and count files were deposited in GEO under this accession identifier: GSE281814

Gene expression analysis

We determined the median counts per million (CPM) across the whole experiment for each gene and applied a cut off of 10 raw counts, removing genes with a median of less than 0.5 CPM from the analysis. 16 315 genes remained representing our LCMD transcriptome, this dataset was used in all subsequent analysis. Three samples were excluded from the RNAseq analysis because they had low read counts and/or low RIN values and formed outliers in the initial data quality PCA analysis. In the final RNAseq analysis the numbers of animals for each group analysis were n= 6 in Prehib; Torpid; LP and n= 5 in Late Prehib; IBE; Refractory. Significance in this study was defined as a false discovery rate below 0.05.

Differential expression analysis of the RNAseq data were performed in R, with the Rstudio interface, using the EdgeR package (McCarthy et al. 2012; Chen et al. 2014; Zhou et al. 2014). In brief, a generalized linear model (GLM) analysis following the EdgeR manual was performed to determine which genes were differentially expressed between the groups. All genes with an FDR less than 0.05 were used in a PCA analysis using the package PCAtools (Blighe and Lun 2019). The same genes were plotted as a heatmap with five clusters (k-means) with the use of the package ComplexHeatmap (Gu et al. 2016). GOterm enrichment

199 analysis on each cluster was performed using ShinyGO (Ge et al. 2020) and EnrichGO (Wu et
200 al. 2021).

201 The package EnhancedVolcano (Blighe K, Rana S 2024) was used to make a volcano plot of
202 genes upregulated in the IBE and Torpid states, with an FDR cut off of 0.05 and no log2-fold
203 change cut off.

204 *Other statistical analysis*

205 Core body temperature data from iButtons (Maxim) were handled and analysed in R, with the
206 Rstudio interface utilizing the Tidyverse (Wickham et al. 2019) package. Graphpad prism was
207 used to analyse and plot the mean core body temperature data, iBAT, testes weight and plasma
208 testosterone concentration. One-way ANOVA and a Tukey test for multiple comparison was
209 used. P value less than 0.05 were considered significant.

210 All scripts used to generate the figures are available in our github repository:
211 https://github.com/ShonaWood/SeasonalTanycytes

Results

Physiological responses over the course of a short-photoperiod induced hibernation season

Our protocol for induction of a hibernation season in golden hamsters involves transferring animals from LP 22°C to SP 8°C (Figure 1A). In line with our published work, this initiates a shift towards an Autumn/Winter program, first shutting down the reproductive axis (Figure 1 A, D, E), and entering a pre-hibernation state characterised by a downward adjustment of the core-body temperature (T_b) and an increase in brown adipose tissue (BAT) (Figure 1A, B, C)(Chayama et al. 2016; Markussen et al. 2024). After approximately 8-12 weeks in SP 8°C T-A cycling commences, defined by multi-day bouts of torpor, during which T_b is close to ambient temperature (approximately 8°C), separated by spontaneous return to euthermic temperatures (interbout euthermia (IBE)) (Figure 1A). Then, after approximately 20 weeks in SP 8°C, the animals spontaneously cease to show T-A cycling and start to re-grow their testes (refractory state) (Figure 1A, D, E). The refractory state is associated with a progressive increase in T_b but this does not reach the T_b values recorded during LP (Figure 1B).

Divergent gene expression dynamics in the tanycytic region over the course of the hibernation season

To assess how changes in tanycyte characteristics mirror hibernation status, we sampled animals from LP, SP 8°C 4 weeks (pre-hibernation), SP 8°C 8-12 weeks (late pre-hibernation), during hibernation (IBE and torpid), and finally once animals had entered the refractory state (Figure 1A). Using a LASER capture microdissection (LCMD) approach, we generated tanycyte-enriched samples (Melum et al. 2024) (Figure 1F and Supplementary Figure 1A) from each of our physiologically defined groups and these were then subjected to RNAseq.

Among the euthermic animals, we found that over 15% of all detectable transcripts showed significant changes in expression (FDR<0.05) over the whole experiment (seasonal differentially expressed genes (DEGs) (Supplementary Table 1). Performing a PCA analysis of the seasonal DEGs, shows that 76.8%, between sample variation in gene expression was accounted for by a single principal component, resolving samples according to seasonal status (Figure 1G).

Focusing on these seasonal DEGs, we used K-means hierarchical clustering to resolve five distinctive expression profiles showing different dynamics over the course of the hibernation season (Figure 2A). Genes constituting clusters 1 (388 genes) are characterised by high expression under LP which then declines upon exposure to SP. Cluster 1 genes maintain reduced expression under SP even in the refractory state. This suggests that cluster 1 genes represent a group whose expression is primarily dependent on photoperiodic input as opposed to seasonal hibernation status. In line with this view, two canonical photoperiod-regulated genes (Aldh1a1 & Dio2 (Hanon et al. 2008, 2010; Shearer et al. 2010)) are members of cluster 1 (Figure 2B & Supplementary Table 1).

We used both Krypto encyclopedia of genes and genomes (KEGG) and Reactome pathway analysis to gain insights into the likely functional consequences of observed changes in gene expression in clusters 1 - 5 (Supplementary table 2, Figure 2B). Cluster 1 shows strong pathway enrichment related to amino acid metabolism (3.92-fold enrichment, 0.00034 FDR), retinol metabolism (10.35-fold enrichment, 0.03 FDR), PPAR signalling pathway (7.25-fold enrichment, 6.36×10^{-5} FDR) and fatty acid metabolism (3.99-fold enrichment, 0.0029 FDR). A closer look at the PPAR pathway enriched genes (Supplementary Figure 1B) shows that lipogenesis and fatty acid transport related genes are up-regulated, concurring with earlier work noting that tanycytes transport fatty acids and in combination with astrocytes regulate lipid metabolism (Hofmann et al. 2017). This pathway enrichment also reflects the well

documented direct effects of photoperiod in retinoic acid (RA) signalling in mammals (Shearer et al. 2010) (Supplementary Figure 1C).

Cluster 2 (463 genes) is defined by low expression in the pre-hibernation and hibernation animals and high expression in LP and refractory animals. This group shows strong pathway enrichment for neurotransmitter uptake in glial cells and G-protein coupled receptor (GPCR) ligand binding (Figure 2B & Supplementary Table 2), echoing our previous work describing strong photoperiodic effects on ciliation in the tanycytic region of Siberian hamsters (*Phodopus sungorus*)(Melum et al. 2024). Consistent with this, we found strong enrichment of GO terms linked to ciliary function (Figure 2C & Supplementary Table 2), and the expression patterns for key cilia genes (Tubb4b, Cfap20, Cfap47) nicely demonstrate the cluster 2 expression pattern (Figure 2A).

Cluster 3 (233 genes) does not show a strong overall seasonal expression trend, but a lower expression in the mid-hibernation season (IBE) state compared to either the late-pre-hibernation state or in the refractory state (Figure 2A). This was the smallest cluster and is enriched for neurotransmitter recycling and synapse pathways (Figure 2B & Supplementary Table 2). GO term analysis also revealed genes involved in clathrin sculpted vesicles (Gad1, Gad2, Rab3a) (Supplementary Table 2 & Figure 2B), which have been proposed to be important in the communication of tanycytes to neurons (Pasquettaz et al. 2021).

Genes constituting Clusters 4 (545 genes) and 5 (566 genes) are characterised by low levels of expression in LP, which then increase upon exposure to SP and entry into the hibernation phase, before a subsequent decline in the refractory state (Figure 2A). These two clusters differ from one another in that declining expression is seen earlier in cluster 4, when animals are still undergoing T-A cycling, than in cluster 5, in which a decline in expression occurs in the refractory state (Figure 2A).

Cluster 4 shows pathway enrichment linked to mitogen-activated protein kinase (MAPK) signalling and calcium signalling as defining the pre-hibernation state (Figure 2B). The MAPK transduction pathway relates to cell growth, division and differentiation, suggesting remodelling of the tanycytic region in response to SP exposure. Consistent with this interpretation and previous descriptions of its expression dynamics in golden hamsters, Dio3 is a member of cluster 4 (Figure 2A)(Milesi et al. 2017). We also note that Slc2a5, a fructose transporter, is up-regulated in the pre-hibernation state, concomitant with a decrease in Slc2a1, a glucose transporter (Figure 2A, D & Supplementary Figure 2A). Phosphofructokinase (Pfkp), the key enzyme in glycolysis that catalyses the phosphorylation of fructose-6-phosphase is also a member of cluster 4, along with Gapdh and Eno2, all important members of the glycolysis pathway (Figure 2A, D).

Cluster 5, constituting genes whose expression is increased during the hibernation season and then decline in the refractory state, is strongly enriched for “metabolism” pathways (Figure 2B) and the GO terms relating to catabolic processes and oxidoreductase activity (Supplementary Table 2). Specifically, genes relating to the pathways; Glycine, serine and threonine metabolism and carbohydrate metabolism show increased expression in the hibernation season (Figure 2B), as do several genes linked to glycolysis (Adpgk, Tpi1, Pgk1, Pck2, Ldhd) (Figure 2D). Similarly key elements of glucose-6-phosphatase activity including catalytic subunit 3 (G6pc3), Slc37a4 (G6pt), and Adpgk, are found in cluster 5 (Figure 2A, D). We also note that glycogen phosphorylase (Pgym), which breaks down glycogen was present in cluster 5, suggesting depletion of glycogen stores in preparation for, and, during hibernation (Figure 2A, Supplementary Figure 2B), potentially to supply neurons with glucose via the G6pase system (Barahona et al. 2024).

Immediate early gene expression and RNA splicing during torpor

To investigate the difference between torpid tanycytes and interbout euthermic tanycytes, we performed RNASeq on animals at the mid-point of torpor (average 13.3 hours) at a T_b of 8°C and contrasted the expression profile with that of IBE animals (Figure 3A). This revealed 1674 DEGs (FDR<0.05), 668 of which were up-regulated during torpor (Figure 3B & Supplementary Table 3). We noted that a striking number of immediate early genes were upregulated during torpor (including c-Fos, Jun, Junb, Egr1) (Figure 3B & C), with c-Fos showing the most impressive induction in terms of counts per million (Figure 3C). Also, amongst the most up-regulated genes during torpor were the RNA splicing/processing genes; Srsf5 and Pnisr (Figure 3B), reflected in the pathway and GOterm enrichment analysis which showed strong enrichment for RNA splicing (Figure 3D & Supplementary Table 4). Furthermore, pathway analysis also revealed an up-regulation of genes related to the cellular response to hypoxia during torpor (Figure 3D). Wsb1, a target of HIF1, with links to glucose and TH metabolism (Dentice et al. 2005; Haque et al. 2016), is up-regulated (Figure 3C). We also note a small up-regulation of Dio3 during torpor that is mirrored by a small up-regulation of Dio2 during IBE (Figure 3B).

By focusing on IBE, we noted Eif5, a translation initiation factor, Dyrk1b, a kinase involved in double strand break repair and transcriptional silencing, Mlx, a BHLH-zip transcription factor, and Kctd21, a histone deacetylase (Figure 3B, C), were among the most up-regulated DEGs (Figure 3B). GO Enrichment analysis indicated genes relating the RNA-induced silencing complex (RISC) and histone methyltransferase activity were up-regulated (Figure 3E). Collectively these data suggest that translation, gene silencing via microRNAs, and epigenetic regulation processes are up-regulated in the interbout euthermic phase.

Discussion

Motivated by an accumulating literature indicating that tanycytes play a core role in the regulation of energy homeostasis in mammals (Bolborea and Dale 2013; Langlet 2014; Rizzoti and Lovell-Badge 2017; Prevot et al. 2018; Dali et al. 2023), and that seasonal adjustments in metabolic physiology may be initiated by changes in tanycyte function (Ebling 2014; Lewis and Ebling 2017; Ebling and Lewis 2018; Dardente et al. 2019; Melum et al. 2024), we sought in the present study to characterise changes in tanycyte phenotype across the hibernation season in the golden hamster. To this end we undertook transcriptomic profiling of LCMD samples from the tanycytic region taken at specified points during the hibernation season defined by telemetric monitoring of T_b. Based on the reasonable assumption that changes in transcriptomic profile reflect underlying changes in cellular physiology the following inferences can be drawn about changes across the season as a whole:

Firstly, among the set of seasonal DEGs, fewer than 20% (cluster 1) appear to primarily be controlled by photoperiod as opposed to seasonal status. This demonstrates that while, in the golden hamster, the initiation of the hibernation season requires SP exposure, subsequent progression through the season from pre-hibernation to the refractory state constitutes an innately driven temporal sequence of events. The presence of Dio2, Aldh1a1 and related genes in this photoperiod-regulated subset is consistent with the current consensus that nuclear hormone receptor signalling through thyroid hormone receptor (THR), retinoic acid and retinoid receptor (RAR-RXR) interactions, is central to photoperiodic triggering of changes in tanycyte function downstream of melatonin-dependent changes in TSH production by the PT (reviewed in: (Dardente et al. 2019)). The broader enrichment of this group for genes linked to amino acid and lipid metabolism is possibly an indicator of photoperiod-induced alterations of tanycyte-astrocyte communication to regulate lipid metabolism in the hypothalamus (Hofmann et al. 2017).

The second inference focuses on the larger group of DEGs that reflect the sequential seasonal state transitions (clusters 2, 4 & 5). Here, there is clear evidence for shifting metabolic fuel use within the tanycytic region, with genes linked to fructose transport and glycolytic function showing higher expression during the pre-hibernation and hibernation state compared to LP or refractory states (Figure 2D). Use of the fructose pathway and endogenous production of fructose can shift an organism towards energy conservation with decreased mitochondrial activity and enhanced glycolytic activity, potentially representing an evolutionary conserved "survival" pathway (Johnson et al. 2020). Our data are consistent with a model in which tanycytes undergo a photoperiod-driven/innately timed metabolic switch to conserve energy by shifting towards glycolysis and an enhanced use of tanycyte glycogen stores. Photoperiodic regulation of genes involved in glycogen and glucose metabolism in tanycytes of Siberian hamsters have also been reported (Nilaweera et al. 2011). This hypothesised shift in tanycyte function would reduce tanycytic energy requirements and might enhance glucose supply to neighbouring cells via the glucose 6 phosphatase system (Barahona et al. 2024). This response can be seen as part of an organism-wide adjustment of fuel requirements to support hibernation, which is at the same time is highly tissue and brain region-specific (Williams et al. 2005; Schwartz et al. 2013; Vermillion et al. 2015).

Our third inference is that inverse to the above-mentioned changes in fuel metabolism, genes linked to the construction and function of cilia are a major feature of the seasonal DEGs. These show a marked decline in expression with the onset of the hibernation phase and then recovery to LP levels with the onset of the refractory state. Recently, we reported a similar result in juvenile Siberian hamsters (*Phodopus sungorus*), with exposure to SP during gestation and the juvenile period causing a significant reduction in the expression of ciliary gene expression and the numbers of cilia present on the ependymal surface in the basal 3rd ventricle (Melum et al. 2024). In both these studies, the described changes in ciliary gene

expression are paralleled by changes in G-protein coupled receptor (GPCR) gene expression, reflecting the role of cilia as scaffolds for cell-surface GPCRs to perform their signalling functions (reviewed in:(Schou et al. 2015)). Hence these results suggest that, in seasonal rodent species, the overwintering state may be characterised by reduced tanycytic sensitivity to signals in the CSF bathing their apical surface.

In addition to characterising transcriptomic change over the course of the hibernation season, we also compared the expression profiles of torpid and inter-bout euthermic animals. Echoing published *in situ* hybridization-based studies in golden hamsters and in hibernating ground squirrels (Bratincsák et al. 2007; Markussen et al. 2024), we saw a striking increase in the level of expression of c-Fos in the tanycytic region of torpid animals. Moreover, this effect is seen for several other well-known immediate early genes (IEGs), including Egr1, Jun and Junb. These genes have been widely used as acute markers for cellular (and especially neuronal) activation in response to stimulatory signals acting through second messengers such as intracellular calcium or cAMP (reviewed in:(Lara Aparicio et al. 2022)). IEG acute sensitivity to stimulus relies on the fact that IEG response does not depend upon synthesis of other transcriptional regulators (reviewed in: (Bahrami and Drabløs 2016)). On this basis, the most obvious interpretation of our results is that increased IEG expression in torpor represents a tanycytic response to stimulation. This raises the interesting issue of what stimuli are responsible for this effect. At the same time, we cannot exclude the possibility that the observed changes in IEG expression are a secondary consequence of changes in tanycytic protein synthesis rate. Since IEGs exhibit negative auto-regulation through transcriptional auto-repression (Gius et al. 1990), a general suppression of protein synthesis may lead to enhanced IEG transcription. Consistent with this interpretation, global suppression of translation during torpor and the resumption of protein synthesis in the inter-bout euthermic phase has been reported in 13-lined ground squirrels (Frerichs et al. 1998; Logan et al. 2019),

and in the current study the expression of the translation initiation factor, Eif5 was suppressed during torpor. Alternatively, given the highly brain region specific pattern of c-Fos induction during T-A cycling (Bratincsák et al. 2007; Fu et al. 2021; Markussen et al. 2024; Haugg et al. 2024), a likely scenario is that the observed tanycytic IEG response represents the actions of as yet unidentified local stimuli enhanced by suppression of translation-based autoregulatory feedback. Clearly further studies to isolate candidate stimuli and test their effects on tanycytes are now warranted.

Pathway analysis of DEGs with increased expression in torpor highlights the hypoxia response and effects on the control of RNA splicing, both of which have previously been implicated in hibernation physiology (Maistrovski et al. 2012; Sano et al. 2015; Fu et al. 2021). Notably, Wsb1 a HIF1-α induced gene (reviewed in:(Haque et al. 2016)) has been linked to ubiquitination, and hence targeted degradation of DIO2 (Dentice et al. 2005; Zavacki et al. 2009). This suggests that TH metabolism may be modulated during T-A cycling by post-translational mechanisms. While exogenous T3 delivered to the hypothalamus blocks torpor in Siberian hamsters (Murphy et al. 2012; Bank et al. 2017), the equivalent experiment is yet to be conducted in a deep hibernator. Furthermore, measurement of deiodinase enzyme activity during a T-A cycle has not been done, therefore a role for TH metabolism in the regulation of the T-A cycle rather than just the overall seasonal physiology remains to be evaluated.

During IBE, the increased expression of Mlx, a BHLH-zip transcription factor, was of particular interest. Playing a crucial role in glucose homeostasis, MLX along with MLXIP translocates to the nucleus in response to high glucose-6-phosphate conditions, targeting glucose-sensitive genes for transcription (Stoltzman et al. 2008). One of these is Txnip, which prevents the uptake of glucose into the cell, thereby forming a negative feedback loop limiting the conversion to glucose to glucose-6-phosphate for glycolysis (Stoltzman et al. 2008).

Expression of Txnip in the mediobasal hypothalamus (i.e. the tanycytic region) is induced in response to fasting in mice, daily torpor in Siberian hamsters (Hand et al. 2013), torpor in the garden dormouse (Haugg et al. 2024) and the 13-lined ground squirrel (Schwartz et al. 2013). We see no change in Txnip expression in the golden hamster tanycytes despite the up-regulation of Mlx (Supplementary table 1). Recently, it was shown that MLX sequestered to lipid droplets in the cytoplasm cannot enter the nucleus in response to glucose, preventing it from exerting transcriptional effects (Mejhert et al. 2020). Tanycytes are rich in lipid droplets (reviewed in: (Rodríguez et al. 2019)), therefore, we speculate that MLX may be sequestered to lipid droplets in the IBE phase. Since golden hamsters eat in the IBE phase, this may provide a mechanism to ensure tanycytic sequestering of glucose to support glycolysis upon re-entry to torpor.

Conclusions

While RNA profiling does not permit the drawing of firm conclusions about how tanycytic function changes over the course of the hibernation season, the data we present serve a useful hypothesis-generating function for future studies. Based on our analysis, we identify the following priorities for further research: 1) defining how tanycytic sensitivity to metabolites and other extracellular signals changes over the course of the hibernation season 2) understanding how tanycytic energy metabolism changes and the relationship between this and the function of tanycytes and neighbouring hypothalamic cells and 3) understanding the causes of the dramatic changes in tanycytic IEG expression during T-A cycling and the consequences of these for tanycytic function during torpor.

Acknowledgements

We wish to acknowledge Clarisse Quignon for her help with sample collection. We are grateful to Dominique Ciocca and Sophie Foisset Reibel for teaching animal husbandry technique. We are also grateful to all the technical staff at the chronobiotron for their support. Further, we thank Stian Olsen and Anne Grethe Hestnes for invaluable technical assistance and guidance on the LASER capture microdissection instrument. Finally, VJM would like to thank Alex C. West, Gerard Clarke and Yin-Chen Hsieh for insightful comments on an early draft of the manuscript.

Funding

The work was supported by grants from the Tromsø forskningsstiftelse (TFS) starter grant TFS2016SW and the TFS infrastructure grant (IS3_17_SW) awarded to S.H.W. It was also co-funded by the European Union (ERC, HiTime, 101086671). Views and opinions expressed are however those of the author(s) only and do not necessarily reflect those of the European Union or the European Research Council. Neither the European Union nor the granting authority can be held responsible for them. The Arctic seasonal timekeeping initiative (ASTI) grant and UiT strategic funds support D.G.H. & S.H.W.

References

Bahrami, S., and Drabløs, F. 2016. Gene regulation in the immediate-early response process. Adv. Biol. Regul. **62**: 37–49. doi:10.1016/j.jbior.2016.05.001.

Bank, J.H.H., Cubuk, C., Wilson, D., Rijntjes, E., Kemmling, J., Markovsky, H., Barrett, P., and Herwig, A. 2017. Gene expression analysis and microdialysis suggest hypothalamic triiodothyronine (T3) gates daily torpor in Djungarian hamsters (Phodopus sungorus). J. Comp. Physiol. B **187**(5–6): 857–868. Springer Berlin Heidelberg. doi:10.1007/s00360-017-1086-5.

Bank, J.H.H., Kemmling, J., Rijntjes, E., Wirth, E.K., and Herwig, A. 2015. Thyroid hormone status affects expression of daily torpor and gene transcription in Djungarian hamsters (Phodopus sungorus). Horm. Behav. **75**: 120–129. Academic Press. doi:10.1016/j.yhbeh.2015.09.006.

Barahona, M.J., Ferrada, L., Vera, M., and Nualart, F. 2024. Tanycytes release glucose using the glucose-6-phosphatase system during hypoglycemia to control hypothalamic energy balance. Mol. Metab. **84**(April): 101940. The Authors. doi:10.1016/j.molmet.2024.101940.

Blighe K, Rana S, L.M. 2024. EnhancedVolcano: Publication-ready volcano plots with enhanced colouring and labeling. R package version 1.22.0.

Blighe, K., and Lun, A. 2019. PCAtools: everything Principal Components Analysis.

Bolborea, M., and Dale, N. 2013. Hypothalamic tanycytes: potential roles in the control of feeding and energy balance. Trends Neurosci. **36**(2): 91–100. Elsevier. doi:10.1016/j.tins.2012.12.008.

Bolborea, M., Pollatzek, E., Benford, H., Sotelo-Hitschfeld, T., and Dale, N. 2020.

494 Hypothalamic tanycytes generate acute hyperphagia through activation of the arcuate
495 neuronal network. Proc. Natl. Acad. Sci. **117**(25): 14473–14481.
496 doi:10.1073/pnas.1919887117.

497 Bratincsák, A., McMullen, D., Miyake, S., Tóth, Z.E., Hallenbeck, J.M., and Palkovits, M.
498 2007. Spatial and temporal activation of brain regions in hibernation:c-fos expression
499 during the hibernation bout in thirteen-lined ground squirrel. J. Comp. Neurol. **505**(4):
500 443–458. doi:10.1002/cne.21507.

501 Campbell, J.N., Macosko, E.Z., Fenselau, H., Pers, T.H., Lyubetskaya, A., Tenen, D.,
502 Goldman, M., Verstegen, A.M.J., Resch, J.M., McCarroll, S.A., Rosen, E.D., Lowell,
503 B.B., and Tsai, L.T. 2017. A molecular census of arcuate hypothalamus and median
504 eminence cell types. Nat. Neurosci. **20**(3): 484–496. doi:10.1038/nn.4495.

505 Chayama, Y., Ando, L., Tamura, Y., Miura, M., and Yamaguchi, Y. 2016. Decreases in body
506 temperature and body mass constitute pre-hibernation remodelling in the Syrian golden
507 hamster, a facultative mammalian hibernator. R. Soc. Open Sci. **3**(4): 160002.
508 doi:10.1098/rsos.160002.

509 Chen, Y., Lun, A.T.L., and Smyth, G.K. 2014. Differential Expression Analysis of Complex
510 RNA-seq Experiments Using edgeR *.

511 Chmura, H.E., Duncan, C., Saer, B., Moore, J.T., Barnes, B.M., Loren Buck, C., Christian,
512 H.C., Loudon, A.S.I., and Williams, C.T. 2022. Hypothalamic remodeling of thyroid
513 hormone signaling during hibernation in the arctic ground squirrel. Commun. Biol. **5**(1):
514 492. doi:10.1038/s42003-022-03431-8.

515 Dali, R., Estrada-Meza, J., and Langlet, F. 2023. Tanycyte, the neuron whisperer. Physiol.
516 Behav. **263**: 114108. doi:10.1016/j.physbeh.2023.114108.

517 Dardente, H., Hazlerigg, D.G., and Ebling, F.J.P. 2014. Thyroid Hormone and Seasonal
518 Rhythmicity. Front. Endocrinol. (Lausanne). **5**: 19. Frontiers.
519 doi:10.3389/fendo.2014.00019.

520 Dardente, H., Wood, S., Ebling, F., and Sáenz de Miera, C. 2019. An integrative view of
521 mammalian seasonal neuroendocrinology. J. Neuroendocrinol. **31**(5): e12729.
522 doi:10.1111/jne.12729.

523 Darrow, J.M., Yogev, L., and Goldman, B.D. 1987. Patterns of reproductive hormone
524 secretion in hibernating Turkish hamsters. Am J Physiol Regul Integr Comp Physiol **253**:
525 329–336.

526 Dentice, M., Bandyopadhyay, A., Gereben, B., Callebaut, I., Christoffolete, M.A., Kim, B.W.,
527 Nissim, S., Mornon, J.-P., Zavacki, A.M., Zeöld, A., Capelo, L.P., Curcio-Morelli, C.,
528 Ribeiro, R., Harney, J.W., Tabin, C.J., and Bianco, A.C. 2005. The Hedgehog-inducible
529 ubiquitin ligase subunit WSB-1 modulates thyroid hormone activation and PTHrP
530 secretion in the developing growth plate. Nat. Cell Biol. **7**(7): 698–705.
531 doi:10.1038/ncb1272.

532 Dobin, A., Davis, C.A., Schlesinger, F., Drenkow, J., Zaleski, C., Jha, S., Batut, P., Chaisson,
533 M., and Gingeras, T.R. 2013. STAR: ultrafast universal RNA-seq aligner. Bioinformatics
534 **29**(1): 15–21. doi:10.1093/bioinformatics/bts635.

535 Duquenne, M., Folgueira, C., Bourouh, C., Millet, M., Silva, A., Clasadonte, J., Imbernon,
536 M., Fernandois, D., Martinez-Corral, I., Kusumakshi, S., Caron, E., Rasika, S., Deliglia,
537 E., Jouy, N., Oishi, A., Mazzone, M., Trinquet, E., Tavernier, J., Kim, Y.-B., Ory, S.,
538 Jockers, R., Schwaninger, M., Boehm, U., Nogueiras, R., Annicotte, J.-S., Gasman, S.,
539 Dam, J., and Prévot, V. 2021. Leptin brain entry via a tanycytic LepR–EGFR shuttle
540 controls lipid metabolism and pancreas function. Nat. Metab. **3**(8): 1071–1090.

doi:10.1038/s42255-021-00432-5.

Ebling, F.J.P., and Lewis, J.E. 2018. Tanycytes and hypothalamic control of energy metabolism. Glia **66**(6): 1176–1184. doi:10.1002/glia.23303.

Ebling, F.J.P.P. 2014. On the value of seasonal mammals for identifying mechanisms underlying the control of food intake and body weight. Horm. Behav. **66**(1): 56–65. Elsevier B.V. doi:10.1016/j.yhbeh.2014.03.009.

Frerichs, K.U., Smith, C.B., Brenner, M., DeGracia, D.J., Krause, G.S., Marrone, L., Dever, T.E., and Hallenbeck, J.M. 1998. Suppression of protein synthesis in brain during hibernation involves inhibition of protein initiation and elongation. Proc. Natl. Acad. Sci. **95**(24): 14511–14516. doi:10.1073/pnas.95.24.14511.

Fu, R., Gillen, A.E., Grabek, K.R., Riemondy, K.A., Epperson, L.E., Bustamante, C.D., Hesselberth, J.R., and Martin, S.L. 2021. Dynamic RNA Regulation in the Brain Underlies Physiological Plasticity in a Hibernating Mammal. Front. Physiol. **11**. doi:10.3389/fphys.2020.624677.

Gaston, S., and Menaker, M. 1967. Photoperiodic control of hamster testis. Science (80-.). **158**(3803): 925–928.

Ge, S.X., Jung, D., Jung, D., and Yao, R. 2020. ShinyGO: a graphical gene-set enrichment tool for animals and plants. Bioinformatics **36**(8): 2628–2629. Oxford Academic. doi:10.1093/BIOINFORMATICS/BTZ931.

Gius, D., Cao, X.M., Rauscher, F.J., Cohen, D.R., Curran, T., and Sukhatme, V.P. 1990. Transcriptional activation and repression by Fos are independent functions: the C terminus represses immediate-early gene expression via CArG elements. Mol. Cell. Biol. **10**(8): 4243–4255. doi:10.1128/MCB.10.8.4243.

564 Gu, Z., Eils, R., and Schlesner, M. 2016. Complex heatmaps reveal patterns and correlations
565 in multidimensional genomic data. Bioinformatics **32**(18): 2847–2849.
566 doi:10.1093/bioinformatics/btw313.

567 Gwinner, E. 1986. Circannual rhythms. Springer Verlag, Berlin Heidelberg.

568 Hand, L.E., Saer, B.R.C., Hui, S.T., Jinnah, H.A., Steinlechner, S., Loudon, A.S.I., and
569 Bechtold, D.A. 2013. Induction of the metabolic regulator txnip in fasting-induced and
570 natural torpor. Endocrinology **154**(6): 2081–2091. doi:10.1210/en.2012-2051.

571 Hanon, E.A., Lincoln, G.A., Fustin, J.-M., Dardente, H., Masson-Pévet, M., Morgan, P.J., and
572 Hazlerigg, D.G. 2008. Ancestral TSH mechanism signals summer in a photoperiodic
573 mammal. Curr. Biol. **18**(15): 1147–52. doi:10.1016/j.cub.2008.06.076.

574 Hanon, E.A., Routledge, K., Dardente, H., Masson-Pévet, M., Morgan, P.J., and Hazlerigg,
575 D.G. 2010. Effect of photoperiod on the thyroid-stimulating hormone neuroendocrine
576 system in the European hamster (Cricetus cricetus). J. Neuroendocrinol. **22**(1): 51–5.
577 doi:10.1111/j.1365-2826.2009.01937.x.

578 Haque, M., Kendal, J.K., MacIsaac, R.M., and Demetrick, D.J. 2016. WSB1: from
579 homeostasis to hypoxia. J. Biomed. Sci. **23**(1): 61. doi:10.1186/s12929-016-0270-3.

580 Haugg, E., Borner, J., Stalder, G., Kübber-Heiss, A., Giroud, S., and Herwig, A. 2024.
581 Comparative transcriptomics of the garden dormouse hypothalamus during hibernation.
582 FEBS Open Bio **14**(2): 241–257. doi:10.1002/2211-5463.13731.

583 Hazlerigg, D., and Simonneaux, V. 2015. Seasonal reproduction in mammals. *In* Knobil and
584 Neill's physiology and reproduction, 4th edition. *Edited by* T. Plant and A. Zeleznic.
585 Academic Press. pp. 1575–1660.

586 Hofmann, K., Lamberz, C., Piotrowitz, K., Offermann, N., But, D., Scheller, A., Al-Amoudi,

A., and Kuerschner, L. 2017. Tanycytes and a differential fatty acid metabolism in the hypothalamus. Glia **65**(2): 231–249. doi:10.1002/glia.23088.

Hut, R.A.A., Dardente, H., and Riede, S.J.J. 2014. Seasonal Timing: How Does a Hibernator Know When to Stop Hibernating? Curr. Biol. **24**(13): R602–R605. Cell Press. doi:10.1016/j.cub.2014.05.061.

Johnson, R.J., Stenvinkel, P., Andrews, P., Sánchez-Lozada, L.G., Nakagawa, T., Gaucher, E., Andres-Hernando, A., Rodriguez-Iturbe, B., Jimenez, C.R., Garcia, G., Kang, D.H., Tolan, D.R., and Lanaspa, M.A. 2020. Fructose metabolism as a common evolutionary pathway of survival associated with climate change, food shortage and droughts. J. Intern. Med. **287**(3): 252–262. doi:10.1111/joim.12993.

Klosen, P., Sébert, M.-E., Rasri, K., Laran-Chich, M.-P., and Simonneaux, V. 2013. TSH restores a summer phenotype in photoinhibited mammals via the RF-amides RFRP3 and kisspeptin. FASEB J. **27**(7): 2677–86. doi:10.1096/fj.13-229559.

Langlet, F. 2014. Tanycytes: A Gateway to the Metabolic Hypothalamus. J. Neuroendocrinol. **26**(11): 753–760. doi:10.1111/jne.12191.

Lara Aparicio, S.Y., Laureani Fierro, Á. de J., Aranda Abreu, G.E., Toledo Cárdenas, R., García Hernández, L.I., Coria Ávila, G.A., Rojas Durán, F., Aguilar, M.E.H., Manzo Denes, J., Chi-Castañeda, L.D., and Pérez Estudillo, C.A. 2022. Current Opinion on the Use of c-Fos in Neuroscience. NeuroSci **3**(4): 687–702. doi:10.3390/neurosci3040050.

Lewis, J.E., and Ebling, F.J.P. 2017. Tanycytes As Regulators of Seasonal Cycles in Neuroendocrine Function. Front. Neurol. **8**: 79. Frontiers. doi:10.3389/fneur.2017.00079.

Lhomme, T., Clasadonte, J., Imbernon, M., Fernandois, D., Sauve, F., Caron, E., da Silva Lima, N., Heras, V., Martinez-Corral, I., Mueller-Fielitz, H., Rasika, S., Schwaninger,

610 M., Nogueiras, R., and Prevot, V. 2021. Tanycytic networks mediate energy balance by
611 feeding lactate to glucose-insensitive POMC neurons. J. Clin. Invest. **131**(18).
612 doi:10.1172/JCI140521.

613 Logan, S.M., Wu, C.-W., and Storey, K.B. 2019. The squirrel with the lagging eIF2: Global
614 suppression of protein synthesis during torpor. Comp. Biochem. Physiol. Part A Mol.
615 Integr. Physiol. **227**: 161–171. doi:10.1016/j.cbpa.2018.10.014.

616 Lyman, C.P., Willis, J.., Malan, A., and Wang, L.C.. 1982. Hibernation and torpor in
617 mammals and birds. *Edited By*C.P. Lyman. Academic Press, New York.

618 Maistrovski, Y., Biggar, K.K., and Storey, K.B. 2012. HIF-1α regulation in mammalian
619 hibernators: role of non-coding RNA in HIF-1α control during torpor in ground squirrels
620 and bats. J. Comp. Physiol. B **182**(6): 849–859. doi:10.1007/s00360-012-0662-y.

621 Markussen, F.A.F., Cázarez-Márquez, F., Melum, V.J., Hazlerigg, D., and Wood, S. 2024. C-
622 Fos Induction in the Choroid Plexus, Tanycytes and Pars Tuberalis Is an Early Indicator
623 of Spontaneous Arousal From Torpor in a Deep Hibernator . J. Exp. Biol.
624 doi:10.1242/jeb.247224.

625 McCarthy, D.J., Chen, Y., and Smyth, G.K. 2012. Differential expression analysis of
626 multifactor RNA-Seq experiments with respect to biological variation. Nucleic Acids
627 Res.: 1–10. doi:10.1093/nar/gks042.

628 Mejhert, N., Kuruvilla, L., Gabriel, K.R., Elliott, S.D., Guie, M.-A., Wang, H., Lai, Z.W.,
629 Lane, E.A., Christiano, R., Danial, N.N., Farese, R. V., and Walther, T.C. 2020.
630 Partitioning of MLX-Family Transcription Factors to Lipid Droplets Regulates
631 Metabolic Gene Expression. Mol. Cell **77**(6): 1251-1264.e9.
632 doi:10.1016/j.molcel.2020.01.014.

633 Melum, V.J., Sáenz de Miera, C., Markussen, F.A.F., Cázarez-Márquez, F., Jaeger, C.,
634 Sandve, S.R., Simonneaux, V., Hazlerigg, D.G., and Wood, S.H. 2024. Hypothalamic
635 tanycytes as mediators of maternally programmed seasonal plasticity. Curr. Biol. **34**(3):
636 632-640.e6. Cell Press. doi:10.1016/J.CUB.2023.12.042.

637 Milesi, S., Simonneaux, V., and Klosen, P. 2017. Downregulation of Deiodinase 3 is the
638 earliest event in photoperiodic and photorefractory activation of the gonadotropic axis in
639 seasonal hamsters. Sci. Rep. **7**(1): 17739. doi:10.1038/s41598-017-17920-y.

640 Morin, L.P., and Zucker, I. 1978. Photoperiodic regulation of copulatory behaviour in the
641 male hamster. J. Endocrinol. **77**(2): 249–258. J Endocrinol. doi:10.1677/JOE.0.0770249.

642 Murphy, M., Jethwa, P.H., Warner, A., Barrett, P., Nilaweera, K.N., Brameld, J.M., and
643 Ebling, F.J.P. 2012. Effects of Manipulating Hypothalamic Triiodothyronine
644 Concentrations on Seasonal Body Weight and Torpor Cycles in Siberian Hamsters.
645 Endocrinology **153**(1): 101–112. doi:10.1210/en.2011-1249.

646 Nilaweera, K., Herwig, A., Bolborea, M., Campbell, G., Mayer, C.D., Morgan, P.J., Ebling,
647 F.J.P., and Barrett, P. 2011. Photoperiodic regulation of glycogen metabolism,
648 glycolysis, and glutamine synthesis in tanycytes of the Siberian hamster suggests novel
649 roles of tanycytes in hypothalamic function. Glia **59**(11): 1695–1705.
650 doi:10.1002/glia.21216.

651 Parkash, J., Messina, A., Langlet, F., Cimino, I., Loyens, A., Mazur, D., Gallet, S., Balland,
652 E., Malone, S.A., Pralong, F., Cagnoni, G., Schellino, R., De Marchis, S., Mazzone, M.,
653 Pasterkamp, R.J., Tamagnone, L., Prevot, V., and Giacobini, P. 2015. Semaphorin7A
654 regulates neuroglial plasticity in the adult hypothalamic median eminence. Nat.
655 Commun. **6**: 6385. doi:10.1038/ncomms7385.

656 Pasquettaz, R., Kolotuev, I., Rohrbach, A., Gouelle, C., Pellerin, L., and Langlet, F. 2021.

Peculiar protrusions along tanycyte processes face diverse neural and nonneural cell types in the hypothalamic parenchyma. J. Comp. Neurol. **529**(3): 553–575. doi:10.1002/cne.24965.

Prevot, V., Dehouck, B., Sharif, A., Ciofi, P., Giacobini, P., and Clasadonte, J. 2018. The Versatile Tanycyte: A Hypothalamic Integrator of Reproduction and Energy Metabolism. Endocr. Rev. **39**(3): 333–368. doi:10.1210/er.2017-00235.

Revel, F.G., Saboureau, M., Pévet, P., Mikkelsen, J.D., and Simonneaux, V. 2006. Melatonin regulates type 2 deiodinase gene expression in the Syrian hamster. Endocrinology **147**(10): 4680–7. doi:10.1210/en.2006-0606.

Rizzoti, K., and Lovell-Badge, R. 2017. Pivotal role of median eminence tanycytes for hypothalamic function and neurogenesis. Mol. Cell. Endocrinol. **445**: 7–13. Elsevier. doi:10.1016/J.MCE.2016.08.020.

Rodríguez, E., Guerra, M., Peruzzo, B., and Blázquez, J.L. 2019. Tanycytes: A rich morphological history to underpin future molecular and physiological investigations. J. Neuroendocrinol. **31**(3). doi:10.1111/jne.12690.

Ruf, T., and Geiser, F. 2015. Daily torpor and hibernation in birds and mammals. Biol. Rev. **90**(3): 891–926. doi:10.1111/brv.12137.

Sáenz de Miera, C., Hanon, E.A., Dardente, H., Birnie, M., Simonneaux, V., Lincoln, G.A., and Hazlerigg, D.G. 2013. Circannual variation in thyroid hormone deiodinases in a short-day breeder. J. Neuroendocrinol. **25**(4): 412–21. doi:10.1111/jne.12013.

Sáenz de Miera, C., Monecke, S., Bartzen-Sprauer, J., Laran-Chich, M.-P., Pévet, P., Hazlerigg, D.G., and Simonneaux, V. 2014. A Circannual Clock Drives Expression of Genes Central for Seasonal Reproduction. Curr. Biol. **24**(13): 1500–1506.

680 doi:10.1016/j.cub.2014.05.024.

681 Sano, Y., Shiina, T., Naitou, K., Nakamori, H., and Shimizu, Y. 2015. Hibernation-specific
682 alternative splicing of the mRNA encoding cold-inducible RNA-binding protein in the
683 hearts of hamsters. Biochem. Biophys. Res. Commun. **462**(4): 322–325. Biochem
684 Biophys Res Commun. doi:10.1016/J.BBRC.2015.04.135.

685 Schou, K.B., Pedersen, L.B., and Christensen, S.T. 2015. Ins and outs of GPCR signaling in
686 primary cilia. EMBO Rep. **16**(9): 1099–1113. doi:10.15252/embr.201540530.

687 Schwartz, C., Hampton, M., and Andrews, M.T. 2013. Seasonal and Regional Differences in
688 Gene Expression in the Brain of a Hibernating Mammal. PLoS One **8**(3): e58427. Public
689 Library of Science. doi:10.1371/journal.pone.0058427.

690 Shearer, K.D., Goodman, T.H., Ross, A.W., Reilly, L., Morgan, P.J., and McCaffery, P.J.
691 2010. Photoperiodic regulation of retinoic acid signaling in the hypothalamus. J.
692 Neurochem. **112**(1): 246–257. doi:10.1111/j.1471-4159.2009.06455.x.

693 Stoltzman, C.A., Peterson, C.W., Breen, K.T., Muoio, D.M., Billin, A.N., and Ayer, D.E.
694 2008. Glucose sensing by MondoA:Mlx complexes: A role for hexokinases and direct
695 regulation of thioredoxin-interacting protein expression. Proc. Natl. Acad. Sci. **105**(19):
696 6912–6917. doi:10.1073/pnas.0712199105.

697 Vermillion, K.L., Anderson, K.J., Hampton, M., and Andrews, M.T. 2015. Gene expression
698 changes controlling distinct adaptations in the heart and skeletal muscle of a hibernating
699 mammal. Physiol. Genomics **47**(3): 58–74. doi:10.1152/physiolgenomics.00108.2014.

700 Wickham, H., Averick, M., Bryan, J., Chang, W., McGowan, L., François, R., Grolemund,
701 G., Hayes, A., Henry, L., Hester, J., Kuhn, M., Pedersen, T., Miller, E., Bache, S.,
702 Müller, K., Ooms, J., Robinson, D., Seidel, D., Spinu, V., Takahashi, K., Vaughan, D.,

Wilke, C., Woo, K., and Yutani, H. 2019. Welcome to the Tidyverse. J. Open Source Softw. **4**(43): 1686. The Open Journal. doi:10.21105/JOSS.01686.

Williams, D.R., Epperson, L.E., Li, W., Hughes, M.A., Taylor, R., Rogers, J., Martin, S.L., Cossins, A.R., and Gracey, A.Y. 2005. Seasonally hibernating phenotype assessed through transcript screening. Physiol. Genomics **24**(1): 13–22. doi:10.1152/physiolgenomics.00301.2004.

Wood, S.H., Hindle, M.M., Mizoro, Y., Cheng, Y., Saer, B.R.C., Miedzinska, K., Christian, H.C., Begley, N., McNeilly, J., McNeilly, A.S., Meddle, S.L., Burt, D.W., and Loudon, A.S.I. 2020. Circadian clock mechanism driving mammalian photoperiodism. Nat. Commun. **11**(1): 4291. doi:10.1038/s41467-020-18061-z.

Wu, T., Hu, E., Xu, S., Chen, M., Guo, P., Dai, Z., Feng, T., Zhou, L., Tang, W., Zhan, L., Fu, X., Liu, S., Bo, X., and Yu, G. 2021. clusterProfiler 4.0: A universal enrichment tool for interpreting omics data. Innov. **2**(3). Cell Press. doi:10.1016/J.XINN.2021.100141.

Zavacki, A.M., Arrojo e Drigo, R., Freitas, B.C.G., Chung, M., Harney, J.W., Egri, P., Wittmann, G., Fekete, C., Gereben, B., and Bianco, A.C. 2009. The E3 Ubiquitin Ligase TEB4 Mediates Degradation of Type 2 Iodothyronine Deiodinase. Mol. Cell. Biol. **29**(19): 5339–5347. doi:10.1128/MCB.01498-08.

Zhou, X., Lindsay, H., and Robinson, M.D. 2014. Robustly detecting differential expression in RNA sequencing data using observation weights. Nucleic Acids Res. **42**(11): e91. doi:10.1093/nar/gku310.

Figure legends

Figure 1: Photoperiod driven initiation and spontaneous termination of hibernation in golden hamsters (*Mesocricetus auratus*) relates to tanycyte transcriptional profile

A) Illustration of the experimental set-up and characteristic animal behaviour in response to shifting from long photoperiod 22°C (LP, 14 hours of light, 10 hours of dark) – summer like state, to short photoperiod (SP, 10 hours of light 14 hours of dark) and cold (8°C) – initiation of Autumn/Winter programme, followed by the eventual anticipation and initiation of Spring/Summer programme. Representative core body temperature (T_b) measurements are shown in parallel illustrate the physiological groups sampled in the experiment. T_b indicated in yellow relates to animals at LP 22°C, and T_b in blue relates to animals at SP 8°C. Ambient temperature (T_a) of the room is denoted by the grey dotted line. Pre-hib = Pre-hibernator 4 weeks after SP 8°C, Late pre-hib = pre-hibernator 8 to 12 weeks after SP 8°C, IBE = inter-bout euthermic.

B) Mean euthermic core body temperature (T_b) throughout the experimental conditions. Each dot represents each individual mean euthermic T_b defined as each experimental group listed on the x-axis. For this analysis the refractory group was split into Refr. 0, 1 and 2 representing weeks after last torpor bout. Results of one-way ANOVA indicate a difference between the group mean T_b (**** = $p<0.0001$). LP = long photoperiod, pre-hib = Pre-hibernator 4 weeks after SP 8°C, L. pre-hib = pre-hibernator 8 to 12 weeks after SP 8°C, IBE = inter-bout euthermic, Refr. = refractory.

C) Each dot indicates each individual visible dissected interscapular brown adipose tissue (iBAT) weight in grams (y-axis) for the experimental groups (x-axis). Results of one-way ANOVA indicate a group mean difference in iBAT amount (*** = $p<0.001$). LP =

long photoperiod, pre-hib = Pre-hibernator 4 weeks after SP 8°C, L. pre-hib = pre-hibernator 8 to 12 weeks after SP 8°C, IBE = inter-bout euthermic.

D) Each dot represents individual testes weight in grams for each experimental group at sampling. Results from one-way ANOVA indicate a difference between the group mean in testis weight (**** = $p<0.0001$). LP = long photoperiod, pre-hib = Pre-hibernator 4 weeks after SP 8°C, L. pre-hib = pre-hibernator 8 to 12 weeks after SP 8°C, IBE = inter-bout euthermic.

E) Blood plasma levels of testosterone. Each dot is each individual`s testosterone levels (ng/ml) for the experimental group indicated on the x-axis. Results from one-way ANOVA indicate a difference between the group mean in plasma testosterone levels (**** = $p<0.0001$). LP = long photoperiod, pre-hib = Pre-hibernator 4 weeks after SP 8°C, L. pre-hib = pre-hibernator 8 to 12 weeks after SP 8°C, IBE = inter-bout euthermic.

F) Diagram to show the workflow from frozen whole brain through frozen cryosections to LASER Capture Microdissection (LCMD) of the ependymal layer of the tuberal part of the 3rd Ventricle (3V), which were further processed for Illumina RNA-seq.

G) Principal component analysis of differentially expressed genes (DEG) across the euthermic time points. The % variation contributing to each principle component (PC) are indicated on the x and y axis. The reproductively active animals, long photoperiod (LP) and refractory group together. The animals preparing for hibernation, pre-hibernation (pre-hib) and late pre-hibernation (late pre-hib) separate from the animals that have entered hibernation and are interbout euthermic, IBE). SP = short photoperiod.

Figure 2: Changes in ciliary genes and the glycolytic pathway in tanycytes defines the seasonal response to short photoperiod

A) Heatmap of seasonal DEGs (n= 2291) with k-means clustering into 5 clusters. Next to each cluster is a normalized counts per million (cpm) plot for all genes within each cluster to indicate direction of change between the groups as listed on the x-axis. Shown as cluster mean normalised cpm (black line), shading ± Standard deviation and certain genes of interest color-coded as indicated.

B) Dot plot of enriched pathway for genes in the respective clusters using shinyGO analysis, both KEGG and reactome database results are shown. Size of dot represent number of genes. The colour of the dot represent -$\log_{10}$ transformed False discovery rate (FDR) value. The x-axis is the enrichment.

C) Specific GOterm enrichment for the genes in cluster 2. Size of dot represent number of genes. The colour of the dot represent -$\log_{10}$ transformed FDR value. The x-axis is the enrichment.

D) Cellular metabolic map of the glycolytic pathway, with the differentially expressed genes color-coded as indicated.

Figure 3: Increased immediate early gene expression and RNA splicing in the tanycytic region of torpid animals

A) Representative illustration of the core body temperature (T_b) recordings of an animal cycling from torpor to the interbout euthermic state and back again to torpor. Days spent in short photoperiod denoted on the x-axis.

B) Volcano plot for gene expression changes between interbout euthermic (IBE) and torpor. Dotted horizontal line indicate the false discovery rate, FDR= 0.05 threshold; Data are presented as $\log_2$ fold change, upregulated in inter bout euthermic (IBE) in red, upregulated in torpor in blue, genes with an FDR>0.05 are shown in green.

C) Counts per million plots across all samples for Fos, Wsb1, Eif5, Mlx. Each dot represents an individual count per million defined as each experimental group listed

on the x-axis. A generalized linear model (GLM) analysis was used to assess the group mean gene expression differences (**** = FDR greater than 0.0001); specific statistical values are in supplementary table 1.

D) Dot plot of enriched pathways for genes upregulated in torpor using shinyGO analysis, both Krypto encyclopedia of genes and genomes (KEGG) and reactome database results are shown. Size of dot represent number of genes. The color of the dot represent -$\log_{10}$ transformed FDR value. The x-axis is the enrichment.

E) Dot plot of enriched pathways for genes upregulated in interbout euthermic (IBE) using shinyGO analysis, both Krypto encyclopedia of genes and genomes (KEGG) and reactome database results are shown. Size of dot represent number of genes. The color of the dot represent -$\log_{10}$ transformed FDR value. The x-axis is the enrichment.

Supplementary figure 1

A) Average counts per million (cpm) across all samples for genes defined by Campbell et al. (Campbell et al. 2017) to be cell-type specific cluster markers. Error bars indicate the Standard error of the mean (SEM).

B) Krypto encyclopedia of genes and genomes (KEGG) diagram over Peroxisome proliferator-activated receptors signalling pathway. Genes within the pathway that are upregulated under long photoperiod are denoted in red.

C) Krypto encyclopedia of genes and genomes (KEGG) diagram over retinol metabolism. Genes within the pathway that are upregulated under long photoperiod are denoted in red.

Supplementary figure 2

A) Counts per million plots across all samples for Slc2a5 (Glut5) and Slc2a1 (Glut1). Each dot represent individual count per million defined as each experimental group

listed on the x-axis. A generalized linear model (GLM) analysis indicate the group mean gene expression to differ between the experimental groups (*** FDR< 0.001, * FDR< 0.05). Pre-hib = Pre-hibernator 4 weeks after SP 8°C, L. pre-hib = pre-hibernator 8 to 12 weeks after SP 8°C, IBE = inter-bout euthermic.

B) Schematic showing genes involved in glycogen creation and depletion, with the differentially expressed genes color-coded as indicated.

Supplementary table 1 – Differential gene expression analysis using a generalised linear model to assess the changes across all euthermic experimental groups. Log fold change of gene expression, the false discovery rate (FDR) and respective cluster assignment for differentially expressed genes (FDR<0.05) are listed.

Supplementary table 2 – Results for the curated GOterm, Krypto encyclopedia of genes and genomes (KEGG) and reactome pathway enrichment for each cluster using shinyGO analysis.

Supplementary table 3 - Differential gene expression analysis using a generalised linear model to assess the changes between the interbout euthermic (IBE) and torpid group animals. Log fold change of gene expression, the false discovery rate (FDR) and respective cluster assignment for differentially expressed genes (FDR<0.05) are listed.

Supplementary table 4 - Results for the curated GOterm, Krypto encyclopedia of genes and genomes (KEGG) and reactome pathway enrichment for genes upregulated when interbout euthermic or torpid using shinyGO analysis.

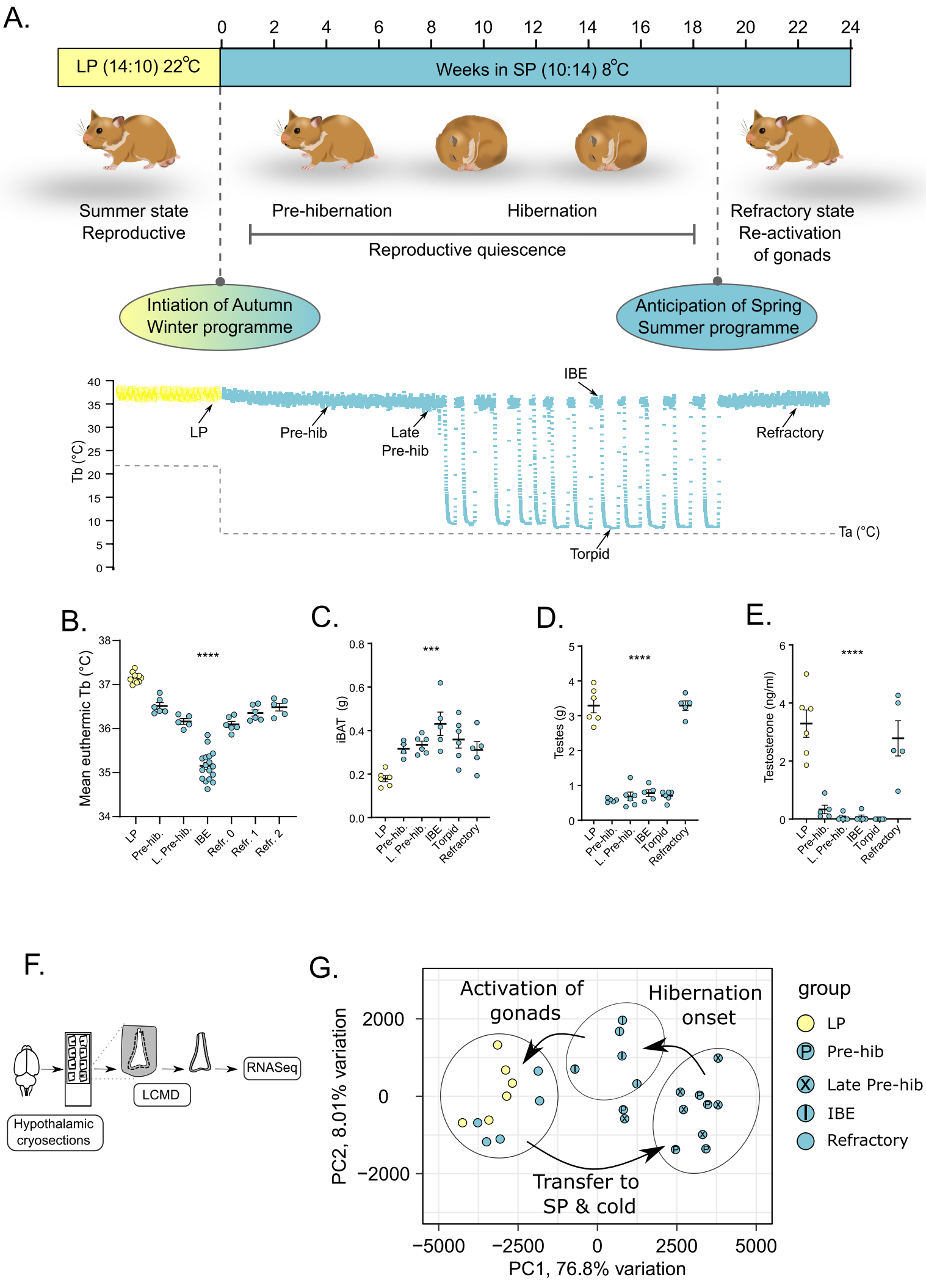
A.
0 2 4 6 8 10 12 14 16 18 20 22 24
LP (14:10) 22°C
Weeks in SP (10:14) 8°C
Summer state
Reproductive
Pre-hibernation
Hibernation
Refractory state
Re-activation
of gonads
Reproductive quiescence
Intiation of Autumn
Winter programme
Anticipation of Spring
Summer programme
Tb (°C)
LP
Pre-hib
Late
Pre-hib
IBE
Refractory
Torpid
Ta (°C)
B.
Mean euthermic Tb (°C)
****
LP
Pre-hib.
L. Pre-hib.
IBE
Refr. 0
Refr. 1
Refr. 2
C.
iBAT (g)
***
LP
Pre-hib.
L. Pre-hib.
IBE
Torpid
Refractory
D.
Testes (g)
****
LP
Pre-hib.
L. Pre-hib.
IBE
Torpid
Refractory
E.
Testosterone (ng/ml)
****
LP
Pre-hib.
L. Pre-hib.
IBE
Torpid
Refractory
F.
Hypothalamic
cryosections
LCMD
RNASeq
G.
Activation of
gonads
Hibernation
onset
Transfer to
SP & cold
PC2, 8.01% variation
PC1, 76.8% variation
group
LP
Pre-hib
Late Pre-hib
IBE
Refractory

Figure 1

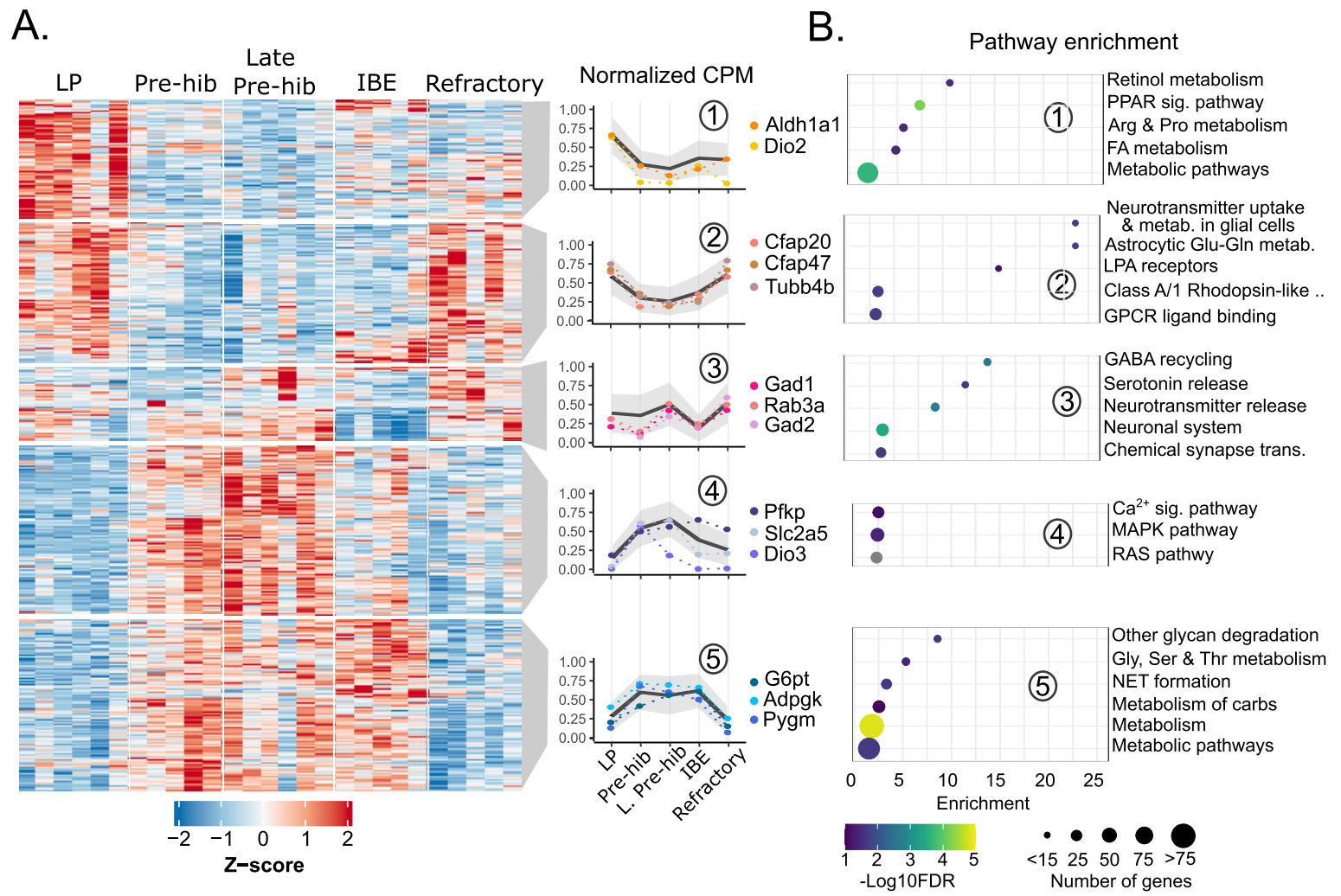
A.
LP
Pre-hib
Late Pre-hib
IBE
Refractory
Normalized CPM
Aldh1a1
Dio2
Cfap20
Cfap47
Tubb4b
Gad1
Rab3a
Gad2
Pfkp
Slc2a5
Dio3
G6pt
Adpgk
Pygm
Z-score
B.
Pathway enrichment
Retinol metabolism
PPAR sig. pathway
Arg & Pro metabolism
FA metabolism
Metabolic pathways
Neurotransmitter uptake & metab. in glial cells
Astrocytic Glu-Gln metab.
LPA receptors
Class A/1 Rhodopsin-like ..
GPCR ligand binding
GABA recycling
Serotonin release
Neurotransmitter release
Neuronal system
Chemical synapse trans.
Ca2+ sig. pathway
MAPK pathway
RAS pathway
Other glycan degradation
Gly, Ser & Thr metabolism
NET formation
Metabolism of carbs
Metabolism
Metabolic pathways
Enrichment
-Log10FDR
Number of genes

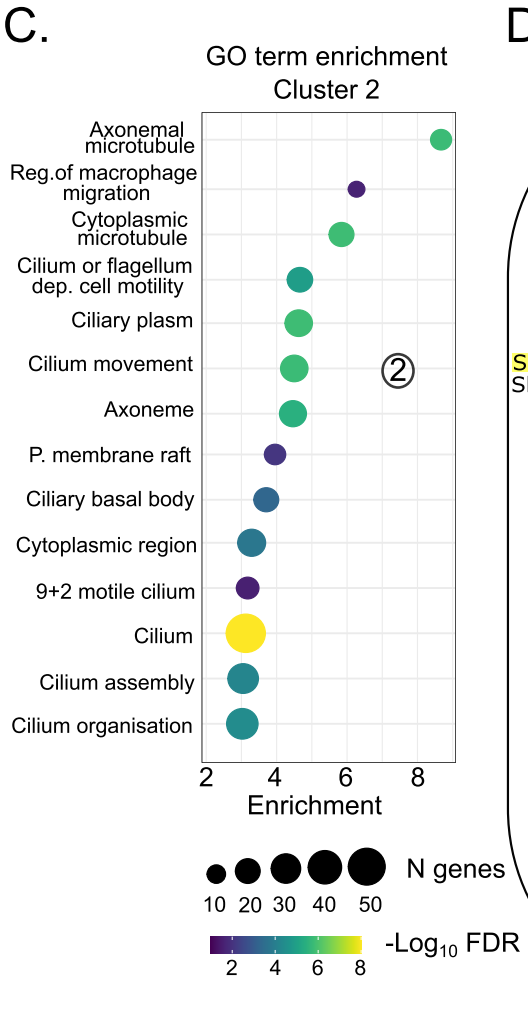
C.
GO term enrichment
Cluster 2
Axonemal microtubule
Reg.of macrophage migration
Cytoplasmic microtubule
Cilium or flagellum dep. cell motility
Ciliary plasm
Cilium movement
Axoneme
P. membrane raft
Ciliary basal body
Cytoplasmic region
9+2 motile cilium
Cilium
Cilium assembly
Cilium organisation
Enrichment
N genes
-Log10 FDR

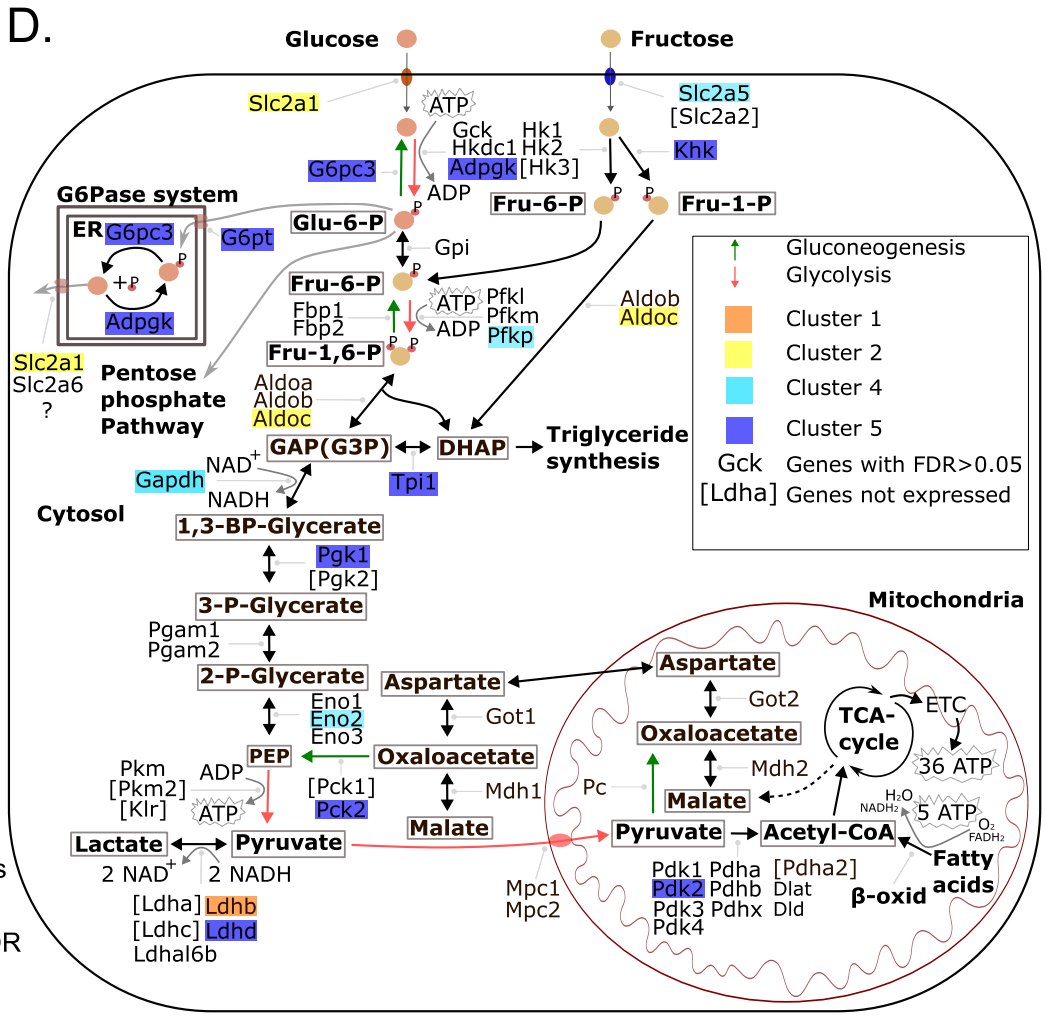
D.
Glucose
Fructose
Slc2a1
ATP
Gck
Hk1
Hkdc1
Hk2
Adpgk [Hk3]
Slc2a5 [Slc2a2]
Khk
G6pc3
ADP
G6Pase system
ER
G6pc3
Adpgk
G6pt
Glu-6-P
Fru-6-P
Fru-1-P
Gpi
Fbp1
Fbp2
ATP
Pfkl
Pfkm
ADP
Pfkp
Fru-1,6-P
Aldob
Aldoc
Slc2a1
Slc2a6
?
Pentose phosphate Pathway
Aldoa
Aldob
Aldoc
GAP(G3P)
DHAP
Triglyceride synthesis
Gapdh
NAD+
NADH
Tpi1
Cytosol
1,3-BP-Glycerate
Pgk1
[Pgk2]
3-P-Glycerate
Pgam1
Pgam2
2-P-Glycerate
Eno1
Eno2
Eno3
PEP
Pkm
[Pkm2]
[Klr]
ADP
ATP
[Pck1]
Pck2
Lactate
Pyruvate
2 NAD+
2 NADH
[Ldha] Ldhb
[Ldhc] Ldhd
Ldhal6b
Aspartate
Got1
Oxaloacetate
Mdh1
Malate
Mitochondria
Aspartate
Got2
Oxaloacetate
TCA-cycle
ETC
36 ATP
Mdh2
Pc
Malate
H2O
NADH2
5 ATP
O2
FADH2
Pyruvate
Acetyl-CoA
Fatty acids
β-oxid
Mpc1
Mpc2
Pdk1 Pdha [Pdha2]
Pdk2 Pdhb Dlat
Pdk3 Pdhx Dld
Pdk4
Gluconeogenesis
Glycolysis
Cluster 1
Cluster 2
Cluster 4
Cluster 5
Gck Genes with FDR>0.05
[Ldha] Genes not expressed

Figure 2

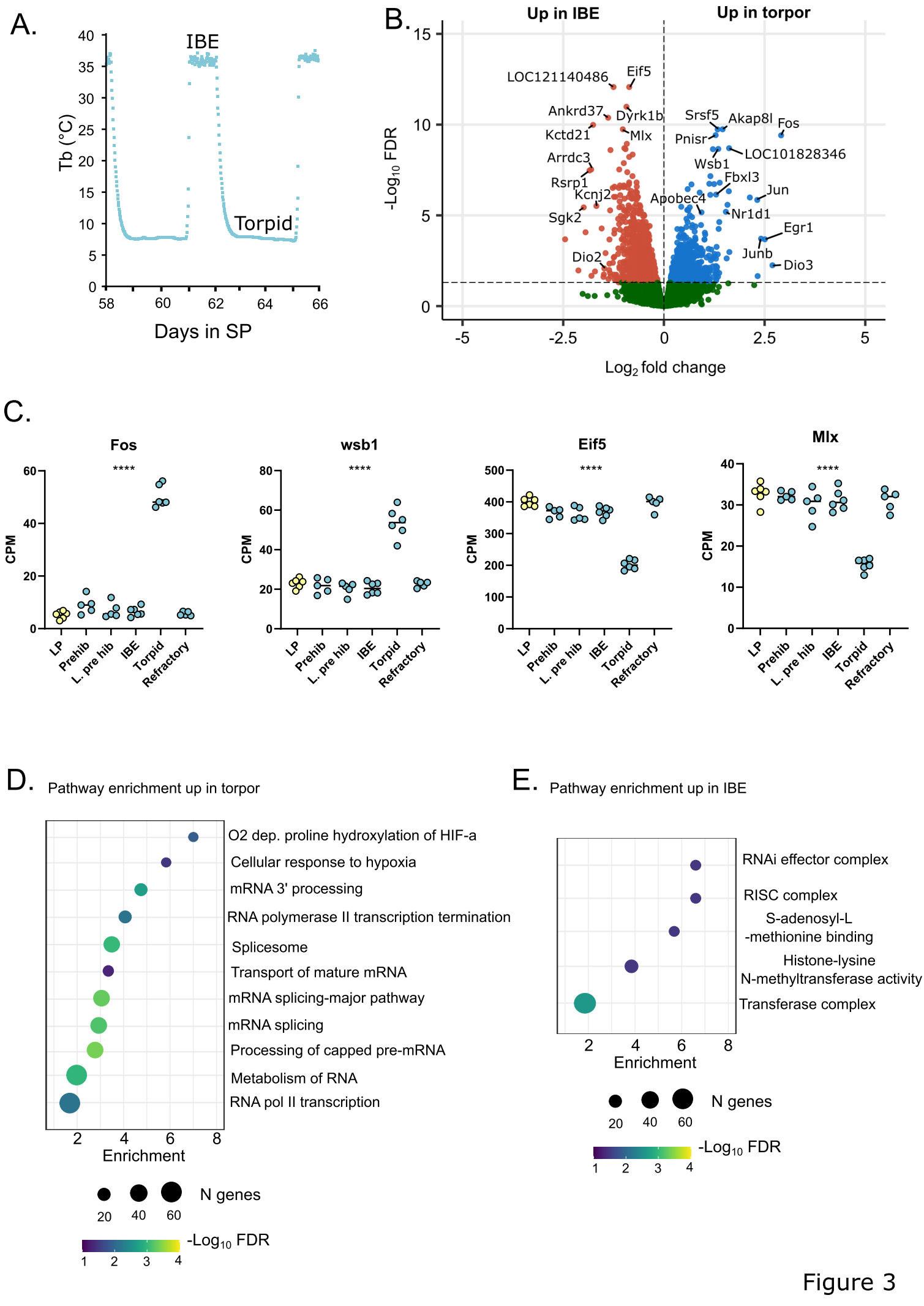
A.
IBE
Torpid
Tb (°C)
Days in SP
B.
Up in IBE
Up in torpor
LOC121140486
Eif5
Ankrd37
Dyrk1b
Kctd21
Mlx
Arrdc3
Rsrp1
Kcnj2
Sgk2
Dio2
Srsf5
Akap8l
Fos
Pnisr
LOC101828346
Wsb1
Fbxl3
Jun
Apobec4
Nr1d1
Egr1
Junb
Dio3
-Log10 FDR
Log2 fold change
C.
Fos
wsb1
Eif5
Mlx
CPM
LP
Prehib
L. pre hib
IBE
Torpid
Refractory
D.
Pathway enrichment up in torpor
O2 dep. proline hydroxylation of HIF-a
Cellular response to hypoxia
mRNA 3' processing
RNA polymerase II transcription termination
Splicesome
Transport of mature mRNA
mRNA splicing-major pathway
mRNA splicing
Processing of capped pre-mRNA
Metabolism of RNA
RNA pol II transcription
Enrichment
N genes
-Log10 FDR
E.
Pathway enrichment up in IBE
RNAi effector complex
RISC complex
S-adenosyl-L
-methionine binding
Histone-lysine
N-methyltransferase activity
Transferase complex
Enrichment
N genes
-Log10 FDR

Figure 3

A

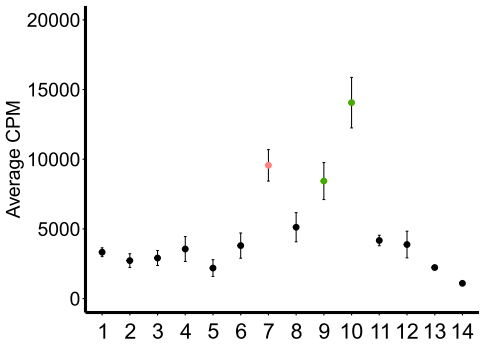

1. Oligodendrocytes
2. Endothelial cells
3. Mural cells
4. NG2/OPC
5. PVMs & microglia
6. VLMCs
7. Ependymocytes
8. Astrocytes
9./10. Tanycytes
11. Neurons
12. Pars Tuberalis
13. Present Campbell -1
14. Absent Campbell

B

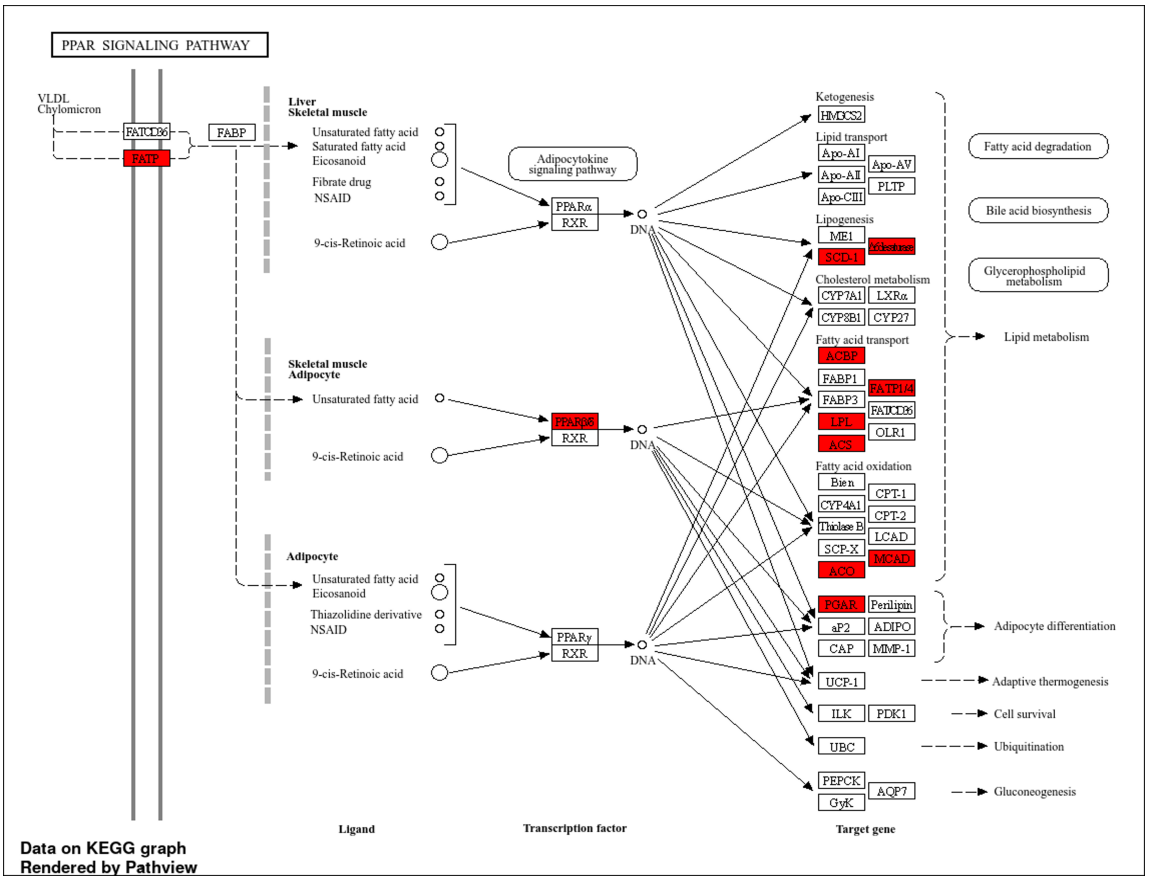

C

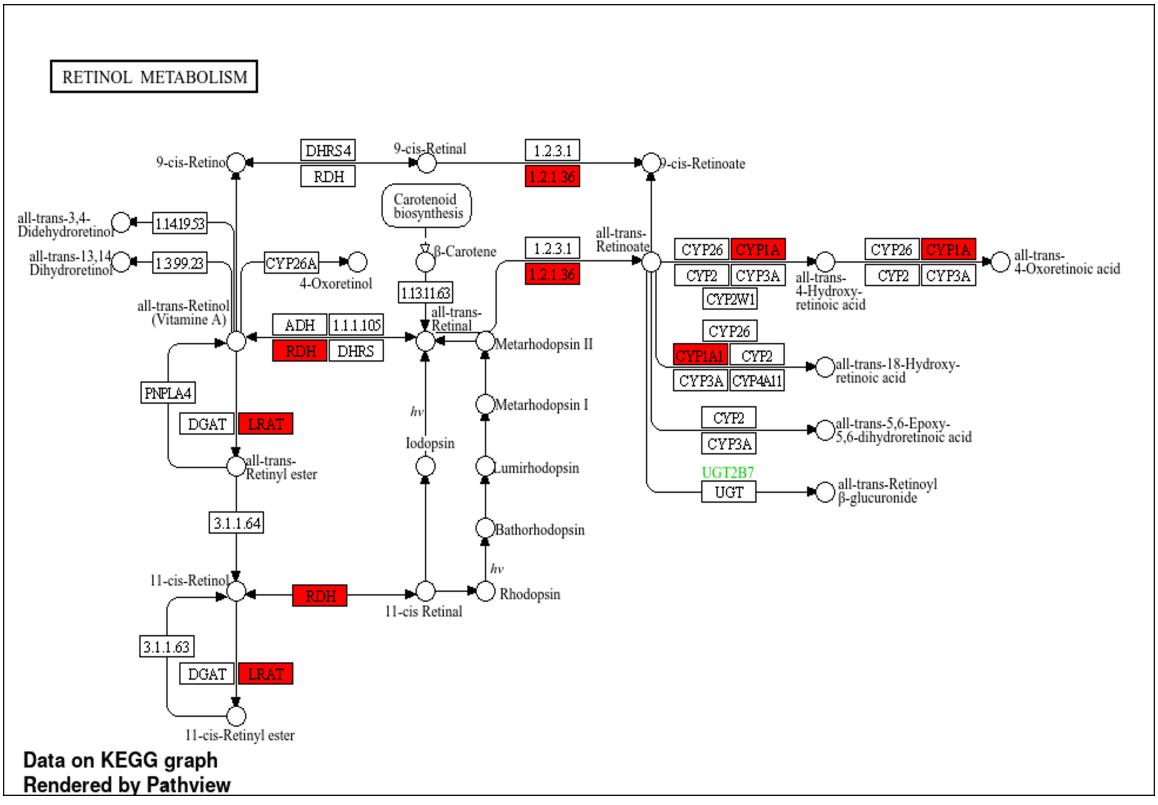

S.Figure 1

A.

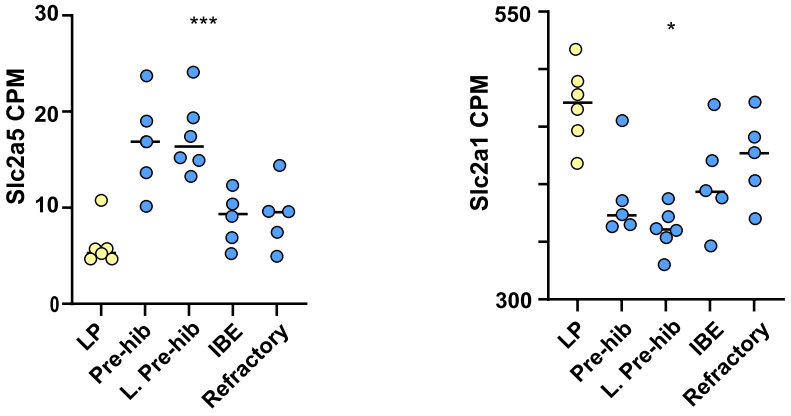
Slc2a5 CPM
30
20
10
0
***
LP
Pre-hib
L. Pre-hib
IBE
Refractory
Slc2a1 CPM
550
300
*
LP
Pre-hib
L. Pre-hib
IBE
Refractory

B.

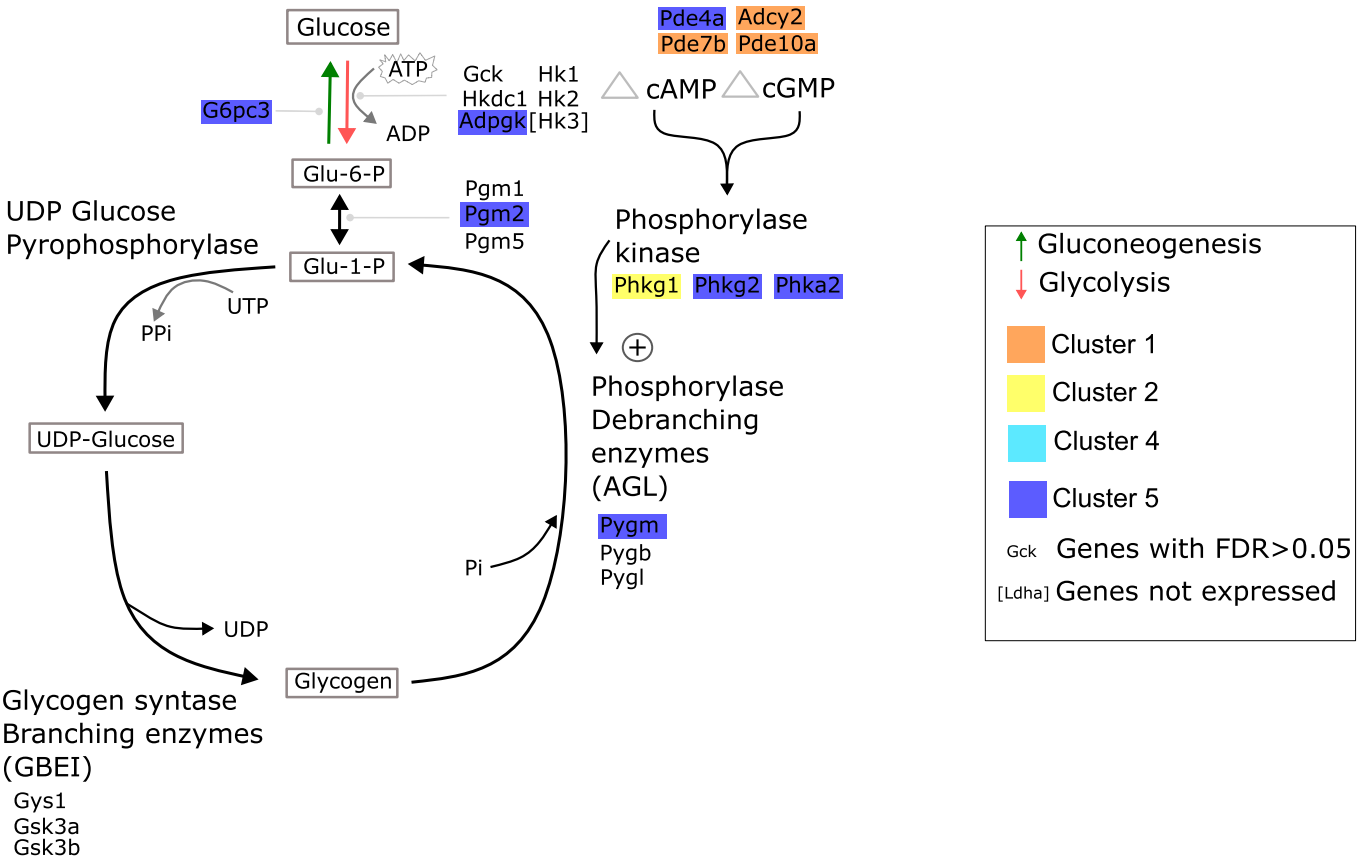
Glucose
ATP
ADP
G6pc3
Gck
Hkdc1
Adpgk
Hk1
Hk2
[Hk3]
Pde4a
Adcy2
Pde7b
Pde10a
cAMP
cGMP
Glu-6-P
Pgm1
Pgm2
Pgm5
UDP Glucose
Pyrophosphorylase
Glu-1-P
UTP
PPi
Phosphorylase
kinase
Phkg1
Phkg2
Phka2
Phosphorylase
Debranching
enzymes
(AGL)
Pygm
Pygb
Pygl
UDP-Glucose
Pi
UDP
Glycogen
Glycogen syntase
Branching enzymes
(GBEI)
Gys1
Gsk3a
Gsk3b
Gluconeogenesis
Glycolysis
Cluster 1
Cluster 2
Cluster 4
Cluster 5
Gck Genes with FDR>0.05
[Ldha] Genes not expressed

S.Figure 2

Vebjoern Jacobsen Melum

Rhéostasie et temporalité : un processus médié par les tanycytes

Résumé

Les propriétés géophysiques de la Terre entraînent des changements annuels dans l'irradiation solaire, entraînant des fluctuations saisonnières de la température et de la disponibilité alimentaire. Dans ce contexte, l'objectif principal de cette thèse était d'élucider la signature moléculaire des tanycytes dans deux paradigmes saisonniers qui modifient le métabolisme ; la programmation photopériodique maternelle (chez le hamster sibérien, *Phodopus sungorus*) et l'hibernation (chez le hamster doré, *Mesocricetus auratus*). Ici, nous avons également observé une modification des gènes liés aux cils en réponse à la photopériode et à l'état réfractaire. Collectivement, les résultats présentés dans cette thèse suggèrent que les changements dans l'expression des gènes liés aux cils et dans le nombre de cils sur les tanycytes pourraient, via des altérations dans la signalisation des métabolites, être un mécanisme rhéostatique altérant la régulation métabolique vers l'hypothalamus, permettant à un animal d'adapter sa physiologie métabolique à l'environnement

Mots clés : hamster sibérien, hamster doré, tanycytes, rhéostasie, plasticité, saisonnière, physiologie, métabolisme

Abstract

The overarching objective of this thesis was to elucidate the molecular signature of tanycytes in two seasonal paradigms that shift metabolism; maternal photoperiodic programming (Siberian hamster, *Phodopus Sungorus*) and hibernation (golden hamster, *Mesocricetus auratus*). Collectively, the findings presented in this thesis suggest that changes in cilia-related genes and numbers of cilia on tanycytes and, therefore presumably alterations in metabolite signalling via tanycytes, may be a rheostatic mechanism altering metabolic feedback to the hypothalamus allowing an animal to match their metabolic physiology to the environment.

Keywords : Tanycyte, rheostasis, metabolism, chronobiology, physiology, hamster, neurobiology, melatonin, seasonal, endocrinology,